Technical University of Munich
Department of Electrical and Computer Engineering
Chair of Energy Economy and Application Technology

MIGRA-NEST: Mixed Granularity Nested Energy System Toolbox

Evaluating National Energy Transition Pathways under Global Greenhouse Gas Emission Budgets - A Case Study on South Africa

Clara Luisa Orthofer, M.Sc.

Vollständiger Abdruck der von der Fakultät für Elektrotechnik und Informationstechnik der Technischen Universität München zur Erlangung des akademischen Grades eines

Doktor-Ingenieurs (Dr.-Ing.)

genehmigten Dissertation.

Vorsitzender

Prof. Dr.-Ing. Rolf Witzmann

Prüfer der Dissertation

1. Prof. Dr.-Ing. Ulrich Wagner
2. Prof. Dr. Miranda Schreurs

Die Dissertation wurde am 17.6.2020 bei der Technischen Universität München eingereicht und durch die Fakultät für Elektrotechnik & Informationstechnik am 21.9.2020 angenommen.

Abstract

Energy is a key driver for socio-economic development. However, it is also the single biggest non land-use related source of greenhouse gas (GHG) emissions. Thus, limiting climate change means transforming the global energy supply. Today a multitude of low-emission energy supply options exist that could support such a transition. However, the potential cost increase, as well as uncertainty about the socio-economic sustainability, technological feasibility and practical implementability of the transition process, have thus far discouraged many countries from embracing these new supply options. Furthermore, while climate change mitigation is a global issue, energy system planning, and the implementation of the energy transition is a matter of local responsibility. Hence, a disparity exists: establishing globally sustainable GHG emission trajectories that are in line with tolerable levels of climate change depends upon a global perspective, but finding ways to implement them, demands country-level knowledge. Identifying robust transition strategies, therefore, requires energy system models that incorporate both a representation of the global GHG emission balance as well as national techno-economic detail.

In this dissertation, I have developed a novel modelling toolbox - MIGRA-NEST: Mixed Granularity Nested Energy System Toolbox - that allows for such analyses. By providing methods to model national energy systems in a global context, the toolbox supports (i) creating simplified stand-alone representations of complex national energy systems, and (ii) nesting them into global model calibrations. This approach is innovative, as such combined model types are rarely considered in other works, that either model the whole world without any country-level detail, or to model on a national or sub-national level without representation of the rest of the world. In contrast, nested models allow exploring national energy supply strategies on country scale, while providing interactions with the international commodity markets and the global GHG emission balance as a backdrop. Additionally, two add-on modules, developed for the toolbox, provide for (i) a structured scenario analysis and (ii) a global sensitivity analysis of the resulting model calibrations.

To demonstrate the capability of the toolbox, a case study was carried out on South Africa. The country is particularly interesting, as its energy system is about to embark on a period of transition that will phase out old infrastructure, leaving space for replacing and expanding it with new technologies. Due to South Africa's vast renewable as well as fossil energy resources, a wide portfolio of options for an energy system upgrade exist. However, undergoing an emerging economy, the affordability of the energy supply is of the utmost importance, as eliminating poverty and eradicating inequality have priority over the transition to clean energy. Hence, the aim of the case study was to identify cost-optimal transition strategies for South Africa that are evaluated in the context of their potential contribution to global GHG mitigation. By first employing the *Rapid Prototyper* and the *Model Nester*, a mixed granularity model of South Africa in the global context was generated that was then employed in a scenario analysis that compares four mitigation strategies: two national strategies that explore the impact of constraining South Africa's GHG emissions to the NDC pledges, and two global strategies that explore the transition pathways along the RCP climate scenarios.

The results of the case study point out that average global GHG emissions reduction costs can be lowered by utilising the mitigation potential of countries with large renewable energy potentials and rapidly growing energy systems (such as South Africa). However, the case study also reveals that while a decarbonisation of the energy system in these countries would lower the global average mitigation costs, it would be a large burden for the respective countries. Hence, utilising the cost benefits of international concerted climate change mitigation action requires international compensation mechanisms that balance unequal contributions to the common goal: limiting climate change.

Kurzfassung

Energie ist ein wichtiger Faktor für die sozioökonomische Entwicklung von Ländern und Regionen. Energie ist aber zugleich die (abgesehen von der Landnutzung) größte Quelle von Treibhausgasemissionen (THG-Emissionen). Die Begrenzung der globalen anthropogenen Erderwärmung erfordert daher eine Umgestaltung der globalen Energieversorgung. Es gibt bereits viele emissionsarme Energieversorgungsoptionen, die eine solche Umgestaltung unterstützen könnten. Der damit verbundene potenzielle Kostenanstieg sowie die Ungewissheit über die sozioökonomische Nachhaltigkeit, die technologische Durchführbarkeit und die praktische Umsetzbarkeit eines solchen Transformationsprozesses haben jedoch bisher viele Länder davon abgehalten, diese neuen Versorgungsoptionen zu nutzen. Darüber hinaus ist die Eindämmung des Klimawandels zwar ein globales Thema, aber sowohl die Planung als auch die Realisierung einer Energiewende liegen in nationaler Verantwortung. Daraus ergibt sich eine Diskrepanz: die Festlegung globaler THG-Emissionsbudgets erfordert eine globale Perspektive, die Übersetzung dieser Budgets in real umsetzbare Handlungsempfehlungen jedoch Kenntnisse auf nationalem Niveau. Die Ermittlung optimaler Übergangsstrategien braucht daher Energiesystemmodelle, die sowohl eine Darstellung der globalen THG-Emissionsbilanz als auch nationale techno-ökonomische Details enthalten.

Im Rahmen dieser Dissertation habe ich eine Modellierungs-Toolbox entwickelt, die solche Analysen ermöglicht. Durch die Bereitstellung von Methoden zur Modellierung nationaler Energiesysteme in einem globalen Kontext unterstützt die Toolbox (i) die Erstellung einfacher Prototypenmodelle komplexer nationaler Energiesysteme und (ii) deren Einbettung in globale Modellkalibrierungen. Dieser Ansatz ist innovativ, da solche kombinierten Modelltypen in anderen Arbeiten nur selten berücksichtigt werden. Darüber hinaus ermöglichen zwei zusätzliche Module (i) eine strukturierte Szenarioanalyse und (ii) eine globale Sensitivitätsanalyse der resultierenden Modellkalibrierungen.

Der Leistungsumfang der Toolbox wird anhand einer Fallstudie zu Südafrika demonstriert. Darin werden kostenoptimale Übergangsstrategien für Südafrika im Kontext ihres potenziellen Beitrags zur globalen THG-Minderung bewertet. Die Szenarioanalyse vergleicht vier Minderungsstrategien: (i) zwei nationale Strategien, welche die Auswirkungen einer THG-Emissionsbeschränkung in Südafrika untersucht, (ii) eine globale THG-Minderungsstrategie, bei der die Dekarbonisierungspfade kostenoptimal auf alle Modellregionen verteilt werden, und schließlich (iii) eine globale Minderungsstrategie, bei der die THG-Emissionsreduktion nach dem Prinzip eines *gleichen Reduktionsanteils* auf die Modellregionen verteilt wird.

Die Fallstudie zeigt, dass durch die Nutzung des kostengünstigeren Minderungspotenzials von Ländern mit großen erneuerbaren Energiepotenzialen und schnell wachsenden Energiesystemen die durchschnittlichen globalen Minderungskosten gesenkt werden. Die Fallstudie zeigt aber auch, dass die Kostenbelastung durch eine solche Minderungsstrategie ungleich verteilt ist: während die Nutzung dieser Dekarbonisierungspotenziale die globalen durchschnittlichen Minderungskosten senkt, erhöhen sie die Minderungskosten auf nationaler Ebene. Die Nutzung der Kostenvorteile international konzertierter Klimaschutzmaßnahmen erfordert daher internationale Kompensationsmechanismen, welche die ungleichen Beiträge zum global gemeinsamen Ziel, nämlich der Begrenzung der globalen anthropogenen Erderwärmung, ausgleichen.

Acknowledgements

First and foremost I want to thank my family, Maria, Rudi, Anna and Andro for believing that I was able to do this, for coaxing me to complete it, and for supporting me all the way to the finish line. I also want to thank my *Munich family*, my flatmates and friends. I am extremely grateful to Alexis Zankowitch, Franziska Bamberg, and Nicolas Staub for their support throughout this project; the delicious meals and strong shoulders they offered as well as their understanding were extraordinary. Further, I am extremely grateful to Christian König, Daniel Zinsmeister, Michel Zadé, Sebastian Lumpp, and Sebastian Tuttas for their friendship, as well as for their critical feedback and for the many insightful comments they made.

Moreover, I want to thank the team at the *IIASA* energy program, here especially Daniel Huppmann and Volker Krey, for their patience in introducing me to energy system modelling, for including me in their team, and for repeatedly scrutinising my research with me.

Finally, I want to express my gratitude to Prof. Dr.-Ing. Ulrich Wagner and Peter Tzscheutschler for giving me the opportunity to write this dissertation, entrusting me with so many different projects, and for the high degree of creative freedom they offered and encouraged as well as to Prof. Dr. Miranda Schreurs for providing a whole new perspective to my research. Thank you!

Contents

List of Figures

List of Tables

Chapter 1

Introduction

Ensuring a tolerable climate future
requires immediate global action.

Lamontagne et al. (2019)

1.1 Motivation

In 2015 the members of the party to the United Nations Framework Convention on Climate Change (UNFCCC) agreed to strive for limiting global anthropogenic average end-of-century warming to well below 2°C above pre-industrial levels and to further pursue efforts to limit warming to 1.5°C (UNFCCC 2015a). In order to relate these envisioned end-of-century goals to today's actions, such temperature targets can be translated into radiative forcing levels and further into greenhouse gas (GHG) emissions budgets that quantify the amount of GHG that can still be emitted into the atmosphere and vice versa. In figure 1.1 six potential GHG emission trajectories are compared with respect to their effect on end-of-century warming. These trajectories are examples of so-called "climate change scenarios", which are coherent descriptions of possible climate change futures. Such scenarios either explore plausible future pathways based on current developments (e.g. *Current policies* in figure 1.1) or invert the process, and hence describe feasible trajectories towards reaching certain goals (e.g. *2° C consistent* in figure 1.1).

For the global community the envisioned *2° C trajectory* entails a reversal of the century-long trend of ever-increasing global GHG emissions. Such a global turnaround, however, calls for coordinated GHG mitigation. Because if each country decides separately if, when and how to act, this will lead to sub-optimal or insufficient mitigation results (Pittel et al. 2012). As such, climate change mitigation is one of the challenges that the world has to confront as an international community. However, while the common goal has to be pursued by the world as a whole, the required mitigation burden has to be broken down into specific, clearly defined measures and apportioned to specific regulatory authorities to be enforced, tracked, and adjusted if necessary. The Nationally Determined Contributions (NDCs) submitted to the UNFCCC under the Paris Agreement and its predecessor the Kyoto Protocol are first steps in this direction. Nonetheless, the NDCs have each been

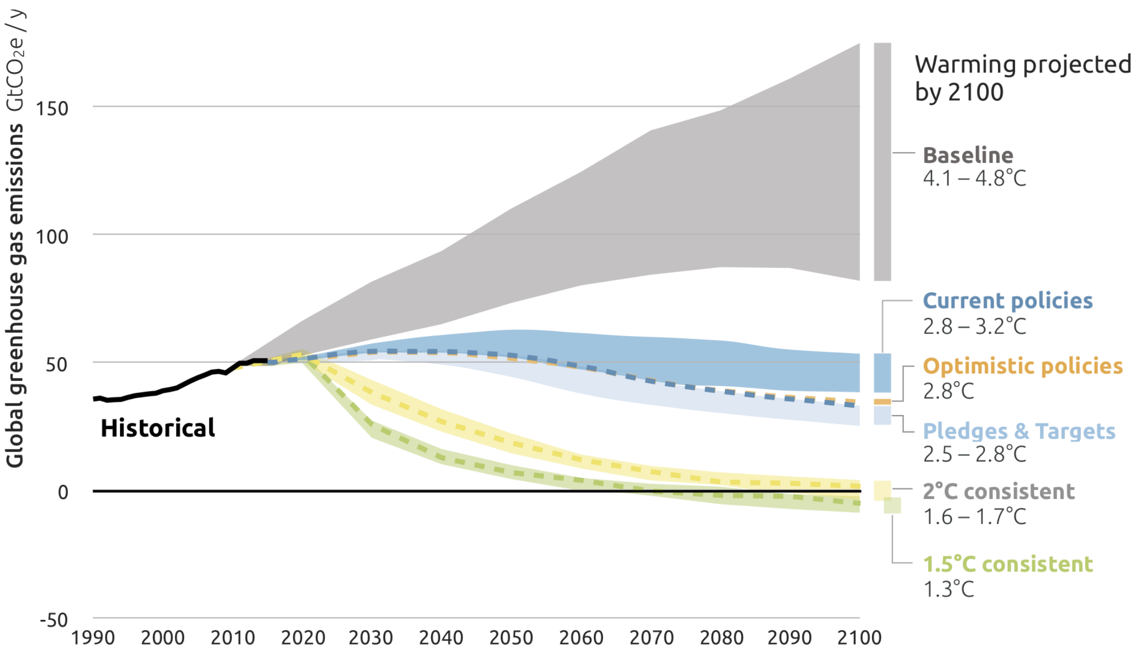

Figure 1.1: History and projections of the global greenhouse gas emissions in gigatons of CO_2 equivalents per year ($GtCO_{2e}/y$) and the related end-of-century anthropogenic global warming potential measured in °C above pre-industrial (1850) levels. The six depicted trajectories show: the no-action baseline (grey), the current policies (dark blue and orange), the pledged NDCs (light blue), and the GHG emissions trajectories required for limiting global warming of annual global anthropogenic GHG emissions (i.e. excluding emissions from semi-natural process such as land use, land use change & forestry (LULUCF)) to 1.5-2°C (green and yellow) (CAT 2019b).

independently developed by national governments and the established means are thus not coordinated among signatory nations. Hence, while the ambitions developed individually will together achieve a significant deviation from the reference scenario (leading to a median anthropogenic warming of 2.6-3.1°C by 2100), further action will be required in order to close the temperature gap (Rogelj et al. 2016). In order to achieve the envisioned goal it is necessary to establish globally coordinated measures that can be scaled down to national action levels.

1.1.1 Climate Change Scenarios

Several attempts of translating the desired end-of-century goals into GHG emission budgets and necessary action levels, have been undergone so far. To do so, first, the global warming targets are translated into end-of-century atmospheric radiative forcing levels, which are then translated into multi-decade long global GHG emission budgets. Subsequently, in order to translate these budgets into emission allowances per fuel, technology, region, capita or per century, these emission trajectories are matched with scenarios on political, technological, and social developments.

The most recent scenario set, which tackles the former, are the so-called Representative

Concentration Pathways (RCPs). To date a fleet of RCPs has been developed (IPCC 2013). Each pathway is named after the calculated end-of-century increase in radiative forcing levels (caused by anthropogenic GHG emissions) compared to pre-industrial (1850) levels (van Vuuren et al. 2011). The term *representative* is used in the name, as the described pathways are representations for the much larger set of scenarios that would allow reaching the envisioned forcing level target. The RCPs and their induced end-of-century warming levels are presented in table 1.1.

The narrative of global social, economic, as well as political development over the next century, is mapped out by the Shared Socioeconomic Pathways (SSPs). The SSPs describe different, but internally coherent, socio-economic storylines that include a quantification of parameters important for modelling, such as population and GDP growth, political stability, international willingness to cooperate, etc. (O'Neill et al. 2014). The RCPs can be combined with the SSPs. Together they can be arranged into a matrix that combines the socio-economic narratives as described by the SSPs with different levels of anthropogenic end-of-century global warming (van Vuuren et al. 2014).

Table 1.1: Expected average anthropogenic global warming above pre-industrial (1850) levels by 2100 in the RCP scenarios in °C. Data from the SSP data base (Riahi et al. 2017; Gidden et al. 2019; Rogelj et al. 2018).

[°C]	RCP8.5	RCP6.0	RCP4.5	RCP3.4	RCP2.6	RCP1.9
min.	3.0	3.2	2.5	2.1	1.7	1.3
max.	5.1	3.3	2.7	2.3	1.8	1.4

The scenarios presented in this dissertation are based on the "middle-of-the-road" SSP scenario (SSP2), which is described by Fricko et al. (2017). The emission trajectories that relate to the SSP2-RCPs are summarised in appendix B.2.

1.1.2 Climate Change and Energy

The energy sector is the dominant source of annual global anthropogenic GHG emissions excluding land-use, land-use change and forestry (LULUCF) (Bruckner et al. 2014).[1] Thus, reversing the global GHG emission trajectory requires a drastic transition of the energy system. This transition includes, first and foremost, the conversion from a high-carbon energy system to low-carbon or no-carbon energy system ("a decarbonisation of the energy system"), as well as a push towards increased energy efficiency.

Embarking on such a transition is a sensitive matter, as supplying reliable and affordable energy is a key driver to economic development around the world (Terrapon-Pfaff et al. 2018). In their Sustainable Development Goals (SDGs), the United Nations (UN)' "*blueprint to achieve a better and more sustainable future for all*" (UNFCCC 2015b) the UN states:

[1]In 2017 the energy sector was accountable for 36.5 $GtCO_2eq$, while the total global GHG emissions excluding GHG emissions from land-use, land-use change and forestry (LULUCF) were recorded at 49.4 $GtCO_2eq$ (Gütschow et al. 2019).

> "*Energy is central to nearly every major challenge and opportunity the world faces today. Be it for jobs, security, climate change, food production or increasing incomes, access to energy is essential.*" (UNFCCC 2015b)

An environmental, social, and economical sustainable development depends upon a successful transition of the energy sector (Arndt et al. 2016; Fankhauser and Jotzo 2018). Especially to emerging economies, finding this balance between economic development and ecological responsibility is of growing importance. While, according to the UNFCCC, countries with emerging economies have in the past contributed a comparatively small share to global GHG emissions, their rapid economic progression has put this group among the top emitters. Today the group of emerging economies is accountable for about 60% of global anthropogenic GHG emissions (Fankhauser and Jotzo 2018). Thus, if international emissions are to be reduced, developing countries and emerging economies cannot follow the carbon intensive growth path as the industrialised countries did, but will need to break new ground in their approaches to development (Fankhauser and Jotzo 2018). Establishing optimal strategies for the energy system transitions, inevitable in the face of fossil resource depletion and anthropogenic climate change, is key to ensuring sustainable development for the world.

1.2 Energy System Modelling

A country's energy supply, transformation, and system is an extremely complex web of sources and flows among a variety of stakeholders. Such systems require adequate complex tools in order to analyse the behaviour of the overall system as a response to disturbances or changes. In engineering, methods from operations research, developed for military purposes in the 1940s, pioneered the methodological approach to energy system modelling (Messner 1997). Those planning methods have since been adapted, advanced, and applied to energy systems numerous times. Simultaneously the methods from economics found introduction into energy research. While less specific on technical detail, these methods offer a broader view on the interactions between macroeconomic development and the energy supply and demand. Recently, and in line with increasing availability of major computational resources, attempts at combining these two approaches have been gaining importance (Herbst et al. 2012).

Additionally, and in the recent wake of increasing interest in the environmental impact of the energy sector, more methods from new fields such as ecology and geo-informatics have been adapted for and applied to the evaluation of energy systems. Environmentalists, such as Howard et al. (2013), apply the dynamic methodologies that embody the environment as a living organism, in order to understand the interaction of the energy system and the surrounding environment. Researchers from geo-informatics, as for example Blaschke et al. (2013) apply geographic information systems (GISs) and other map-based methods to understand the spatial dimension of interactions such as land-use demands, land-use options and potentials (e.g. renewable energy potentials and their geographic position, the demand locations, grid-expansion options, etc.) related to the energy-supply. However, engineering and economics remain the dominant disciplines and thus, the development of the energy-economic perspective to energy system modelling, characteristic to these two approaches, is introduced below.

1.2.1 Historical Developments

While energy system modelling dates back to the beginnings of operations research in the 1940's, interest in it only gained attention in the 1970s, when the first oil crisis shocked the energy supply systems around the world and revealed their vulnerability (Messner 1997). All of a sudden, providing a deep understanding of the energy sector, its long-term development options and related costs, was, for many countries, of national importance (Dioha 2017). Ever thereafter, many policymakers were concerned with long-term energy planning and the deliberate design of rational energy use strategies (Dioha 2017; Bhattacharyya and Timilsina 2010b). Hence, the interest in energy sector modelling then was twofold and focused on the questions of: (i) *How can the energy system be altered so that the oil import dependency is reduced?*, and (ii) *How will such energy policies affect the economy?* (Messner 1997).

Accordingly, two model approaches were established. On the one hand, and with a focus on the first question, researchers from the engineering field developed a fleet of technology-driven simulation and optimisation models (so-called *bottom-up* models). Their main design aim was energy planning and, hence to explore benefits and shortfalls of various energy system designs in the context of constraints on the availability of competing resources and technologies. On the other hand, and with the second question in mind, researchers from the field of economics have developed models that portrayed the energy sector as a sub-sector of the overall economy (so-called *top-down* models).

One of the first and most influential early energy system models of the engineering type was the *Brookhaven Energy Systems Optimisation Model (BESOM)* (Kydes 1980). While *BESOM* is no longer in use, several of the models dating back to that generation are still amidst the models most frequently utilised today. Among the most prominent examples from that generation are the *MARKet ALocation (MARKAL)* model, first developed by the *Energy Technology Systems Analysis Program (ETSAP)* of the International Energy Agency, the *Model for Energy Supply Strategy Alternatives and their General Environmental Impact (MESSAGEix)* model developed at the *International Institute for Applied Systems Analysis (IIASA)* and the *EFOM* model developed by European Union (Seebregts et al. 2002; Hall and Buckley 2016; Subramanian et al. 2018; Huppmann et al. 2019).

Starting in the 1980s, increasing concerns about environmental pollution and global warming, both stemming to a great extent from the continuously growing energy sector, brought a third objective to the field of energy research. The question posed was: *How does the energy sector interact with the environment?* The search for an answer to this question led to the development of a new generation of tools. These new tools incorporated environmental features and brought the evaluation of climate change mitigation strategies into energy system modelling (Messner 1997). Driven by this new interest, many models, for example the *MARKAL* and the *MESSAGEix* model formulation, were extended to include representations of the interaction with other economic sectors and the environment (e.g land-use change through agriculture and forestry). Hence, they transformed from plain energy system models into the new model class, the so-called Integrated Assessment Model (IAM) (Klaassen and Riahi 2007).

To date a plurality of country-level scenarios but also global level scenarios have been implemented using the *MARKAL* model and its more recent successor *The Integrated MARKAL-EFOM System (TIMES)*, making it today's probably most used energy system model framework (Hall and Buckley 2016; Subramanian et al. 2018). In similar way, *MESSAGEix* is used for many current applications. With its representation of the global energy-emissions-land-use nexus the *MESSAGEix* models find great recognition in global energy assessments (GEA 2012; Pachauri and Meyer 2014; Klaassen and Riahi 2007) as well as in the development of country-level energy strategy plannings (Orthofer et al. 2019).

1.2.2 Recent Developments

Over the last decades energy system research has remained an active research field. With a strong focus on energy system modelling, the field advanced in line with the increasing complexity of the energy sector. The new challenges of today's energy supply are manifold, ranging from the increasing number of market participants through the liberalisation of the energy markets and the introduction of *prosumers*[2], the market-distorting effects induced by the introduction of subsidies and other policy incentives, across to new technological challenges, induced by the increasing share of intermittent renewable energies, decentralised power generation, and the inter-linkage of different energy sectors, to the increasingly pressing issue of global warming (Bhattacharyya and Timilsina 2010b).

Hence, portraying these new dimensions of intricacy on the market as well as recent technological innovations are two of the main drivers that currently extend energy modelling efforts. On both the economic and technological ends, these continued efforts, in combination with the rapid increases in available computing power, have led to the development of new types of models. For example, agent-based models for the description of the new market players, or machine learning algorithms for short-term market price forecasting are just two novel model approaches that were introduced to energy system modelling over the last decade. For the description of the new technological challenges, the increased calculation power was frequently invested into increasing the model detail and scope by refining the model granularity while widening the coverage on a spatial, temporal as well as on sectoral level.

Today, energy system models of all spatial levels exist: from models covering the entire world on a continental or regional scale to models covering a single household on electric appliance level (see figure 1.2). The same holds true for the temporal range. Here, on the one hand, models for grid optimisation and grid operations planning explore timeframes at the scale of minutes at a millisecond granularity, while on the other hand, models for global energy supply planning and emissions balancing span across centuries with annual granularity. A comprehensive review study on current energy system models is given by Ringkjøb et al. (2018), who in their meta-study compare 75 energy system models by their general logic as well as their spatio-temporal resolution.

[2] The term is a composition of "producer" and "consumer" and refers to electricity consumers who also produce electricity and vice versa.

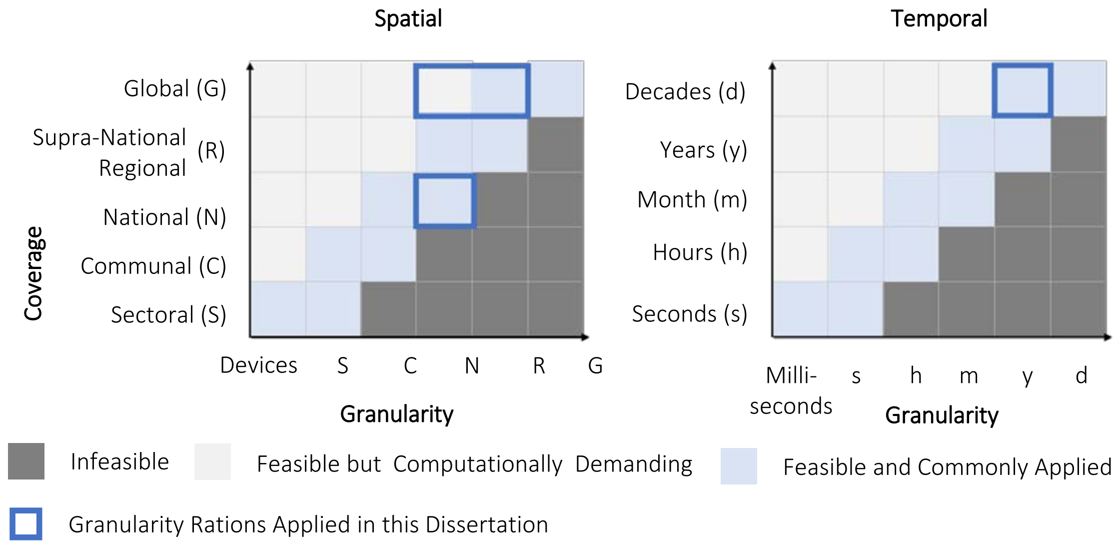

Figure 1.2: Common spatial and temporal coverage-to-granularity ratios used in energy system modelling. The figures show feasible and commonly applied (blue), infeasible (dark gray), and feasible but computationally demanding (light gray) coverage-to-granularity ratios. The blue hatched areas indicate the ratios as modelled in this dissertation.

In this dissertation, the aim is to provide a tool that allows to identify globally sustainable as well as nationally feasible scenarios for potential energy system development paths. Therefore, the minimum spatial coverage requirement for the research question at hand is national and hence, in the following, models of lower coverage (communal or household level) are not further investigated.

National & Regional Energy System Model Applications

Over the past decades, governments, non-governmental organisations (NGOs) as well as private corporations, together with researchers from various disciplines have developed a large variety of models describing and exploring the energy systems on national levels in depth. Numerous energy system model-based analyses have been conducted on most industrialised nations with a special focus on countries that have ambitious GHG-emission mitigation goals, and which seek to implement far reaching *energy transitions*. In their study on the energy system model landscape of the UK, Hall and Buckley (2016) identified over one hundred model calibrations recently referenced in academic literature, for the UK alone.

Emerging economies, faced with the challenges connected to fast growing energy demands and an often outdated and inefficient energy system, have also received increased attention from the modelling community. For example, for South Africa seven major models are currently in use and for each of these models several calibrations exist.[3]

[3]The most recent model calibrations for South Africa are:
(i) Winkler (2007) has calibrated MARKAL (Turton et al. 2013) to the South African energy system.
(ii) Musango et al. (2009) have developed the *T21* model, a new national model for South Africa that is

The fleet of national and sub-national regional models spreads across a vast methodological space, including different sectors and time frames, each model geared towards answering a specific research question. Most of these models are similar in that they focus on one specific country. While the majority of these models do include energy trade to some extent, only some models include other relevant countries (e.g. neighbouring countries, trade partners) for a more explicit understanding of international interactions. The same holds true for energy system models with a supra-national focus, such as the 36 regional models (26 EU-scale, 10 multi-national sub-European-scale models) listed by the Energy Modelling Platform for Europe (EMP-E)[4]. While they, by definition, cover a multitude of countries, most of them have hard system boundaries that do not consider energy trade with countries or regions outside the model's scope.

Such national and sub-national regional models can deliver great insight on country or regional level and are therefore well suited for developing and testing national policy recommendations. However, they fall short in representing global feedback effects or balancing global emissions (see figure 1.3).

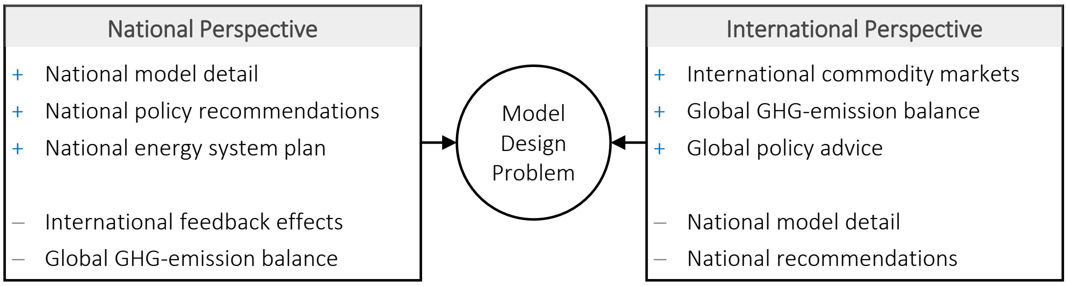

Figure 1.3: Schematic of the contradicting perspectives on energy system modelling from a national and an international perspective.

Global Energy System Models

A variety of global models have been developed to supplement the national and supra-national regional models, described above. In contrast to the national- and regional models' policy focus, the primary objective of global models are issues related to long-term energy

embedded in an integrated energy-economic-social-environmental framework.
(iii) ERC (2013) have calibrated the inter-temporal bottom-up partial equilibrium optimisation model *ANSWER-TIMES* to the South African energy system (*SATIM*). *SATIM* is based on the *TIMES* (Loulou and Labriet 2008) model, which itself is a version of MARKAL but extended by an economic approach top-down modelling approach.
(iv) Arndt et al. (2016) have extended the *SATIM* model by linking it to a general equilibrium model.
(v) NREL (2017) have calibrated a linear expansion and dispatch optimisation model of the South African power sector based on the commercial market simulation software *PLEXOS* (*PLEXOS Integrated Energy Model* 2019).
(vi) Brown et al. (2018) have developed the *PyPSA* model, a national linear partial equilibrium power flow model of the South African grid.
(vii) Orthofer et al. (2019) have calibrated the techno-economic *MESSAGEix-MACRO* (Huppmann et al. 2019) model framework for applications in emerging carbon-fuel rich economies and applied the model for South Africa as a case study - in work prior to this dissertation.

[4] http://www.energymodellingplatform.eu/resources.html

supply scenarios. This includes sensitive concerns on economic development, but also on global equity in allocating finite resources and dealing with the mitigation of GHG emissions from the energy sector.

The most renowned energy models applied in this context are the three model frameworks calibrated for the Intergovernmental Panel on Climate Change (IPCC) reports on climate change (Pachauri and Meyer 2014): *REMIND* (Bauer et al. 2016), *GCAM* (Calvin et al. 2012) and *MESSAGEix* (Riahi et al. 2012). Furthermore, two other models have gained recognition in global energy system modelling: *MARKAL* (Turton et al. 2013) was used for the *World Energy Scenarios* (WEC 2019) and the World Energy Model (IEA 2019b) was used for the widely-cited *World Energy Outlook*.

While these model calibrations provide deep insights into international energy market dynamics and global GHG emissions, they cannot be applied to provide country-level insights and thus national policy recommendations because they lack country-specific detail (see figure 1.3).

1.3 Research Gap

The discussion above shows that today many models are available that have been optimised and calibrated for various spatio-temporal as well as sectoral coverages. On a temporal scale, common model approaches range from milliseconds (for power-system optimisation) to decades (see figure 1.2). On a spatial scale, the coverage varies from household and community levels, as typically used for operational and process control purposes, to national and global scale, as required for strategic energy modelling to consider ecological and economic influences. In line with spatial coverage, granularity varies: with reasonable computational and calibration effort, households can be modelled either on household or device level, nations can be modelled on national or sub-national community level and models of global scope tend to use a supra-national regional resolution, as any higher granularity would result in unreasonably high computational demand and calibration effort.

Of course, some models are well calibrated for the energy-focused assessment of countries, supra-national regions and even of the entire world. However, to date, most of these models have been designed for a single coverage-to-granularity ratio. The literature indicates that (i) almost all models on global scale have a focus on a supra-national regional granularity, (ii) regional models are commonly calibrated to countries or sub-national regions and (iii) national models come in many granularities ranging from communities, districts to arbitrary sub-national divisions (Ringkjøb et al. 2018).

To the best of my knowledge, the only published national model that includes the global energy system and thus computes international commodity trade dynamics is *GCAM-US*. This model portrays the energy supply and demand in the fifty states of the United States of America on state level and the rest of the world in the shape of thirty-two sub-national regions (Zhou et al. 2014). However, in contrast to the toolbox proposed here, this model does not provide a frame- or code-base for creating such models for other nations. Furthermore, while the underlying scenario assumptions of *GCAM-US* are well documented, the model calibration data itself is not publicly available, which makes the model irreproducible for unaffiliated researchers.

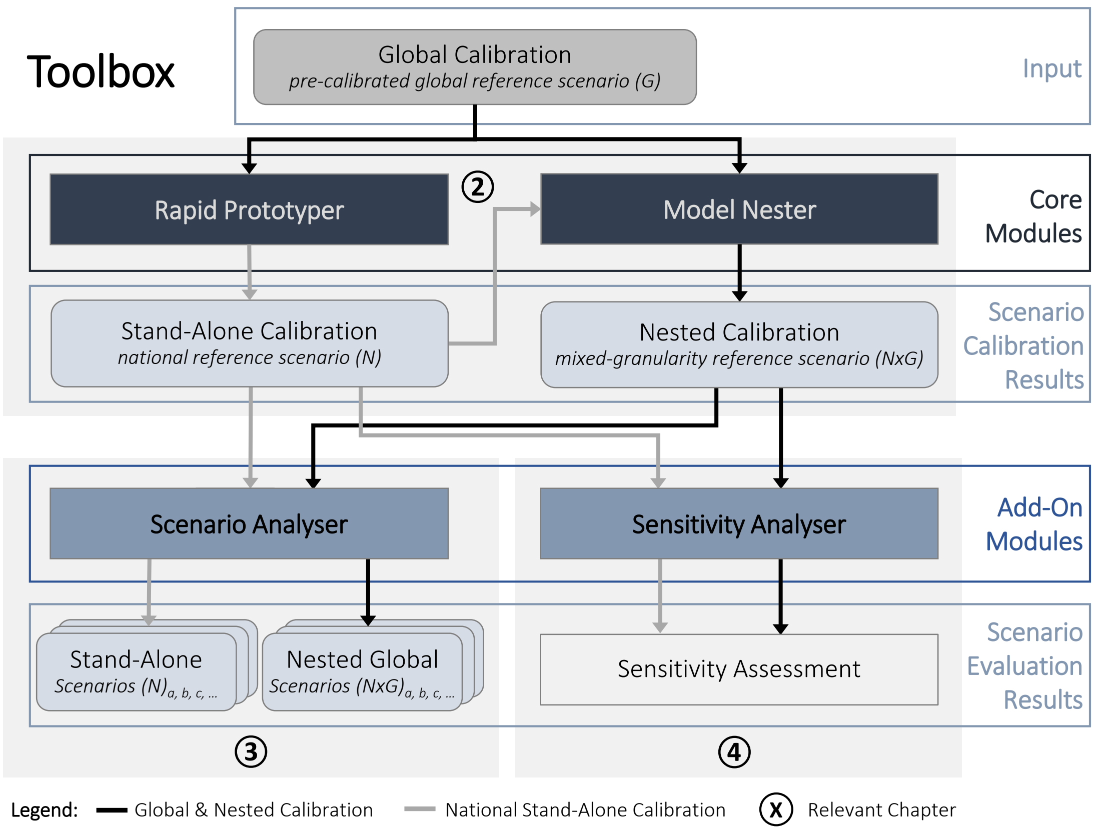

Figure 1.4: Schematic of MIGRA-NEST. The two dark-blue boxes represent the two core-modules, the Rapid Prototyper and the Model Nester that are described in detail in chapter 2. The two add-on modules, the Scenario- and the Sensitivity Analyser are covered in chapters 3 and 4, respectively. The light blue shapes indicate the model calibrations.

1.4 Contribution

A review of national energy system modelling studies reveals that - despite most models showing a strong awareness of the implications of global interaction effects - only a limited number of models exist that endogenously portray the international commodity market. While such national energy system models are well suited to examine the national energy supply, they lack the scope to model international feedback on national policy choices. Global models on the other hand tend to deliver global or supra-national regional insights and hence cannot provide tangible insights for national policy makers.

This dissertation addresses the aforementioned shortcomings by providing a toolbox - MIGRA-NEST: Mixed Granularity Nested Energy System Toolbox - for nesting national energy system model calibrations within model representations of the global energy supply. These new models allow for illustrating transition pathways for energy systems and are well suited for identifying national GHG mitigation strategies in a global context. Figure 1.4 shows a schematic of the novel model toolbox that enables the development of robust national energy system scenarios, which incorporate international feedback effects.

MIGRA-NEST consists of four independent modules: two core modules that make up the basis of the toolbox and together allow for the creation of the mixed-granularity model calibrations.

- The *Rapid Prototyper* module aims at reducing the technical barriers to energy system modelling that potential users might fear. By introducing a tool to prototype national energy system models, I provide an easy to operate integrated input-data to output-plot, tool-based, Python workflow that enables quick model creation without programming ability requirements.
- The *Model Nester* module is a novel workflow to embed national energy system models into integrated assessment models of global coverage and, hence, introduce a standardised workflow to create mixed-granularity model types.

The two add-on modules support the scenario- and sensitivity analysis of created models.

- The *Scenario Analysis* module provides scripts and workflows for defining, evaluating, and visualising sets of scenarios. By separately handling the calibrated reference scenario and the applied scenario alterations, it provides for a synoptic scenario description.
- The *Sensitivity Analysis* module allows for a standardised global sensitivity analysis and, thus, the evaluation of the sensitivity of the model results towards the model calibration. By allowing the user to estimate the uncertainties that are inherent to global long-term modelling the module provides a means for researchers to take a proactive stance towards model uncertainties that are often overlooked.

Both core modules are described in detail in chapter 2. The function of the *Scenario Analysis* module that contains the model run results is described in chapter 3, the *Sensitivity Analysis* module and its application are described in chapter 4.

Alongside the toolbox description, I present a case study that explores the real-world application of the model toolbox by evaluating the challenges and opportunities faced by

South Africa, an energy-resource rich emerging economy. By applying the *Scenario Analysis* module to a mixed-granularity model calibration of South Africa, I compare different GHG mitigation strategies and exemplify how the novel integrated approach might help reveal previously overlooked internationally-coordinated mitigation strategies. Finally, the toolbox is equipped with a module for global *Sensitivity Analysis*. The standardised workflow for testing the sensitivity of the model output upon the model input factors, completes the toolbox.

Reducing the Barrier to Energy System Modelling

Model frameworks exist today that allow for the calibration of national models. However, deep modelling expertise, and in most cases programming experiences as well as substantial techno-economic data sets are required to calibrate even a simple stand-alone one-node model. With the *Rapid Prototyper* presented in this dissertation, I provide a tool that enables the fast prototyping of national stand-alone models without extended programming knowledge or the need for extensive techno-economic data.

For countries where detailed energy system model representations exist, the prototyped models are not to be considered equivalent to these. Instead of regarding the prototyped models as a replacement of existing models, they should be considered a valid starting point for modellers who do not have access to a pre-calibrated model of their country of interest. With the prototype providing the initial model structure, no limits are set for further calibration refinement. Furthermore, by standardising the workflow and recycling the techno-economic calibration data of well documented models, the *Rapid Prototyper* increases the overall reproducability and transparency of the modelling process.

Standardised Workflow for Mixed-Granularity Models

Many energy system model calibrations at national and international levels exist today. However, to the best of my knowledge, no open framework for the integration of national-scale energy system models into global model calibrations is available to date. With the *Model Nester*, presented in this dissertation, I supply a blueprint for the generation of mixed-granularity-models by providing a tool for embedding national energy system models into integrated assessment models of global coverage. By standardising the nesting process, I again support the overarching goal of current modelling activities: increasing reproducability and transparency of the modelling process and the results.

Internationally-Coordinated, National Emission Mitigation Strategies

Achieving ambitious climate goals will require internationally-coordinated measures (Pittel et al. 2012). Within a globalised world and its international commodity markets, mitigation strategies of national governments should not be considered additive but interconnected. While some national strategies might yield global synergies, others might result in unintended negative feedback effects.

In this dissertation I present a case study that evaluates the national mitigation strategies for emerging economies exemplified by South Africa. By applying, first, the *Rapid Prototyper* to create a national stand-alone model calibration of the South African energy system and second, the *Model Nester*, to embed the national stand-alone calibration in a pre-existing global model calibration, I develop a mixed-granularity model calibration of the South African energy system. The calibration covers the South African energy system on a national level and the global energy system on a supra-national regional level. Based on this model calibration I conduct a scenario analysis to evaluate the efficiency of various national and international GHG emission reduction strategies.

Dealing with Uncertainties in Global Long-Term Modelling

Finally, energy system models are data- and law-driven and their results are thus strongly connected to the model input parameters and applied development assumptions. While long time-horizons are necessary to represent the long-lasting decision processes experienced in the energy industry, they increase the uncertainty connected to any of the model results. By highlighting input factors of special importance with respect to the model output, a global sensitivity analysis can point out inputs, which have to be calibrated with special caution, or are of special interest to be further investigated in a scenario analysis. Furthermore, the sensitivity approach provides insights into the reliability of the model results in dependence on the variance of model calibration input data. However, only very few energy system model publications exist that employ such a consistent integrated sensitivity analysis. By integrating a tool for sensitivity analysis in a workflow for parallel computation of multiple scenarios, I allow users to test their models using a global sensitivity analysis despite the computational challenge posed by this task.

1.5 Structure

This dissertation is structured as follows:

Chapter 2 presents the overall model concept, the design and function of MIGRA-NEST. Furthermore, it introduces a case study on South Africa, in which a national stand-alone model calibration and a global model calibration are combined to form a mixed-granularity model calibration of the South African energy system within the global energy context.

Chapter 3 contains a description of the scenario analysis conducted with the mixed-granularity model of the South African energy system, which was introduced in chapter 2. By evaluating eighteen different scenarios, the analysis compares different national and international mitigation strategies.

Chapter 4 is devoted to a global sensitivity analysis that tests the reliability of the model results against variations in the input data calibration and identifies the main levers and inhibitors to GHG emission reduction.

Chapter 5 summarises the results by evaluating the presented work and by providing an outlook for future research.

1.6 Definitions

In order to avoid potential problems through misunderstandings among terminologies, this section defines the key terms used throughout this dissertation.

Energy System

In analogy to the latest *Global Energy Assessment* (GEA 2012), this dissertation defines the term *energy system* as the process chain between acquiring and using energy. This comprises the extraction of primary energy resources, the utilisation of renewable energy sources as well as all transformation steps required to convert energy carriers into useful energy services.

Model Formulations

Figure 1.5 summarises the relevant modelling terminology. The terms are:

Mathematical Model: a generic set of equations that provides for the description of an energy system. The mathematical model formulation consists of decision variables, the objective function, constraints, and parameters. The equations constituting the mathematical model define the abstraction level, of the real-world problem. A mathematical model, could, in theory, be created by pen and paper as it is, for example, a set of equations describing a version of a linear optimisation problem, which is equipped with the formulations of the boundary conditions required to describe limitations common to energy and land related systems.

Model Framework: a mathematical model that has been realised in a software environment. For example the implementation of a specific mathematical model in GAMS, python, MATLAB, etc. The model framework *MESSAGEix*, a GAMS implementation of a linear optimisation model designed for the representation of the land-, energy-, air- and water-nexus, is applied in this dissertation.

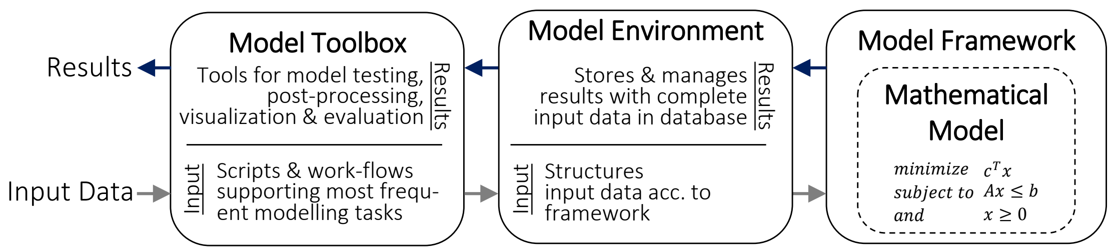

Figure 1.5: Definition of the modelling terminology occurring within the model toolbox, as used in this dissertation. The figure indicates the relationship of the terms Model Toolbox, Model Environment, Model Framework and the contained Mathematical Model as seen by the modeller.

Model Environment: an extension to a model framework designed to supply functionalities related to the modelling process. The model environment applied in this dissertation is *ixmp*. It provides a user interface for *MESSAGEix* and supports data management related to the modelling process.

Model Toolbox: an assembled palette of functionalities (e.g. scenario creation, visualisation, post-processing), which are built around a model environment. The MIGRA-NEST toolbox created in this dissertation consists of four modules: (i) the *Rapid Prototyper* that provides for creating parsimonious national stand-alone model calibrations based on existing global model calibrations, (ii) the *Model Nester* that integrates national stand-alone model calibrations into a global model calibration, (iii) the *Scenario Analyser* that is tailored for creating and evaluating sets of scenarios, and (iv) the *Sensitivity Analyser* that provides the tools for standardised global sensitivity analyses. While the toolbox provides the workflow and scripts required for the given task, it utilises the model environment for communicating the input data to the model framework and the mathematical model formulation, which provides the computation.

Model Application

Figure 1.6 summarises the scenario related terminology. The terms are:

Model Calibration: a data set tailored to describe an energy system, based on a specific model framework. The data itself depends on the energy system that is to be modelled, the data structure, however, has to be adjusted to the applied model framework. The name giving process of fitting the data to describe the modelled energy system, is called *calibrating* a model.

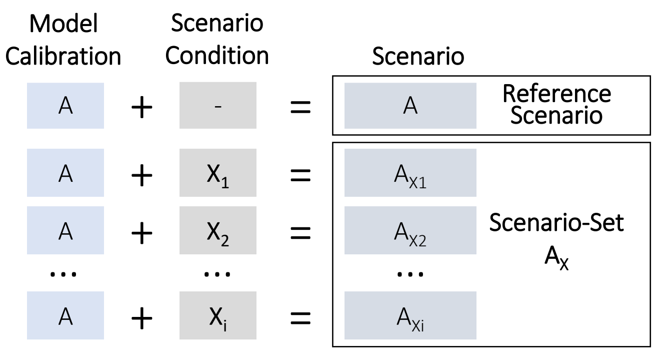

Figure 1.6: Definition of the scenario terminology occurring within the model toolbox, as used in this dissertation. The figure explains the relationship between the terms model calibration, scenario condition, scenario, reference scenario, and scenario set.

Scenario: an adaptation of a model calibration that is applied to an analysis.

Reference Scenario: a counterfactual for measuring the impact of a change in the calibration on the model results. In this dissertation two reference scenarios of the South African energy system are created. One describing the energy system as a national stand-alone model and another describing it as part of a model calibration of the global energy system.

Scenario Condition: a formalised variation of the existing calibration, such as the introduction of a carbon price, a modification in the demand development or the availability of a certain technology.

Scenario Set: in energy system analysis, insights are most commonly gained by the comparison of multiple scenarios, so-called *scenario sets*, which compare various possible future developments to a counterfactual.

Model Years

In the presented case study a model is calibrated for the projection of scenarios of the South African energy system. Figure 1.7 summarises the terminology that relates to the model years presented in the case study. It shows the ten-year time slicing that is applied in the case study calibration. The time slicing means that every tenth year is a modelled year. In a ten-year time slicing every modelled year represents the year itself and the nine years before it (e.g. values calculated for 2030 represents the average value for the time horizon 2021-2030). In the presented case study, the first model year is 2030, the last model year is 2070. The last two periods, 2060 and 2070, are add-on periods that are only calculated in order to suppress end-of-horizon effects. The base year that concludes the historic calibration is 2020.

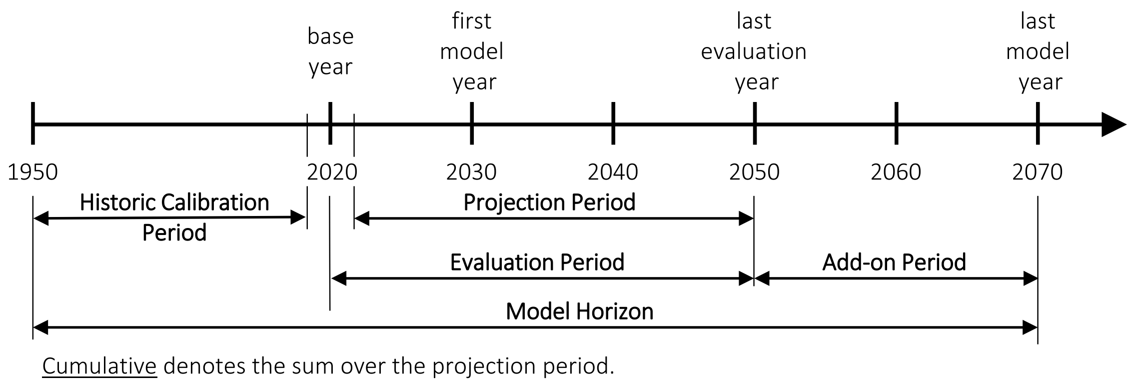

Figure 1.7: Definition of the time horizon related terminology as used in this dissertation. The figure explains the relationship between the model horizon (1950-2070), the calculated model years (2030, 2040, 2050, 2060, 2070), the base year (2020) and as well as the model sub-horizons: the projection (2021-2050), the evaluation (2020-2050), and the add-on period as well as the historic calibration period (1950-2019).

The terms used in the case study are:

Projection Period: denoted by the modelled years 2030-2050, covers the time period 2021-2050. Throughout the presentation of the case study the term *cumulative*, strictly refers to this time horizon.

Evaluation Period: extends the projection period by the base year (2020-2050).

Base Year Calibration: national energy statistics are created based on a wide variety of numeric input data. As such, they are time intensive to create and are thus always one to several years behind the current date. Hence the term *2020 Values* refers to a data set that is calculated by linear interpolation between the last available statistical data point (usually the year 2017 if not indicated otherwise) and the first model year (2030).

Numerical Model Outputs

Renewable Energies: Renewable energies are defined as to include biomass, direct solar energy, geothermal energy, hydropower, and wind energy. This definition presumes that all these renewable energy sources, especially biomass, are extracted at a rate equivalent to the natural rate of replenishment. Furthermore, in the presented results, *fuel consumption* of solar and wind power generation facilities is calculated according to the direct equivalent method, hence at a theoretical 100% production efficiency. This means that in order to produce 1 GWh of electricity, 1 GWh of *wind* and or *solar energy* is "consumed". Biomass, however, is balanced at the actual technology efficiency. For a more detailed description of the balancing method see Pachauri and Meyer (2014).

Global Warming Potential: The term global warming potential (GWP) is used as a metric to compare the emissions of different greenhouse gases with potentially different effects on radiative forcing. In this work, the GWP refers to the relative standard global warming potential of greenhouse gases over a 100-year horizon, as compared to the primary greenhouse gas CO_2. This is in line with the most recent IPCC report, and most current literature on GHG emissions and global warming ambitions (Myhre et al. 2013). However, in order to establish consistency between the applied global parent model calibration and the nested model calibration, the 100 year time horizon global warming potential of methane gas is defined to be 25, despite more recent studies suggesting higher values (Etminan et al. 2016).

Net Nodal Energy System Costs: Net nodal energy system costs are here defined as the discounted nodal costs as calculated by the global model calibration (source based), minus the revenue generated through commodity exports and the carbon tax (if applied), but plus the costs stemming from commodity imports.

Mitigation Costs: The term *Mitigation Costs* refers to *average* mitigation costs for GHG emission reduction, i.e. the ratio between the amount of GHG mitigated measured in CO_2-equivalent and the net energy system cost increase, both compared to the reference scenario. This is in contrast to the often-applied *marginal abatement cost*, which refers to the cost of the most expensive ton of emissions reduction.

Chapter 2

MIGRA-NEST

My interest is in the future
because I am going to spend the
rest of my life there.

Charles F. Kettering (1876-1958)
quoted after Andrews (1989)

The following chapter describes MIGRA-NEST (Mixed Granularity Nested Energy System Toolbox) and its architecture that consists of two core-, and two add-on modules (see figure 1.4). Additionally the theoretical background necessary for energy system modeling and the choice in the applied model framework are discussed. The chapter closes with a demonstration of the core modules' capabilities in a case study on the South African energy system.

The description of the modules in this chapter focuses on the two core modules - the *Rapid Prototyper* that allows the creation of national stand-alone model calibrations, and the *Model Nester* that provides the nesting process plus the testing and visualisation of the integrated mixed-granularity model calibrations - as these two generate the core scenario calibration for the South African test case. The two add-on modules - the *Scenario Analyser* that provides scripts and workflows for defining and evaluating scenarios, and the *Sensitivity Analyser* that allows the evaluation of the sensitivity of the model output upon the model input factors - which directly depend on the outputs of the core modules, are described in connection with the South Africa case study in chapters 3 and 4, respectively.

2.1 Toolbox Concept & Problem Definition

The aim of this dissertation is to provide model calibrations that allows to, (i) identify suitable national energy system development scenarios in the context of international commodity market developments; (ii) evaluate national GHG mitigation potentials induced by these developments; and (iii) break down international GHG emission targets to national contributions. Such models need to be of mixed spatial granularity, thus integrating a concise country-scale model into a global model calibration of limited national detail.

As to the best of my knowledge, no model toolbox exists today that provides for the creation of such mixed-granular models, I have designed and realised a transparent model toolbox - MIGRA-NEST. The toolbox enables the model creation and supports the exploration of the feedback effects between national and international policy decisions on energy system planning, and the resulting GHG emission trajectories in a transparent, standardised and easy-to-reproduce manner.

Model Concept

In order to meet the model requirements described above, MIGRA-NEST's design combines the strengths of both national and global model calibrations by integrating a national stand-alone model into a global model calibration and connecting them via trade links (figure 2.1). While in this dissertation the created toolbox is applied to the energy system of South Africa, this is not exclusive, as the dynamic toolbox can be applied to any country.

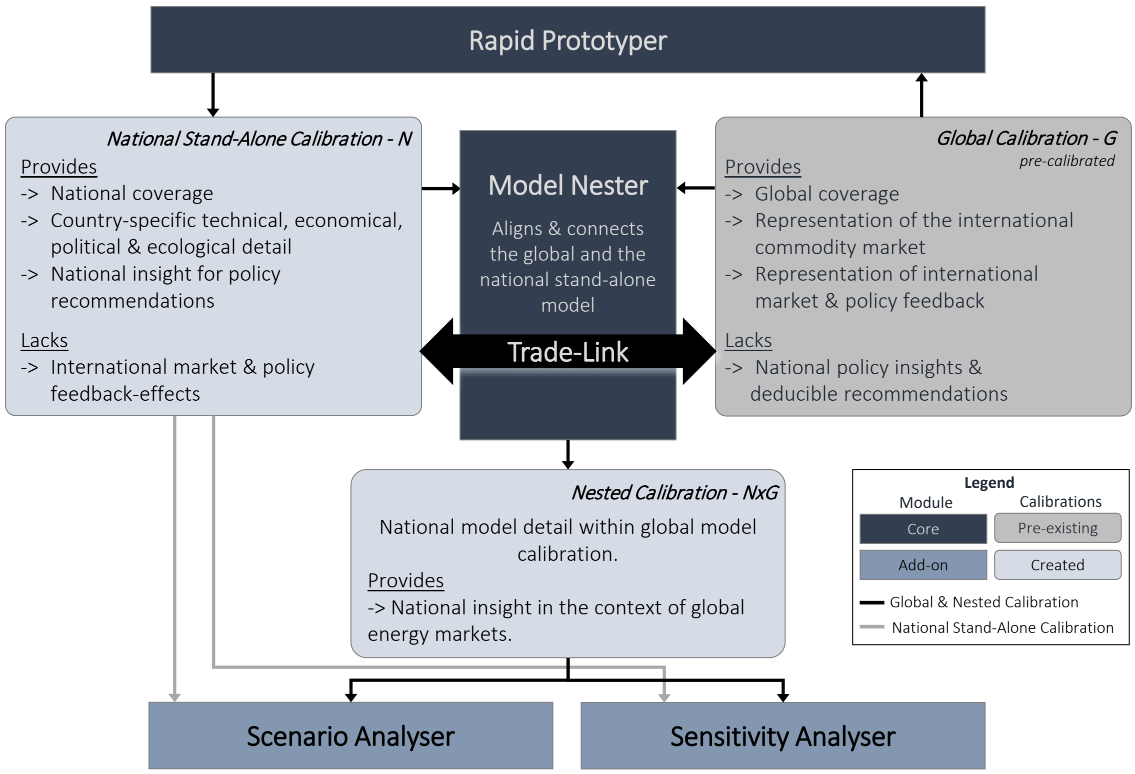

Figure 2.1: Schematic of the generalised MIGRA-NEST concept: connecting a national stand-alone model calibration and a global model calibration via trade links to create a model calibration of mixed spatial granularity. The Rapid Prototyper module uses data from an existing global model calibration (G) and creates a national stand-alone model calibration (N). The Model Nester uses both the existing global model calibration and the newly created national stand-alone model calibration to create a nested calibration of a national model (NxG) with a global model. These results feed into the add-on modules that provide the tools required for a standardised scenario and a sensitivity analysis.

In order to ensure that the resulting model calibrations are reproducible and transparent - two factors that are key to modern energy system modelling (DeCarolis et al. 2012; Dodds et al. 2015) - MIGRA-NEST standardises the model creation workflows and the data handling processes. The toolbox thus provides the complete code base required for:

1. Prototyping and calibration of national stand-alone models;
2. Embedding of national stand-alone models into global model calibrations;
3. Testing and visualisation of the national stand-alone as well as mixed-granularity global model calibrations; and
4. Data handling related to the modelling process.

2.2 Toolbox Architecture & Workflow

MIGRA-NEST is a toolbox for creating mixed-granularity nested energy system models and scenarios. The toolbox consists of four interconnected modules. The modules are each self-contained, each one with a specific purpose. Yet, the full functionality and usefulness of the overall system requires all four modules to be arranged and interconnected.

In this section the architecture and workflow of MIGRA-NEST are introduced. As mentioned before, this section focuses mainly on the two core modules (the *Rapid Prototyper*and the *Model Nester*) that both provide for the creation of model calibrations. The two add-on modules (the *Scenario* and the *Sensitivity Analyser*) that support the evaluation of the created models are documented in detail in chapters 3 and 4, respectively.

2.2.1 Rapid Prototyper - Creating National Stand-Alone Models

The first core module of MIGRA-NEST is the *Rapid Prototyper.* As suggested by the name, the idea behind this module is to provide the tools that enable the fast prototyping of simple national stand-alone energy system models. This idea is pursued by adopting and refining the reference energy system (RES) of existing model calibrations of similar or lower spatial granularity and adapting them to national specifications.

The module consists of three methods, which support (i) the rapid prototyping, thus adopting the selection of a RES from the pre-existing model calibration; (ii) the capacity calibration, thus substituting missing data points from the historic calibration by approximations; (iii) model testing and visualisation that together provide for feasibility and sanity-checks of the resulting model (see figure 2.2). As the testing and visualisation tools are common to the *Rapid Prototyper* and the *Model Nester* they are discussed separately subsequent to the introduction of the modules.

Rapid Prototyping: Adopting Scenarios from Existing Model Calibrations

The rapid prototyping method is the primary, and hence naming giving method within the rapid prototyping module. The basic idea is to adopt the reference energy system from an existing model calibration (*parent model*) and to later fill in the available country-specific data points. Using the same principle, the *Rapid Prototyper* can also be used to approximating missing data points in an otherwise country-specific RES based on a *parent model* calibration (see figure 2.3).

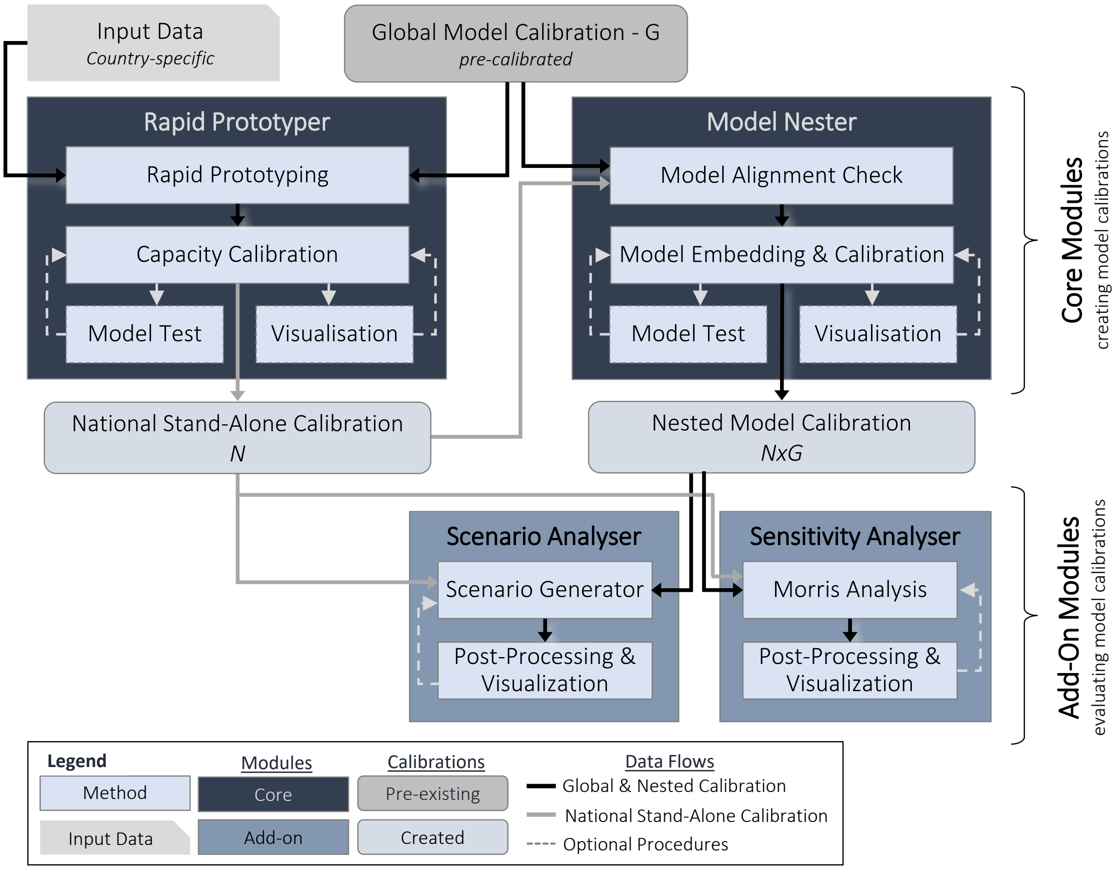

Figure 2.2: Functional schematic of the MIGRA-NEST set-up. The full lines show the data flows as used in MIGRA-NEST. The dashed lines indicate optional procedures used for calibration purposes.

The *Rapid Prototyper* enables the fast and systematic development of national stand-alone models with limited country-specific data available. In other words, when using the *Rapid Prototyper* the user has the option to adopt a subset of a pre-existing reference energy system, i.e. the user can choose to extract the commodity flows and technology specifications, from any pre-calibrated *MESSAGEix* model. A particular feature is that if more country-specific data are available (which is indeed the case in many developed countries) this principle can also be reversed in the sense that the model is based on national data and only missing data points are approximated based on a global model calibration.

In order to adopt a subset of the RES from a parent model, the user specifies the selected subset within a predefined spreadsheet. This spreadsheet communicates the relevant technology and commodity flow specifications to the *Rapid Prototyper*. Thus, the spreadsheet specifies the subset of technologies and also the so-called *parent region*, which is the model region (node) that the *Rapid Prototyper* copies the parameters from. In the current version, the *Rapid Prototyper* allows for up two prioritised *parent regions*. If a technology and or commodity does not exist in the model calibration of the specified primary parent region, the *Rapid Prototyper* replicates the data from the secondary parent

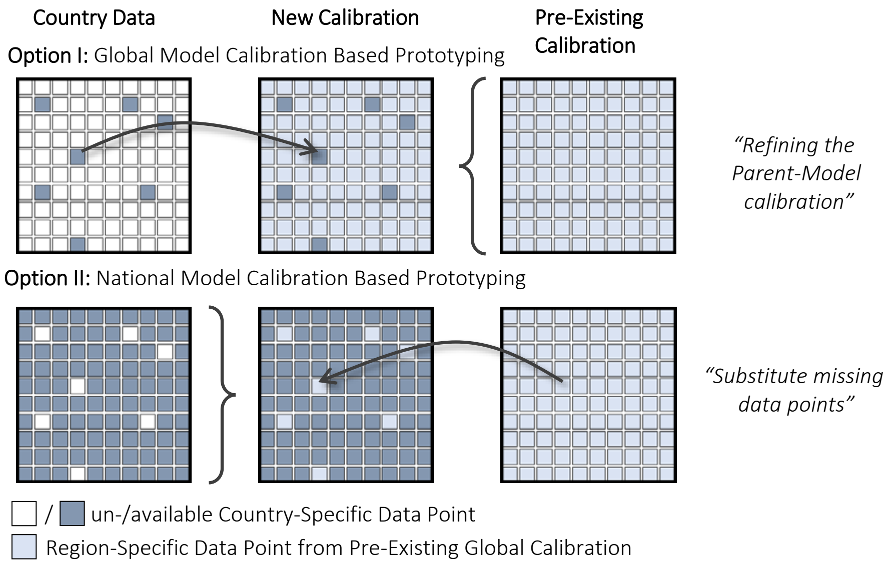

Figure 2.3: Schematic of the functionality of the Rapid Prototyper showing the two principle operation modes. Option I (top): Refining a pre-existing parent model calibration by adopting its Reference Energy System (RES) and filling in for country-specific data points. Option II (bottom): Substitute missing data points by creating a country-specific RES and approximating missing values based on the pre-existing parent model calibration.

region. While at the moment a maximum of two ranked *parent regions* is integrated in the workflow, the *Rapid Prototyper* is developed in a dynamic and easy-to-extend way, such that it can be modified to allow for more than two *parent regions*. While by default, all selected technologies are transferred from the *parent region* as-is, the *Rapid Prototyper* also allows for the modification of technologies before adding them into the new model. Furthermore, the standardised spreadsheet-based workflow enables the integration of new technologies into the prototyped model without programming skills.

This easy model creation tool does not only lower the threshold of creating energy system models for users new to the field, but also allows for synoptic and comprehensible input data handling by experienced users. Furthermore, this very structured approach to model creation supported by the *Rapid Prototyper* allows maximising the benefits of well-calibrated and documented models, provided by the modelling community, and thus raises model quality standards and assists collaboration efforts within the research field.

International Commodity Trade Although the national stand-alone model calibrations, which are created using MIGRA-NEST, are country-level applications, modelling trade with other countries and the international market is made possible by using a proxy trade node. In order to calibrate the virtual trade with the proxy trade-partners, certain assumptions about commodity prices and trade volumes must be made. For consistency and comparability among the national stand-alone model runs, the international commodity prices are adopted from the results of the global trade node of the *parent model*. However, these prices are marginal costs as they are derived from the dual solution of the optimisation problem. Hence, in order to represent the trade prices in the country model and to prevent circular trade (i.e. import of vast quantities for re-export) within the stand-alone model, commodity prices for the country are adjusted. In the predefined calibration the adjustment is set to + 20% on the price for the import, and - 20% on the export of commodities. Furthermore, to reflect the inertia of trade agreements and infrastructure, trade volumes are confined to an annual change rate of ± 7%.

Capacity Calibration - Substituting Missing Data

Apart from the RES definition, the technology parameterisation and the expected technology transition rates that the *Rapid Prototyper* adopts from the *parent regions*, the stand-alone models require calibration concerning the fossil and renewable resources and reserves, the historical capacity stock, the established energy use patters, and a demand forecast. While data on fossil and renewable resources and reserves is mostly readily available, the *Rapid Prototyper* supports the user in filling in missing data points in the historical capacity stock. The predominant energy use patterns, and the demand forecast, however, have to be provided by the user.

For most countries, the technological description of the existing technology stock is well documented and publicly available for the majority of central power stations and transformation facilities such as refineries and or coal gasification/liquefaction plants. However, data on the installed capacities of smaller end-use units, such as the industrial process sector and mobility services, is mostly undocumented. In order to compensate for this missing data, the *Capacity Calibration* calculates the historical capacity stock (CAP) of a technology (t) based on the minimum capacity requirement according to the energy consumption (E_{in}) as documented in the energy balance and the technology specific capacity-factor (cf_t).

$$CAP_t = \frac{E_{in,t}}{cf_t} \tag{2.1}$$

If the energy input is unavailable it can be substituted through the energy output (E_{out}) and the technology specific energetic efficiency η_t as follows:

$$E_{in,t} = \frac{E_{out,t}}{\eta_t} \tag{2.2}$$

In order to represent the age-dependent decommissioning of technologies where no details on commissioning dates are available, the minimum required capacity is assumed to have been installed at a uniform distribution across its lifetime. Thus, the capacity installed per historic year (y) is calculated to be the fraction of the minimum capacity requirement calculated in equation 2.1 and the technology specific technical lifetime (tf).

$$CAP\_NEW_{t,y} = \frac{CAP_t}{tf_t} \tag{2.3}$$

2.2.2 Model Nester - Creating Mixed-Granularity Calibrations

The second core module of MIGRA-NEST is the *Model Nester*. The idea behind the module is to produce mixed-granularity model calibrations of national energy systems within a global framework for the analysis of country-level policies that consider international feedback effects especially from the global commodity markets. This idea is pursued by nesting a national stand-alone model calibration into a global model calibration. The module workflow consists of two processing (ii, iv) and two testing (i, iii) steps: (i) testing the alignment of the models; (ii) embedding the national stand-alone in the global model calibration; (iii) testing the embedded model; (iv) finalising the nesting process by establishing trade links between the two sub-models and adjusting the global model parameterisation (see figure 2.4).

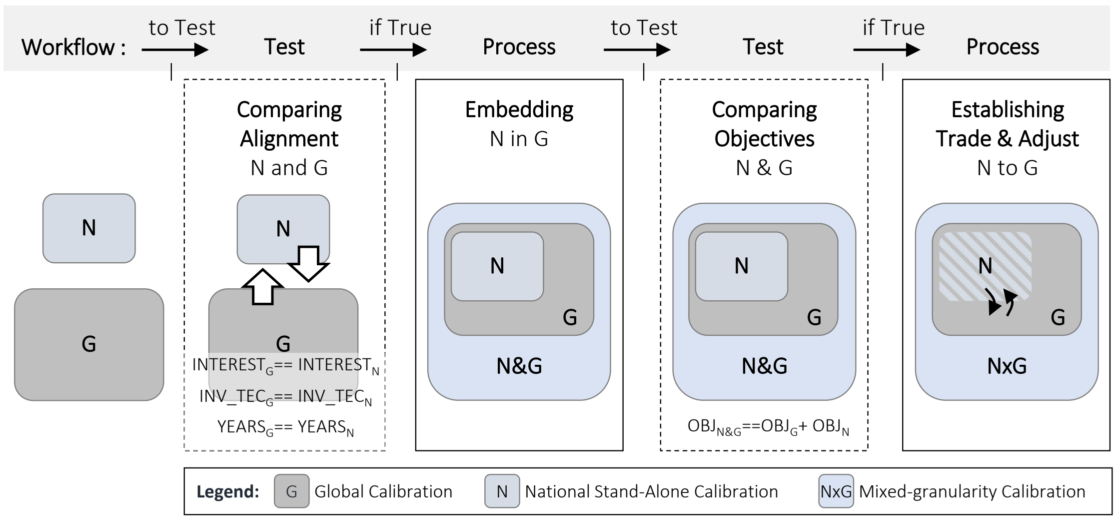

Figure 2.4: Schematic of the functionality of the Model Nester showing the implemented nesting workflow. (i) testing the alignment of the models, (ii) embedding the national stand-alone in the global model calibration, (iii) testing the embedded model, (iv) finalising the nesting process by establishing trade links between the two sub-models and adjusting the global model parameterisation .

Aligning and Embedding

Before embedding the national model calibration into the global model calibration, the main parameters of both model calibrations have to be tested for compatibility. This is relevant for three non-node specific global parameters: (i) the model horizon; (ii) the global interest rate; and (iii) the sub-set of technologies that are specified as investment technologies, (i.e. all technologies that have investment costs and a technical lifetime assigned to them). These three parameters have to match in both models in order to allow for a successful nesting of the national stand-alone model calibration within the global model calibration. If one of these three indicators does not match, the nesting process is interrupted. If the global and the national model calibration pass the test and prove to be compatible, the embedding process starts.

The embedding starts by adding first the sets and then the parameters of the national model calibration into the global calibration one-by-one. Once the parameters are transferred, the embedding process is completed, and the new model calibration can be solved.

Comparing Objectives

After embedding the national stand-alone model calibration into the global model calibration the success full completion of the embedding process is tested. For the newly created embedded model calibration to pass the test, its objective ($OBJ_{N\&G}$) has to be equal to the sum of the objectives of the global (OBJ_G) and the national stand-alone model (OBJ_N) as described in equation 2.4.

$$OBJ_{N\&G} == OBJ_G + OBJ_N \tag{2.4}$$

Equation 2.4 must hold true for the embedded model, as whiteout trade option, the two sub-models (N and G) cannot yet interact. Thus, the objective function must find the same solution for the two sub-systems, which leads to the objective of the embedded model equalling the sum of the two sub-objectives.

Establishing Commodity Trade & Adjusting Global Calibration

In order to connect the two model calibrations (N and G) of the embedded calibration ($N\&G$) and to allow interaction among them, commodity trade technologies are introduced. In the resulting mixed-granularity calibration NxG all trade is directed via a proxy node that represents the international commodity market (i.e. international trading node: GLB_G). In line with this calibration the national stand-alone calibration (N), directs all trade to the trade node (GLB_N) that represents all international trade partners (see section 2.2.1). To connect both calibrations the trade node of the stand-alone calibration (GLB_N) is merged into the trade node of the global calibration (GLB_G) by changing the origin and destination node of the related export as well as import technologies from GLB_N to GLB_G. These adjustments are done for all globally traded commodities. For commodities that are not traded globally - such as the grid-bound commodities natural gas and electricity - trade activity is restricted to the exchange between the national node and the primary *parent region*. This grid-bound trade is enabled by a trade technology between the national node and the *parent region*.

In the global calibration, each country is represented as part of a *parent region*. Therefore, after adding the national stand-alone calibration as a separate node, the parameters from *parent region* need to be adjusted with the respective contributions from the national calibrations. To do so, the national contributions are subtracted from the *parent region*. This subtraction affects the useful energy demands, the fossil and renewable energy resources and potentials, as well as the historical capacity stock and the historical energy use.

During this automated subtraction process special attention is given to the plausibility test before the subtraction process. Thus, in order to prevent calibration inconsistencies (e.g. the country node has larger coal reserves than the *parent region*) the process will raise warnings whenever the country node accounts for an unexpectedly high share of a resource or demand.

Limitations

By using the novel nesting methodology, any national stand-alone calibration can be embedded into the global calibration.

However, several limitations apply. To date MIGRA-NEST is tailored for handling model calibrations for the *MESSAGEix* framework using the *ixmp* interface (see 2.3.3 for the decision basis). While the idea as well as the workflows can be transferred to any other model framework and or environment, the code base of the toolbox would need to be adjusted. The following limitations thus apply exclusively to the application of the *MESSAGEix* framework. Namely those are, (i) as the set "year" cannot be specified per node in *MESSAGEix*, the model time horizon of the parent and the nested calibration have to be aligned; (ii) the same holds true for the applied interest rate, which is used by the model to calculate the global discount factor; (iii) as technologies are mapped on a global rather than on a nodal level as either with or without investment costs, this definition has to be consistent among the two calibrations (N and G). If these limitations are respected, the *Model Nester* allows for the systematic and synoptic creation of energy system models of mixed spatial granularity.

Integrated Model Testing

Both core modules (i.e. the *Rapid Prototyper* and the *Model Nester*) are used to perform a thorough testing of the model. This is important because the national stand-alone models and even more, the nested mixed-granularity models contain a RES of about one hundred technologies. Each technology describes an energy transformation process with many inputs and outputs of various commodities on several energy levels. Any one of these technologies is furthermore described by several dozen techno-economical parameters (costs, build rates, life-times, operation factors, utilisation rates, etc.) that are modulated over the several decades of the time-horizon described by the model. Thus, manually auditing the functionality of each of these technologies is very time-consuming and cannot be reproduced systematically. An automatic feasibility test for all technologies is therefore implemented as a testing method that can be run every time the input data are updated throughout the modelling process. The testing method is based on the testing script as developed by Zipperle (2020).

The implemented algorithm systematically tests all technologies by first reducing the variable cost of the tested technology to a marginal proxy-value of 0.1 USD/kWh and setting all other cost parameters of the tested technology to zero. Then the model is solved, and the test is finalised by evaluating the model results. In other words, after each model run, the test algorithm compares the activity value of the tested technology in the solution to the expected value (> 0). If the activity-level is equal to zero (meaning that the technology is not used despite its low costs) this technology is highlighted in the test report, in order to be further investigated by the user as this might indicate a calibration issue that prohibits technology's utilisation.

2.2.3 Scenario Analyser - Exploring Possible Energy System Futures

In Integrated Assessment Models (IAMs) and energy system modelling, scenario-analysis has become a common tool in understanding and describing potential future developments. Especially in long-term models, the importance of understanding the impact of calibration assumptions increases as in such models a significant portion of the calibration data describes points in the far future, which are subject to a high degree of uncertainty (e.g. *How will the demand develop over the next decades? Will commodity prices rise or fall in the next century?*). While sensitivity and uncertainty analyses in many cases provide a deeper understanding of the model's sensitivity to calibration assumptions (see chapter 4), long computation times and computing power demands often leave the scenario analysis as an alternative for (or a first step to) understanding the model's dynamics and to explore a multitude of future development options. In addition, such analyses are a common tool to evaluate different policy options; e.g. a scenario analysis can be applied in order to compare the cost, GHG emission and technology impacts of various climate-policies (e.g. *What is the impact of a carbon price? What does a GHG emission constraint?*).

Due to the inherently lean character of both the national stand-alone model as well as nested mixed-granularity global model calibrations, they are well suited for exploring a multitude of long-term scenarios and thus for investigating various feasible development pathways. Hence, MIGRA-NEST is equipped with a *Scenario Analyser* add-on module that provides all functionality required to set up, execute and evaluate a scenario analysis. To structure and document the scenario creation process, the *Scenario Analyser* strictly separates the input data of the reference scenario from the scenario assumptions. Every scenario is defined by a specific reference (as a starting point calibration) and a set of separately defined functions that are used to modify the reference scenario (e.g: (i) apply a carbon-tax of 50 USD/tCO_2eq and (ii) increase the demand by 10%). Using this one-to-one scenario definition ensures the reproducibility and transparency of the scenario creation process and analysis.

In order to support the comparative evaluation (which is key to the scenario analysis), the *Scenario Analyser* aggregates all common scenarios of interest to *scenario sets.* Those scenario sets are defined by a common reference scenario and the scenarios' unique modifying functions. In addition to the post-processing of the individual scenarios (applying the same post-processing as the *Rapid Prototyper*), the *Scenario Analyser* offers post-processing that is tailored to the comparative analysis of the scenarios in the scenario sets (see chapter 3).

2.2.4 Sensitivity Analyser - Quantifying the Relative Importance of Input Factors

As stated above, understanding the uncertainty and sensitivity connected to the parametric calibration of the resulting scenarios is key to correctly interpreting their results and to constructively engage with the complexities and uncertainties inherent to any energy system. Consequently, MIGRA-NEST is equipped with a workflow for an attached sensitivity analysis. The *Sensitivity Analyser* is tailored to ease and guide the modeller through the entire process connected to the global sensitivity analysis, hence the six steps defined as:

1. Selecting the model outputs to test in the sensitivity analysis: e.g. the GHG emissions, total energy system costs, share of renewable energy in the transformation sector;
2. Selecting the input factors to test in the sensitivity analysis, apply grouping and define their domain;
3. Sampling the input factors;
4. Executing the model on the sampled input factors in a parallelised model execution workflow;
5. Evaluate the model results;
6. Aggregate and visualise the results for interpretation.

The implemented global sensitivity analysis applies the Method of Morris for sampling and evaluation as implemented in the Sensitivity Analysis Library in Python (SALib) by Herman and Usher (2017). Aim of this add-module is to reduce barrier to conduct such an important, however, to date in the field of energy systems analysis, rarely used model scrutiny. A detailed description of the integrated sensitivity analysis can be found in chapter 4.

2.3 Energy System Modelling Fundamentals

Energy system models are common tools for the exploration of potentially viable energy system futures. The core output of these models are costs, technology mixes, and often also environmental descriptors such as water use and GHG emission levels, which together describe the scenario-specific consequences of different development pathways. By offering a structured and more objective approach to the exploration and evaluation of the energy-emission-policy-cost nexus, they have become the backbone of decision-making processes in energy system and climate politics (Connolly et al. 2010; Pfenninger et al. 2014). To date, several hundred energy system models have been developed using a variety of different model frameworks, each tailored to assess one of the numerous challenges related to energy systems analysis (Ringkjøb et al. 2018). In line with their general purpose, the designs differ in capability, spatio-temporal but also sectoral resolution as well as modelling approach and software requirements.

The following sections contain an overview of different modelling approaches as well as the various currently available frameworks, a discussion of technical requirements as related to the research question of this dissertation, and finally my conclusion with respect to the model approach chosen as the basis of MIGRA-NEST.

2.3.1 Modelling Approaches

The following introduction to energy system modelling is based on the detailed modelling guideline report prepared by Mai et al. (2013) for the International Energy Agency (IEA) and the extensive model comparison by Ringkjøb et al. (2018). The IEA report provides a broad overview of the different modelling approaches commonly used in energy system modelling and related fields today. The paper by Ringkjøb et al. introduces several dozen recent energy system models and their calibrations.

When comparing energy system models, two main model properties have to be differentiated between: on the one hand there is the mathematical approach of model formulation, and on the other hand, there is the model calibration. While the model approach is inherent to the core model framework and defined by the mathematical formulation of the models' equations, the specific calibration is, for most model frameworks, open to the user of the model to decide upon. Figure 2.5 shows a schematic for common approaches in energy system modelling and the approach chosen for the MIGRA-NEST model architecture.

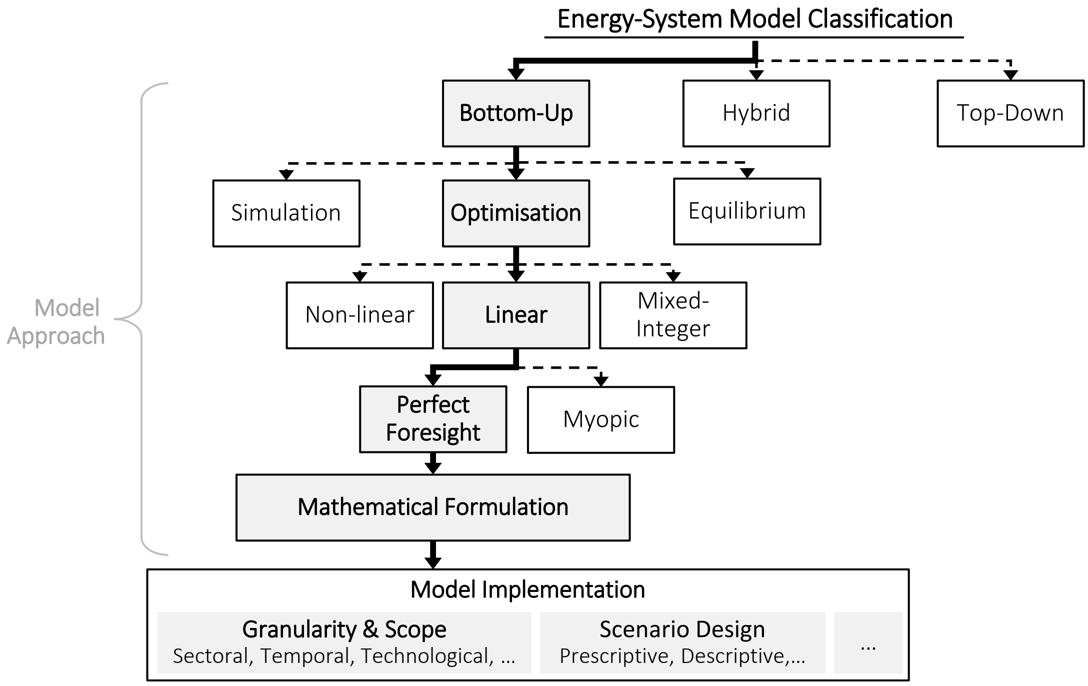

Figure 2.5: Schematic decision tree for common approaches in energy system modelling. The bold path outlines the model topology chosen in the presented work, the dashed lines indicates the other available options.

Bottom-Up vs. Top-Down

The general modelling approach of an energy system model calibration is predefined by its model framework, and thus by the mathematical formulation of the underlying equations. Today, a wide variety of such modelling approaches exists. However, as described in the introduction (see section 1.2), in the field of long-term energy scenario analysis two modelling approaches have to date established themselves as "go-to" solutions: bottom-up or *engineering type* models and top-down or *econometric type* models, as well as hybrid models that link those two approaches (see figure 2.5).

Bottom-up models are based on a detailed representation of technologies and thus capture technology-specific relations and physical constraints. Top-down models, in contrast, capture macroeconomic relationships, such as market behaviour and economic preferences while being hardly aware of physical constraints. Instead of physical correlations, econometric models use historic developments to forecast future behaviour. As such, they perpetuate behavioural patterns under estimates of deviation. This approach makes econometric models well suited for short- and medium-term forecasting where deviation from historical patterns is not yet among the factors with the strongest influence on the model outcome. However, this approach is unsuited for long-term time horizons because deviations from historical pattern increase in significance over time (Jebaraj and Iniyan 2006). Hence, for models with time horizons in the decades, bottom-up approaches are recommended (Jebaraj and Iniyan 2006). However, these models are blind to macro-economic feedbacks, such as demand elasticity. In order to combine the benefits of both approaches, an increasing number of hybrid models are being developed and employed (Ringkjøb et al. 2018). Yet, with increasing model complexity, the computation times as well as the parameterisation effort increases dramatically. The results of such complex models become more difficult to interpret, and model mistakes and calibration errors become more challenging to identify. Thus, choosing the model framework wisely, in accordance to the modelling purpose and research questions is imperative (Ellenbeck and Lilliestam 2019).

The research questions explored in this dissertation focuses on the technical feasibility of different sustainable development pathways and policy choices. Hence, the representation of the physical constraints is key. Accordingly, MIGRA-NEST is designed as a toolbox for creating bottom-up model calibrations.

Simulation vs. Optimisation vs. Equilibrium

Another major difference between modelling approaches concerns the mathematical methodology to solve the underlying problem: namely if the model is of the simulation, the equilibrium or the optimisation type. As suggested by the name, simulation models are prescriptive in the sense that they calculate a process according to a set of prescribed rules and equations. Hence, they perpetuate a certain system state under given boundary conditions to mimic system behaviour in a predefined state. Consequently, simulation models are computationally very lean but unable to map out previously unthought-of scenarios. In contrast, optimisation and equilibrium models find the final model state endogenously. They calculate the mathematical solution for the problem under the given boundary conditions. To do so, optimisation models, minimise or maximise a quantity (e.g. GHG emissions and cost or utility, respectively) under given techno-economic constraints (e.g. limited fossil resources). In contrast equilibrium models, balance the energy system as part of the flow of goods and services in an economy.

Aim of this work, is to explore novel and so far unknown, however, technically-feasible and desirably cost-optimal system developments. Therefore, MIGRA-NEST is designed for creating bottom-up, cost-minimising optimisation model calibrations.

Linear vs. Non-Linear vs. Mixed-Integer vs. Heuristic Models

As depicted in figure 2.5, optimisation models can be subdivided according to the structure of the mathematical formulation of their objective function and their boundary conditions. The forms most commonly applied are linear, mixed-integer, non-linear and heuristic model types.

While linear models are computationally the most efficient, their objective function as well as their boundary conditions have to be strictly linear. This means that they restrict the model to the description of all-linear relations. Consequently, all non-linear behaviour components must be mathematically linearised to be considered in the modelling process.

While to date most energy system models of the optimisation type have been linear models, the rapid increase of computation power has led to increasing utilisation of mixed-integer and non-linear models. Such non-linear model types allow for binary decision variables (e.g. *Was the power plant running in the time slice before or not?*) and the representation of other non-linear relationships.

While this added mathematical flexibility provides a more accurate mathematical description of complex techno-economic correlations, the higher modelling resolution is accompanied by several shortcomings. First and best known are the longer solve times and higher demands for computational power induced by the increased mathematical complexity. Moreover, the issue of correctly calibrating the input-data and correctly interpreting the results have often proven to be even more troublesome than the mere technical feasibility. Several researchers have pointed out that an increased model complexity significantly increases the model uncertainty (Pfenninger et al. 2014; Usher and Strachan 2012).

MIGRA-NEST calibrates global, long-term, bottom-up optimisation models, which are, by definition, data-heavy. Hence, calibration and computation are limited by the available calibration data and computation power, respectively. This limitation is amplified when considering the uncertainty inherent in any long-term forecast and the high numbers of scenarios required to generate stable results (see chapter 4). Therefore, MIGRA-NEST is designed to calibrate linear, bottom-up cost-minimising optimisation models.

Perfect Foresight vs. Myopic Models

Based on the foresight time, which an optimisation model considers for the calculation of the objective function, it can be categorised as either of the *myopic* or so-called *perfect foresight* model type.

While *perfect foresight* models make all decisions for the entire model time horizon simultaneously, myopic models take decisions in stages, with limited information about future conditions. Because myopic models only consider a sub-horizon time interval, they take investment decisions without knowledge of their performance beyond these time frames. Thus, while the myopic approach might be more reflective of real decision-making processes, these decisions can, in retrospect, be shortsighted and sub-optimal. This effect is averted by *perfect foresight* models, which, by using the inter-temporal approach, will take the *perfect* decision on investment options and will thus provide the more optimistic scenario.

The aim of the presented research is not to simulate real development but rather to explore cost-optimal and technically feasible scenarios. Therefore, all optimisation results presented in this work are calculated under *perfect foresight* conditions.

Other Mathematical Model Characteristics

Apart from the differentiation in mathematical model formulations mentioned above, the major difference between model formulations can be found in their algebraic description of technology types and the set-up of their objective function.

Considering the technology description specifics, many published model frameworks used to be of great similarity. They offered equations, tailored to describe the techno-economic characteristics of energy supply technologies and their behaviour over time, as well as additional sets of equations to describe the extraction of fossil energy resources. However, the special characteristics of renewable energy sources (especially non-dispatchable electricity generation from wind and solar energy) were mostly described through unique, user-defined and thus data-intensive relations. Until recently, these descriptions proved to be sufficient, as on a global level, (non-dispatchable) renewable energy sources contributed only little to the total energy supply, but today the situation has changed. With increasing significance of renewable energy sources, many model frameworks added explicit mathematical formulations to the code base. In this dissertation, a special focus was put on the explicit representation of (i) volatile renewable energy sources, (ii) the characterisation of storage technologies, (iii) the display of demand side flexibility.

For the energy transition pathways that are to be explored using MIGRA-NEST, renewable energy sources are of great relevance. Hence, the model framework is required to portray the unique characteristics of (volatile) renewable energy supply in necessary detail while allowing for a low-resolution (ten-year time-slicing) long-term (several decades) time horizon (see section 2.4.1).

Another significant model characteristic determining the suitability of the selection of given model frameworks for MIGRA-NEST is their handling of GHG emissions. The main difference here exists between energy system models that balance GHG emissions endogenously by the model formulation versus models that balance GHG emissions ex-post as part of the post-processing of the model results. While the ex-post GHG emission calculation reduces the mathematical and numerical model size, only models that explicitly calculate emissions endogenously can be used for GHG emission-mitigation-driven, exploratory scenario analyses. Hence, for the scenario analysis envisioned to be executed with MIGRA-NEST (e.g. limit cumulative GHG emissions to a certain level or put a price on GHG emissions), endogenous GHG emission balancing is a requirement.

As stated above, another major difference between modelling approaches is defined by the algebraic formulation of the objective function. Here, a function to find the minimal-discounted-cost for the investment, fixed and variable costs for the dispatch and capacity planning of the entire energy system by an inter temporal approach is applied.

2.3.2 Model Calibration

Under a general definition *model calibration* describes the adjustment of the model parameters to obtain a model representation of the processes of interest that satisfies pre-agreed criteria. In this dissertation the model frameworks are considered constants and thus, the verb *calibrate* only refers to the adjustment of model input data (e.g. adjusting the demand forecast, the costs, etc.). As a noun, the term *model calibration* is used for a carefully arranged data set that is tuned to describe a specific energy system using a selected model framework (e.g. a data set to model the South African energy system as a national stand-alone model using the *MESSAGEix* framework.).

Most model frameworks and their underlying mathematical model formulations allow for a variety of calibrations. For example, a linear optimisation model could be either calibrated as country model used for long-term planning of the power sector of a country, focusing on transmission and distribution, or as a model of the global energy system with focus on international energy trade and GHG emissions balancing. The coverage in scope and granularity, may it be spatial, temporal, sectoral or technological, as well as the scenario design, is, in most cases, independent of the applied model framework. However, despite being dependent on numerical calibration data and modelling choices - rather than mathematical formulation - the model calibration is of great significance in tailoring a model to a specific research question. The most relevant calibration descriptors are discussed in the following.

Model Scope and Granularity

The *scope* as well as the *granularity* are two significant properties used to describe the coverage, the scale, and the level of detail featured by a model, respectively. While the terms scope and granularity can be used to characterise either a mathematical model or a specific model calibration, here it is considered a property inherent to a specific model calibration.

Spatio-Temporal Scope & Granularity The temporal resolution is described by the time-slice length (a second, a day, a moth, a year, a decade, etc.) and the model horizon (short-term: seconds, hours, days, months; long-term: years, decades). The spatial resolution is defined by the geographical coverage (municipals, regions, nations, continents, global, etc.) and the number of so-called *nodes*. The term *node* describes the fragmentation of the spatial scope (e.g. one node per continent in a global model calibration). Both parameters vary widely among models: while the time-step length varies from milliseconds (mainly used in power systems analyses tools) to multiple decades (e.g. for long-term planning), the model horizon can accordingly lie either in the range of seconds or centuries. The same applies for the spatial resolution, where node numbers range from single node models to several dozen nodes covering a wide range from a household up to the entire world.

MIGRA-NEST is designed to create models that analyse national energy systems under the influence of global energy market development scenarios. Therefore, the toolbox is tailored to generate long-term models of global scope.

In order to remain computationally lean the spatio-temporal granularity is by design as high as necessary but as low as possible. With respect to spatial granularity, the mixed-granularity model calibrations cover the entire world at a mixed-granularity of national to regional (supra-national) resolution. With respect to temporal resolution the models describe a time frame of several decades as this is the minimum required for omitting stranded assets in the investment-heavy long-living energy sector. In order to limit the computational demand to reasonable requirements, despite these long-time frames, a ten-year time-slicing is applied.

Sectoral Scope & Granularity The sectoral coverage describes the parts of the energy-economy-environment nexus that are considered by a model: e.g. electricity only, all energy carriers, energy and water, energy and water and food, energy and GHG emissions. The commonly applied coverage varies from a limited scope such as electricity or mobility service supply only to the wide range of sectors, which is often the case in integrated assessment models.

MIGRA-NEST is designed to create models that portray the entire relevant energy system sectors across the full supply chain from source to sink, from fossil or renewable energy resource to the useful energy demand (mobility, electric, and thermal demand in industry, commerce and the residential sector). However, in order to keep the models parsimonious, the models created by MIGRA-NEST do not include any water or land-use related parameters.

Techno-Economic Resolution Another major difference between model calibrations is the technological and economic resolution. This dimension refers to the detail and means the energy supply, the transformation, distribution and consumption technologies that are portrayed. As stated above, mixed-granularity model calibrations portray the entire energy system. However, with the focus on energy system development pathways under various GHG emission mitigation strategies, the models put the main emphasis on the secondary transformation with a major focus of the power sector.

Prescriptive vs. Descriptive Scenarios

The main difference in how scenarios are designed is if they are either prescriptive or descriptive. While prescriptive scenario designs, as mostly used in simulation models, are designed to identify how to reach a predefined state at a predefined point in time, descriptive scenarios analyse, which development to expect, under given conditions.

In order to identify potentially novel transition pathways under international policy, the scenarios for evaluation established with MIGRA-NEST are calibrated and designed as descriptive. These scenarios predefine certain conditions (e.g. introduction of a carbon tax, reduction of demand) but not the resulting system state. Thus, the system reaction to those scenario conditions are left to be determined endogenously by the model.

2.3.3 Selection of the Mathematical Model

MIGRA-NEST is based on a pre-existing mathematical energy system model framework, namely *MESSAGEix*. This design follows the current trends towards an open and transparent modelling practice. By relying on an openly available, well established and tested mathematical framework, this approach eliminates a major source of error in the modelling process and simultaneously increases the comparability of the results with published and reviewed scenario-outcomes. MIGRA-NEST bases the modelling process on a linear, bottom-up, optimisation model that allows following features:

1. Simultaneous dispatch and capacity expansion planning across all energy sectors;
2. Endogenous GHG emission balancing;
3. An aggregated but accurate representation of non-dispatchable renewable energy supply;
4. Dynamic adaptation of the temporal and regional granularity.

A key requirement for any mathematical framework is that is well maintained, thoroughly documented as well as publicly available under an open source licence. The final and most practical requirement for MIGRA-NEST is the availability of a well-documented and maintained global model calibration, as this global calibration builds the backbone of the rapid-prototyped country models and the framework of the mixed-granularity nested models. Figure 2.6 summarises the requirements for the mathematical model framework that builds the basis of the toolbox.

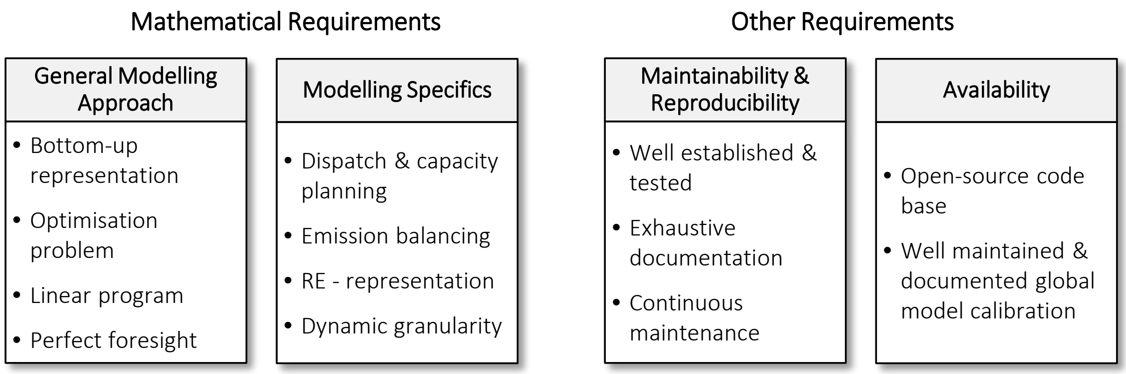

Figure 2.6: Requirements for the mathematical model framework that builds the basis of MIGRA-NEST. (RE: Renewable Energy)

Dozens of energy system model frameworks are published and used by many scientific and industrial institutions today.[5] However, among these many are not available under an open source licence. Among the open source models, *MESSAGEix* proved most suitable as it fulfils all above stated criteria and was thus chosen as the mathematical model base for MIGRA-NEST.

2.4 Mathematical Model Framework

The mixed-granularity model calibration combines the benefits of national and global energy system model calibrations by physically integrating a spatially limited national model calibration into a complex global calibration. By nesting the national stand-alone model into a global model calibration, the resulting model complexity is inevitably increased. Thus, for the model to remain computable, comprehensible, transparent, reproducible and intelligible, the mixed-granularity models are calibrated to be of reduced mathematical

[5]Thorough reviews of existing energy system model calibrations as well as model frameworks have been done by Ringkjøb et al. (2018), Gargiulo and Gallachóir (2013), Bhattacharyya and Timilsina (2010a), Connolly et al. (2010), and Dioha (2017).

outlay (thus also of reduced spatio-temporal resolution and computational complexity). The main aim of the model design, therefore, is to find an acceptable compromise between the level of detail, degree of flexibility and conciseness.

The following sections contain a description of *MESSAGEix*, which provides the mathematical framework for MIGRA-NEST plus the communication between the *MESSAGEix* and the MIGRA-NEST modules.

2.4.1 *MESSAGEix* and the *ixmp* Modelling Platform

In line with the requirements, *MESSAGEix* is a computationally lean, linear optimisation model that allows for both the optimisation of the dispatch as well as the investment decisions of the entire energy sector. Due to its parsimonious design, *MESSAGEix* is well suited for modelling long-term time horizons covering a wide spatial area. Those characteristics are essential for the investigation of development paths in the investment-intensive and slow-to-transition energy sector. Furthermore, the temporal and regional resolution in *MESSAGEix* is configurable, which is necessary for the model approach in the mixed-granularity model calibration design (in which higher-resolution nation-state model calibrations are embedded into a lower-resolution, global model calibration of supra-national regional granularity). In addition, this framework balances GHG emissions within the model, and thus it allows GHG emission limits and levies to be mapped in regional and global scenarios.

In addition to its mathematical suitability, the *MESSAGEix* developers also provide a globally calibrated and well-documented input data set (SSP2).[6] This frequently used, thoroughly documented and peer-review published data set forms the reference scenario for global development. Other important features that underpin the selection are (i) that I was very familiar with the framework as during my research I had the opportunity to contribute to the implementation of the renewable energy formulation (Huppmann et al. 2019); (ii) the bottom-up structure of the model framework that allows for detailed mapping of physical and technical feasibility limits, as well as (iii) the Python interface that allows to integrate *MESSAGEix* into MIGRA-NEST and workflow. *MESSAGEix* is published on GitHub under the Apache license version 2.0.[7]

Framework History

The *MESSAGEix* model framework was originally developed under the name MESSAGE at the IIASA in the 1970s (Häfele 1976; Agnew et al. 1979). Since then, the framework has been constantly improved (Messner 1984; Messner and Strubegger 1995; Riahi et al. 2012). Thus far, dozens of studies all over the world have used and extended the core model formulation. Some of the most recent studies include: Zhang et al. (2020) who apply *MESSAGEix* to quantify the relationship between industrialisation, the energy system, and GHG emissions within the context of the Paris Accord; Harmsen et al. (2019) who compare

[6]SSP2 is one of the five Shared Socioeconomic Pathway (SSP) that were developed by an international team of climate scientists, economists and energy system modellers, which examine how global society, demographics and economics might change over the next century (IIASA 2018). Among the five SSP scenarios SSP2 is the "middle-of-the-road" scenario.

[7]`https://github.com/iiasa/message_ix`

MESSAGEix with its *GLOBIOM* land-use extension to seven other IAM on their assessment of short-lived climate gases; and McCollum et al. (2018b) who evaluate global investment needs for limiting global warming to well below 2°C by linking *MESSAGEix*, among others, to the air pollution model *GAINS*, the energy access model *Access*, and the land- and water-use representation *GLOBIOM*. The *MESSAGEix* framework has to date received much attention in the modelling community as many models for international energy supply and GHG mitigation assessments are based on it. The most prominent examples are the renowned *Global Energy Assessment* (GEA 2012), which presents an integrated analysis of and a comprehensive outlook on the future energy challenges faced by the countries around the world, and the comprehensive IPCC (2018) report on climate change. Furthermore, the *MESSAGEix* based research conducted at IIASA's Energy Program has in recent years received increasing attention, as it has made most of its data sources publicly available (Huppmann et al. 2018). The input parameters as well as the majority of calculation results for the SSPs model calibrations can be accessed via the online database (IIASA 2018).

MESSAGEix-ixmp **Set-Up**

In 2019 the former MESSAGE model framework was re-released as the *MESSAGEix* framework. The big progress of the new *MESSAGEix* framework is that has been embedded into the *MESSAGEix - ix modeling platform (ixmp)* environment (Huppmann et al. 2019). The *MESSAGEix-ixmp* environment consists of an improved mathematical formulation of the *MESSAGE* model (coded in General Algebraic Modeling System (GAMS)) and integration of an interface to the novel modelling platform called *ixmp*. Figure 2.7 shows the model interaction between the *ixmp* modeling platform, the *MESSAGEix* model framework comprising of the mathematical model formulation and the database environment provided by the *ixmp* environment.

Among other features, the modelling environment provides a dedicated database infrastructure for version-controlled management of input data and model results and an application programming interface (API) with programming languages *Python* or *R* (see figure 2.7). This new modelling infrastructure improves the transparency, reproducibility and comprehensibility of the model and its results by separating the model framework - thus the mathematical model formulation - from the input data calibration. In the course of the new release, modern scientific workflows and transparent processes for processing and storing data were integrated into the framework. The new structure is designed to support efficient scientific workflows, transparent input data and result documentation. Huppmann et al. (2019) provide a detailed description of the new *MESSAGEix* framework as well as the *ixmp* model platform.

MESSAGEix **Model Fundamentals**

MESSAGEix is a technology-based, bottom-up, linear optimisation model for the systematic and comprehensive analysis of energy systems in one or multiple regions. If required, *MESSAGEix* can be calibrated as an Integrated Assessment Model (IAM), modelling not only the energy system but also the land- and water-nexus. In this dissertation, *MESSAGEix* is an applied in the shape of an energy-only model. The model is designed to

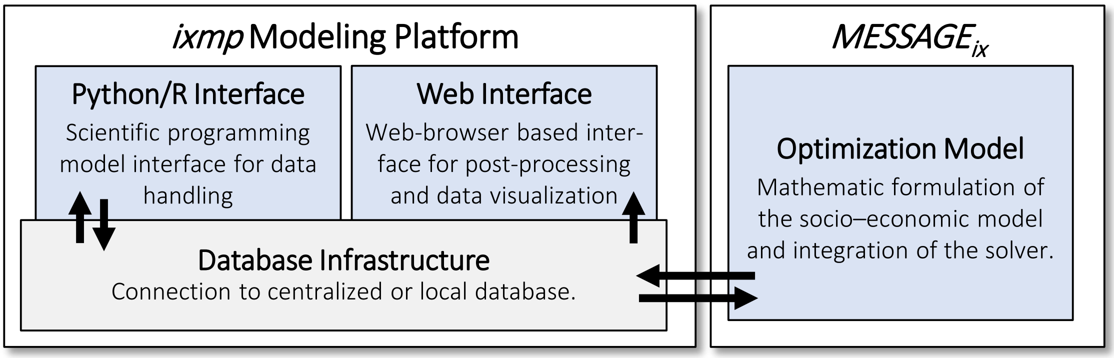

Figure 2.7: The model environment comprising of the mathematical model framework MESSAGEix and the scientific user interface ixmp (adapted from Huppmann et al. (2019)).

guide inter-temporal investment and the configuration of the supply chain over long-time horizons. The objective function minimises the net present value of the annualised total system costs under predefined technical, economic, and ecological constraints. In its current layout, *MESSAGEix* can be run as a perfect foresight model as well as in myopic mode. The spatial and the temporal resolution of the framework are customisable; thus, both can be adapted to the specific use case as defined by the modeller. While the temporal resolution is in theory customisable, to the best of my knowledge, no applications of *MESSAGEix* is a short-term model, which optimises dispatch decisions and or grid use, have been undertaken so far.

Linear Programming *MESSAGEix* is a linear optimisation model, which can also be called a linear programming (LP). This means that the objective function of the model (i.e. the minimisation of the total discounted costs) as well as all constraints (e.g. the uninterrupted supply of demand, GHG emission constraints, technological growth and or capacity constraints) need to be described as system of linear equalities and inequalities. While the exact form of the boundary conditions may differ among models, any linear optimisation model can be transformed into the following standard form (Luenberger and Ye 2016):

$$\begin{aligned} \min_{x} \quad & c^T x \\ \text{subject to} \quad & Ax \leq b \\ \text{and} \quad & l \leq x \leq u \end{aligned} \tag{2.5}$$

Here b, c and A are the fixed real constants, and x are the unknowns. x and c are n-dimensional and b is an m-dimensional column vector. A is an $m \times n$ matrix.

While this linear formulation prohibits the numeric representation of non-linear system-behaviour (e.g. ramping efficiency losses of power plants), several good reasons exist for using linear rather than non-linear or mixed integer programming for long-term energy system modelling. Even though the relative computational simplicity might appear to be the most obvious advantage for the use of linear rather than non-linear or mixed integer programs, experts agree that the main advantages of linear programs are primarily found within the formulation and analysis rather than within the solution phase of the modelling process (Luenberger and Ye 2016). This is connected to the linear or near-linear nature of many constraints commonly applied in operations research and the difficulty inherent to the descriptions as well as parameterisation of non-linear behaviour (Luenberger and Ye 2016). Linear models have recently been re-gaining increased interest as more and more researchers find that they do not require additional (mathematical) complexity, but rather a reduced form or simplified approach in order to improve their model results by making the results more understandable, transparent and robust (Ellenbeck and Lilliestam 2019; Pfenninger et al. 2017).

The Reference Energy System As a tool for medium- to long-term energy planning and policy analysis, *MESSAGEix* provides a framework to represent energy systems, including inter-dependencies and system dynamics. Thus, *MESSAGEix* can portray the energy flow from resource, to primary, to secondary, to final energy carrier all the way to the end-use energy service (e.g. lighting, space conditioning, industrial process heating, or mobility). Despite offering user-defined energy system description depth and detail, all *MESSAGEix* models, as most bottom-up energy system models, can be formalised through a specified set of energy carriers, conversion processes, sources and sinks (Pfenninger et al. 2014). The conceptual setup of such models can be laid out in a network representation called a reference energy system (RES). Figure 2.8, shows the generalised RES schematic of a *MESSAGEix* model.

The main user inputs are the definition and calibration of the energy carriers, conversion processes, sources and sinks, as well as the techno-economic boundary conditions. The main model outputs are the required capacity investment and dispatch strategy of the cost-optimal energy system configuration, as well as the primary, secondary and final energy use required to cover the demand. Furthermore, the model calculates the related GHG emissions. *MESSAGEix* is therefore well designed to compare the effectiveness of different GHG mitigation scenarios and to develop policy-driven decision guidelines for the energy sector.

(Non-dispatchable) Renewable Energy Representation

Since 2019 the *MESSAGEix* framework includes new mathematical formulation for the representation of renewable energy sources. During this dissertation I had the opportunity to work together with the developers of *MESSAGEix* in implementing and improving this part of the model formulation. While this new representation concerns all renewable energy sources, this was particularly important for the representation of power generation from non-dispatchable so-called volatile renewable energy (VRE) sources, such as solar photovoltaics (PV) and wind power, and their integration into the power supply system. While a full mathematical description of the formulation can be found in Huppmann et al. (2019), the section below is intended as a brief introduction that provides a general understanding of the functional principle and the implications for the modelling process mainly relevant to users new to MIGRA-NEST and or *MESSAGEix*.

For all energy system models of low temporal resolution, it is quite challenging to adequately consider short-term sensitive technical equipment (such as the power grid that

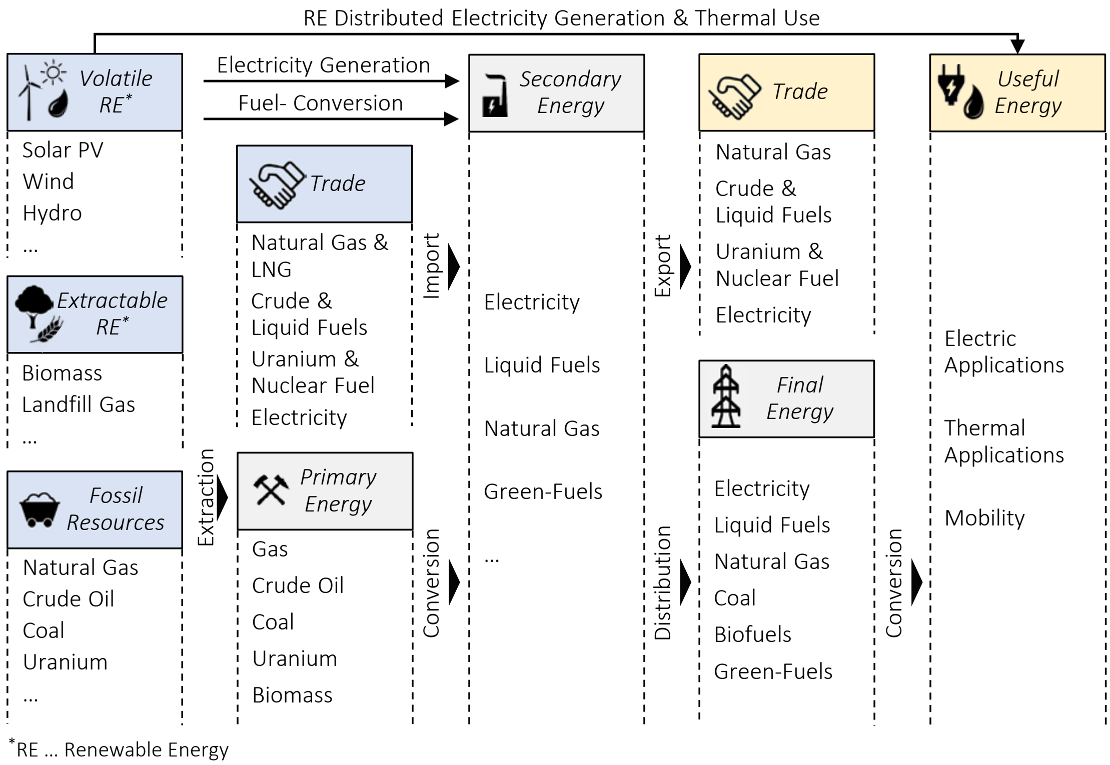

Figure 2.8: Reference energy system schematic of a MESSAGEix model. Sources are indicated in blue, intermediate energy levels technologies in grey and sinks are indicated in yellow.

at any moment needs to be in perfect balance in order to prevent black-outs). However, several robust approaches have thus far been developed that all ensure constant balancing between electricity feed-in and consumption, even at low temporal model resolution. The majority of these approaches apply the basic presumption that if the electricity generation capacity that is available to the grid at all points in time throughout the year, the *firm capacity* (CAP_{firm}) lies above the peak load experienced by the grid (P_{peak}), then the grid can be operated safely and without black-outs:

$$CAP_{firm} \geq P_{peak} \tag{2.6}$$

Wherein the firm capacity available to a grid can be calculated as the sum of the gross capacities (CAP_{gross}) of all dispatchable power plants (PPL_d):

$$CAP_{gross,d} = capacity\_factor_d * operation\_factor_d * CAP_{rated,d} \tag{2.7}$$

$$CAP_{firm} = \sum_{d=1}^{PPL_d} CAP_{gross,d} \tag{2.8}$$

However, the presumption that only an insignificant number of outages occurs coincidently throughout the year, exclusively holds true if (i) there is a sufficiently high number of dispatchable power plants available to the grid, and (ii) most outages of the plants are planned outages that can be scheduled in accordance with the grid operator (described by the *operation_factor*). While these presumptions, by definition, hold true for most dispatchable power supplies, they fail at describing non-dispatchable renewable power generators as the occurrence of unpredictable outages is inherent to all VRE sources.

In the past, most power systems were dominated by dispatchable power generation and most still are. Hence, the failing of the capacity hypothesis for non-dispatchable power generators was insignificant as their capacity share was marginal, and power system stability was still guaranteed by dispatchable power plants. However, with the recent surge in non-dispatchable power generation facilities (especially solar PV and wind turbines) the capacity hypothesis was further questioned as reality proved that non-dispatchable power generators can also, to a certain degree, contribute to the firm grid capacity. In earlier versions of *MESSAGEix* as in many other energy system models, this problem was handled through the implementation of a set of user-defined equations. Those equations ensured (i) that sufficient firm capacity is available to the grid at any point in time, (ii) that non-dispatchable power generators can contribute to the firm capacity, (iii) that the installed renewable power generation capacity does not exceed renewable energy potential, and (iv) that the flexibility of the grid remains uncomprimised at all times. While this description allows the accurate representation of renewable power generation and its integration into the grid, it simultaneously increases model complexity as it adds several dozen additional equations per model node and year to the model calibration.

In order to omit the added complexity while continuing to accurately represent the properties unique to renewable energies, a new mathematical formulation to represent VREs in a reduced form was included in the 2019 re-release of *MESSAGEix* (Huppmann et al. 2019). The new formulation is based on a novel approach that was first proposed by Sullivan et al. (2013) and later advanced by Johnson et al. (2017). It is designed to accurately depict the grid impact of VRE power generation potentials, despite the low spatio-temporal resolution and computational slenderness inherent to long-term scenario analyses.

The new formulation adds a set of explicit parameters that provide a transparent description of the VRE power generation. By separating the properties of the power generation technology (e.g. the costs and maintenance times of a wind mill) and the characterisations of the VRE resource potential, the new formulation integrates well into the existing description of the dispatchable power generation facilities. In order to correctly describe the *quality* of the VRE potentials, the new formulation allows to subdivide the resource potentials by location, quantity, and grade. For example, the onshore wind energy resource potential assigned to a certain model node can be split by its distance to the grid or the closest consumer as well as into quality grades by annual full load hours. In the new formulation each technology that feeds into the grid can contribute (with a flexibility factor: 0 to 1) or demand (with a flexibility factor: -1 to 0) a certain degree of flexibility. This ensures that at any point in time enough capacity can be ramped up or down to supply the flexibility required. Thus, while highly flexible dispatchable power plants, (e.g. open-cycle gas turbines), can provide high degrees of flexibility, volatile power generation capacities and inflexible demands increase the flexibility demand on the overall grid. Thus, both volatile wind and solar PV power generation have slightly negative flexibility values because they require additional system flexibility to smooth out fluctuations (Sullivan et al. 2013).

In addition to this explicit technology and resource description, the new formulation acknowledges the fact that VRE power generation facilities, despite being by definition less reliable than dispatchable power stations, can, to some extent, contribute to the required reliable power generation capacity stock. In contrast to many energy system models, in which the firm capacity is modelled to be supplied by conventional dispatchable power generation facilities only, the new *MESSAGEix* model allows that all installed capacity of dispatchable power generation facilities counts towards the firm capacity. Hereby the degree, to which intermittent and VRE power generation facilities can contribute to the firm capacity is determined by the penetration percentage of the technology. By assuming that *high-quality* locations for VRE power generation, i.e. the locations of highest and most reliable full load hours are connected first, and that the concomitance increases with increasing penetration shares, the contribution of a certain technology towards the firm capacity stock decreases with increasing penetration. The calibration of which share of capacity contributes to which degree can be defined by the user.

In this dissertation, I use the calibration suggested by Sullivan et al. (2013) that proposes to split the power generation share into four bins of 5%, 15%, 20% and 60%, within which the VRE capacity contributes to 90%, 60%, 30%, and 0%, respectively. Figure 2.9 illustrates the model representation of the VRE power capacity contribution to the firm capacity.

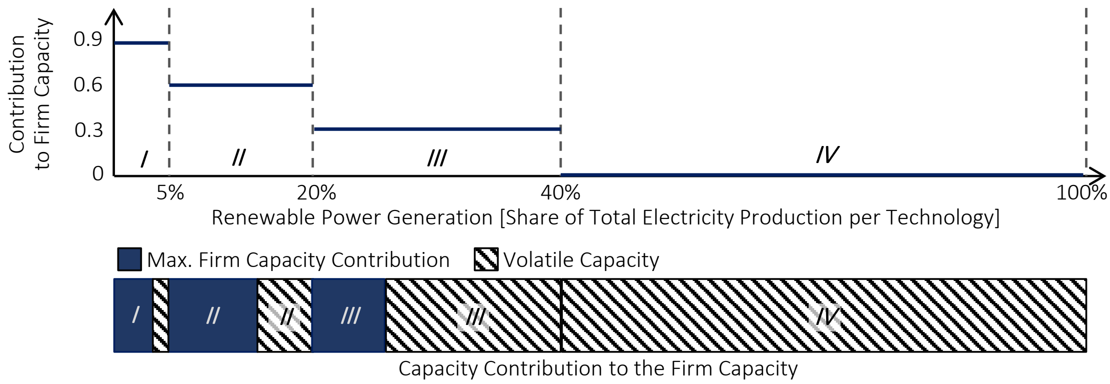

Figure 2.9: Schematic illustration of the model representation of the volatile renewable energy power capacity contribution to the firm capacity. Representation based on Sullivan et al. (2013). The figure shows the renewable energy contribution to firm capacity as a function of the share, to which the renewable energy source contributes to the total electricity production. The top figure shows the sectioning of the total electricity generation, the so-called bins I-IV. The bottom indicates the firm capacity contribution. e.g. if 12% of the total annual consumed electricity is supplied by onshore wind turbines, the first 5% of total generation fall into section I and are hence assumed to be installed at very high quality locations with reliable wind conditions and low concomitance among another. Thus, 90% of the capacity in these high quality locations contributes to the firm capacity. The remaining 7%, however, are produced by second grade locations (bin II) and only 60% of its capacity contributes towards the firm capacity requirement.

2.4.2 Integrating *ixmp* into MIGRA-NEST

With its 2019 release, the mathematical model framework *MESSAGEix* was extended by a modelling environment named *ixmp*. While *MESSAGEix* as the mathematical model formulation remained the core of the model environment, the platform extends the environment by a set of tools. These tools provide an API with the programming languages *Python* and *R* for the communication of input data and model results between the model user and the *MESSAGEix* model formulation. As such the *ixmp* environment provides the tools necessary to create new model calibrations as well as to store and track any changes applied to the model calibration data.

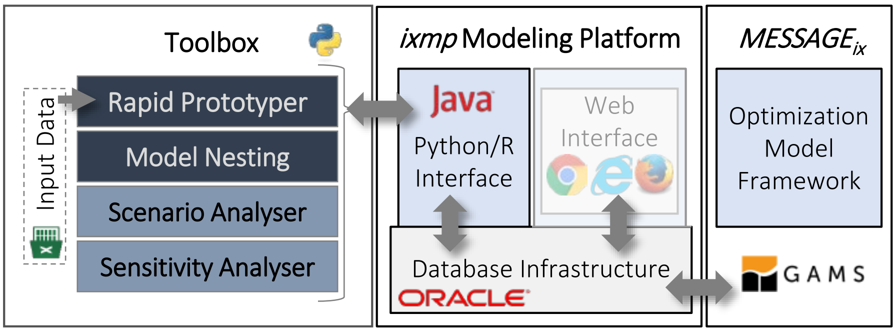

Figure 2.10: Functional schematic of the communication between MIGRA-NEST, the ixmp platform, and the MESSAGEix model framework.

The modules of MIGRA-NEST build upon this environment and employ the *ixmp* for data handling. Figure 2.10 shows a functional schematic of the integration of the *MESSAGEix-ixmp* environment into the MIGRA-NEST workflow.

While the functionalities of all modules of MIGRA-NEST vary widely, the utilisation of the *ixmp-MESSAGEix* environment remains the same: in every module, existing models are loaded from the database (e.g. the *Rapid Prototyper* and the *Model Nester* both load the global model calibration) edited by the module (e.g. the *Rapid Prototyper* replicates a global region in the shape of a country model), and finally saved in the database and handed on to *MESSAGEix* to solve.

2.5 Case Study: South Africa's Energy System in a Global GHG Context

In order to scrutinise the capabilities of MIGRA-NEST, I apply the core modules to create an energy system model of South Africa. By applying the *Rapid Prototyper* to a global energy system model calibration (*GLO*) I first create a national stand-alone model calibration (*ZAF*). The generalised model calibration structure (N) is filled with data to represent the South African energy system. Subsequently, by applying the *Model Nester*, I combine those two calibrations to synthesise the mixed-granularity model calibration. By applying the current policy framework assumptions, the general South African calibration is further refined to the *CURPOL* scenario.

Using MIGRA-NEST add-on modules, the *Scenario Analyser* and the *Sensitivity Analyser*, the results are assessed in order to explore the solution space of possible energy system transition pathways under various national and international GHG mitigation scenarios.

2.5.1 Parameterisation

The main feature of the *Rapid Prototyper* is that it allows to *recycle* existing model calibrations for creating prototypes of national stand-alone models. The basic calibration is achieved through a selection of a subsection of an energy system. This selection includes the definition of the parent model, the parent node and the technology subset. From this basic input definition, the *Rapid Prototyper* creates a reference energy system that comprises the techno-economic description of all commodities and technologies across the defined time horizon. For this case study on South Africa, I use the *MESSAGE-GLOBIOM* SSP2 (Fricko et al. 2017) calibration provided by IIASA in two ways. First, as an input to the *Rapid Prototyper* to create the national stand-alone model calibration of the South African energy system. Second, for the *Model Nester* and hence, as the global framework to the mixed-granularity scenario *CURPOL*.

For the national calibration, in addition to the data that can be adopted from the global model calibration, country-specific calibration data are required. This is particularly important for the calibration of the fossil and renewable energy resources, the historical capacity stock, the established energy use patters, as well as a demand forecast. Below, the calibration of the national stand-alone model is presented together with the rational for the data selection.

Structural Calibration

The global model calibration that is used as *parent model* for the rapid-prototyping process defines the temporal as well as the sectoral granularity of the national stand-alone models. However, the coverage of both parameters as well as the scope of the GHG emissions balancing can be user-defined. The following brief description of the *CURPOL* calibration provides an overview of the most relevant pre-defined and user-defined calibration dimensions.

Temporal Resolution The general approach of the *Model Nester*, to embed national stand-alone calibrations into global model calibrations, requires matching temporal resolution among both calibrations. Hence, the time horizon and time slicing of both the historic and the future model horizon of these two models have to match. Consequently, a subset of the temporal coverage of the global calibration (*GLO*) is used as a temporal resolution for the creation of the national stand-alone model calibration (*ZAF*). With this approach the national stand alone as well as the mixed-granularity model calibrations cover a model horizon from 1950 to 2070.[8] Due to the legacy of *GLO*, the model horizon between 1950 and 2010 operates on a five-year slicing. In order to reduce the model size and the computational demand, the granularity is set to ten years for the time period after 2010. 2030 is the first model year (representing the period from 2021-2030), calculated by the optimisation model.

Sectoral Resolution The global model calibration (*GLO*) not only depicts the power sector, but the entire energy system, including liquid fuels and direct thermal energy end-use applications. In order to also account for such sectoral interconnections in the mixed-granularity calibration and to furthermore be able to compare results of both the national and global calibrations, the mixed-granularity calibration adopts such an extended sectoral resolution. However, while all energy sectors are covered by the model, the end-use sector, being the most small-scale and diverse, is only portrayed in limited detail.

The demand sector is aggregated to seven categories, which are supplied by 59 technology options. The secondary transformation sector (refining and power supply) however, as the to date dominant GHG emission source, is described in greater detail offering more than 120 technology options for fuel transformation on the secondary level, 60 of which are technologies for power generation.

GHG Emission Representation In *MESSAGEix* emissions are endogenously balanced. This means that the model itself keeps track of the GHG emissions released and removed from the system, based on a source and sink methodology (see section 2.3.1). By applying emission factors to energy transformation processes (i.e. *technologies*) the model balances both GHG emissions from combustion and fugitive GHG emissions from extraction, transport, and storage. Accordingly, GHG emission sources, (from combustion and use of national resources and fuel imports) add to the GHG emission balance while GHG emission sinks (carbon sequestration technologies such as carbon capture and storage (CCS) and exports) reduce this balance. The energetic use of biomass is considered to be neutral with respect to GHG emissions.

The global *parent model* calibration (*GLO*) accounts for all six GHGs that are defined in the Kyoto protocol: CO_2, CH_4, HFCs, PFCs, N_2O, SF_6. As CO_2 and CH_4 are dominant in the energy system, only these two greenhouse gases have been considered in the presented calibration.

[8] In order to suppress any possible end-of-horizon effects inherent to optimisation problems, only the results until 2050 are analysed and presented in this dissertation.

Data Calibration

Fossil Energy Reserves In order to make the results of this work comparable to the national energy scenario planning of South Africa, the data used for fossil energy reserves are based on national assessments and reports. The fossil resources and related sources are listed in the appendix A.3. However, to date, only limited data about the structure, the cost and availability of the reserves are available. Therefore, and in order to stay in line with the global model calibration, the available reserves are allocated into the subcategories based on the shares of the *parent region*.

Renewable Energy Potential Literature provides an abundance of different estimates of the global renewable energy potential. In this case study, the three major renewable energy resources (solar PV, solar concentrated solar power (CSP) and wind energy) are based on global assessments by Pietzcker et al. (2014) and Eurek et al. (2017). The (in the case of South Africa) smaller scaled potentials (e.g. biomass, solar thermal applications and hydro power) are estimated based on national assessments. The considered renewable energy potentials and related sources are summarised in in appendix A.3.

Historical Energy Supply & Capacity Stock Any meaningful energy system model has to consider the historic stock of installed capacity. While size and commissioning dates of the legacy of large energy infrastructure from the fossil fuel extraction as well as the power and the refining sector are mostly available online, the capacity stock of smaller energy infrastructure, such as house appliances, in most cases, remains undocumented. However, such small infrastructure is often investment intensive, which results in low exchange rates and long life times.

In order to capture this behaviour in the model despite the lack of calibration data, the *Rapid Prototyper* supplies an *automatic calibration* feature (see section 2.2.1). Based on the allocation of historic energy use to the available technologies, the *automatic calibration* calculates the minimum required capacity stock in this period. As long as no other specifications are imposed, the automatic calibration will assume that the minimum required capacity in any one year is installed according to a uniform distribution over the technology's lifetime.

In this case study, the capacity stock of the refining and the power sector is calibrated based on national reports (see appendix A.2 and A.1). As no data on the historical capacity of the other energy infrastructure is available, to date, the *automatic calibration* is used with publicly available national energy balances as well as energy use data published by the IEA in case national data are unavailable (SA DoE 2020; IEA 2018).

Energy Demand In line with the *parent model*, in the presented calibration the energy demand is represented as *useful energy* demand, hence, as the demand for specific energy services such as electric applications, heat, or mobility. This representation ensures that the model can endogenously determine the optimal mix of technologies to supply the service. Demand is split into three sectors: residential and commercial (RC), industrial, and transportation. Furthermore, the demand is categorised into four services: (i) specific electric supply, (ii) thermal energy services, (iii) mobility, and (iv) feedstock. The applied energy demands are listed in appendix A.4.

Energy Trade In a national stand-alone model, trade is optimised based on the commodity cost or revenue of import and export technologies. Hence, the international market price is applied as variable costs to the trade technology. By default, the *Rapid Prototyper* applies the marginal costs of the commodities as calculated by the global model calibration as international market prices. Although this approach is a valid and frequently applied method it may cause problems because it assumes that costs are a constant rather than a function of the demand. For example: if marginal costs for coal export are higher than the costs of coal extraction the optimal solution would export as much coal as fast as possible. Reality, however, would be different as the international markets would react to such an export surge with decreasing prices, which would in turn discourage further exports and hence stabilise at an equilibrium. In the model, this undesired behaviour is controlled by limited technology build rates.

Energy- and Emission-Relevant Policies One major driver of energy system costs and cost-independent developments are energy-related policies. Through subsidies, taxes and restrictions, policy makers can influence utility and cost curves and thus alter decision making processes in the desired direction.

If those effects are intended to be transferred into the model calibration, an appropriate representation of these policies has to be applied. For the presented parameterisation a variety of South Africa's relevant policies has been checked. Of the many policies the two most relevant were selected: (i) the national carbon tax, and (ii) capacity prescriptions from the renewable as well as the non-renewable *Independent Power Producer Procurement Programme (IPPPP)*.

A national carbon tax was introduced in June 2019 (SA SCF 2018). This important policy instrument has been included in parameterisation at an effective economy-wide rate of 2.7 USD per ton of CO_2eq, which is increased by 3% per annum in the years thereafter. This growth estimate is based on intention of the carbon bill to raise the tax in line with Gross Domestic Product (GDP) growth, and the GDP growth forecast indicated in South Africa's most recent Integrated Energy Plan (IEP) (SA DoE 2016a). As the bill does not specify any long-term plans, this increase is applied until 2050 and is kept constant for the final model periods thereafter.

The IPPPP was introduced in 2010 to support the fragile power system through endeavours in the private sector (Calitz and Wright 2019). The program aims to diversify the fuel mix and ownership structure and to further use the concomitant rise in market competition to increase the efficiency. The IPPPP targets to procure 30 GW of power capacity from the private sector in a competitive tendering system, to be connected to the grid by 2025 (IPPO 2019). Based on the historic realisation rates, this goal was included as 80% successful in the parameterisation .

2.5.2 Results of Reference Scenario

In the following, I present the results of the reference scenario calibration from the case study on South Africa that were generated using the mixed-granularity model calibration. In line with the initial definition (see section 1.6) the term *reference scenario* is used here as this initial calibration to the current policies will be used as a counterfactual for all following analyses. This reference scenario considers the most relevant current energy-related policies as they are published to date, however, does not make any assumptions about whether or not these policies are going to be tightened, extended or removed and is thus called *current policies* scenario (*CURPOL*). This summary is structured into sections about (i) country-specific results, (ii) a view of the global dimension of the results, and (iii) an integrative conclusion.

Country-specific Results

As mentioned above, the reference scenario includes the most relevant energy- and GHG emission-relevant policies in place to-date, namely the national carbon tax and the IPPPP act.

Figure 2.11 shows the development of (a) the GHG emissions and (b) the average energy efficiency factors. Sub-figure 2.11a depicts the development of South Africa's energy-related GHG emission in the reference scenario and the pledged NDC emissions range. The upper range limit indicates South Africa's unconditional NDC pledge, while the lower limit indicates the envisioned GHG emission trajectory that is conditional to the backing of more developed country parties "*... relating to financial resources, development and transfer of technology, and capacity building.*" (UNFCCC 2016).

The results indicate that in the reference scenario South Africa's GHG emissions develop not in line with the NDC pledge. While GHG emissions remain close to constant in the first period, they increase thereafter to peak at a level of 586 $MtCO_2eq/a$ and decline thereafter. Over the projection period the GHG emissions accumulate to 16.9 $GtCO_2eq$. This is 15% to 95% above the upper and lower cumulative GHG emission ranges pledged to in the 2016 NDC, respectively (8.4-14.3 $GtCO_2eq$).

Sub-figure 2.11b summarises the development of the average energy efficiency. The plot shows that energy conversion efficiencies between the primary and useful energy sectors, as well as between the final and useful energy sectors are increasing over the evaluation period (2020-2050), from 0.4 to 0.67 and from 0.65 to 0.81, respectively. While the efficiency of the more fragmented and diverse power sector improves continuously over the evaluation period, the more clustered refining sector - with just six major plants constituting the entire refining capacity - experiences a jump in efficiency over the first model period and remains at around this level thereafter.

This drastic leap (from 0.68 to 0.93) in efficiency between 2020 and 2030 is caused by the rapid phase-out of South Africa's single major coal-to-liquid facility. While significant efficiency gains are implemented throughout the energy supply chain, the highest gains are achieved in the transformation (secondary-to-final) sector. The final-to-useful energy efficiency increases by 25% over the evaluation period, the primary-to-useful conversion

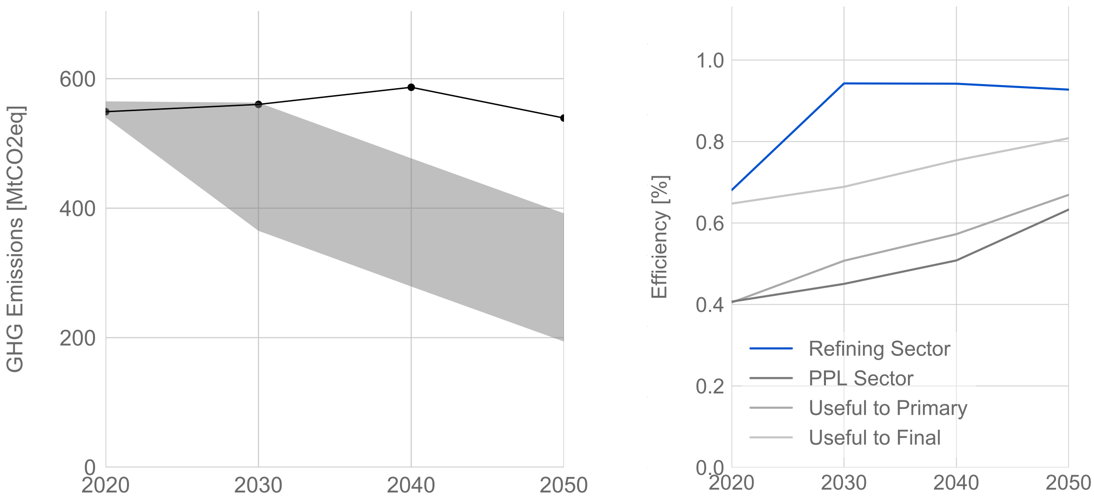

(a) Greenhouse gas emissions *(b) Average Energy Efficiency*

Figure 2.11: Results of the current policies reference scenario for South Africa (CURPOL): (a) Development of GHG emissions (solid line) in comparison the pledged NDC emission range (grey box). (b) Development of the for key energy efficiency indicators: (i) energy transformation in the refining sector (blue line), (ii) energy transformation in the power sector (dark grey line), (iii) energy conversion between the primary and useful energy sectors (grey line), and (iv) energy conversion between the final and useful energy sectors (light grey line).

efficiency increases by 68%. This effect, predominantly induced by a modernisation of the power sector and a fade-out of inefficient coal liquefaction, is explained below.

The panels in figure 2.12 summarise the development of key indicators of the energy system as calculated in the reference scenario, which provide further insights into the development of: (a) energy supply, (b) trade balance, (c) final energy consumption, and (d) electricity output of the power sector.

Sub-figure 2.12b shows the development of the energy commodity trade balance over the evaluation period. The global demand for coal remains strong up to 2040 and therefore, South Africa's coal exports are expected to grow until then: coal export capacities will more than double by 2040 (from 2.0 EJ/a in 2020 to 4.3 EJ/a in 2040). Simultaneously, the import of higher-grade fuels grows at the double rate.

Sub-figure 2.12c shows the development of the final energy consumption over the evaluation period. The figure indicates how the efficiency gains in the final energy use (as discussed above) are brought about. The efficiency rise is induced by a shift in thermal application technologies: overall energy efficiency can be increased by 25% over the evaluation period by replacing inefficient thermal applications (such as non-commercial biomass and simple gasoline fuelled combustion stoves) with more efficient and cleaner technologies (such as gas stoves, electric water heaters, thermal solar water heaters).

Finally panel (d) in figure 2.12 shows the electricity output of the power sector subdivided by power plant category.[9] The plot shows that the power sector does not only grow fast due

[9]For easier representation the power plants are summarised by fuel.

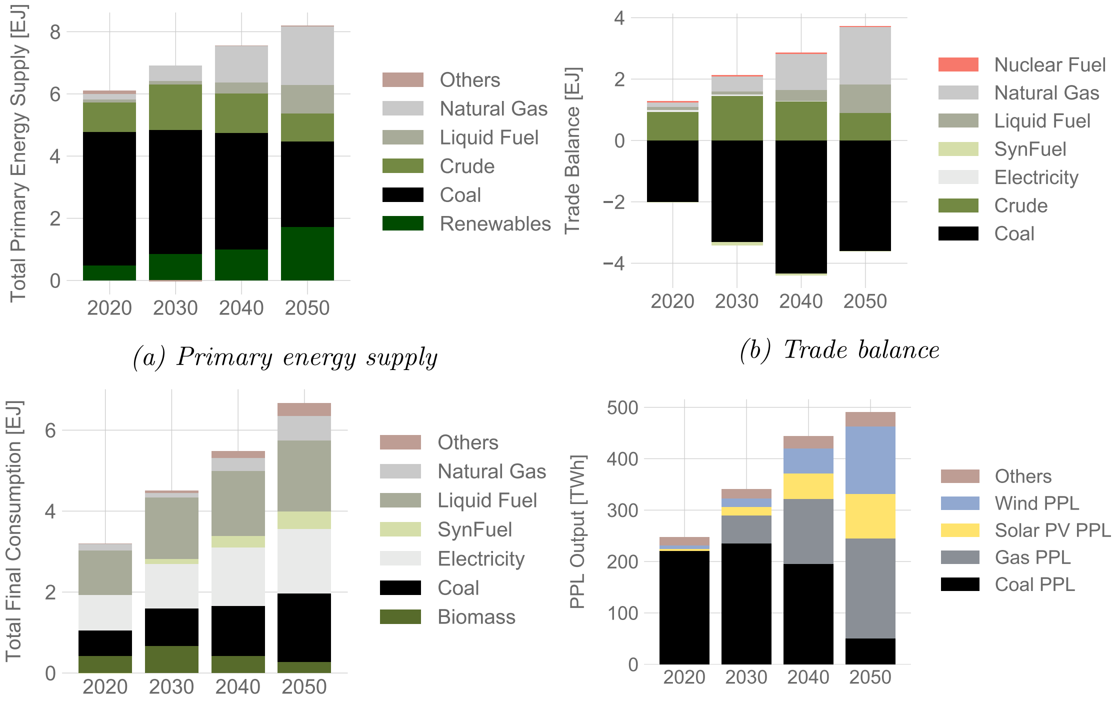

(a) Primary energy supply *(b) Trade balance*

(c) Final energy consumption *(d) Electricity output*

Figure 2.12: Results of the current policies reference scenario (CURPOL) for South Africa showing the fuel mix of: (a) the primary energy supply, (b) the energy commodity trade balance (positive values indicate net imports, negative values indicate net exports), (c) the final energy consumption, and (d) the technology mix of the power generation sector (power plant (PPL)).

to the increasing electrification of the final energy supply, but also undergoes a transition. Throughout the evaluation period the rapidly growing power sector is altered from an inefficient coal-dominated conventional power portfolio (with an average efficiency of 40%, see figure 2.11b) to a modern and diverse portfolio that is dominated by power generation from renewable energy sources. While in 2020 89% of electricity is produced in coal-fired thermal power plants, this share decreases to 10% by 2050. Correspondingly, the renewable power will be turning into the dominant energy source (with wind, solar, and biomass together supply about 50%) and gas (with a share of around 40%) providing the necessary flexibility and reliability.

The Global Context

Figure 2.13 summarises the global-scale results of the mixed-granularity model in the *current policies* reference scenario (*CURPO*): the development of global primary energy supply and global final energy demand, categorised by energy commodities.

Sub-figure 2.13a depicts the total primary energy supply over the model evaluation period subdivided by energy carrier. The figure shows that annual total primary energy supply grows by 43% over the evaluation period from 550 EJ/a in 2020 to 787 EJ/a 2050.

Simultaneously and in line with the development presented for South Africa, a commodity shift takes place on the global scale, too. While the demand for crude remains constant, and the demand for coal increases by only 27%, demand for natural gas increases by 101% and the demand for renewable energy sources rises by 78%.

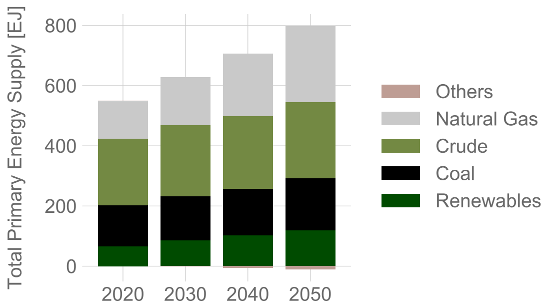

(a) Global total primary energy supply

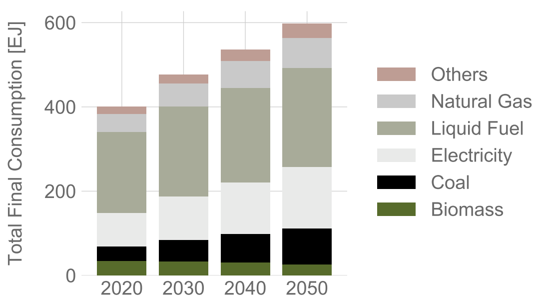

(b) Global total final energy consumption

Figure 2.13: Results of the current policies reference scenario on a global scale: (a) development of the total global primary energy supply and (b) development the total global final energy consumption subdivided by energy commodity.

Sub-figure 2.13b depicts the development of the total final energy consumption subdivided by energy commodity. It shows that final energy consumption increases over the evaluation period (49% between 2020 and 2050). However, the figure indicates that the commodity shift of the supply side passes through to the final energy demand only to some degree. Hence, the energy mix of the final energy consumption only changes marginally with a slight decrease in liquid fuel and biomass use (from a 48% share in 2020 to 40% in 2050 and from 9% to 4%, respectively), which is compensated to equal parts by an increase of the coal and electricity share. This minor fuel switch in the reference scenario leads to an increase in the global average primary-to-useful energy efficiency from 65% in 2020 to 76% in 2050.

Figure 2.14 shows the development of GHG emissions, as calculated in the reference scenario. Global GHG emissions increase by 54% (from 36.9 $GtCO_2eq/a$ in 2020 to 56.7 $GtCO_2eq/a$ in 2050). Although there is a significant increase in fuel demand, GHG emissions do not grow at the same rate. This is because over the evaluation period the specific average GHG emission intensity is slightly reduced from 108 $MtCO_2eq/EJ$ to 96 $MtCO_2eq/EJ$. This reflects the increased use of more energy-efficient and less GHG-releasing fuels such as renewable energies and natural gas. However, this commodity shift does not happen simultaneously in all regions, and thus the GHG emission intensities of the world regions do not change uniformly. While the regions centrally planned Asia and China (CPA), North America (NAM) remain among, and South Asia (SAS) joins the group of dominant emitters over the evaluation period, the GHG emission increase varies widely among the regions from a 176% increase in SAS to a mere 10% increase in CPA.

Figure 2.14 also shows the GHG emission trajectories for the five representative RCP scenarios (RCP 6.0-RCP 1.9). As stated above, the five scenarios relate to average end-of-century temperature increases of 3.3° C to 1.3° C, respectively. The figure shows that in the reference scenario global GHG emissions lie well above the RCP 6.0 scenario, which in turn indicates a trajectory to an average end-of-century global warming of well above 3.3° C above pre-industrial levels.

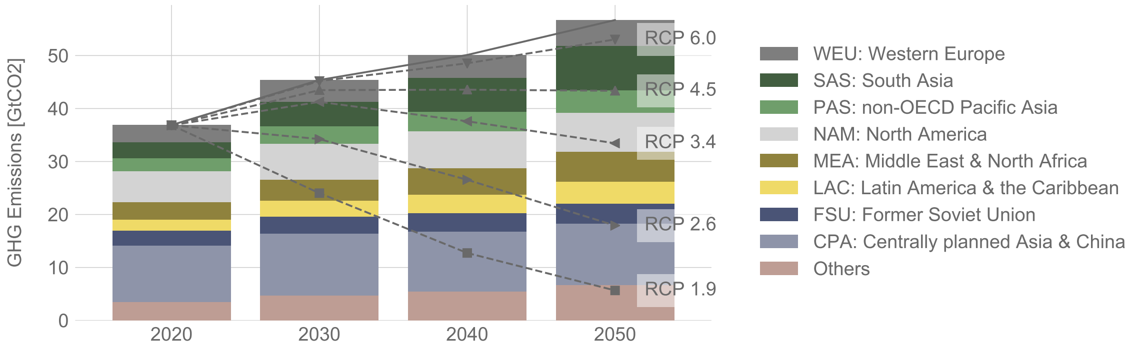

Figure 2.14: Results of the current policies reference scenario (CURPOL) in a global context: development of greenhouse gas emissions by emitting region. The dashed grey lines indicate the adjusted RCP emission trajectories (see appendix B.2). The regions are defined in appendix B.1.

The results indicate that in order to limit average end-of-century global warming to values well below 2.0° C (or even below 1.5° C) above pre-industrial levels, as agreed upon by the signatory parties in the *Paris Accord*, significant deviations from the reference development must be targeted.

Conclusions

The results indicate that South Africa's GHG emissions first increase to a peak in 2040 and decrease in the decade thereafter. While a shift towards more efficient fuels and energy applications can be identified, this is not sufficient to reduce GHG emissions to the peak-plateau-decline trajectory proposed in South Africa's NDC.

Furthermore, the reference scenario indicates that global primary energy demand continuously increases between 2020 and 2050. This development, despite being driven by a growth in demand for natural gas, leads to a surge in global GHG emissions. While all global regions contribute to the total growth of 69%, the emerging economies of Sub-Saharan Africa (AFR), South Asia (SAS), Middle East and North Africa (MEA), Latin America and the Caribbean (LAC), and non-OECD Pacific Asia (PAS), are accountable for the major part (71%) of the increase. With their high demand growth and continuing strong dependence on fossil fuels, these five emerging regions together raise their contribution to the total global GHG emissions from below 25% in 2020 to 45% 2050.

The resulting projected trajectory of global GHG emissions lies well above the GHG emission trajectory required for limiting global average end-of-century warming to 2° C above pre-industrial levels. Hence, in order to reach the globally agreed upon global warming goals, strong mitigation efforts are required.

2.5.3 Benchmarking the Reference Scenario

The *Rapid Prototyper* produces - as its name suggests - parsimonious archetype representations of country-level energy systems rather than detailed and refined bottom-up representations. Hence, in order to identify the limitations of the prototyped model calibrations, the results of the *current policies* reference scenario (*CURPOL*) are bench-marked against results from national energy system simulations that provide much greater details.

Thus, results of the reference scenario for South Africa are compared to two sources from literature. One is the Integrated Energy Plan (IEP) as published by South Africa's Department of Energy (SA DoE 2016a). The IEP is designed as a "*roadmap of the future energy landscape for South Africa, which guides future energy infrastructure investments and policy development*" (SA DoE 2016a). The other is an independent and more recent peer-reviewed study on the power sector transition of South Africa by Wright et al. (2019).

The IEP, constituting of several sub-reports, provides an energy roadmap in four scenarios (*Base Case*, *Environmental Awareness*, *Green Shoots*, *Resource Constrained*), each covering the whole energy supply system, including separate results for the power and the liquid fuel sector. The detailed analysis by Wright et al. (2019) compares three separate long-term scenarios for South Africa (a *Business-as-Usual*, a *Least-Cost*, and a *Decarbonised* scenario) but it covers the electricity sector expansion planning only. The results of both studies are summarised and compared in appendix A.6.

Figure 2.15 summarises the results of the model benchmarking, namely the comparison of key benchmark variables from the *current policies* reference scenario (*CURPOL*) against the results from four scenarios from the IEP (SA DoE 2016a; SA DoE 2016b) and three scenarios from the power sector expansion study by Wright et al. (2019). The benchmark variables refer to (i) installed capacity for power generation, (ii) the power generation, and (iii) final energy consumption. All results refer to the year 2050 and are end-of-evaluation period values for all scenarios. This late point in time was chosen for the comparison, as the deviation from today is expected to be greatest there, which enhances the significance of the comparison.

The figure indicates that the *CURPOL* scenario compares well to the model results of the more detailed national model calibrations. Within the comparison of the seven (four for the final energy demand) scenarios, the reference scenario does not strike as an outlier. Only for natural gas use in power generation and in final energy, the results of *CURPOL* lie outside the range covered by the benchmark scenarios. This variance, however, is within an acceptable low percentage range. While this brief model benchmark cannot be considered an exhaustive test of the plausibility of the model as such, it stands as a first sanity check of the *CURPOL* scenario results. However, the robustness of the results, and the quality of the model calibration and structure cannot be assessed this way, as this requires a more in-depth analysis. Such an analysis is conducted in the form of a global sensitivity analysis in chapter 4.

2.6 Summary & Discussion

In this chapter I have introduced the MIGRA-NEST toolbox that I developed as part of this dissertation. I furthermore demonstrated the functionality of its two core modules -

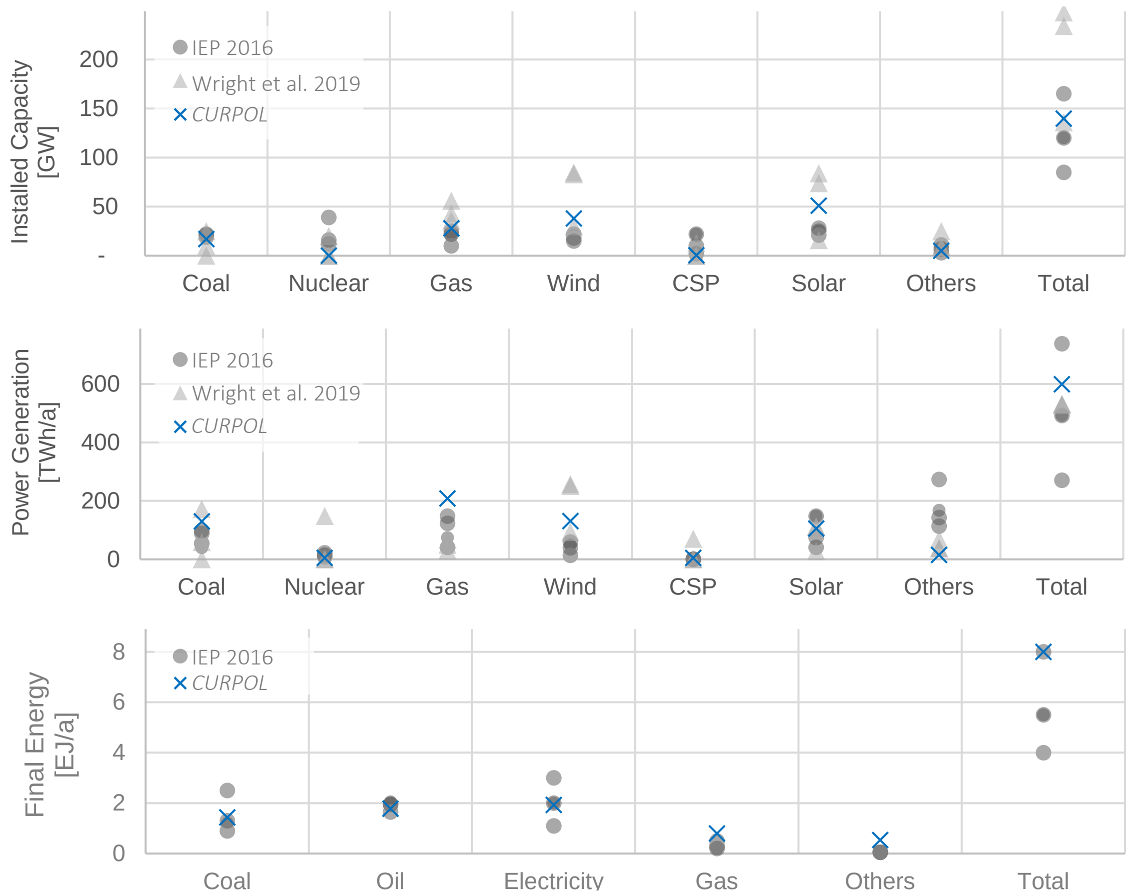

Figure 2.15: Comparison of the results from the current policies reference scenario (CURPOL) against the results from four scenarios from the IEP (SA DoE 2016a; SA DoE 2016b) and three scenarios from the power sector expansion study by Wright et al. (2019). The benchmarked variables refer to (i) the installed capacity for power generation (top), (ii) the power generation (middle), and (iii) final energy consumption (bottom). All benchmark values refer to the year 2050.

the *Rapid Prototyper* and the *Model Nester* - in a case study on South Africa.

The results of the case study have shown that the overall design of the MIGRA-NEST system (in this first step, the rapid prototyping of the national stand-alone models and the interaction between the two core modules) is practicable and useful for creating first, national stand-alone model calibrations and subsequently integrating them into global model calibrations. The substantial advantage of such an integration is that it allows to assess national energy scenarios within a global context.

Why is this important? All models have limitations - and models that refer to different aggregation levels have different limitations. A model is a mathematical tool that is specifically created to support answering model-specific questions, and these questions are quite different for different spatial and temporal or structural scales. Thus, scenarios that are projected with models of a different aggregation level are usually not comparable.

A global energy system model that supports scenarios for options of country contributions to global GHG emission reduction targets might be useful for UNFCCC negotiations, but it would be of no help to determine the feasibility of alternative development paths in the country's economical and energy sectors. On the other hand, a detailed national energy model that incorporates the countries production and consumption sectors, and the overall governance system of a country's energy system, can be extremely complex. This complexity and detail also has some disadvantages associated with it. For instance, the high degree of detail provided by such models often comes at the cost of long computation times. Hence, while a more advanced and detailed model may capture more inter-linkages, it limits the numbers of scenarios that can be solved and evaluated due to computing time requirements (Hedenus et al. 2013). Detailed national models are also often not comparable with other national models with respect to spatial and structural granularity, and often also in terms of semantics. Furthermore, very few of advanced detailed national energy system models are available under an open source license and cannot be scrutinised nor utilised by potential users.

The MIGRA-NEST approach tries to overcome this problem by establishing a simplified model calibration from national energy system models and merging them with global model calibrations, so that alternative national scenarios in a country can be assessed within a global context. While the modelling idea of applying different levels of spatial detail, to national energy system models is not new, to the best of my knowledge no open framework for creating such models of mixed spatial granularity in a standardised manner exist. The MIGRA-NEST model set-up follows current trends to decrease model complexity for the sake of an increased result discussion and narrative (Ellenbeck and Lilliestam 2019). By providing a workflow for embedding national stand-alone calibrations into model calibrations the toolbox offers the methods required to explore potential national energy transition pathways in a global context.

Of course, this approach requires the introduction of simplifications. For instance, the national stand-alone model prototypes generated by the *Rapid Prototyper* are not comparable to specific detailed and explicit national energy system model designs and calibrations. The necessary lower spatial and temporal resolutions, for example, exclude an explicit description of transmission and distribution infrastructure and or energy storage within a country. The reduced complexity also has some important advantages. It reduces the barrier of entrance to energy system modelling while providing a legitimate starting point for national energy system modelling that is open to further improvement through refining and extension of the prototype country model for more detailed analyses.

The test case for South Africa has demonstrated valuable insights to the practical application of the MIGRA-NEST concept. First, the benchmarking exercise has shown that the results of the *current policies* scenario are well aligned with the selected key benchmark values from seven very detailed South African national stand-alone scenarios. It projects reasonably the likely development of many parameters of the South African energy system and the implications of this development on the global GHG emission balance.

However, the model is not without limitations. An energy system model must cope with the drastic uncertainty that inherently characterises any future development (e.g. energy demand, technological capabilities, or commodity costs). Thus, energy system models should not be mistaken as forecasts of an actual development but must rather be interpreted as a comprehensible and stringent mathematically optimised transition pathway defined by the techno-economic calibration of a scenario. The question an energy system model may answer cannot be: *How is the energy system going to develop?* but rather: *What would be a technically feasible and under given assumptions cost-effective transition pathway look like?*

As such, the model results, can be interpreted as "an optimal energy supply strategy under given assumptions". These assumptions might be of a quite variable quality, and often are simply guesses. Thus, all these assumptions must be carefully scrutinised for their influence on the final results. Such scenario results can, thus, be used as informative guidelines for developing an understanding of:

- How could the energy system develop under given policy framework conditions?
- Is this development in line with an envisioned goal?
- What are the consequences of such a development of the energy system in the means of energy supply costs and the GHG emission trajectory?
- Is the envisioned system technically feasible and how could a transition to this new system look like?
- Which (maybe unintended) side-effects are caused by certain changes of political and technical changes in the framework condition?

The best response to assess such uncertainties lies in the exploration of the model sensitivity. Such global sensitivity analysis requires a very high number of model executions, which will result in high computational demand. Lean systems such as the model created by MIGRA-NEST provide the option to analyse a wide range of scenarios as well as to explore the global sensitivities of the produced models.

Hence, while the models created with MIGRA-NEST have a limited degree of detail, and although several parameters (e.g. resource quantity distribution) are only estimates, the created models offer a starting point for further calibration efforts or thorough scenario and sensitivity analyses.

Chapter 3

Scenario Analysis

> The purpose of scientific computing is insight, not numbers.
>
> Arthur M. Geoffrion 1976

A scenario analysis is a key component of most energy system studies. By comparing a multitude of scenarios, insights on the system dynamics of a model and the key drivers to the relevant results (e.g. energy system costs, GHG emissions, import dependence) can be gained. However, such an analysis is based on a plurality of scenario definitions and result data. The *Scenario Analyser* supports such an analysis by providing the means tailored to comparative scenario analyses.

The special feature of the *Scenario Analyser* is that it clearly separates and standardises all components that constitute a scenario analysis. Thus, as shown in figure 3.1, two pre-defined classes with a pre-defined set of properties exist, namely (i) *scenarios* and (ii) *scenario sets*.

Scenarios are defined by:

- a unique scenario name, a description, and optionally a synonym;
- a reference scenario that the scenario is based on;
- a (set of) functions calls that describe the variations, which distinguish the scenario from the reference scenario (e.g. *first apply a carbon price of 10 USD/tCO_2eq, then a demand reduction of 10%*); and
- the post-processing specifications: scenario colour, marker and line style, output file directory etc.

Scenario sets are defined by:

- a unique scenario set name, a description and optionally a synonym;
- a the collection of unique scenarios that the scenario set consists of;
- the post-processing specifications such as output file directory.

In addition to the data organisation system, the *Scenario Analyser* also contains the functions that apply the scenario conditions, which distinguish any scenario from the reference scenario. This separation averts mistakes by ensuring a synoptic code base for

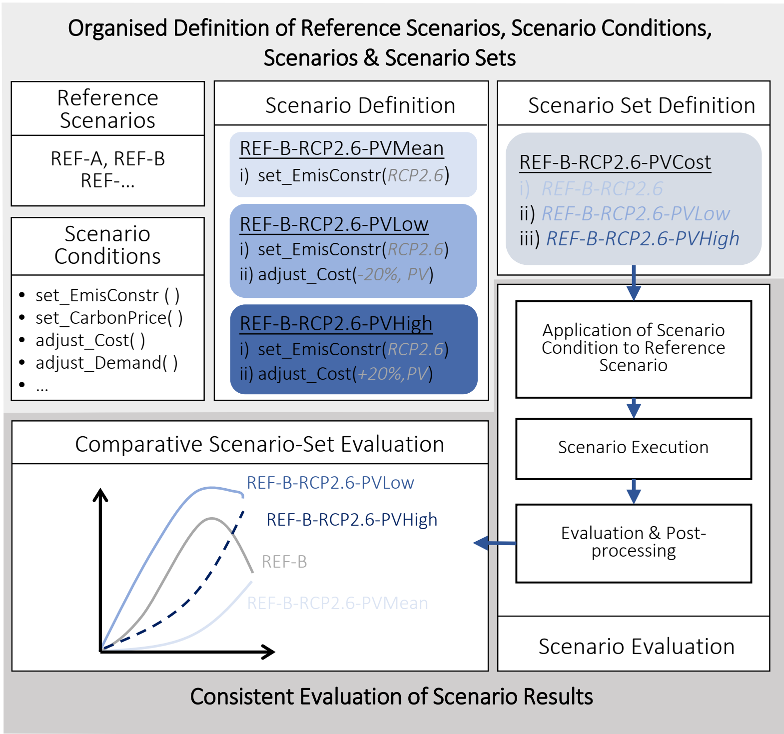

Figure 3.1: Schematic of the functioning of the MIGRA-NEST Scenario Analyser module. The Scenario Analyser allows (i) an organised definition of scenarios based on reference scenarios and scenarios conditions, and (ii) a stringent evaluation of the respective results. Scenarios are established defining scenario conditions for a variety of parameters and a reference scenario to apply them to. Scenario sets are defined as groups of scenarios with a common lineage of conditions and a common reference scenario (e.g. REF-B). The Scenario Analyser organises the parameterisation (condition setting) and the evaluation of scenarios and scenarios sets, and allows an automatic execution of the defined scenarios and a comparative evaluation of the results.

the scenario definition and a standardised set-up of the scenario analysis. Furthermore, the *Scenario Analyser* provides a standardised methodology for post-processing and visualisation of temporally disaggregated results for single scenarios and comparative aggregated results of scenario sets.

The following chapter presents a scenario analysis of the South Africa case study. The purpose of the scenario analysis is to demonstrate the design, functioning and performance of the *Scenario Analyser*. In this analysis I compare two national and two global mitigation strategies with respect to their impact on national energy supply, energy supply costs and GHG emissions, as well as on global energy supply and GHG mitigation costs. The analysis is based on scenarios that build upon the *current policies* reference calibration (*CURPOL*) of the globally embedded country-level representation of the South African energy system, presented in chapter 2.5.2. While the results of this reference calibration offered a first introduction to the South African energy system, the aim of the following scenario analysis is to evaluate GHG mitigation driven transition pathways for South Africa's energy system.

In this analysis a special focus is put on the potential benefits and challenges for creating internationally coordinated mitigation strategies.

The chapter is structured as follows. First the scenario set-up of the seventeen scenarios that constitute the national and the global mitigation strategies are described in their variation to the *current policies* reference (see figure 3.2). Thereafter the results of the seven scenarios that explore the national mitigation strategies are presented and their implications are discussed. Subsequently the results of the ten scenarios that were used to investigate the two global mitigation strategies are compared. The chapter closes with a summary and a conclusion on the benefits and challenges posed by internationally coordinated GHG mitigation strategies as experienced by the different cooperating parties.

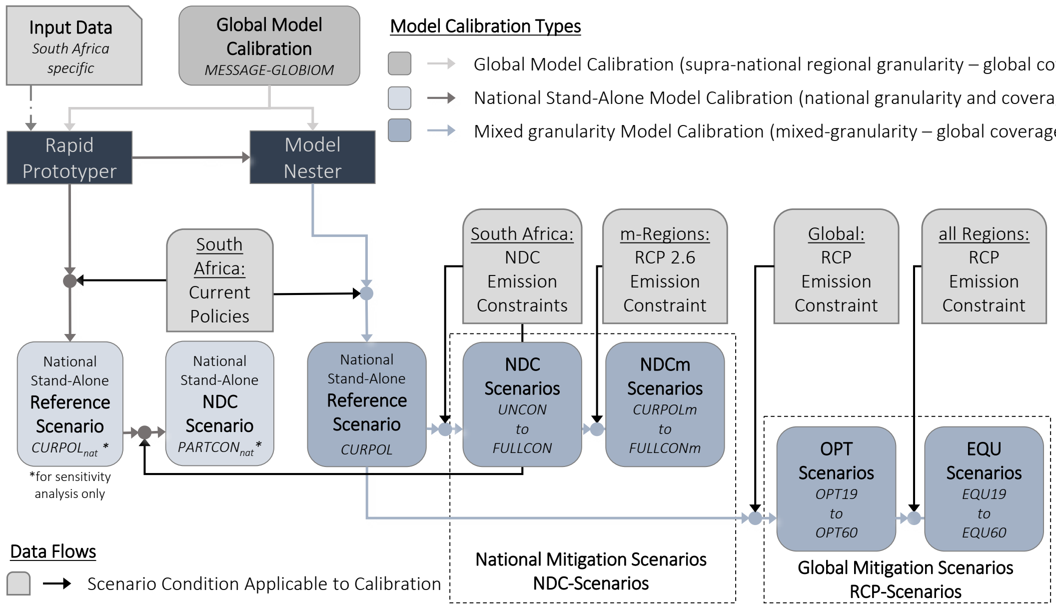

Figure 3.2: Map of the model calibrations as applied in this dissertation. The figure shows, how: (i) the Rapid Prototyper is used to create the national stand-alone model calibration of the South African energy system based on the global model calibration (MESSAGE-GLOBIOM); (ii) these two calibrations are merged in the Model Nester to create the mixed-granularity calibration; (iii) the current policy assumptions are applied as scenario conditions in order to create two reference calibrations (CURPOL and CURPOLnat); (iv) the remaining scenario conditions are applied to create the NDC and the RCP scenarios as required for the scenario analysis.

3.1 Scenario Design

In order to evaluate the technical feasibility, the cost, and the system effects of different national as well as global mitigation strategies, four different scenario sets are defined and presented in the following (see figure 3.2). First, two sets of national mitigation scenarios are developed that focus on South Africa's national GHG mitigation goals, as determined in the NDC. This scenario set evaluates the technical feasibility and potential cost increase induced by limiting South Africa's GHG emissions to the implied constraints.

Second, two global mitigation scenario sets are designed. Aim of these scenario sets is to explore cost-optimal strategies for reaching global GHG mitigation targets and to quantify the benefits of internationally coordinated efforts. A special focus is put on South Africa's potential contribution towards such a global mitigation strategy.

Both scenario sets build upon the *CURPOL* reference scenario that was presented before (see section 2.5.2). In the following, the main characteristics as well as the aim and design of the national and the global mitigation scenario sets are presented.

3.1.1 Current Policies Reference Scenario

The reference scenario is designed as a counterfactual to compare the GHG emission mitigation scenarios to. It is presented in detail in section 2.5.2 and is, therefore, designed under the assumption that for the country of interest (i.e. South Africa in the case study presented here) the GHG emission-relevant energy policies in place today (e.g. for South Africa the carbon tax and the IPPPP - section 2.5.2) are maintained over the model horizon and that no other climate-relevant policies are introduced. It is therefore called the *current policies* (*CURPOL*) scenario. While the energy demand of South Africa is anticipated to develop in line with the national energy demand forecast, all techno-economic developments are expected to develop in line with the global model calibration.

The rest of the world is expected to develop according to the SSP2 scenario model calibration without radiative forcing targets as described by Fricko et al. (2017). As the middle-of-the-road scenario with respect to mitigation and adaptation challenges, this SSP2 scenario results in a projected average end-of-century anthropogenic global warming of nearly 4 °C relative to pre-industrial levels (Fricko et al. 2017).

3.1.2 National Mitigation Scenarios - Aiming for the NDCs

In response to the agreement established in the Paris Accord, South Africa pledged in the 2016 Nationally Determined Contribution (NDC) to limit its future GHG emissions to a peak-plateau-decline trajectory range, with an emission peak of 398-614 $MtCO_2eq$ between 2025 and 2030.[10] While the upper limit of the GHG emissions range is the unconditional goal, independent from international support, the lower limit is conditional to sufficient international backing (UNFCCC 2016).

The national mitigation scenarios are designed to evaluate (i) the impact of national GHG mitigation efforts upon reaching national mitigation targets and on global climate

[10]It is noteworthy that South Africa is one of very few countries, not listed in Annex I of the Kyoto Protocol, which nevertheless has committed itself to absolute emission limits (Pauw et al. 2019).

goals and (ii) the impact of global mitigation efforts on South Africa's mitigation ambitions that are proposed in the NDC. It is important to note that while NDC trajectories cover all GHG emission sectors (including LULUCF), this dissertation focuses on the energy-related GHG emissions from CO_2 and CH_4 (which covers 92% of total GHG emissions - see appendix C.1).

Additionally, to the unconditional and conditional NDC pledges, a mid-range trajectory is constructed in this analysis, which stands as a proxy for a trajectory resulting from partial international support. Table 3.1 summarises South Africa's greenhouse gas emission limits as pledged in the NDC (UNFCCC 2016), and the adjusted GHG emission (limited to the energy sector, and to CO_2 and CH_4 emissions) as applied in this dissertation under the three mitigation pledges: (i) unconditional to international support (*UNCON*), (ii) conditional to partial international support (*PARTCON*), and (iii) conditional to full international support (*FULLCON*). These three trajectory assumptions are based on the *CURPOL* reference scenario (introduced in section 2.5.2). In each of these a constraint is applied to the annual GHG emissions of South Africa while the rest of the world remains without carbon restraint.

Table 3.1: South Africa's emissions reduction trajectories. Top: GHG emissions (all GHGs and all sectors incl. LULUCF) as pledged in the NDC (UNFCCC 2016). Bottom: Adjusted NDC emission trajectories (and according scenario names) as applied in this dissertation.

NDC GHG emission mitigation pledges

[$MtCO_2eq$]	**by 2030**	**by 2050**
Unconditional to international support	614	428
Conditional to full international support	398	212

Adjusted NDC GHG emission mitigation pledges as modelled*

[$MtCO_2eq$]	**Scenario**	**2030**	**2040**	**2050**
Unconditional	UNCON	563	477	392
Conditional to partial int. support	PARTCON	464	378	293
Conditional to full int. support	FULLCON	365	279	194

*constraints include CO_2 & CH_4 from energy applications only.

As the South African energy system and thus, the country's GHG emissions depend upon the international commodity market, four additional scenarios are developed and evaluated. In these four additional scenarios - *CURPOLm*, *UNCONm*, *PARTCONm*, *FULLCONm* the GHG emission trajectories of the countries aggregated in the economically most advanced model regions North America (NAM), Western Europe (WEU), and the Pacific OECD (PAO) are assumed to strictly adhere to emission reduction requirements as described in the RCP2.6.[11] These scenarios are marked with a *m* for *most economically advanced* in the scenario acronym and are thus referred to as *m*-scenarios. The three regions NAM, WEU, and PAO are referred to as *m*-regions.

[11] The modified RCP2.6 reduction trajectory as defined in appendix B.2 is applied here.

The three *m*-regions were selected to proxy for a *fair-share* distribution that allocates the majority of the mitigation burden to the most developed regions. While this is a non-exclusive selection that is not based on current policy ambitions, these scenarios stand in for a narrative where parts of the world embark on a GHG emission reducing trajectory while others remain unconstrained. The trajectory in line with the RCP2.6 is selected to surrogate an ambitious mitigation target that corresponds to the agreed global warming target from the Paris Accord. In order to support comparability of the results between the *m*-scenarios and their *non-m* counterparts, all other scenario assumptions remain the same. Table 3.2 summarises the scenario assumptions and notations used in this scenario set.

Table 3.2: Summary of the scenario assumptions and notation used in the NDC scenario set. All scenarios defined for South Africa have a global mitigation counterpart indicated by an m in the scenario name. In these mitigation scenarios the GHG emissions of the three economically most advanced regional nodes North America (NAM), Pacific Asia OECD (PAO) and Western Europe (WEU) are defined to follow the emission reduction equivalent to the global reduction required for being in line with the trajectory of RCP2.6.

Scenario Abbreviation	Applied NDC Constraint	Global Effort*	Scenario Symbols	
CURPOL	-	-	●	—
CURPOLm	-	✓	▲	- - -
UNCON	Unconditional NDC pledge	-	●	—
UNCONm		✓	▲	- - -
PARTCON	Partially conditional to international support	-	●	—
PARTCONm		✓	▲	- - -
FULLCON	Conditional to full international support	-	●	—
FULLCONm		✓	▲	- - -

*Greenhouse gas emission from the regions NAM, PAO, WEU are constrained to RCP2.6

3.1.3 Global Mitigation Scenarios - Aiming for the RCPs

In the global mitigation scenarios, the global GHG emissions are limited to the values in line with the SSP2 RCPs marker scenarios (see table 3.3).

However, while the model presented in this dissertation is a representation of the energy sector that considers only the most energy-relevant GHGs (CO_2 and CH_4), the marker scenarios include all climate-relevant GHG emissions and all emission-relevant sectors (e.g. energy, agriculture, land use). Hence, the respective GHG emission trajectories applied to the case study are adjusted accordingly. The adjustments made to the trajectories are described in appendix B.2.

As stated in the introduction, experts agree that limiting global warming to levels below 2 °C requires immediate and globally concerted action and that such concerted action can be of many different ways. However, determining the most economical ones will increase the likelihood of implementation of any of them. In this case study I, therefore, compare two different subsets of global mitigation scenarios. In the first scenario set, the GHG

Table 3.3: Summary of the scenario assumptions and the notation used in the RCP scenario set. For all RCP trajectories, two scenarios are designed: one that applies the trajectory as a globally cumulative constraint (OPT), and one that applies a equal emission reduction share to each node (EQU).

Scenario Abbreviation	Mitigation Trajectory	GHG Constraint global	GHG Constraint nodal	Scenario Symbols	
CURPOL	-	-	-	●	—
OPT60	RCP 6.0	✓	-	●	—
EQU60		✓	✓	★	- - -
OPT45	RCP 4.5	✓	-	●	—
EQU45		✓	✓	★	- - -
OPT34	RCP 3.4	✓	-	●	—
EQU34		✓	✓	★	- - -
OPT26	RCP 2.6	✓	-	●	—
EQU26		✓	✓	★	- - -
OPT19	RCP 1.9	✓	-	●	—
EQU19		✓	✓	★	- - -

emission constraints are applied at global level and hence, the regional allocation of the GHG mitigation is established by the optimisation problem. Therefore, these scenarios are referred to as *globally optimised* or *OPT* scenarios. In the second scenario set, in contrast, the GHG emission constraints are applied at an equal share to each model region separately. They are referred to as *equal-share* or *EQU* scenarios. This reduction strategy does neither align with currently debated "fair" distributions of the mitigation endeavour nor does it represent current policy ambitions. However, it is here chosen as a proxy for an uncoordinated global mitigation strategy. In this dissertation in the *EQU* scenarios the GHG emissions of every model region are limited to the global reduction target compared to their reference, if feasible. For example: under the RCP2.6 emission constraint, the GHG emissions of every model region are reduced equally by -23% in 2030, -46% in 2040, and -67% in 2050 (as compared to their reference values). Only if limiting emissions to this extent leads to infeasible model solutions, the GHG emission constraints are loosened to the highest feasible GHG emission for that model region for that year. Table 3.3 summarises the scenario assumptions and notations used in this scenario set.[12]

[12] The original scenario set contains two scenarios that represented the emission reduction in line with the "Paris Scenario" RCP1.9. However, under the *EQU19* scenario assumptions the model proves to be infeasible, while in the globally optimised scenario *OPT19* the model is taken to the limb of feasibility (e.g. decoupling of the export revenue for South Africa and raising commodity trade prices to the twenty-fold). These limitations can be interpreted in several ways. (i) it points at the level of ambition inherent to this mitigation scenario: halving emission within the next decade and further reducing global emission to net-negative values by 2050 as required might pose a real-world challenge for the global community, which has also been found in other studies (Grubler et al. 2018; van Vuuren et al. 2014; UNEP 2019). (ii) These results can also be interpreted as an indicator for an overly restrained model calibration that limits technological change and efficiency gains to values below values actually achievable in reality. Therefore, this interpretation will be revisited in the sensitivity analysis in order to evaluate the degree, to which

3.2 Results of the National Mitigation Scenarios

3.2.1 Greenhouse Gas Emission Trajectories

The global GHG emission trajectories and the emission trajectories for South Africa in the six national mitigation scenarios and the *m* as well as *non-m* variation of the *current policies* reference are illustrated in figure 3.3. The GHG emissions depicted in the figure include all energy-related CO_2 and CH_4 emissions.

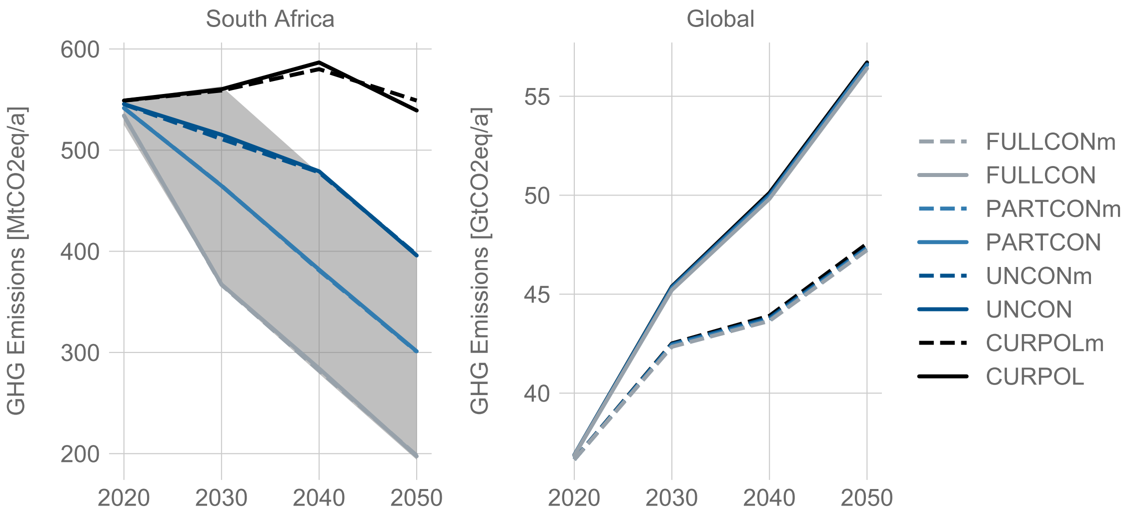

Figure 3.3: Development of the GHG emission trajectories in the current policies and the NDC scenarios (see table 3.2). Left: GHG emissions in South Africa (grey area refers to range of NDC pledges). Right: global GHG emissions.

The comparison of the national and the international emission trajectories exposes the different GHG emission trends already discussed before in the review of the reference scenario (see section 2.5.2): while in the *CURPOL* reference scenario the GHG emissions in South Africa follow a peak-plateau-decline trajectory, worldwide GHG emissions increase throughout the evaluation period. This global trend persists in the *m*-scenarios, in which GHG emissions decline in the *m*-regions (WEU/PAO/NAM).

Furthermore, the plots in figure 3.3 show that while the South African GHG emission constraint has a significant impact on the South African emission trajectory, the impact exerted by the global emission constraints remains marginal. This suggests that for South Africa limiting emissions to the pledged levels is technically feasible whether or not GHG emissions are reduced in other regions. Global GHG emissions, however, are only slightly impacted by South Africa's emission trajectories, which is in line with the relatively low share, to which South Africa contributes to the global GHG emission balance. Global GHG emissions are, however, significantly reduced by the strict carbon cuts that are realised in the *m*-regions in the *m*-scenarios. To put it in a nutshell, deviating the GHG emission trajectories from the *current policies* reference is technically feasible on both the national as well as the global scale.

technological transition speeds contribute to the limited GHG emission reduction potential.

While the outcome stated above was among the expected results, the model results also expose an interesting and unexpected effect for South Africa. It shows in the comparison of the two unconditional mitigation scenarios (*UNCON* / *UNCONm*). In these two scenarios the 2030 model-projected emissions are lower than the maximum allowance of the GHG emission constraint for the scenario. Thus, in the year 2030 the unconditional GHG emission constraint allows GHG emissions of maximum 563 $MtCO_2eq/a$ but the model projects GHG emissions of 516 $MtCO_2eq/a$. This indicates that under cost-optimal conditions there is an earlier-than-expected transition from carbon-intensive fuels (in South Africa: coal) to less carbon-intensive fuels (in South Africa: mainly natural gas) than anticipated in the initial setting of boundary conditions.

The effect is linked to the limited technological transition speed and the longevity of energy sector infrastructure. Hence, for economic operation, most energy technologies have to be operating throughout several decades. Therefore, installing carbon-intensive infrastructure to "exploit" the lenient GHG emission constraint for the first period does not make economic sense in the context of the more stringent GHG emission constraint that follows in the periods thereafter. Furthermore, the existing capacity stock and the available technology supply structure (such as the existing new-technology industry capacity as well as its growth potential) limit the transition speed of the energy sector. While in reality, such transition speeds can be increased by monetary measures such as subsidies, state investments as well as technology imports, the model represents these extra costs by considering so called *soft constraints* on the technology growth rates. Hence, by starting the energy system transition as soon as possible, the model omits costs of exceeding the transition speed constraints that would otherwise be required to perform the system transition necessary to limit GHG emissions in 2040 to below 477 $MtCO_2eq$ in the *UNCON* scenario, respectively. This model effect can be interpreted as the real-world requirement to start the energy system transition in time for the domestic industry and expertise to grow with the rising demand.

3.2.2 Energy Supply Costs

As figure 3.3 shows there is hardly any impact of the global GHG constraints on the GHG emissions in South Africa. However, there are considerable impacts on costs. The total net energy system costs summarised over the projection period (2021-2050) for the *m* and *non-m* variation of the *current policies* scenario and the six national mitigation scenarios are shown in figure 3.4. On the left hand side, the cost components that constitute the total energy system costs are shown individually. On the right hand side, the summarised total discounted net energy system costs are provided. The figure shows the influence that the national emission constraint and the international mitigation efforts have on the energy system costs in South Africa (compare the *non-m* - circles - to the *m*-scenarios - triangles). In this dissertation the net costs are defined as the total discounted energy system costs, less the carbon price and export revenue. As the carbon price is, from an economic point of view, not considered a cost component but rather a revenue that balances to net zero, it is not depicted in figure 3.4.

Several effects can be observed in the plots. First, the subplot showing the total net system costs indicates that the introduction of a national GHG emission constraint raises

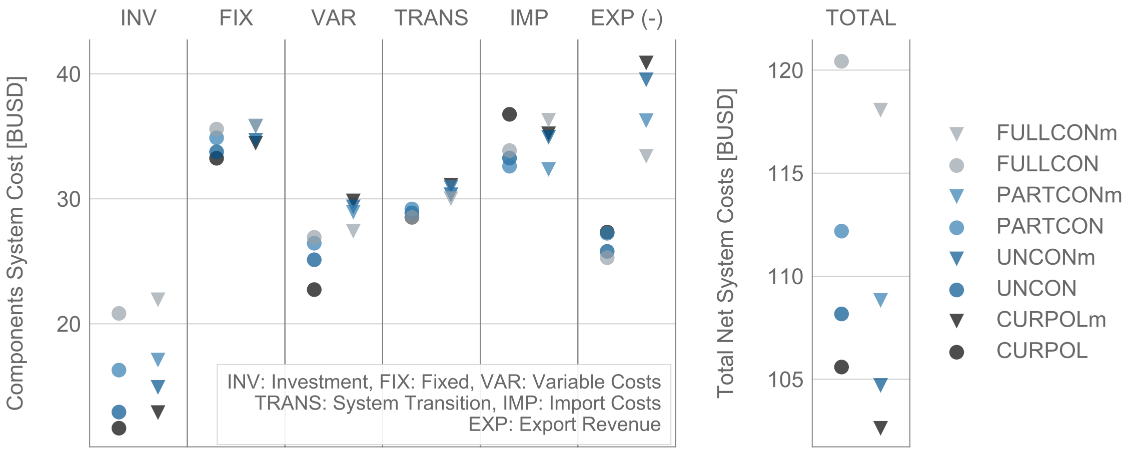

Figure 3.4: Total discounted net energy system costs and the energy system cost components for South Africa in the current policies (CURPOL/CURPOLm) and the NDC scenarios (see table 3.2). The total net system costs are equal to the sum of the technology costs (INV, FIX, VAR), the transformation costs (TRANS) and the fuel import costs (IMP) minus the export revenue (EXP).

total energy system costs (right in figure 3.4). For the *non-m* scenarios - indicated by the round markers - total energy system costs increase from 105.6 billion USD in the *CURPOL* reference, to 108.2 billion USD under the *unconditional* NDC constraint, to 112.0 billion USD under the *partially conditional* NDC constraint, and to 120.8 billion USD if GHG emissions are limited to the *fully conditional* NDC constraint.

Adjacent to the mentioned results, figure 3.4 shows the total net system costs in the *m*-scenarios (indicated by the triangular markers). The numbers suggest that by the introduction of a GHG emission constraint for the *m*-regions total energy system costs decrease for South Africa. If emissions are constrained in those regions, and GHG emissions remain unrestrained in South Africa (*CURPOLm*), the net energy system costs decrease to 102.6 billion USD, which is 4% lower than in the *CURPOL* scenario. If a GHG emission constraint is then applied to South Africa, the net system costs, again, increase, rising to 104.7 billion USD under the *unconditional* GHG emission constraint, to 108.8 billion USD under the *partially conditional*, and to 118.1 billion USD under the *fully conditional* GHG emission constraint. However, the negative offset between the *non-m* and the *m*-scenario remains at a similar level throughout the scenarios. This causes the net energy system costs in the *m*-scenarios to remain below those in the only nationally GHG constrained scenarios.

The separation of the six main cost components shown on the left in figure 3.4 provides insights into the cost structure and the formative effects induced by the national and the global emission constraints on South Africa's energy system costs. The figure shows that for South Africa, the "traditional" energy system cost components (the investment, maintenance and variable costs) shown in the first three columns of the figure - contribute up to 70% of the total energy system costs. As dominant share, they significantly shape the total energy system cost structure. In the presented scenarios these cost components follow the expected results: the more stringent the GHG emission constraint, the higher the cost. However, in contrast to the total energy system costs, the introduction of a global emission constraint increases South Africa's energy system technology cost (investment, maintenance, and operation costs).

Trade costs make up the second biggest component of the net energy system costs. While the import costs are rather invariable across all tested scenarios (between 32.4 and 36.8 billion USD) the export revenue varies across the wide range from 25.2 to 41.1 billion USD. Across this range there are several effects to be observed. In the *non-m* scenarios the export revenue remains rather constant. If, however, a stringent GHG emission constraint is applied to the *m*-regions, South Africa's export revenue increases significantly by up to 60%. Especially, if no GHG emission constraint is applied to South Africa, the country can monetise the increasing demand for synthetic fuels on the international market. If however a GHG emission constraint is applied to South Africa, these revenue options decrease as the country (i) is limited in the amount of coal to be refined to synthetic fuels in plants without carbon sequestration and (ii) needs to supply the domestic synthetic fuel demand that rises in line with the stringency of the GHG emission constraint.

Figure 3.5 summarises the energy system costs in the two *current policies* and the six NDC scenarios for South Africa.

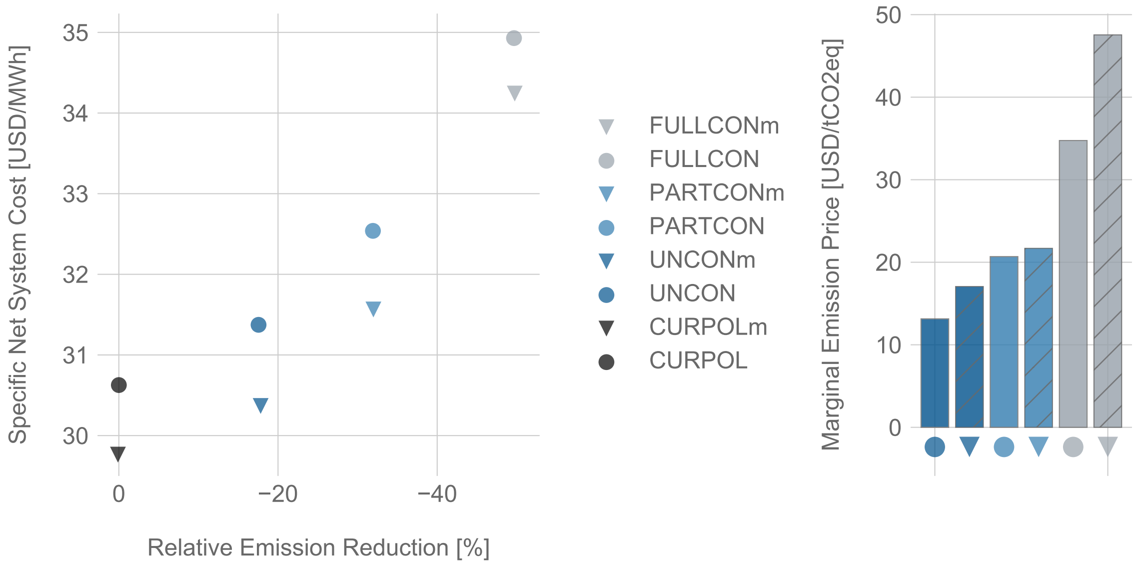

Figure 3.5: Cumulative greenhouse gas emission reduction (2021-2050) in relation to the average specific energy costs (left) and the marginal emission price (right) in South Africa in the current policies and the NDC scenarios (see table 3.2). The grid hatched bars indicate the m-scenario, the dotted hatched bars represent the non-m scenarios.

On the left panel it shows the average specific net energy system costs in relation to the relative cumulative (2021-2050) emission reduction in South Africa. Here, the specific energy system costs are defined as the fraction of the net total energy system costs as numerator and the useful energy demand as the denominator.

The data on the left panel emphasise what has been discussed above: reducing energy system related GHG emissions over the projection period (2021-2050) by up to 49.8% as proposed in South Africa's NDC is technically feasible, it however comes at a cost. By increasing the GHG mitigation effort, the national specific energy supply costs increase from 30.6 USD/MWh to 34.9 USD/MWh (14%). However, international mitigation ambition can reduce the specific net system costs (by up to 3%) by giving South Africa the opportunity to alter its export portfolio from a low-margin coal dominated to a more balanced portfolio including a mix of advanced synthetic fuels of higher margin

The right panel in figure 3.5 compares the marginal emission price for the six NDC scenarios. The marginal emission price is defined as the amount, to which the model objective function can be reduced for each additional unit for which the GHG emission constraint is relaxed. The marginal emission price is often interpreted as the level, to which an economy-wide emission price would need to be raised in order to achieve the desired emission reduction. The figure indicates that the export opportunity, which is induced in the m-scenarios, raises the marginal emission price in South Africa. Hence, in the m-scenarios a higher price would need to be put on GHG emissions in order to limit GHG emissions to desired levels.

3.2.3 Energy Supply System

South Africa's national GHG emission constraint, as well as the constraints on the m-regions has a significant impact on the country's energy supply structure. The projected structural change of South Africa's energy system is summarised in figure 3.6.

In the top row, figure 3.6 presents the total primary energy supply, the second row summarises the development of South Africa's trade balance. In the trade balance negative values indicate net export and positive values net imports. The two panels confirm what was described for the *current policies* scenario (see section 2.5.2): over the evaluation period (2020-2050) total primary energy supply as well as trade activity increases. However, the national as well as the global emission constraint both have an influence on the level of the total increase as well as the distribution of the supply by commodity split.

The application of a national GHG emission constraint (*non-m* scenarios) increases the average efficiency of the energy system and hence decreases the total primary energy required to supply the energy demand. This energy efficiency increase is realised by a continuous fuel switch, away from carbon-intensive fuels such as coal and unrefined crude, towards cleaner and more efficient fuels such as natural gas, clean synthetic and other refined liquid fuels as well as renewable and nuclear energy. While in the reference year 71% of the total primary energy supply is coal-based, this share decreases over the evaluation period to 34% in the current *policies scenario* (*CURPOL*) and even further to 20% if the *fully conditional* GHG emission constraint is applied (*FULLCON*).

In contrast, the liquid and synthetic fuel shares increase from 2% to 11% in the current *policies scenario* (*CURPOL*) and up to 21% under the most stringent national GHG emission constraint (*FULLCON*). Simultaneously the renewable energy consumption more than doubles under *current policy* assumptions (*CURPOL*) and more than quadruples under the *fully conditional* GHG emission constraint (*FULLCON*).

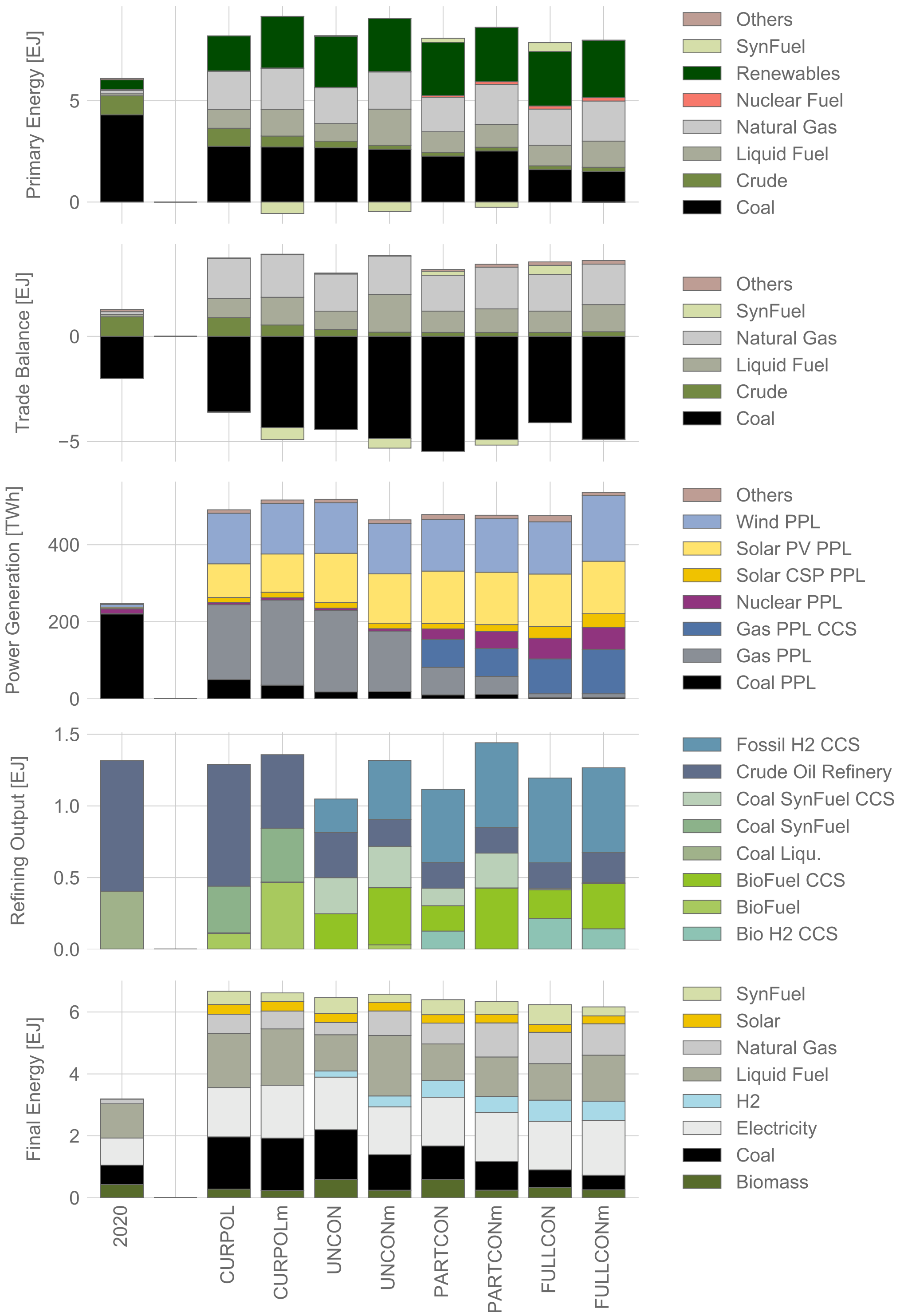

Figure 3.6: South Africa's primary to final energy supply system structure in the reference year 2020 and the last evaluation year (2050) in the NDC scenarios and the current policies reference (see table 3.2). (PPL: power plant, CCS: carbon capture and storage, PV: solar photovoltaics, CSP: concentrated solar power, H2: Hydrogen)

The additional renewable energy use and the majority of the synthetic fuel demand can be supplied by domestic means. However, the shift in the energy commodity supply mix still induces a doubling of the liquid fuel and natural gas imports. Throughout all scenarios natural gas imports from neighbouring countries and the refined fuel import from the international commodity market, supply between 45% under *current policy* assumptions (*CURPOL*) to 36% (*FULLCON*) of the total primary energy demand.

Next to the *non-m* scenarios, figure 3.6 depicts the primary energy demand in the in the respective *m-scenarios*. Across all levels of the emission constraint, the *m*-scenarios exhibit a higher primary energy demand.

The comparison of the primary energy demand in the *m*-scenarios with the *non-m* scenarios suggests that the increased international demand for clean synthetic fuels becomes a main driving force for South Africa's energy system structure. By 2050 the export market opportunity induces an increase in total primary energy demand of 5% under *current policies* (*CURPOLm*) assumptions to 1% under the most stringent national GHG emission constraint (*FULLCON*). This drop in overall energy system efficiency, which can be allocated to the increased production of synthetic fuels for the export market, is compensated to some degree by the increased import of efficient fuels such as natural gas and liquid refined fuels. With increasing stringency of the domestic GHG emission reduction targets, the synthetic fuel production for the international market subsides, and coal, South Africa's single dominant export energy commodity, recurs as a fuel for CCS applications in the carbon restrained *m*-regions.

In the third row figure 3.6 depicts the development of South Africa's power generation portfolio. It suggests that the power generation technology mix depends predominantly on the applied national GHG emission constraint. First, the lenient GHG emission constraint (*UNCON*/*UNCONm*) decreases the share of conventional coal-fired thermal power stations in favour of renewable power stations, such as solar photovoltaics and wind turbines. With increasing stringency, renewable power generation facilities continue to rise, the natural gas fired power stations that supplement the renewable power park are now fitted with carbon sequestration units, making natural gas CCS power plants the dominant non-renewable power source. Simultaneously with the introduction of cost-intensive carbon sequestration units for thermal power stations, new nuclear power facilities are introduced as a (now cost-competitive) base to mid-load power supplier (*PARTCON*/*PARTCONm* to *FULLCON*/*FULLCONm*).

In the second to last row, figure 3.6 describes the refining output in South Africa in 2050. The figure indicates a clear cost order for the different technological fuel production options, which can be described as a function of the marginal carbon price. With increasing pressure resulting from limitations of the GHG emissions the relative share of inexpensive crude oil refinery outputs decreases while outputs from more expensive refining products such as coal-derived synthetic fuels and - most important - hydrogen production from fossil sources increase. Hence, with increasing stringency of the national GHG emission constraint crude oil refinery outputs decrease while outputs from first synthetic fuel and later hydrogen production increase. In the *current policies* scenarios (*CURPOL*/*CURPOLm*), only synthetic fuels are produced from predominantly coal and biomass. However, already under the most lenient GHG emission constraint (*UNCON*/*UNCONm*) carbon sequestration, technologies for synthetic fuel and clean hydrogen production become dominant and the first net-negative emission technologies are introduced into the market (e.g. synthetic fuel production from biomass using CCS). With increased stringency of the GHG emission constraint ($PARTCON/PARTCONm$ to $FULLCON/FULLCONm$) the produced amount of clean hydrogen increases simultaneously to the increase of net negative-emission synthetic fuel production. While this pattern is visible across all scenarios, the introduction of a carbon constraint for the m-regions enhances this effect for all national GHG emission constraint scenarios (m-scenarios).

Finally, in the bottom row of figure 3.6, the final energy supply structure in 2050 in South Africa is outlined. The plot suggests that the South African end-use sector has little scope for change. The plot suggests that by 2050 the overall final energy supply will remain about the same: throughout all scenarios, the final energy demand varies by less than 8%. This is due to the inelastic demand representation of the applied model. On the other hand, the results of the final energy supply structure reflect the limited acceptance of technological changes by the end-use sector that can also be observed in the real world. In contrast to the secondary energy transformation sector, where a small number of large-scale installations are planned and cost-optimised, the end-use sector is characterised by a variety of small-scale applications that are labour-intensive to renew and where high installation costs are considered barriers to the technology transition processes by the investment-decision makers. Hence, in the end-use sector the vintage capacity stock as well as the investment and installation costs are the dominant factors over operation costs. Thus technology choice in the end-use sector is less affected by the marginal carbon price that exerts an effect only via the operation costs. Nevertheless, the GHG emission constraints induce a change in the end-use sector fuel mix. With rising stringency, coal and liquid fuel use are increasingly replaced by electrification and the application of synthetic fuels and hydrogen.

3.2.4 Conclusion

In this section the technical feasibility and the cost- and system-impact of limiting South Africa's GHG emissions to the trajectories proposed in the NDC were tested under two global assumptions: (i) applying GHG emission constraints for South Africa, within the global framework from the *current policies* reference calibration; and (ii) rerun the first set with the modification that the countries aggregated in the three most economically advanced model regions - North America (NAM), Western Europe (WEU), Pacific OECD (PAO) - were additionally constrained to reach GHG emission reduction trajectories equivalent to the RCP2.6 scenario.

The scenario analysis provided several insights. First, significantly reducing GHG emissions compared to *current policies* reference is possible on a national as well as on a global scale. Second, even under the most lenient emission constraint the near-term investment in carbon-intensive energy infrastructure is not economically competitive. In contrast, the model results show that the long run-times and slow infrastructure transition speeds inherent to the energy supply sector require immediate action for even fulfilling the most lenient GHG emission constraint within the next decade.

Third, limiting South Africa's GHG emissions to the trajectories as suggested in the NDC scenarios increases total net energy system costs by up to 15%. However, mitigation synergies can be found if economically more advanced nations implement strong GHG emission reductions. In these scenarios the economically more advanced nations can create international market conditions that provide other nations the option to follow on the mitigation pathway: (i) establishing a surplus of mid-range carbon-intensive fuels (e.g. natural gas) on the international commodity market, makes them cost-competitive with more GHG emission-intensive fuels for countries without or a less stringent carbon constraint; (ii) increasing global demand for new synthetic fuels, provides other countries (e.g. South Africa) with the option to alter the export portfolio and transition it away from low-grade fuels (e.g. coal) in favour of synthetic fuels of bigger margin. Together these effects can lower the mitigation costs for South Africa (up to 4%).

Finally, international mitigation efforts do not only increase the export margin of South Africa but they also increase the marginal carbon price, which in turn means that more stringent policy measures will be required nationally in order to achieve the same level of GHG emission mitigation.

The presented scenario analysis indicates that substantial GHG emission mitigation is technically feasible on a national, and on a global scale and that synergies can be utilised if emission mitigation is coordinated internationally. However, the scenario analysis leaves open how the GHG emission mitigation effort can be distributed among nations for cost-optimal mitigation results. Therefore, in the following sections, two different global mitigation strategies are explored under the aspect, to which degree South Africa could and should contribute to such an *optimal* GHG emission mitigation strategy.

3.3 Results of the Global Mitigation Scenarios

In this section the results of the global mitigation scenarios are presented. As described above, these global mitigation scenarios are designed for exploring cost-optimal strategies on reducing global GHG emissions in line with the adjusted RCP GHG emission trajectories (RCP1.9 - RCP6.0). In order to define the cost-optimal strategy on reducing global GHG emission, the GHG emission constraints were first applied to the global emission sum (*OPT19*-*OPT60*). Thereafter and in order to quantify the effects of non-cooperative emission mitigation strategies, the required percentage reduction was applied to every model region separately (*EQU19*-*EQU60*).

Below, the results of these mitigation scenarios are compared and discussed. However, an *equal-share* emission reduction proved infeasible under the most stringent GHG emission constraint RCP1.9. Therefore, the scenario set *EQU19* and the globally optimised counterpart *OPT19* are removed from the presented scenario results.

3.3.1 Greenhouse Gas Emission Trajectories

The global GHG emission trajectories for the eight evaluated global mitigation scenarios and the *current policies* reference are illustrated in figure 3.7. The modelled GHG emissions include all energy-related CO_2 and CH_4 emissions from the energy sector. Unsurprisingly, the figure shows that the global emission balance follows the four predefined RCP trajectories in all *global mitigation* scenarios, indicating the technical feasibility of limiting global emissions to the proposed levels.

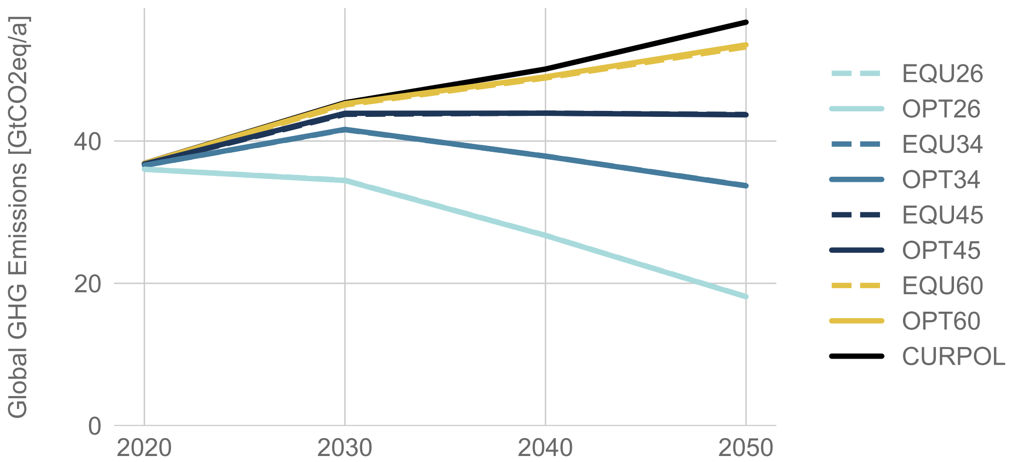

Figure 3.7: Global GHG emission trajectories in the current policies (CURPOL) reference and the global mitigation scenarios (see table 3.3).

3.3.2 Global Energy System Costs

For the eight mitigation scenarios (*OPT26*/*EQU26* to *OPT60*/*EQU60*) and the *current policies* (*CURPOL*) reference, the cost impact is depicted in figure 3.8. On the left hand side, the figure shows the global average specific mitigation costs over the cumulative GHG emission reduction compared to the *CURPOL* reference. On the right hand side, the figure presents the total global energy system cost increase in comparison to the *current policies* reference scenario. All shown values are summed over the projection period and all model regions.

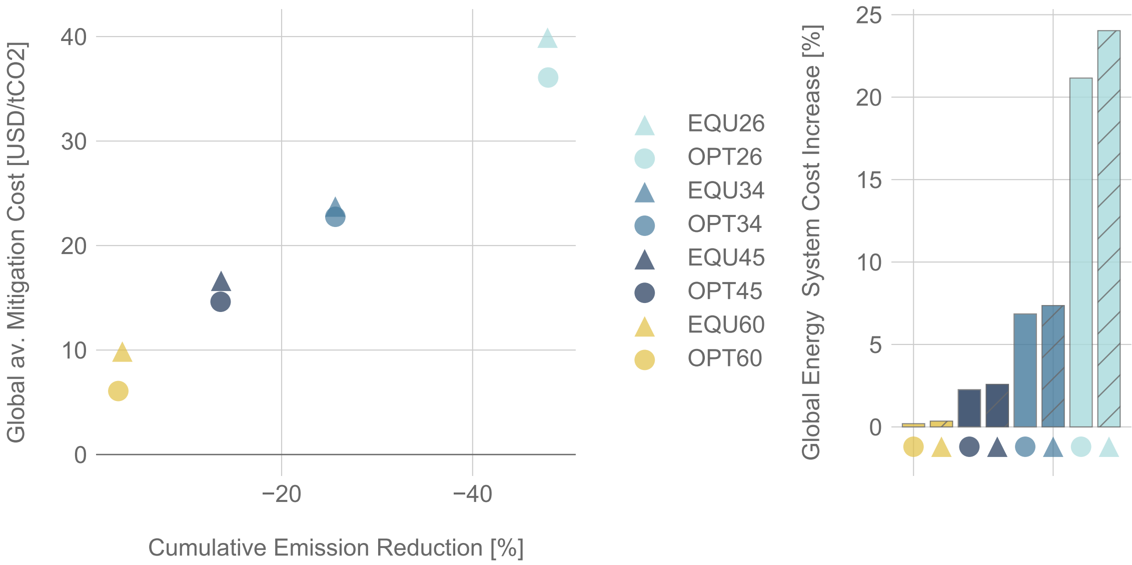

Figure 3.8: Left: global average specific mitigation costs over the GHG emission reduction compared to the current policies (CURPOL) reference. The average specific mitigation costs are defined as the ratio between the total discounted net system cost increase and the GHG emission reduction both summed over the projection period. Right: total global energy system cost increase in comparison to the CURPOL reference. All shown values are summed over the projection period (2021-2050) and all model regions.

The figure indicates that reducing GHG emissions increases global energy system costs. Furthermore, the data suggests that the cost increase is first and foremost influenced by the GHG emission constraint, but, to a lesser extent, also by the GHG emission mitigation strategy. With increasing stringency the total energy system costs increase by 0.1-0.4% under the RCP6.0, 2.3-2.6% under the RCP4.5, 6.9-7.4% under the RCP3.4 and 21.2-24.0% under the RCP2.6 GHG emission constraint with the respective lower values representing the *globally optimised* (*OPT*) scenarios (see figure 3.8 right).

As the cumulative (2021-2050) GHG emission reduction in the RCP scenarios is, by definition, dictated by the applied GHG emission constraint, in both the *equal-share* (*EQU*) and the *OPT* scenarios, the total global energy system cost increase is also reflected in the average specific mitigation costs. Here too the stringency of the GHG emission constraint is the dominant influence on the mitigation costs while the mitigation strategy has a subordinate effect. Nevertheless, all *OPT* scenarios realise the imposed emission reduction at lower costs (see figure 3.8 left). The figure shows the global average specific mitigation costs to range from about 6-10 USD/tCO_2eq for the relatively lenient RCP6.0 scenarios, 15-17 USD/tCO_2eq for the RCP4.5 scenarios, 23-24 USD/tCO_2eq for the RCP3.4 scenarios, and 36-40 USD/tCO_2eq for the RCP2.6 scenarios. The difference between the mitigation costs in the OPT an the EQU scenario is larger at both ends of the tested scenarios.

3.3.3 National Energy System Costs

Figure 3.9 depicts the regional average specific mitigation costs over the GHG emission reduction in the *globally optimised* (OPT) and the *equal-share* (EQU) scenarios. The most prominent difference between the two scenario sets, is, as expected, the distribution of GHG emission reductions among the model regions. In the EQU scenarios, the model regions are, despite spread across a wide range of national mitigation costs, concentrated around the predefined emission reduction. However, with increasing stringency of the GHG emission constraints, the concentration scatters. This is due to the limited GHG emission reduction potential of several model regions and indicates that the feasibility of the equal-share scenarios is conditional to a certain degree of lenience in the definition of an "equal" share (see below for further detail).

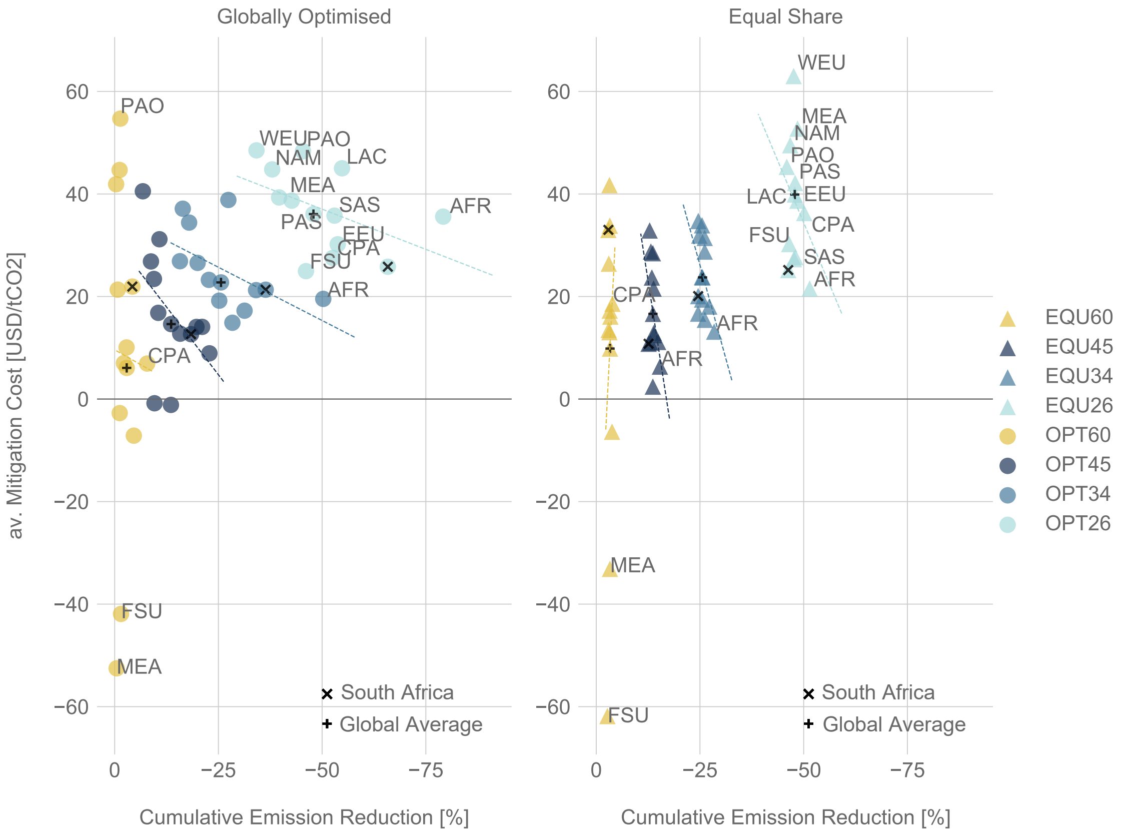

Figure 3.9: Model results showing the average specific mitigation costs over the GHG emission reduction in the globally optimised (OPT) (left) and the equal-share (EQU) scenarios (right). The average specific mitigation costs are defined as the ratio between the total nodal (regional) discounted net system cost increase and the total nodal GHG emission reduction, both summed over the projection period (2021-2050). The dashed lines indicate the least square error trends. The strong negative emission mitigation costs for Former Soviet Union (FSU) and Middle East and Africa (MEA) regions under the RCP6.0 constraint are related to a price increase for natural gas on the international commodity market (see discussion of market prices below).

In the *OPT* scenarios, the global emission reduction goal is achieved through the strong GHG mitigation of some model regions rather than the equal emission reduction of all model regions. For example the Sub-Saharan Africa (AFR) region reduces its cumulative (2021-2050) GHG emissions over the projection period by more than 50%, South Africa (ZAF) by more than 40%, while the Middle East and North Africa (MEA) region merely reduce emissions by 20%. In contrast, in the *EQU* scenarios that are designed to proxy for a *globally uncoordinated* emission mitigation strategy, the mitigation of every model region is defined to be exactly the same. However, if the mitigation target is infeasible to reach for any one model region the excess GHG emissions can be compensated for by another region. This share of emission reduction that has to be reallocated from one region to another rises from 3% to 10% with increasing stringency of the GHG emission constraint.

The second effect visible in figure 3.9 is a steepening of the *mitigation cost-to-emission* *reduction diagonal*. This is because of the prescribed emission reduction targets. Thus, in the *OPT* scenarios the regions, which experience higher than average mitigation costs reduce fewer emissions (top left markers of every colour, e.g. Western Europe (WEU) in the *OPT26* scenario) and regions that are confronted with lower costs reduce more (lower right markers, e.g. AFR in the *OPT26* scenario). In the *EQU* scenarios, however, this beneficial distribution is not an option. Thus, regions with large economic GHG emission reduction potentials limit their emission reduction to the prescribed global average and hence also their average GHG mitigation costs (i.e. they move left and down), while regions with lower economic GHG emission reduction potentials have to increase their mitigation efforts (i.e. move right and up).

The mitigation costs are spread among the regions, thus indicating their different GHG emission reduction potentials and technological shift capacities. Hence, while Western Europe's GHG emission reduction is dependent on a region-wide technology transition and on clean fuel imports, resource-rich economies with great GHG emission reduction potential - such as South Africa - can provide high quality clean fuels to other, more emission-restricted model regions and hence profit of their enhanced export portfolio. This effect can be observed to cause the negative mitigation costs for the MEA and the Former Soviet Union (FSU) region under the least stringent GHG emission constraint RCP6.0.

3.3.4 Economic GHG Emission Reduction Potential

One of the most important parameters for successful and cost-effective climate mitigation measures is the economic GHG emission reduction potential, which is defined as the amount of GHG that can be cost-competitively mitigated by a model region compared to the *current policies* reference scenarios (*CURPOL*). As there is no absolute value to compare the cost competitiveness against, it is here established as being less costly than in the other model regions - and hence showing as a bigger/smaller emission reduction compared to global average in the *globally optimised* scenarios (*OPT*).

Figure 3.10 shows the cumulative greenhouse gas (GHG) emissions per region in the *CURPOL* reference (grey bars) and the offset of the regional cumulative GHG emission reduction compared to the global average required to reach the RCP target trajectory in the *OPT* scenarios. Among the *equal-share* scenarios (*EQU*) the deviation is, by scenario design, limited and therefore not relevant to exploring the economic GHG emission reduction potential. By comparing the offset from the global average mitigation, the figure provides insights into the uneven distribution of the economic GHG emission reduction potential among the model regions. The figure shows a ranking of the individual model regions in the *OPT* scenarios: while Sub-Saharan Africa (AFR), South Africa (ZAF), South Asia (SAS), Latin America and the Caribbean (LAC), Central and Eastern Europe (EEU), and centrally planned Asia and China (CPA) exhibit a positive offset from the mitigation target (i.e. they mitigate more than the global average), the regions Middle East and North Africa (MEA), non-OECD Pacific Asia (PAS), Former Soviet Union (FSU), North America (NAM), Pacific OECD (PAO) and Western Europe (WEU) reduce less GHG emissions than targeted.

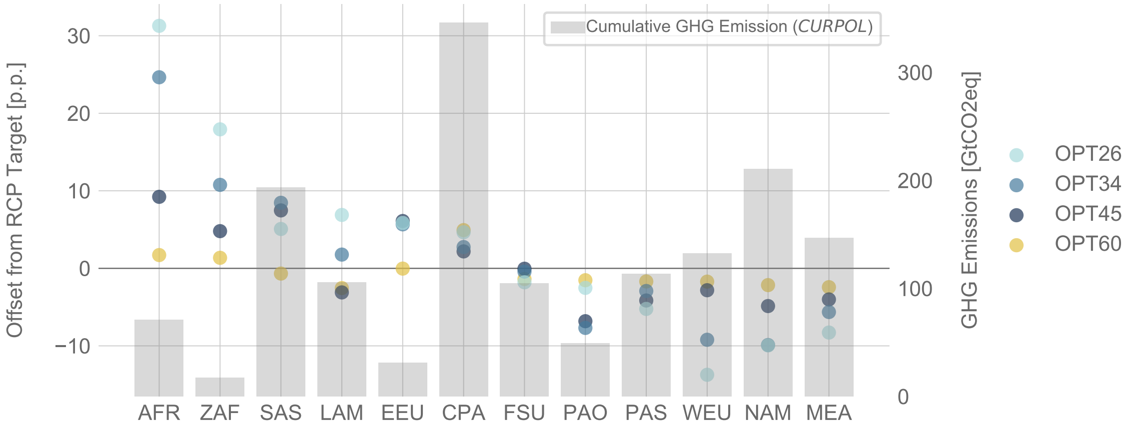

Figure 3.10: Cumulative GHG emissions per model region in the current policies reference scenarios (grey bars) and the offset of the cumulative GHG emission reduction compared to the global average in the globally optimised scenarios (OPT). A positive offset indicates a surplus in GHG emission reduction, while negative values indicate the opposite. The offset is measured in percent points (p.p.), the total cumulative GHG emissions are shown in $GtCO_2eq$, all cumulative values are summed over the projection period (2021-2050). The regional acronyms are defined in the appendix B.1.

Understanding the Variation in the GHG Emission Reduction Potential

As described above, the economic GHG emission reduction potential varies significantly among the model regions. The structural dynamics within the mixed-granularity model, which lead to this wide spread, are numerous and will be explored exemplary for South Africa in detail (see section 3.3.5).

However, figure 3.11 provides some general insights into the suspected main causes for the regional variation by showing some of the most important factors that influence the economic GHG emission reduction potential. It shows the correlation between the GHG emission reduction and the (i) useful energy demand growth over the projection period, (ii) the share of coal and (iii) the share of renewable energies in total primary energy supply in the *current policies* reference scenario (*CURPOL*). The degree of GHG mitigation in a region in the *OPT* scenarios is used as a measure for its economic GHG emission reduction potential.

Aim of this analysis is to test two hypotheses on the regional economic GHG emission reduction potential. The first hypothesis is that a fast increase in demand allows for a rapid economic system improvement as the influence of vintage capacity loses significance. The second hypothesis is that the energy mix in the *current policies* reference (*CURPOL*) has an impact on the change capabilities of the energy system.

Although *correlation* does not necessarily indicate *causation*, figure 3.11 is useful to understand the main levers in defining the regional mitigation costs and hence the GHG emission reduction potential. The Pearson coefficient is provided to quantify the degree of the correlation. By definition the Pearson coefficient can vary between -1 and +1, with a negative sign indicating a negative and a positive sign indicating a positive linear correlation. Here, however, the correlation between positive factors (e.g. the share of coal) and a negative factor (GHG emission reduction) is tested and hence the sign of the Pearson coefficients is inverted. A negative Pearson coefficient should, thus, be interpreted as a measure for a positive linear correlation between e.g. the share of coal in primary energy and the emission reduction. As a measure of the statistical significance of the correlation the P-values are provided.

The top plot in figure 3.11 shows the correlation between the GHG emission reductions in the *OPT* scenarios compared to the *CURPOL* reference and the useful energy demand growth over the projection period. The data indicate a positive linear correlation between the economic GHG emission reduction potential of the model regions and the respective demand growth over the projection period. This supports the hypothesis that the more the demand grows, the bigger the economic decabonisation potential of a region or country is. The Pearson correlation coefficient also supports this hypothesis: for all moderate mitigation scenarios (*OPT26*, *OPT34*, *OPT45*) the Pearson coefficient is in the range of -0.7 and hence indicates a moderate linear correlation between the two variables. However, in the very lenient *global mitigation* scenario (*OPT60*), the Pearson coefficient drops to about -0.2 and the P-value rises to around 0.5, which suggests a weak and statistically irrelevant correlation. A plausible explanation for this could be that while in the more stringent *OPT26*-*OPT45* scenarios the vast capacity stock of currently existing energy infrastructure holds back the transition of the energy sector, in the very lenient *OPT60* GHG emissions can be reduced sufficiently by changing the energy supply at the new build rate - hence not requiring decommissioning of historic capacity stock before their end-of-life.

A similar effect can be observed in the two other plots of figure 3.11 that describe the correlation between the GHG emission reductions in the *OPT* scenarios compared to the *CURPOL* reference and the share of coal (center) and the share of renewable energy (RE) (bottom) in total primary energy supply (TPES) in the *CURPOL* reference. The correlation between the share of coal in the total primary energy supply in the *current policies* (*CURPOL*) reference and the cumulative (2021-2050) GHG emission reduction in the *globally optimised* mitigation scenarios (*OPT*) suggests that the coal share can have an impact on the economic GHG emission reduction potential of that region. The Pearson coefficient confirms this hypothesis of a moderate linear correlation for all scenarios, but this linear relationship weakens with increasing stringency of the respective *OPT* scenario. For renewable energy a similar effect can be observed. However, the correlation under the lenient GHG emission constraint (*OPT60*) is weak and becomes more pronounced with increasing mitigation targets (such as in the *OPT34* and *OPT26* scenarios).

In summary, the model results suggest that the mitigation costs of a model region and hence the economic GHG emission reduction potential is correlated to the currently existing energy infrastructure. While the data shows that the demand growth over the projection period correlates with the economic GHG emission reduction potential, this can be interpreted as the GHG emission impact by the existing capacity stock. With its long lifetimes and high investment costs, the energy sector relates slow demand growth with a slow rate of change, as mitigation costs rise if carbon-intensive infrastructure ends operation before end-of-live as stranded asset.

Furthermore, the numbers indicate that model regions, which depend heavily on carbon-

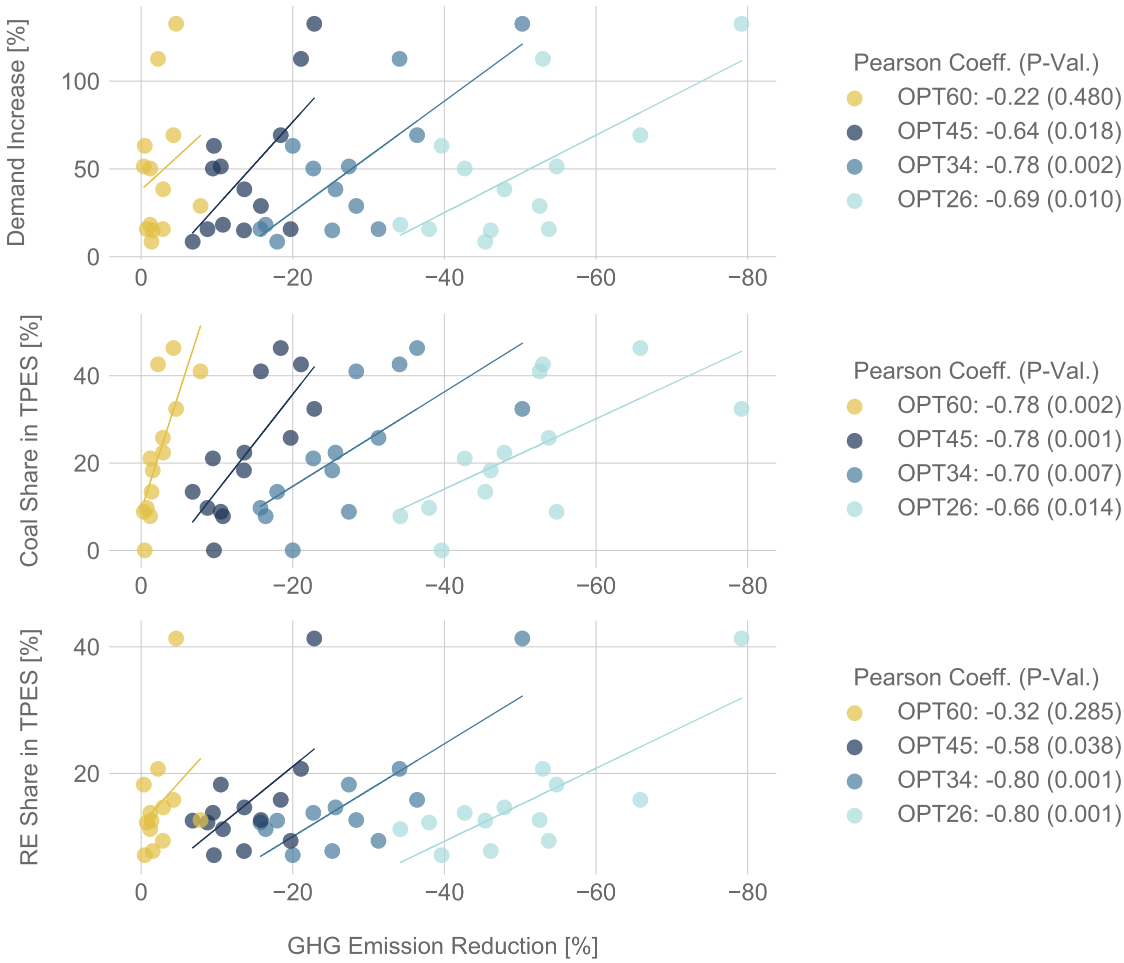

Figure 3.11: Correlation between the GHG emission reduction (summed over the projection period) and the useful energy demand growth over the projection period (top), the share of coal (center) and the share of renewable energies (bottom) both measured as share in total primary energy supply (TPES) in the current policies reference scenario (CURPOL). The shown degree of GHG mitigation in a region in the globally optimised scenarios (OPT) is used as a measure for the economic GHG emission reduction potential. The markers indicate the scenario results in the model regions, the lines indicate the least-square-error linear trend per scenario. The GHG emission reduction is calculated relative to the reference scenario. The Pearson coefficient is a measure of linear correlation (here values <-0.5 are considered an indication for linear correlation), the P-Value is a measure of statistical significance (here values <0.05 are considered an indication for statistical significance). Projection period: 2021-2050

intensive coal infrastructure in the *CURPOL* reference are also the ones that have the best economic GHG emission reduction potential in all but most stringent (*OPT26*) scenario. This can be related to the fact that replacing carbon-intensive coal-based infrastructure with more efficient cleaner fuels provides a significant cost-efficient GHG emission reduction potential. In the most stringent scenario (*OPT26*), however, this restructuring might not be sufficient and hence the correlation fades.

Finally, the renewable energy share correlates with the GHG emission reduction in all but the least stringent scenario (*OPT60*). This indicates that the model regions where renewable energy sources are readily available and cost-effective to deploy in the *CURPOL* scenario, also hold the potential to cost-effectively intensify the utilisation of these natural resources if a GHG emission constraint is applied. However, while the renewable energy deployment in the *CURPOL* reference scenario correlates with the GHG emission reduction, the renewable energy potential does not (see appendix C). This indicates that the total renewable energy potential of each model region is big enough as to not be the limiting factor to GHG emission reduction, but that rather the transition speed of the energy sector is what slows down the system transition and hence, GHG emission reduction.

3.3.5 A View on South Africa

One of the important questions that stimulated the development and realisation of MIGRA-NEST was to find out, what the likely and what the desirable energy system transition options are for a country and how global mitigation actions influence the country's options for achieving a change in its GHG emission targets. The second question of interest was, which role a specific country could play in a global mitigation scenario and how global interactions might benefit and or challenge the country's energy system and mitigation ambitions. Therefore, in the following, South Africa's role in a globally coordinated mitigation strategy (*OPT*), and the cost as well as system impact of this role are evaluated. In order to quantify these impacts the scenarios are compared to the conditions under an *equal-share* (*EQU*) mitigation distribution.

Greenhouse Gas Emission Trajectories

Figure 3.12 shows the model results for the development of South Africa's GHG emissions from the energy sector (CO_2 and CH_4) in the four *OPT* and four *EQU* mitigation scenarios, as well as in the *current policies* reference (*CURPOL*).

The plot indicates that global GHG emission constraints induce a significant GHG emission reduction in South Africa. Already under the RCP4.5 global emission constraint, GHG emissions in South Africa are reduced to values compatible with South Africa's NDC pledge (*OPT45*). Furthermore, in the *OPT26* scenario, South Africa's GHG emissions are cut even to below the conditional NDC target. The results presented in figure 3.12 confirm what was already identified before: in the global emission mitigation scenarios South Africa contributes significantly more to the global GHG mitigation than the international average (e.g. visible as positive offset in figure 3.10). While in the four *OPT* mitigation scenarios South Africa's cumulative GHG emissions over the projection period (2021-2050) are reduced by -4% in the lenient *OPT60* scenario, by -18% in the *OPT45* scenario, by -36% in the *OPT34* scenario, and -66% in the most stringent *OPT26* scenario, the cumulative emission reductions in the *EQU* scenarios are considerably lower, namely -3%, -13%, -25%, and -46%, respectively (see figure 3.12).

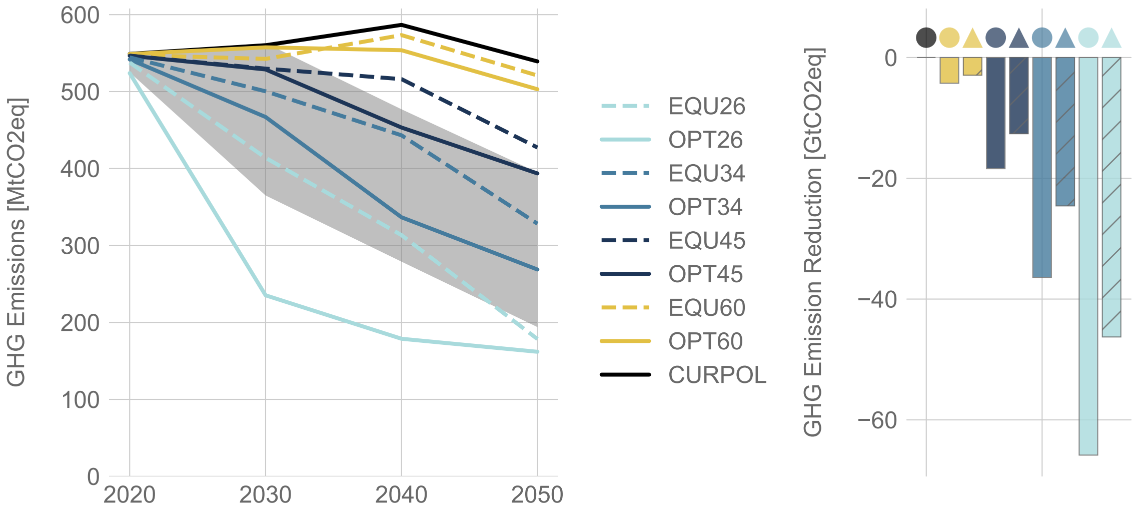

Figure 3.12: South Africa's GHG emissions in the four globally optimised mitigation (OPT) as well as in the four equal-share (EQU) scenarios, and in the current policies reference (CURPOL). GHG emissions refer to the contributions of CO_2 and CH_4 in the energy sector. The grey-shaded area indicates the NDC emission range pledged in South Africa's NDC. The solid lines show the results of the OPT scenarios, the dashed lines indicate the results of EQU scenarios. The bars on the right hand side indicate the cumulative GHG emission reduction over the projection period (2021-2050).

Energy System Costs

Figure 3.13 shows the total discounted net energy system costs in South Africa in the *OPT* and the *EQU* mitigation scenarios, and the *CURPOL* reference. As before (see section 3.2), here too, the constituting cost components as well of the total net energy system costs are depicted separately.

The analysis of the results indicates two effects. First, total net energy system costs relate strongly to the GHG emission reduction and hence, increase with increasing stringency of the GHG emission constraint. However, another effect is visible in the data: for every scenario, the triangular markers are below their circular marker counterparts. This means that South Africa faces higher costs in the *OPT* than in the *EQU* scenarios. This cost-effect is on the one hand related to the lower GHG emission reduction imposed on South Africa by the objective function - i.e. a higher GHG emission allowance permitting the use of carbon-intensive low-cost fuels. On the other hand this is connected to a significantly higher global demand for clean fuels. For South Africa this new demand poses the opportunity to turn into a high-quality clean fuel producer by refining the abundant locally available coal and combining it with carbon capture technologies.

Energy Supply System

Both the global GHG emission constraints, applied as total global (*OPT*) or as *equal share* on model region level (*EQU*), have a significant impact on South Africa's energy system. Figure 3.14 summarises this structural change in both the *OPT* and the *EQU* global

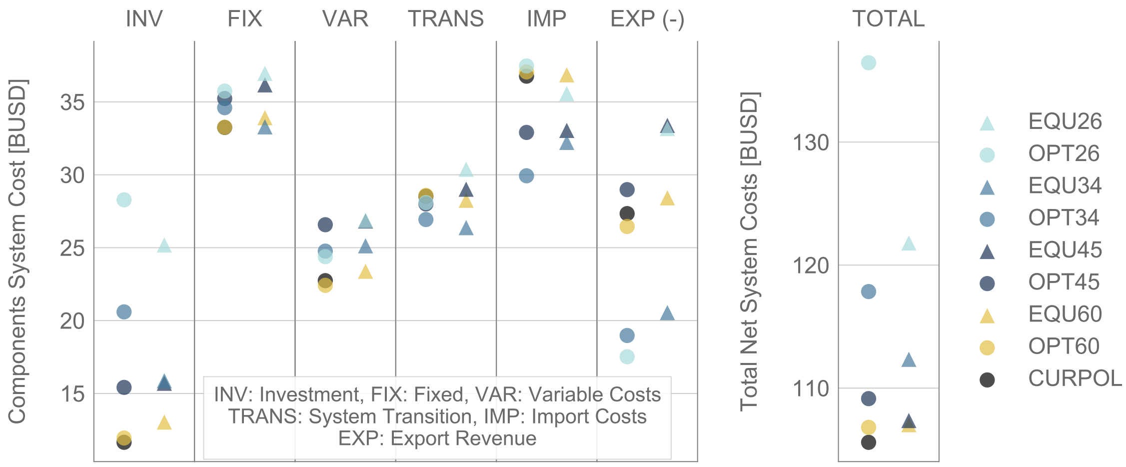

Figure 3.13: Total discounted net energy system costs and the energy system cost components for South Africa in the in the globally optimised (OPT), and the equal-share (EQU) mitigation scenarios as well as in the current policies (CURPOL) reference. The costs are expressed in Billion USD. The total net system costs are equal to the sum of the technology costs (INV, FIX, VAR), the transformation costs (TRANS) and the fuel import costs (IMP) minus the export revenue (EXP).

mitigation scenarios. In line with the results of the *NDC* scenarios presented before, the sub-figures show (i) the total primary energy demand, (ii) the trade balance, (iii) the power generation per fuel type, (iv) the output from the refining sector by energy commodity, and (v) the final energy consumption by fuel. As before, here too, the trade balance accounts for exports by negative values, and imports by a positive sign.

On first sight, the figure indicates two effects: first, the defined global emission scenario has a great influence on the energy system structure. Second, also a clear distinction between the *OPT* and the *EQU* scenarios can be made. However, while the overall stringency level of the GHG emission constraint influences the entire structure of South Africa's energy system, the difference between the respective *OPT* and the *EQU* scenarios seem to focus its effects on the refining sector and the trade balance.

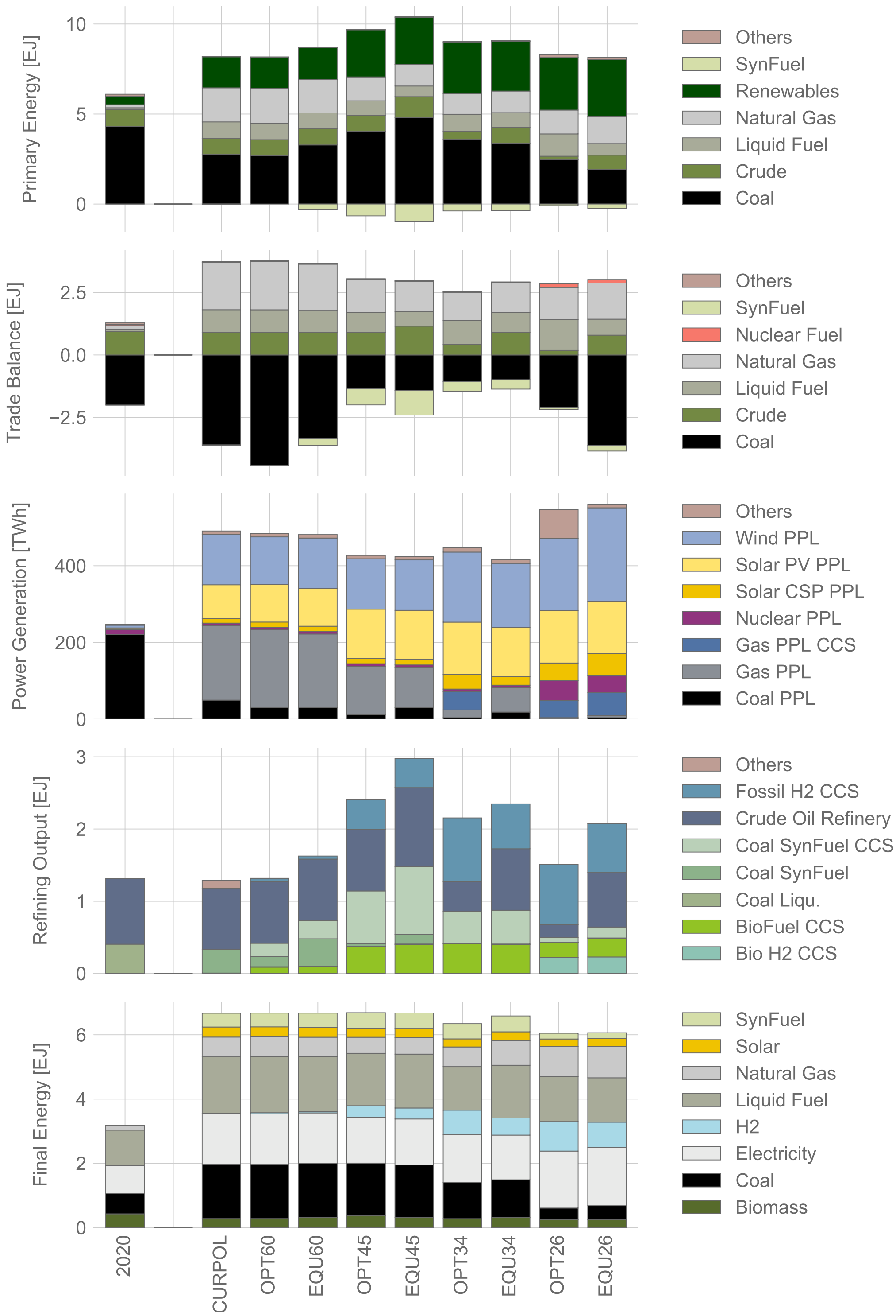

Figure 3.14: South Africa's primary to final energy supply system structure in the reference year 2020 and the last evaluation year (2050) in the globally optimised (OPT) and the equal-share (EQU) mitigation scenarios and the current policies reference. (PPL: power plant, CCS: carbon capture and storage, PV: solar photovoltaics, CSP: concentrated solar power, H2: Hydrogen)

In the first row of figure 3.14 the primary energy supply of South Africa is summarised. Together with the second row, which depicts the trade balance, the figure reveals the dominant factors, which shape South Africa's energy system in both the *EQU* and the *OPT* mitigation scenarios. The figures show how trade and the international commodity market are key drivers for the modelled energy system. Hence, in the least stringent *OPT* scenario (*OPT60*) coal trade remains South Africa's single export commodity. However, if the same emission constraint is applied at *EQU* conditions to each model region, some regions require clean synthetic fuels to cut their GHG emissions in accordance with their GHG emission constraint. As South Africa, with its vast renewable and fossil resources and an expected moderate demand growth, has many other options to decarbonise its energy supply, it can monetise this additional international clean fuel demand. With increasing stringency of the applied GHG emission constraints, this dynamic persists and the synthetic fuel export peaks under the *EQU45* scenario and declines with more stringent RCP requirements to give way to give way to a new global dynamic: namely a new increasing international demand for coal, because the projected demand of the end-use sector for clean electricity will not only be met by renewable energy but also from fossil fuels with subsequent CCS technologies.

The same effects that shape the international demand (and hence also South Africa's primary energy demand and trade balance) are also visible in the development of South Africa's energy transformation and end-use sectors. The subplot in the third row of figure 3.14 shows the development of the power sector. Here, a development similar to the one discussed for the NDC scenarios (see section 3.2) becomes visible as the, currently carbon-intensive, power sector is quick to respond to any emission constraint.

Again, two dynamics are visible: first, under a lenient to moderate carbon constraint (i.e. the *EQU*/*OPT60* to *EQU*/*OPT34* scenarios), total power consumption decreases as efficiency measures in the end-use sector are implemented and total power demand recedes. While this might seem counter-intuitive at first sight, it can be understood in the context of South Africa's energy system: electrification, often discussed as a mitigation measure, is grid-bound, and it is therefore cost-intensive with respect to infrastructure investment and maintenance. While this is already understood as a hindrance to electrification in economically more advanced and densely populated regions, this impediment to electrification amplifies for emerging economies such as South Africa, which are of considerable size and have a comparatively low population density. Here, efficiency measures and the provision of transportable and grid-independent clean fuels seem to be the more economic mitigation choice. However, with increasing RCP-stringency (*EUQ*/*OPT34* and *EUQ*/*OPT26*) this dynamic fades, as electrification becomes a necessary means for remaining within the GHG emission constraint. In these scenarios the electricity sector responds by further reducing specific GHG emissions through an increase of renewable power generation and a retrofit of fossil power stations with carbon sequestration and storage CCS units. This trend lasts throughout the most stringent GHG emission reduction scenarios. In these scenarios, however, the fossil CCS thermal units used for the peaking and mid-range purposes are replaced with solar thermal power stations that are equipped with storage, and with modern nuclear energy facilities.

The second to last row in figure 3.14 depicts the significant structural change induced by both global scenarios on South Africa's refining sector. The figure shows that (as mentioned above) the international demand for synthetic fuels rises with increasing stringency of the GHG emission constraint, peaks at the mid-range emission constraint RCP4.5 (i.e. the *EUQ/OPT45* scenarios) and declines with more demanding GHG emission targets (i.e. in the *EUQ/OPT34* and *EUQ/OPT26* scenarios).

Furthermore, the figure again outlines the *merit order* of the refining sector as a function of the GHG emission constraint and its dual value, the marginal emission price (see section 3.2). With increasing stringency of the GHG emission constraint this order is: The lowest *merits* are with fossil fuels, followed by biomass-sourced synthetic fuels, followed by fossil- (and biomass-) sourced synthetic fuels with CCS technologies, followed by fossil hydrogen production with CCS , followed by the top *merits* allocated to net-negative-emission biomass-sourced hydrogen production.

3.3.6 Conclusion

In this section, the modeling results that relate to the technical feasibility and costs as well as energy system impact of different GHG emission reduction targets under eight different mitigation scenario calibrations were presented and discussed. The scenarios are based on the *current policies* (*CURPOL*) as reference and the four RCP marker scenario developments, namely the RCP6.0, RCP4.5, RCP3.4 and RCP2.6. For all four marker pathways, two different implementations were defined, namely a reduction that is a cooperative *globally optimised* scenario set (*OPT*), and a reduction that is based on an *equal-share* (*EQU*) contribution from all global model regions.

The analysis of these nine situations allows some robust conclusions. On a global level, model results suggest that the economic GHG emission reduction potential varies significantly among the model regions. Thus, while all model regions prove to obtain significant GHG emission reduction margins (all model regions can mitigate up to 50% of the cumulative GHG emissions over the projection period (2021-2050) compared to the *current policies* reference scenario), the cost efficiency of GHG emission reduction varies significantly among the evaluated regions. For example: reducing emissions by -25% as required by the *EQU34* scenario raises the average discounted net energy system costs by 11 USD per ton CO_2eq mitigated in the region Sub-Saharan Africa (AFR), and by 35 USD/tCO_2eq in the regions Pacific OECD (PAO) and Western Europe (WEU).

While a multitude of factors affect the economic GHG emission reduction potential, the demand growth over the projection period as well as the coal and the renewable energy share in the *current policies* reference scenario are identified as key drivers. The analysis furthermore classifies the economically least advanced model regions as the ones with the overall biggest economical GHG emission reduction potential. This finding highlights the importance of the currently ongoing scientific and political debates about international balancing mechanisms, which should incentivise the utilisation of this potential but not burden to the ones contributing the most.

With a close-up view on South Africa, the results indicate that in all *OPT* mitigation scenarios South Africa reduces more GHG emissions than in the parallel *EQU* scenarios. While this is a clear indication of South Africa's vast GHG emission reduction potential it also highlights the economic potential that a globally optimised effort holds for the country. As an export-dependent nation with vast renewable and abundant fossil resources, South Africa can monetise the international demand for clean synthetic fuels in the mitigation scenarios. However, this adaptation of the export portfolio comes at a cost increase that depends on high export revenues to compensate for the investments. Hence, in order to decouple the national mitigation from the export market, other incentives, such as an international emission trading system, will need to be provided in order to utilise the country's GHG emission reduction potential for the global mitigation endeavour.

Chapter 4

Sensitivity Analysis

> Since all models are wrong the scientist must be alert to what is importantly wrong. It is inappropriate to be concerned about mice when there are tigers abroad.
>
> George E. P. Box (1919-2013)

The main purpose of a sensitivity analysis is to identify those input factors that most strongly influence the model output. Establishing those parameters is useful for two reasons. First by knowing the sensitivity of the model output to the calibration data the reliability of the model results in the face of incomplete knowledge of the correct model parameterisation can be established. For long-term model types, as the ones presented in this dissertation, understanding this connection is of particular importance as the uncertainty inherent to any forecast may otherwise become an unintentional driving force of the model results. Second, by identifying the input factors that have a strong influence on the relevant model results, the model operator can learn how much attention needs to be given to the calibration of a certain parameter or set of parameters. Although sensitivity analysis is "*core to honestly communicating the extent, to which model results can be trusted* " (Saltelli 2007) it is often overlooked and not given appropriate attention, especially in the field of energy system modelling.

In order to supply an easy to use access to sensitivity analysis on MIGRA-NEST-style model calibrations I have included an add-on module to MIGRA-NEST that is dedicated to the sensitivity analysis - the *Sensitivity Analyser*. This new module is specifically geared towards evaluating national stand-alone as well as mixed-granularity (MIGRA) energy system models, as the ones created using MIGRA-NEST. The *Sensitivity Analyser* has been designed to automatically perform a sensitivity analysis of user-defined results and input parameters.

In the following, I first provide an introduction to theoretical fundamentals and the mathematical background of global sensitivity analysis, as well as the reasoning for the implemented approach. Thereafter I provide more practical knowledge on the matter in a *user manual* that is geared towards reducing the initial hurdles experienced by energy system modellers new to the field of global sensitivity analysis. Finally, I present the results of a sensitivity analysis that was conducted on three different scenarios of the South African energy system.

4.1 Fundamentals

There are two established methods that support the characterisation of the effects of uncertainty of the calibration of model input factors upon the output of a model: the sensitivity analysis and the uncertainty analysis.

While the names *uncertainty analysis* and the *sensitivity analysis* are often used interchangeably and both analyses are based on a similar methodological theory, they differ in their aim. The sensitivity analysis aims at identifying the input factors that show the most relevant influence on the model output and, hence, at establishing their degree of reliability (Usher 2016; Tennøe et al. 2018). The main objective of an uncertainty analysis, however, is to evaluate and quantify the distribution of the model results in order to calculate their expected value. While the sensitivity analysis is often accompanied by an uncertainty analysis, this is not always necessary or even recommended. Especially if only a fraction of input factors lends themselves to uncertainty quantification (i.e. the knowledge of their likelihood and distribution is well defined) the calibration of the uncertainty analysis becomes uncertain itself. Hence, in such cases where an uncertainty analyses proves inapt, conducting stand-alone sensitivity analyses is recommended (Usher 2015; Saltelli et al. 2019). Therefore, in this dissertation a sensitivity analysis is given priority over an uncertainty analysis.

The deliberations of a sensitivity analysis can be manifold: (i) corroborate the abstract and simplified description of a real-world problem inherent to modelling - especially relevant for top-down-models; (ii) test the model calibration for overparameterisation - especially relevant for bottom-up-models; (iii) validate the mathematical model formulation; (iv) improve the model calibration by identifying relevant and irrelevant input factors; (v) infer uncertainty in the model results of the uncertainties in its input factors; (vi) quantify the model quality by the robustness of the results; and finally (vii) assist the model-based decision making process by indicating the most effective levers impacting future development (Iooss and Saltelli 2017; Norton 2009). However, these aims can be aspired in many different ways and depending on the structural set-up and the analysis' assertion, the methods of the sensitivity analysis can be quite different.

A variety of different sensitivity analysis methods have been developed to date. While extensive overviews of current methods and their application can be found in the literature (Ghanem et al. 2017; Tian 2013), this section gives a brief introduction to the most relevant methods. A focus is put on their strength, weaknesses, and overall applicability, the three characteristics most important to the method selection process. Table 4.1 compares the key characteristics of the selected methods.

The most common differentiation of sensitivity analysis methods is between local and global methods.[13] Local methods investigate how the model output changes with small

[13] In sensitivity analysis the mathematical expression *global* refers to the inclusive and comprehensive nature of the method. This has nothing to do with term *global* used in energy modelling, where it indicates

Table 4.1: Characterisation of four approaches for sensitivity analysis. The table is based on Zipperle (2020) and extended according to Saltelli (2008), and Kristensen and Petersen (2016).

	Local	**Global Methods**		
	Method	**Factorials**	**Morris**	**Sobol**
Method	One-at-a-Time	Factorial Fractions	Elementary Effect	Variance Based
Sample Source	levels	levels	levels	distribution
Setting	FP	FP,FF	FP, FF	FP,FF
Computational Cost	2(k+1)	k to 2k	N(k+1)	n(k+2)
Relative Effort	low	low	moderate	high
Recommended for model setting:				
max. Factors[1]	< 100	> 100	20 to 100	< 20
max. Run Times	<1h	<10h	<1h	<1 min

[1] by grouping the number of factors (k) can be increased for all global methods
k: number of factors; n: sample size ≈ 500 - 1000
C: number of model runs; N: number of trajectories ≈ 10 - 30
FP: Factor Prioritisation; FF: Factor Fixing

changes of only one to a few input values (e.g. *one-at-a-time analyses*) around a fixed point in the parameter space. Global methods consider the impact caused by the simultaneous change of all parameters of interest across the entire possible value range (Tennøe et al. 2018). As such, local methods are conceptually simpler and hence easier to conduct. By design, all local methods rely on the (often unjustified) assumptions that the tested model is linear, and all parameters behave in an additive manner (Ferretti et al. 2016). This shortcoming can be obviated by applying global sensitivity methods as they provide a much more robust measure of the influence of input factors on the model results (Saltelli 2008). Global methods, on the other hands, by design, require a large number of model executions and may therefore not be applicable to computationally demanding models. Several mathematical approaches have been developed so far in order to reduce this number. The advantages and shortcomings of the most relevant of these approaches (see table 4.1) will be discussed in the following.

Error Types

Two error types are distinguished in statistical hypothesis testing, as applied during the sensitivity analysis methods described here: Type-I and Type-II errors. Type-I errors, also called *false positives*, denote the false rejection of a true null hypothesis. Type-II errors, so-called *false negatives*, describe the non-rejection of a false null hypothesis. In sensitivity analysis, as applied in this dissertation, Type-I errors, or false positives, are preferred over Type-II errors, as false positives flag non-influential factor as important while false negatives identify important input factors as irrelevant (Usher 2015).

a worldwide coverage.

4.1.1 Local Sensitivity Screenings & Scenarios

Local or One-at-a-time (OAT) methods are the most common among the currently used sensitivity testing techniques (Usher 2015). As suggested by the name, during an OAT analysis, only one or a small number of input values are changed at a time while the other parameters remain fixed. The sensitivity of these input factors in relation to the model output is thus determined by the sequential change (e.g. partial derivation) of the individual parameters. The advantage of this method is that they are simple to perform and that the implied computational effort is kept low, as most of the time only a small number of parameters is tested. Thus, modellers can use this method to identify model errors because faulty model results are easily traceable to a specific input factor.

The most commonly applied OAT method is the analysis of so-called sensitivity scenarios (Usher 2016) which consist on an evaluation of several well-defined scenarios that represent the distinct variation of the input factor calibrations, e.g. *Which technologies will be available when and at what cost? How will fuel prices develop over time? How fast are the technology adoption rates in certain areas?* (Hedenus et al. 2013). Such an analysis provides good insights into the influence connected to certain input factors on the output of the model. However, due to the restricted number of observations, only a limited and subjective understanding of the model's sensitivity can be gained (Hedenus et al. 2013). Ferretti et al. (2016) add to the list of disadvantages of the OAT method: first, by moving only one parameter at a time, the OAT method leaves all interactions between factors disregarded. Second, the results of such sensitivity scenarios are interpreted subjectively by the model operator and hence the results are local, partial, and potentially biased. Third, when moving only one factor within a multidimensional space of uncertain factors at a time, the majority of that space is left unexplored. This is due to the so-called *curse of dimensionality* that suggests that:

> *"[...] the mass of a hyper-cube tends to concentrate in its edges and corners at increasing dimensionality – corners which are not visited if one moves factors away from their baseline one at a time."* (Ferretti et al. 2016)

Hence, while the OAT methods are a good introduction into sensitivity analysis, they are insufficient to describe a model's sensitivity and quantify the reliability of the model results to an adequate degree. Nevertheless, for a computationally extremely demanding Integrated Assessment Model (IAM) that portrays the energy sector integrated into the land-water-food nexus and in interaction with the economy and often even the air quality, these sensitivity scenarios prove to be the only feasible sensitivity assessment. Bosetti et al. (2016), Rogelj et al. (2017), and McCollum et al. (2016) provide three thorough examples of such *sensitivity scenario* based evaluations using *MESSAGEix*-based IAM models.

4.1.2 Global Sensitivity Methods

By varying all relevant input factors simultaneously, and by exploring the entire model input range, global sensitivity methods provide a tool to generate an objective and deep understanding of a model and its results. With their mathematical methodology having been available for several decades, they have become state-of-the-art in many research fields.

However, in the field of energy system modelling, its application has thus far remained low (Saltelli et al. 2019).

In their capacity to test the entire model input factor domain, global methods provide the required insights that can be used to (i) fix parameters with little influence on the output (factor fixing - FF), (ii) prioritise parameters with big influence (factor prioritisation FP), and (iii) give insights into the reliability of the obtained model results (Hamby 1994). These three options are also referred to as the three sensitivity analysis' settings (Saltelli 2007). Depending on the aim of the sensitivity analysis, the recommended method varies and hence, several methodologies have been developed thus far. Saltelli (2008) provides an in-depth discussion on a broad spectrum of methods and their range of application.

In the following the three global sensitivity analysis types that are most commonly applied today will be discussed. Those employ *fractional factorials*, *variances* or the *elementary effects* methods (see table 4.1). A brief introduction into these methods follows below.

Fraction Based Methods - Fractional Factorial

The fractional factorial method is a global sensitivity analysis approach that is based on the idea of the *full factorial experimental design*, common to statistics. In a full factorial experimental design, the experiment is executed as often as necessary such that each discrete possible value of each factor can be tested within all possible combinations of these levels across all the factors. Hence, for a full factorial experimental design l^{k} (where l is the number of discrete values each of the k factors can take) model executions are required to evaluate the impact of each input factors - e.g. using an Analysis of Variance (ANOVA). However, according to the *sparsity-of-effects* principle, a system is generally dominated by single factor effects (so-called *main-effects*) and *two-factor interaction.* In *argumentum e contrario* this means that all other effects that could occur in a full factorial analysis can be expected to be rare. By choosing the relevant subset of factors, the most important information of the problem at hand can be exposed, while only requiring a fraction of the model executions required for a full factorial model design.

For example, by applying a two-level approach (setting the input factors to the two extremes of their range only, rather than all possible values in between), the fractional factorial design can significantly reduce the amount of scenario runs required. Such a design allows to gain insights into the model's main effects even with a number of models runs that lies below the number of input factors to be tested (Usher 2016). However, by reducing the information the fractional factorials are, by design, incapable of portraying non-linear interaction effects within the model and are hence unsuitable for the evaluation of MIGRA-NEST style models (Saltelli 2008).

Variance-Based Methods - Method of Sobol

Variance-based methods, often referred to as *Sobol methods* (Sobol 2001), are based on the idea that the variance of a model output can be decomposed into fractions, which can be attributed to an arbitrary combination of inputs or sets of inputs (Kristensen and Petersen 2016). There are several methods to calculate the indices that reflect these fractions and hence the influence that inputs have on a model output. While all methods are based on the same theory, they compete in providing a calculation technique that identifies robust estimates of the sensitivity of a factor at the least computational cost (Usher 2016).

In order for even the most efficient procedure to produce significant and robust results, $N * (k + 2)$ model executions are necessary.[14] With N being above 500 and the number of input factors k in the order of magnitude of 100 (typical to energy system models such as *MESSAGEix*), any variance-based model requires a number of model executions that lies in the order of magnitude of ten thousands. With a model execution requiring about one to several minutes, the computation time might accumulate to several months. Hence, the variance-based sensitivity methods are, despite being otherwise frequently applied today, not appropriate for models with high numbers of input factors or high computation times such as the bottom-up models generated by MIGRA-NEST.

Elementary Effects Method - Method of Morris

The Morris method (Morris 1991) is a global sensitivity approach that is based on the method of the elementary effect. Elementary effect methods calculate the ratio of the change in an output for each of the input factors, based upon random permutations of all other input factors and are, hence, able to identify input factors of high importance. As such, the elementary effects method is a global application of an OAT sensitivity analysis that tests the effect of altering one parameter in every possible combination to the other input factor values one after another.

However, in order to limit this otherwise extensive computational effort, the Morris method defines a k-dimensional input space Ω (a dimension for each of the k input factors) that is subdivided into an equidistant grid of p discrete levels and a step width of Δ). Within this grid, a set of trajectories (X) is calculated, by moving all k input factors randomly across the p discrete levels one-at-a-time.

Hence, as one input factor moves step by step, starting from a randomly sampled starting point, at an equidistant step width of Δ, through the grid, all other input factors remain fixed. Each resulting trajectory is hence composed of $(k + 1)$ defined points $\mathbf{X} = (X_1, X_2, ...X_{k+1})$, a randomly sampled starting point and the three corners to every sampled dimension (see figure 4.1). Finally, for each defined trajectory and each output factor of interest $Y = f(X_1, X_2, ...X_{k+1})$, the elementary effect (EE) can be calculated:

$$EE_i(X) = \frac{Y(X_1, \ldots, X_{i-1}, X_i + \Delta, X_{i+1}, \ldots, X_{k+1}) - Y(\mathbf{X})}{\Delta} \tag{4.1}$$

In order to limit the computational effort to acceptable values, the Morris method suggests to compute N elementary effects for each of the inputs ($\mathbf{X}$) by randomly sampling N trajectories $\mathbf{X}^{(1)}, \mathbf{X}^{(2)}, \ldots, \mathbf{X}^{(N)}$ in the input space Ω. Hence, this produces the collection of elementary effects unique to the random sample:

$$EE_i\left(\mathbf{X}^{(1)}\right), EE_i\left(\mathbf{X}^{(2)}\right), \ldots, EE_i\left(\mathbf{X}^{(N)}\right) \tag{4.2}$$

[14] Where k is the number of input factors, and N the sample size (N can be reduced to about 500 when using sequences with quasi-random numbers)

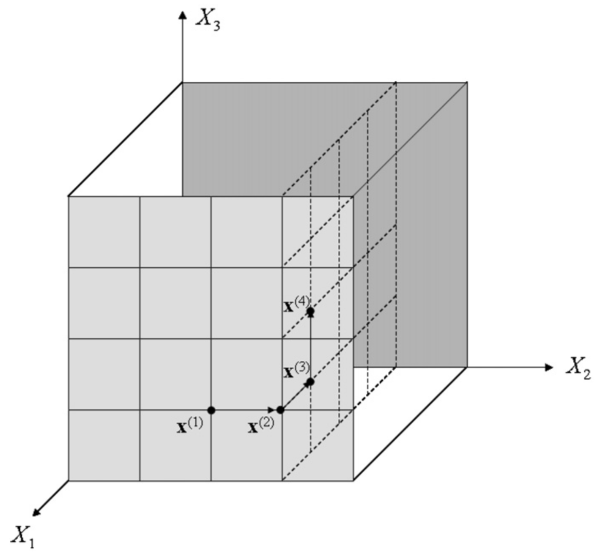

Figure 4.1: Example of a randomly sampled trajectory $\mathbf{X}$ *the 3-dimensional input space* Ω *as shown in Campolongo et al. (2011).*

Based on these random elementary effects the original Morris method proposes to estimate two qualitative sensitivity measures. First, μ, the measure for the overall importance of an input factor upon the output factor of interest Y and second σ, the measure for the degree of non-linearity and interaction effects of the input factor.

$$\mu_i = \frac{1}{N}\sum_{j=1}^{N} EE_i\left(X^{(j)}\right) \tag{4.3}$$

$$\sigma_i = \sqrt{\frac{1}{(N-1)}\sum_{j=1}^{N}\left(EE_i\left(X^{(j)}\right) - \mu_i\right)^2} \tag{4.4}$$

The original sensitivity measure, μ, being defined as the mean of the distribution of the elementary effects of each input, however, falls short in identifying effects within non-monotonic models. In such models, elementary effects of opposite signs can occur, which cancel each other out in the original definition of μ, which can lead to Type-II errors. In their extension to the original Morris method, Campolongo et al. (2007) proposed an additional and more reliable sensitivity measure: μ^*, which is an extension to μ, and defined as the mean of the distribution of the absolute values of the r elementary effects of the input factors (see equation 4.5).

$$\mu_i^* = \frac{1}{N}\sum_{j=1}^{N}\left|EE_i\left(X^{(j)}\right)\right| \tag{4.5}$$

Furthermore, Campolongo et al. (2007) extended the Morris method by suggesting a method to compute optimal combinations of trajectories in a way that they evenly cover the input space and hence, improve the quality of the estimate provided by the limited number of elementary effects. In their original approach, Campolongo et al. (2007) used a brute-force method to identify the optimal combination of trajectories. As this approach is very time-consuming and hence the number of trajectories that can be tested is limited, Usher (2015) suggests treating the problem as a binary integer program. By introducing an optimisation problem for the identification of optimal trajectories among a pool of N randomly generated trajectories the number of tested trajectories can be significantly increased.

With its effective sampling method and its capacity to handle factor grouping the extended Morris method is considered computationally effective, and well suited for the sensitivity screening of large numbers of input factors (Usher 2016; Saltelli 2008). In this dissertation I use the new and improved sensitivity measure $\boldsymbol{\mu^*}$ (Campolongo et al. 2007) and the optimal trajectories as proposed by Usher (2016). The parameterisation chosen in this dissertation for the sensitivity analysis of the case study is presented in section 4.5.

4.2 Selecting a Suitable Approach

The primer on applied sensitivity analysis by Saltelli (2008) provides a general best-practice for applying a sensitivity analysis to a model and for selecting the appropriate method. As stated above, the book emphasises the importance of supporting any sensitivity analysis with an uncertainty analysis. However, in a setting where the uncertainty of the majority of input factors is predominantly not quantifiable, an uncertainty analysis is not applicable (Usher 2016). Hence, I focus on providing the tools for conduction global sensitivity analyses on the mixed-granularity model calibrations.

The model calibrations, which are generated using MIGRA-NEST, can be large and complex. For each model node and year, the models feature several hundred input factors that describe the development of the techno-economic parameters as well as the energy demand and the availability and costs of energy commodities. As these input data concern future developments, the prevailing share of them is based on scenario assumptions and projections rather than assessments of empirical data. By identifying the most influential input factors (factor prioritisation) as well as the inputs, which the relevant model outputs are least sensitive to (factor fixing), the researcher running the model can learn several things. First, as the factor prioritisation reveals the parameters that the model is most sensitive to, the researchers are pointed to these factors that might be worth investigating further in order to reduce the uncertainty surrounding them or to include them in an in-depth scenario analysis for further evaluation. Second, by identifying the non-sensitive parameters, the researchers can either reduce the model complexity by fixing these parameters to defined values or reduce the scope of the scenario analysis to exclude them. Hence, providing these insights requires an approach that provides both a factor prioritisation and a factor fixing setting.

The model equations (the input factors of the *MESSAGEix* models) map out a mathematical problem of significant computational complexity. Together, the large number of input factors in combination with the computational complexity solve times are pushed to lie in the range of one to several minutes and, thus, they make the efficiency of the sensitivity approach of utmost importance. For example, a variance-based sensitivity analysis in the minimum setting (e.g. with sample size n = 500, and a number of tested input factors k of the about same magnitude) would require ten to several hundred thousand model executions and computation times of several hundred days. As such time requirements are obviously unpractical for the analysis, the otherwise powerful, and e.g. by Saltelli (2008) most recommended, pool of variance-based approaches are ruled out for the problem at hand.

However, while the fractional factorials are computationally the cheapest, they are non-optimal for complex models that depend on a large number of input factors. While the underlying approach allows a grouping of factors, and hence testing a larger number of factors at a reduced computational need, the fractional factorial design requires all that factors within a group are permuted and examined collectively. Thus, in such a setting, two influential parameters, if placed in one group, can cancel each other out, and hence lead to so-called *false negatives* (Saltelli 2008). In contrast, when applying grouping with an elementary effect design, all parameters are permuted and examined individually, hence, preventing false negatives by design.

Consequently, for the *Sensitivity Analyser* the elementary effect method, as first developed by Morris (1991) and extended by Campolongo et al. (2007) and Usher (2016), was realised. As stated above, this approach was chosen for two reasons. First, the Morris method is a global sensitivity approach that proves effective in identifying the most influential factors in a model consisting of many factors using a relatively small number of model executions, especially if compared to variance-based sensitivity testing methods. Secondly, the chosen approach copes well with infeasible model executions, which are likely to occur when running a sensitivity analysis and hence testing the model at its limits.

4.3 Software Implementation

Figure 4.2 shows the schematic of the functioning of the *Sensitivity Analyser*. The *Sensitivity Analyser* supports the entire workflow required for a global sensitivity analysis: from construction, over conduction of the global sensitivity analysis, to the evaluation and visualisation of the results.

The *Sensitivity Analyser* implemented as part of MIGRA-NEST is based on SALib, an open source library designed for performing sensitivity analysis (Herman and Usher 2017).[15] As a decoupled library, SALib does not directly interact with *MESSAGEix* or MIGRA-NEST workflow (see figure 1.4). However, SALib provides two core functionalities to the *Sensitivity Analyser*: first, based on an input factor list (a list containing the names as well as upper and lower bounds of all input parameters and constraints) the *sample* function generates the random sample of trajectories, which define the specific input factor values for each model execution. After these model input factors are sampled, the *Sensitivity Analyser* applies them to the selected scenario, executes the model and extracts the relevant output. Second, given the respective model outputs, SALib computes the sensitivity indices using the Morris *analyse* function. The fundamental set-up of the analysis is based on the sensitivity analysis implementation by Zipperle (2020). However, for this dissertation it was

[15] The library is hosted by William Usher and his department at KTH-dESA and is available via GitHub (`https://github.com/SALib`) under the MIT open source license.

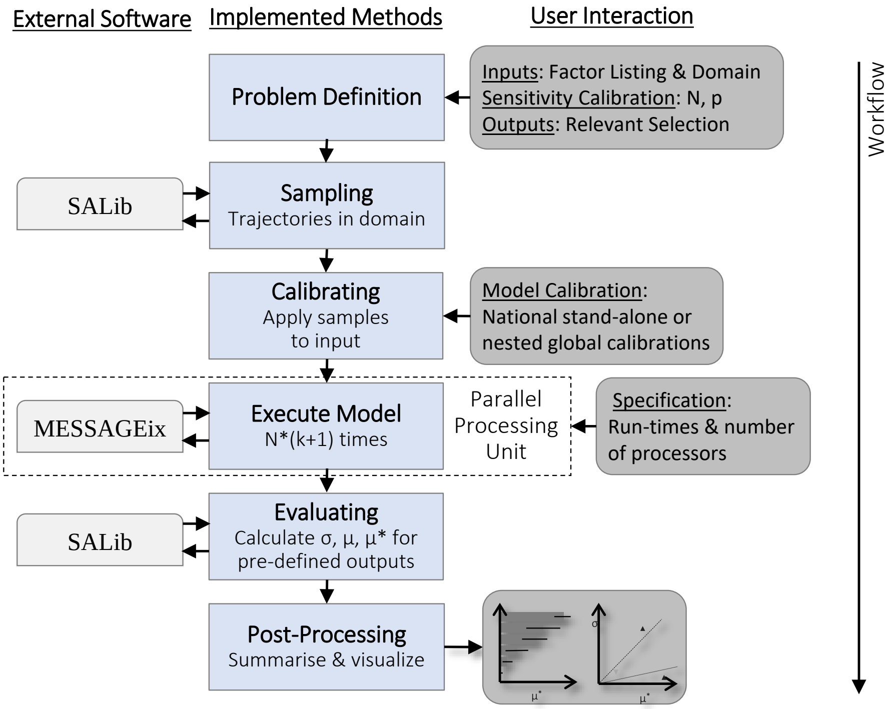

Figure 4.2: Schematic of the functioning of the Sensitivity Analyser. The Sensitivity Analyser allows to (i) construct the sensitivity analysis by sampling relevant trajectories in the domain and by calibrating the samples for the input, (ii) conduct the sensitivity analysis by executing the model multiple times as required, and (iii) evaluate the results by providing sets of sensitivity parameters and by summarising and visualising the results. As a typical workflow at first the user inputs are sampled, then these values are applied to the model parameters, after the model is executed, the relevant results are documented, and in a final step the results are evaluated and visualised.

extended by a framework that supports the modeller throughout the sensitivity analysis such as an auto-generated input factor list and a predefined set of evaluation outputs. The implemented script for running the sensitivity analysis within the *Sensitivity Analyser* follows the workflow suggested by Saltelli (2007):

1. Select the output parameter (model results) of interest: In this step the user chooses, for which model outputs the sensitivity measures will be calculated. The user can choose among ten predefined variables, which have been selected based on the most commonly evaluated model results (see table 4.2). The user can, however, expand the script to evaluate further variables of own choice.
2. Define the input factors: While the script provides a predefined set of factors in the shape of a spreadsheet, any user is strongly encouraged to adapt and enhance the auto-generated sample by removing factors that are known to be irrelevant or by adding factors of interest. Additionally, by assign a grouping, the number of model executions can be further reduced. Furthermore, the user is encouraged to update the domains of all parameters. For the choice of the parameter domain, Usher

(2016) suggests to choose "*A reasonably liberal approach ... right to the bounds of plausibility as the intention is to test the model at extremes as well as within more normal operating ranges.*".

3. Sample the parameters: After the definition of the input factors, the *Sensitivity Analyser* reads the input factor definition from the spreadsheet and generates N sets of randomised trajectories. Per default, the module sets the number of trajectories to ten and the number of levels, p, to four. However, for more detailed analyses, these parameters can be adjusted.
4. Run the model: After sampling of the trajectories, the model is executed $N * (k + 1)$ along the N trajectories. As this is the most time-consuming process step, the *Sensitivity Analyser* provides an algorithm for running several models in parallel. The number of models that can be run in parallel depends on the computational resources available and the model size, and can be defined by the user. All results presented in this dissertation were run on a desktop computer with an Intel Core i7 six core CPU @ 3.2 GHz. The number of parallel processes was varied between eight to twelve depending on the size of the tested model calibration.
5. Capture the results: Following the solve procedure, the predefined model outputs of interest are automatically assessed and summarised. This step is structurally separated from the previous step, in order to prevent re-running all $N * (k + 1)$ model executions if additional outputs of interest are identified ex-post.
6. Analyse the results to identify the most/least sensitive parameters: The *Sensitivity Analyser* automatically generates an output plot summarising the most influential input factors for all predefined output parameters of interest for easy evaluation. Additionally, summary tables are provided that provide an overview of all tested input factors (groups of input factors).

4.4 Guidelines for the Sensitivity Analysis

4.4.1 Choosing the Output Metrics

Key objective of the sensitivity analysis is to establish the sensitivity of the model to the calibration of the input factors. However, here the question arises, how the sensitivity of the model is defined. Choosing meaningful output metrics is decisive for producing insightful results by the means of a global sensitivity analysis. Hence, in this section I provide a reasoning for choosing and or omitting specific output metrics if applying a sensitivity analysis to a MIGRA-NEST-type model.

The models, which are generated when applying MIGRA-NEST, are *MESSAGEix*-based linear optimisation models. Their objective is to minimise total energy system costs, including the discounted sum of total capital investment as well as the fixed and variable costs of energy system operation over the projection period. Hence, the most straightforward output parameter to evaluate, is the model objective, thus, the total energy supply costs summed over the projection period (2021-2050). By testing its sensitivity, insights into which input factors entail the biggest influence on the objective function and, hence, the model solution, can be provided. Therefore, by default, the *Sensitivity Analyser* calculates the sensitivity metrics for the model objective (*OBJ*).

The objective function only has one aim: namely minimising the total discounted energy system costs. In doing so, the objective function is unaware of the underlying energy system structure. Hence, the structural change of an energy system may not be adequately portrayed by the objective, i.e. two energy system structures of unrelated nature can be of similar total cumulative cost. Therefore, choosing further, and more structural output metrics, is advisable. As a general suggestion Usher (2016) recommends to use "... *a quantitative indicator to match what a model user may wish to obtain from the model* ...".

Based on this recommendation, the *Sensitivity Analyser* provides a set of predefined output metrics that can be applied to analyse the structural impact of the tested input factors. Table 4.2 summarises the key output metrics predefined in the *Sensitivity Analyser*. The implemented metrics for the structural analysis focus on the secondary transformation sector, as this is the most dynamic and emission-intensive sub-sector in the energy supply-chain (IEA 2019a). The implemented metrics are: (i) the amount of electricity generated (*PPL-ACT*), which provides insights into the degree of electrification of the energy supply, (ii) the total installed power generation capacity (*PPL-CAP*) as well as the share of power generated by renewable (*RE-PPL-SHARE*), nuclear (*NUC-PPL-SHARE*) and thermal power plants with carbon sequestration (*CCS-PPL-SHARE*) in the total power supply. Furthermore, and as a measure to identify technological transition processes, the total installed capacity of all facilities equipped with carbon sequestration (*CAP-CCS*) is evaluated.

Table 4.2: Key output metrics predefined in the Sensitivity Analyser.

Output Metric	**Symbol**	**Unit**
Discounted cumulative energy system costs	OBJ	Billion USD
Cumulative GHG emissions	EMIS	$MtCO_2eq$
Cumulative electricity output	PPL-ACT	TWh
Installed power generation capacity	PPL-CAP	GW
Share in power supply		
Renewable energy	RE-PPL-SHARE	%
Nuclear energy	NUC-PPL-SHARE	%
With carbon sequestration	CCS-PPL-SHARE	%
Installed carbon sequestration capacity	CAP-CCS	GW
Commodity price for		
Electricity end-use services	COM-COST-ELEC	USD/kWh
Thermal end-use services	COM-COST-THERM	USD/kWh
Mobility	COM-COST-TRP	USD/kWh

All cost-related parameters are calculated excluding the revenue generated by the carbon price.

In addition to these output parameters relevant to the "system perspective", the commodity costs for electric and thermal end-use services as well as for transportation are provided as predefined output parameters. These additional outputs can be used in order to quantify the significance of the tested input factors seen from the "consumer perspective".

In addition to the system cost and the potential technological transition options, the mixed-granularity models generated with MIGRA-NEST provide the GHG emission balance as a key model result (see section 3). Hence, in order to establish the reliability of these model results, the cumulative (summed over the projection period) energy-related GHG emissions as calculated by the model are added as an output metric (*EMIS*).

4.4.2 Selecting the Input Factors

The *Sensitivity Analyser* provides an auto-generator for creating input factor lists. While these auto-generated lists can provide a valid starting point for an initial sensitivity screening, refinement of the list for more detailed analyses is highly recommended. In the following, the reasoning behind the auto-generated input factor lists is explored and additional guidelines on how further refinement could look like are given.

Input Factor Choice

The general guideline on choosing the input factors for the sensitivity analysis by Saltelli (2007) suggests to test as many input factors as computationally possible. However, for a bottom-up style model the totality of single input data points accumulates to several hundred thousand.[16] Hence, testing all input parameters is infeasible within reasonable time frames. Thus, an insightful subset of influential input factors has to be selected. Special care has to be taken, as removing input factors from the list because they are preemptively considered non-influential can lead to undesired Type-II errors.

In the initial step of the auto-generated input factor selection, all input factors constituting the model calibration are added to the input factor list. The consecutive factor reduction is approached based on previous experience with the analysed model calibration. First, all technology parameters are reduced to the representation of only one model year and one vintage[17]. Furthermore, of all the costs factors only the ones that have in previous analyses been identified as dominant are further considered in the sensitivity analysis. Thereafter, by the same approach, the dominant technology growth constraint is selected, and the remaining growth constraints are removed from the selected set. Then, the most significant (hence most utilised in the reference scenario and the most GHG emission-restrained scenario) fossil and renewable resource potential grades are selected, while the remainder are removed from the list.

Input Factor Grouping

As described above, the extended Morris method, which is applied in the *Sensitivity Analyser*, allows for input factor grouping (Usher 2015). By grouping input factors together, the number of independent input factors and hence the required number of model executions can be significantly reduced. Aggregating two factors together into one group reduces the number of input factors k by one and hence the number of model executions by the number

[16]For every technology option up to 22 parameters are defined for every year, every vintage, every node and every mode of operation. Additionally, the node specific quantification of the fossil and renewable energy resources as well as the demand and the historic parameterisation add to the number of input data points (Zipperle and Orthofer 2019).

[17]The installation year of a technology is called the *vintage* of the technology.

of trajectories N (usually between 10-30). A detailed description of the grouping of input parameters according to Morris and the underlying theory of elementary effects is given in Saltelli (2008).

The implemented grouping method is based on previous works of Usher (2015). In this approach all input factors that constitute a group are treated as one input factor for the sampling process. Thus, for each input factor group, only one trajectory is sampled, along which the input factors of the group move simultaneously. While the movement follows along the same sampled trajectory, the movement of each input factor within a group can commence at a different starting point and can move into a different direction. This is necessary in order to allow for the elementary effects and the sensitivity measures μ^*, μ, and σ to be calculated for every input factor individually. Only in the last step, μ^* is summed to serve as sensitivity measure for the entire group. Hence, the sensitivity measure μ^* of a group corresponds to the sum of the mean influence of each of the input factors belonging to one group. While such grouping is possible for the absolute sensitivity measure μ^*, it is not for the direction-indicating sensitivity measure μ and the measure for the standard deviation of the elementary effect σ, as here, sensitivity effects of opposite directions could cancel one another out and hence induce Type-II errors.

With $\mathbf{G}$ being a group membership matrix that assigns the membership of the k input factors to $\bar{G}$ groups ($\mathbf{G}(i, g) = 1$ if the input factor i is member of the group and $\mathbf{G}(i, g)$ $= 0$ otherwise.) and μ_i^* being the absolute sensitivity measure of the input factor i, the sensitivity measure of the group g, μ_g^*, is defined to be:

$$\mu_g^* = \sum_{i=1}^{k} G_{ig} * \mu_i^* \tag{4.6}$$

The selection of the members of a group does not overly affect the results of the sensitivity analysis for the single input factors because the group sensitivity measure is calculated as the group's sum rather than the group's average. As such, it avoids indicating important parameters as non-sensitive just because they are grouped together with parameters of low sensitivity (Type-II errors). However, this formulation can lead to Type-I errors, hence flagging input factors as being of high sensitivity, if they are placed in a group with parameters of high sensitivity (Type-I error).

While the applied definition of the group sensitivity measure reduces the importance of group allocation, some attention should be paid to the grouping process before executing a sensitivity analysis. The groups have to be defined for every sensitivity analysis individually, and thus, I here present several ideas on how to group parameters (Usher 2016). The first idea is to assign input factors into groups of similar properties. These properties can be of the structural (e.g. costs) or of sectoral (e.g. all parameters of a technology) type. The second idea is to group parameters according to their presumed importance, thus, forming larger groups of parameters of low importance in order to allow the non-grouped screening of a higher number of more important input factors. However, while it is recommended to group parameters of similar kind or importance, grouping parameters because of a likely correlation is not necessary.

In the sensitivity analysis of the case study for South Africa, both principles are applied to a certain degree. First, several parameters are grouped by their structural similarity.

For instance, all costs of conventional power plants are grouped together, as knowing the influence of the generation costs of fossil power plants has more interpretational value than knowing the exact significance of every single technology. Second, all parameters that are presumed to be of very-low influence on the relevant outputs are grouped together. By classifying them cumulatively as belonging to a group named "non-significant", the number of required model executions is reduced while possible Type-II errors can be prevented, as any significant input factor falsely placed within that group raises the total groups significance. For further detail see section 4.5.

Input Factor Distribution

Assigning a potentially probable value range is possible for the majority of input factors of any model calibration. However, for most of these input factors no measure of likelihood or predefined distribution can be assigned to. This lack of information is especially pronounced in long-term models as the ones created by MIGRA-NEST. Hence, a distribution of likelihood has to be defined by the user based on little (or even no) knowledge on the actual distribution. The *Indifference Principle* discusses such problems and states: "*if there is no known reason for predicating of our subject one rather than another of several alternatives, then relatively to such knowledge the assertions of each of these alternatives have an equal probability.*" (Keynes 1921). This principle suggests that parameters unsuitable to be described by informed probability distributions can be best described using a uniform distribution.

However, it could be argued that most input factors are assigned not a complete random but rather based on a default value defined by reasonable assumptions and expert knowledge (Bosetti et al. 2016). Such a hypothesis would advocate a normal distribution or, in special cases, a skewed distribution of the input values around their assigned level. However, in line with Usher (2016) and the applied implementation of *SAlib*, a uniform distribution is applied to all input factors in the *Sensitivity Analyser*.

This simplifying choice is acceptable as it will, in most cases, portray the most conservative assumption about the distribution of input factors and will, in the worst case, lead to Type-II errors. The detailed implications are discussed in Usher (2016).

Considering the Time Dependency of Input Factors

Most input factors of the *MESSAGEix* based models that are created using MIGRA-NEST, are in some way time dependent (e.g decreasing technology costs and build rates or the changing energy demand). There are several different ways to test the sensitivity of these parameters. One option would be to treat the values of all relevant input factors of every model year as an independent input factor. However, this would lead to an increase in input factors proportional to the number of model years. While this inflation in input factors could be counteracted by grouping the time-dependent annual parameter samples, this again could cause a series of volatile and hence probably nonsensical trajectories (for example a 20% drop in costs in the first, followed by a 10% increase in the second model period instead of a continuous increase or drop of the e.g. investment costs).

In order to omit those problems, the *Sensitivity Analyser*, in line with previous works by Usher (2016) and Zipperle (2020), only samples the input factor value in the pre-defined sample year (2050 in the model presented in this dissertation). This sample is then used to re-scale the values from the remaining model years by interpolating them between "year zero" (being the first model year) and "sample year". For re-scaling, the hypothesis is applied that the values in the first model period are well defined and hence have a domain of zero. For the model years after the sampling year, the sampling value is maintained (see figure 4.3).

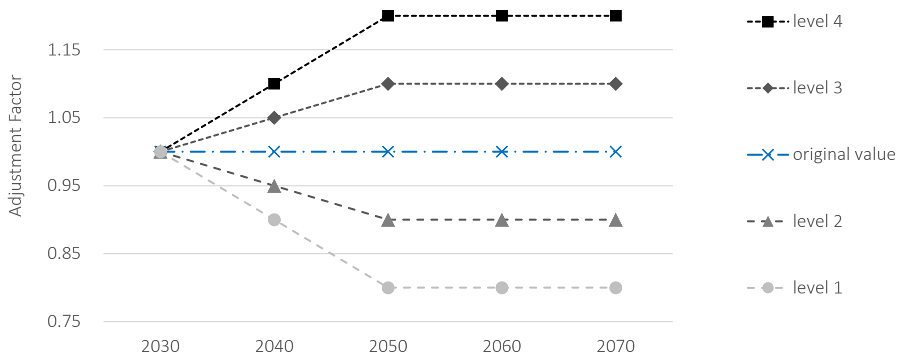

Figure 4.3: Example of the adjustment factor of a time-dependent input factor for a ± 20% domain at four levels. While the 2050 values are scaled by the randomly sampled adjustment factors among the four levels, the values of the remaining years will follow the depicted interpolated and extrapolated trajectories.

The time-independent parameters (e.g. resource volumes and renewable energy potentials) are not interpolated as this could lead to implausible model executions. For those parameters the sampled values were applied on the original input value. Throughout the sensitivity analysis, it is assumed that all of those parameters are statistically independent and that therefore any combination of parameter values is equally likely to occur in order to ease the sampling.

4.4.3 Choosing a Calibration

The calibration of the global sensitivity analysis according to the Morris method has three external input parameters. Those are: (i) the number of levels (p) that the domain of the input factors is split into. p can be interpreted the *granularity* of the sensitivity analysis. (ii) step-width Δ within the grid (Ω) that defines the values the input factor can be varied to, and (iii) the number of trajectories (N) that defines how many independent and randomly sampled trajectories are applied in the sensitivity analysis.

However, these three calibration parameters are not independent. First, as the analysis aims for a uniform distribution of the input factors across their domain, it is recommended to choose p as an even number, and the step-width to be $\Delta = p/[2(p-1)]$ (see Saltelli (2008) for detailed explanations). Furthermore, the number of levels is strictly connected to the number of trajectories N, as higher values of p require a higher number of trajectories to produce the same degree of confidence. This is due to the fact that, assuming a uniform distribution of the input factors across the domain, the sampled values should also represent this distribution. However, with an increasing number of levels, a higher number of sampling *experiments* is required in order to prohibit skewed distributions.

This can be understood in a simple experiment: assuming a global sensitivity analysis for two input factors ($k = 2$) that are both uniformly distributed in $[0, 1]$. If the number of levels is set to two ($p = 2$) the input factors can only take two values $\Delta \subset \{0,\ 1\}$; if the number of levels is set to four ($p = 4$) factors are limited to taking values of $\Delta \subset \{0,\ 1/3,\ 2/3,\ 1\}$; if the number of levels in increased to six ($p = 6$) then both input factors will be able to take the values of $\Delta \subset \{0,\ 1/6, \ldots,\ 5/6,\ 1\}$. Thus, in order to provide a reasonable high probability that the distribution of the samples resembles the intended uniform distribution the number of trajectories has to be in line with the number of chosen levels as otherwise many levels might remain unexplored or the distribution will be skewed. Figure 4.4 shows the results of the randomly sampled input factors for the three levels from the though experiment. While the distribution for the $p = 2$ setting provides an acceptably close to uniform distribution, the distribution in both other settings ($p = 4$ and $p = 6$) is strongly skewed.

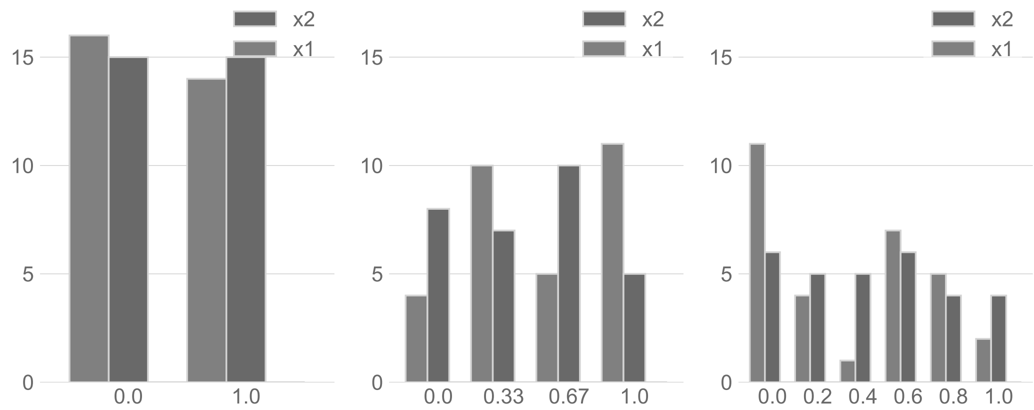

(a) p=2 *(b) p=4* *(c) p=6*

Figure 4.4: Examples from sampling two input factors ($x1$, $x2$), which are both uniformly distributed in $[0, 1]$, on ten trajectories ($N = 10$) for a choice of 2, 4 and 6 levels (p) and $\Delta = p/[2(p-1)]$. The figure shows that with at an increasing number of levels the distribution tends to desert the uniform distribution if the number of sampling operations is not increased accordingly.

To summarise, based on previous experiments, Saltelli (2008) suggest that working at a setting of $p = 4$, $N = 10$ and $\Delta = p/[2(p-1)]$ provides valuable results at an acceptable computational demand. While Usher (2016) follows this recommendation, he reduces the confidence intervals of his results by re-running the initial screening analysis on the top ranking input factor groups at a $p = 8$ and $N = 20$ setting, suggesting the validity of the calibration choice. If not stated otherwise, the results presented in this work are created using the calibration as proposed by Saltelli (2008). While this parameter choice is also pre-defined as default values in the *Sensitivity Analyser*, the module allows any user-defined calibration.

4.4.4 Interpreting the Results

As described above, the extended Morris method, as applied in MIGRA-NEST, provides several sensitivity measures.

For non-grouped input factors these are: μ, the mean of the distribution of the elementary effects that can be interpreted as the measure of the overall importance and σ, the standard deviation of the elementary effect and hence the measure of non-linearity of an input factor.

For groups of input factors, the extended Morris method provides μ^*, the mean of the distribution of the absolute values of the elementary effect as a measure of overall importance. By re-sampling the results of the sensitivity analysis, the extended Morris method additionally calculates a confidence interval of the sensitivity measure μ^* for both the grouped and the non-grouped input factors. In addition to these calculated numeric sensitivity output metrics the *Sensitivity Analyser* produces output plots to support the interpretation of the model results.

As recommended by Usher (2016), for every tested output parameter two plots are produced by the *Sensitivity Analyser.* (i) a bar chart that summarises the μ^* values of all tested input factors (and groups) plus the 95% confidence interval (CI) of the absolute elementary effect, and (ii) a point graph that shows the ratios of the standard deviation of the elementary effect (σ) over the mean absolute elementary effect μ^* for all non-grouped input-factors (see figure 4.5).

The bar chart (that summarises the μ^* values of all tested input factors and input factor groups including their confidence interval) provides a clear ranking of importance of the tested input factors and input factor groups. As described above, μ^* corresponds to the mean absolute elementary effect caused by moving the input factor across its range. The confidence interval, obtained through bootstrapping, provides insights about the mean deviation of the absolute elementary effect of the parameter around the mean. In this first plot, μ^*, the confidence interval as well as the tested output have the same unit. If groups are used, the same applies. However, given the independent behaviour and range of every input factor within a group, the value of μ^* corresponds to the sum of the impact of all input factors within a group (see the section on factor grouping above). Hence, the plot provides several insights: first, the value of μ^*, shown by the length of the respective bars, indicates the absolute sensitivity of the output to every tested input factor or parameter group. The higher a μ^*-value is, the more sensitive is the output to the tested factor (or factor groups). The graph also contains the 95% confidence intervals (CI) shown as error bars; these error bars indicate the range, within which μ^* will lie 95% of the times if the sensitivity analysis is repeated using a new sample. The confidence intervals indicate how certain the ranking of a parameter is, and if the number of model executions done for the sensitivity analysis was high enough in order to produce reliable outputs. Hence, very wide confidence intervals can be interpreted as either that the impact of a parameter (group) on an output varies widely or that the number of model executions was too low.

For all non-grouped input factors the scatter plot (that shows the ratios of standard deviation of the elementary effect (σ) over the mean absolute elementary effect μ^* for all non-grouped input-factors), provides additional insights. This plot provides a measure of the interaction effects, the so-called coefficient of variation (CV). The coefficient of variation shows the variability (σ) of the elementary effect in relation to its mean μ^*. The ratio σ/μ^*

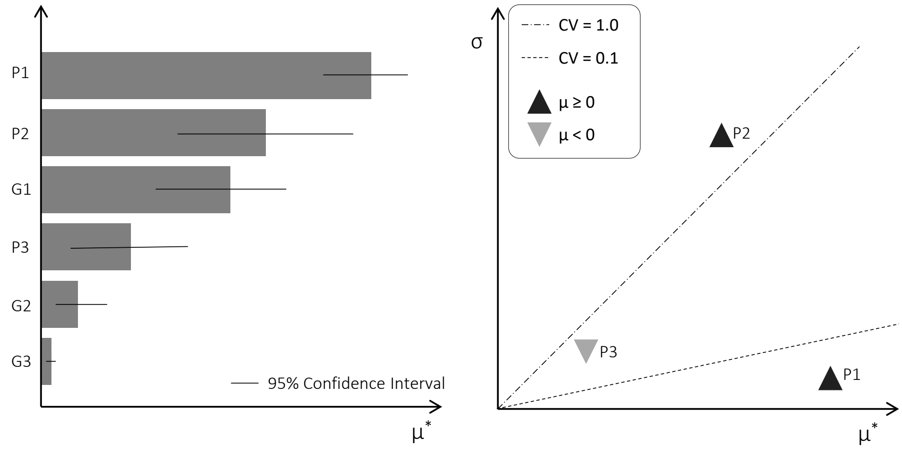

Figure 4.5: Example plots illustrating the visualisation of results of the global sensitivity analysis in the Sensitivity Analyser. Left: The bar chart shows the mean absolute elementary effect μ^* of the tested input factors P1-P3 and the input factor groups G1-G3. The black lines indicate the 95% confidence interval of the absolute elementary effect calculated via bootstrapping. Right: The scatter plot shows the ratios of the standard deviation of the elementary effect σ of the non-grouped input factors (P1-P3) over the mean absolute elementary effect (μ^*). The two indicator lines divide sectors of different ranges of coefficients of variation ($CV = \mu^*/\sigma$). These sectors separate areas with different degrees of non-linearity of the input factors: the higher the ratio, the stronger the non-linearity. In addition this graph also shows the value of μ though the marker type: upward pointed triangles show positive μ values (that indicate direct proportionality between the input and the output parameter), downward pointing triangles shows negative values (that indicate an inverse proportionality).

can be interpreted as the measure of the non-linearity of the effect of the non-grouped input factor upon the tested output. The higher the ratio, the more interactive or non-linear is the impact of this input factor upon the output. In the figure, the non-linearity of the parameters is qualitatively indicated by three sections: (i) $\sigma/\mu^* \leq 0.1$, parameters in this section are non-interactive and hence their effect on the output is near-linear; (ii) $0.1 \geq \sigma/\mu^* \leq 1$, parameters found here are moderately interactive and hence, have a non-linear impact; finally parameters located in section (iii) where $1 \geq \sigma/\mu^*$ are highly interactive and hence, have a strongly non-linear effect. Additionally, and as suggested by Zipperle (2020), two different marker types are used in the scatter plot (upward and downward facing triangles). The different markers are used to indicate the value of the mean elementary effect μ that can be calculated for all non-grouped parameters. Here μ can be interpreted as a measure of the proportionality. If μ is greater or equal to zero, the output value will increase if the input factor is increased. In contrast, if μ takes negative values, the output value decreases if the value of the input factor is increased (inverse proportionality).

4.4.5 Troubleshooting Unexpected Outcomes

While the *Sensitivity Analyser* provides for a relatively easy operation of sensitivity analysis, the complexity inherent to global sensitivity analysis can still confront inexperienced users with unexpected outcomes. By providing an overview of the most common difficulties experienced when conducting a global sensitivity analysis, this section provides a go-to guide for modellers new to this topic. While this list is not exhaustive, it covers the issues most commonly faced when applying the Morris method to MIGRA-NEST-style energy system models.

Very Wide Confidence Intervals

Usher (2016) identifies two reasons for wide confidence intervals: (i) There were not sufficient model executions in order to produce significant results. If this is the case, the confidence intervals should be reduced if the number of model of trajectories and hence the number of model executions is increased. (ii) Confidence intervals can also be very wide, if the chosen output metrics are disaggregated. In this case, the output can only take a very limited number of states (e.g. if the number of levels is set to 4 ($p = 4$), the very disaggregated output can also only vary between these four levels). In this case, the number of levels can be increased to six or eight but at the same time the number of trajectories needs to be increased, too (e.g. $N = 30$).

In the course of this work, the input factor group (size) was identified as another cause for wide confidence intervals. Here, the best solution was found to be re-adjusting the size of input factor groups with inadequate wide confidence intervals after the first screening.

Too High Number of Model Runs

The bottom-up style energy system optimisation models like the ones created with MIGRA-NEST tend to have a very large number of input parameters. One advantage of the extended sensitivity measure for evaluating groups of input factors μ^* is that it represents the sum of the elementary effects of all the input factors contained in one group. This allows to address the sensitivity analysis of a model at a global approach. Hence, theoretically (and if no prior knowledge of the model dynamics exists) all parameters could be assigned into one group, in which one parameter is tested at a time by randomly removing it from the group. However, in most cases, some indication on the model behaviour exists: in such a case parameters can be grouped by into smaller groups of input factors with expected large influence and larger groups of input factors that are anticipated to have a low influence. Furthermore, fixing the least influential parameters to their pre-assumed values does not affect the variation of output metrics caused by the remaining input factors. Thus, if such groups of parameters of low influence can be identified in an initial screening, they can subsequently be removed from the sensitivity analysis.

Non-Solvable Scenarios

The general recommendation for calibrating a sensitivity analysis is to set the domain of each input factor to the outer bounds of the conceivable parameter range. However, such extreme settings, or an unsuitable combination of parameter values, can lead to non-solvable[18] model executions. While this is no problem per se, the non-solvable model executions have to be masked before the elementary effects is calculated.

As suggested by Usher (2016) two options are thinkable: (i) eliminating the model executions that are infeasible from the sample set, or (ii) replacing the missing output metric with the mean average of the output metrics. While both approaches produce insightful results, the *Sensitivity Analyser* applies the second strategy. The reasoning behind this is that, especially for inexperienced modellers, the ex-post analysis of the infeasible scenarios can widen the understanding of the model calibration's working and expose possible structural weaknesses.

Hence, the *Sensitivity Analyser* automatically ends a sensitivity analysis by comparing the input factor values at and around (the last feasible and the first feasible scenario before and after) an infeasible scenario (or scenario set) to identify the input factor values that cause such an ill-posed scenario. By default, a plot featuring all input factors that change before and after that infeasible scenario is produced for every infeasibility.

Implausible Scenarios

When sampling the input factors according to the Morris method every parameter is sampled separately, and hence implausible combinations of parameters can happen. Such an example can be that import costs for a commodity drop while the export revenue for the same commodity increases. While such a combination can only happen for national stand-alone models, other implausible parameter combinations are possible. While in other approaches allow aggregating parameters that will, in real life, move together, this is not possible using the method applied here. Because, in the grouping as suggested by Campolongo et al. (2007), input factors that are grouped together are sampled simultaneously, and hence move simultaneously, they can, however, move from different starting points and in different direction. Thus, grouping does not prevent these combinations here. However, this is not a problem as such, as it will only cause parameters to seem important that would otherwise be of little to no relevance (Type-II errors). Furthermore, these errors can be prevented by carefully selecting the tested input factors for such combinations and only selecting one or the other.

4.5 Results of the Case Study

In the following, a sensitivity analysis is conducted for three different model calibrations of the South African energy system. The goal of this analysis is to identify the input factors with the biggest influence on energy system costs and on GHG emissions in order to generate an understanding about the key drivers and reliability of those two core model outputs used in the scenario analysis (see chapter 3).

[18]In this dissertation, the term non-solvable model calibrations includes (i) infeasible model calibrations (models without an solution space) as well as (ii) model calibration with unbound rays (model calibrations, for which the solution is infinite).

First, an initial screening is carried out for the reference calibration of the national stand-alone prototype model of South Africa (*CURPOLnat* - see section 2.5.2).[19] The aim of this approach is twofold. First, applying the sensitivity analysis to the computationally lean national stand-alone model allows to test a wider range of input factors, than the more complex mixed-granularity model allows for. By running an initial sensitivity screening on the small model, input factors with low influence can be identified and excluded from the analysis of the more complex model. Second, by solving the optimisation problem for the national stand-alone model calibration only, the country-specific costs, emissions and other system drivers can be identified. Subsequently, to this initial screening of the GHG emission-unrestrained national stand-alone reference scenario *CURPOLnat*, an emission constraint that is in line with the partially conditional emission constraint (see section 3.2) is applied to the *CURPOLnat* scenario. Thereafter the sensitivity analysis is rerun on the new scenario (*PARTCONnat*). The aim of this analysis is to identify South Africa's drivers and inhibitors of GHG emission reduction. Finally, a reduced set of input factor groups is evaluated using the more complex nested mixed-granularity model calibration *CURPOL*, in order to analyse the impact of international feedback on South Africa's energy system.

4.5.1 National Stand-Alone Reference Scenario

Calibration of the Sensitivity Analysis

Goal of the global sensitivity analysis is to obtain an unbiased insight into the sensitivity of the main outputs with respect to the input data. Hence, all sensitivity analyses presented in this dissertation are initiated by global screenings of wide scope. In order to include as-many-as-possible but no-more-than-necessary input factors, 344 input factors were selected from the 800 total input factors that constitute a reduced MIGRA-NEST created model calibration (see section 4.4.2).

The input factor selection, as applied here, is first and foremost based on the input factors' degree of uncertainty. Input factor calibrations that are well known and or unlikely to change significantly over the model horizon (e.g. the efficiency of a conventional thermal coal power plant or gas turbine) are excluded from the input factor list. Subsequently the input factor list is further reduced through the application of an effect-equality principle. Hence, similar input factors of equal effect on the output are reduced to the one factor of highest influence (e.g. for technologies featuring investment, annual fixed and variable costs, only the respective dominant cost component is selected).

The selected input factors are aggregated into 61 groups; the remaining (non-selected) parameters are fixed to their pre-calibrated level. The full list of the included input factors and the group memberships can be found in the appendix D.1. With ten trajectories applied to each one of the 61 selected groups the analysis requires 620 model runs. While this would be quite manageable with both stand-alone scenarios (*CURPOLnat*, *PARTCONnat*) such a high number of model executions would be difficult to manage for complex mixed-granularity

[19] *CURPOLnat* is the GHG emission-unrestrained national stand-alone calibration used, together with the global calibration *GLO*, to create the mixed-granularity model calibration *CURPOL*.

global model calibrations, because each screening would take several days to compute.[20] In order to enable the complete screening of both a GHG emission-unrestrained as well as a GHG emission-restrained model calibration, the less complex national stand-alone model calibrations are employed for these initial screenings (*CURPOLnat* and *PARTCONnat*). Due to the inherent structural identity of the national stand-alone and the mixed-granularity global model calibrations, all non-trade related parameters can be assumed to be of the same scale of sensitivity in the global as well as in the national stand-alone model.

For this case study all output metrics as predefined in the *Sensitivity Analyser* (see table 4.2) are calculated. To ensure clarity of information this chapter focuses on the most important output metrics; a summary of all output tables is given in appendix D.2. Concerning the GHG emission-unrestrained scenarios (the national stand-alone *CURPOLnat* and the mixed-granularity *CURPOLnat*), the key outputs are the energy system costs and the GHG emissions in the target year 2050. In the emission-restrained *PARTCONnat* scenario, the evaluation focuses on energy system costs and on the derived carbon prices.

Results

Unless specified otherwise, the following results were created using the GHG emission-unrestrained national stand-alone scenario *CURPOLnat*.

Figure 4.6 summarises the results of the initial screening. The bar charts show the values of the average absolute elementary effect $\boldsymbol{\mu^*}$ for the fifteen input factor groups with the biggest influence on the two selected output metrics ranked in order of influence. The scatter plots below show the standard deviation of the elementary effect of the non-grouped input factors over the mean absolute elementary effect. The depicted output metrics are the energy system cost, and the GHG emissions in the year 2050.

Among the presented results the most influential parameters are distinctly detectable, with a few parameters causing significantly bigger variations that the other factors combined. For both outputs, the top input factor groups are dominated by (i) first and foremost the energy commodity cost, followed by (ii) the demands, and (iii) the applied carbon price.

The lower section of figure 4.6 are scatter plots with the values of the standard deviation of the elementary effect of the non-grouped parameters ($\boldsymbol{\sigma}$) over the mean absolute elementary effect ($\boldsymbol{\mu^*}$) with the direction of the markers indicating the proportionality between the input and the output parameter. The numbers indicate the coefficient of variance of most parameters to be below one, hence indicating an almost monotonous and or additive parameter influence. For the GHG emission balance, the coal export price, however, exhibits a coefficient of variance greater one, which means that its influence on the output is not linear and that interactions with other parameters exist.

However, the confidence intervals of several factor groups are of considerable size for both presented outputs. While this is to be expected from an initial screening, this can mean that input factor groups with overlapping confidence intervals could switch their ranking if a different random sample would have been applied. Three dominant input factor groups are distinguishable: energy resource costs, energy demand, carbon price. These will be discussed in the following.

[20] At approximately 10 minutes solve time per model execution, the computational requirement for one screening lies at 4.3 days and 20 GB of storage.

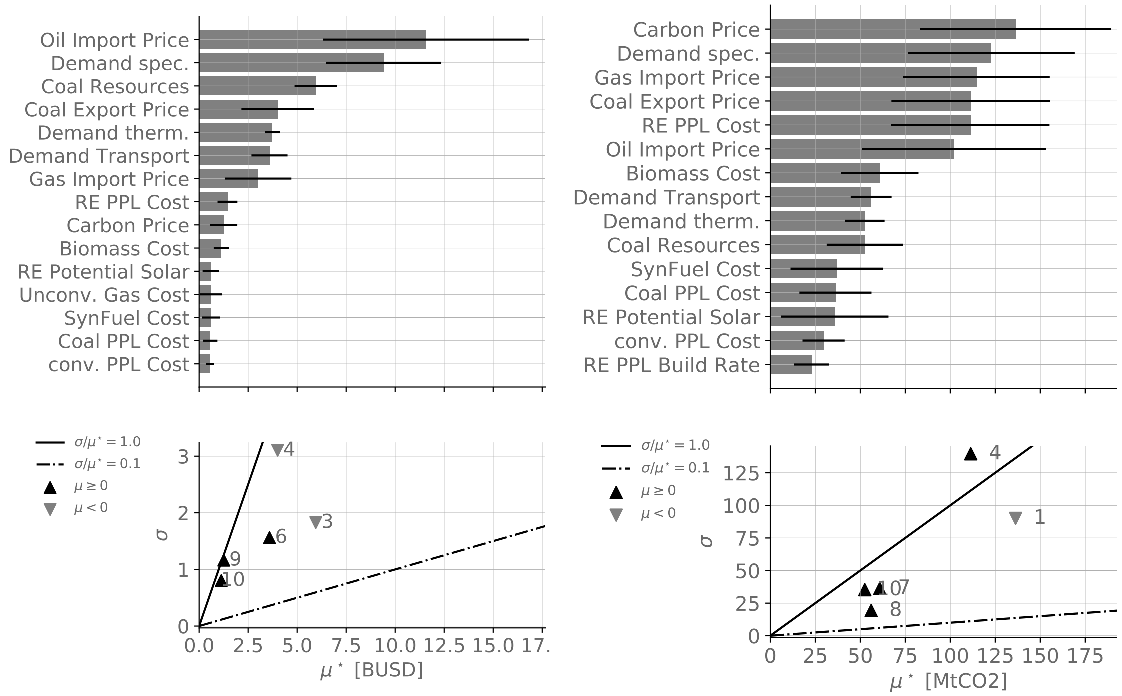

(a) Energy System Cost

(b) GHG Emissions

Figure 4.6: Results of the initial screening of the greenhouse gas emission-unrestrained national stand-alone scenario CURPOLnat showing the 15 most influential input factor groups on the 2050 (a) energy system cost, and (b) GHG emissions. The numbers in the lower plots refer to the parameter rank in the top plot. Abbreviations: Demand spec. = electricity demand, RE = renewable energy, PPL = power plant, conv. = conventional.

Energy Resource Costs The top section of table 4.3 summarises the ranking of the input factor groups that relate to the cost of energy commodities. It shows that the two output factors, the energy system costs and the GHG emissions, are significantly influenced by the energy commodity costs, and here especially the import price of oil and gas as well as the coal export revenue. All three rank among the top ten input factor groups for all evaluated outputs (see full ranking in appendix D.2). This ranking clearly identifies the model's, and hence, the country's trade dependence. In South Africa oil and gas are two fuels that are locked into the system by prior investment decisions (e.g. for thermal applications in the industry sector), and a limited alternative technology portfolio on the other hand (e.g. the mobility sector is heavily dependent on liquid fuels with currently only limited infrastructure available that would support a fuel switch). In combination, these two effects cause a constraint situation where large quantities of oil and gas will be continued to be consumed, even if prices on the international market rise.

However, the high influence of trade costs (here also the revenue generated by the export of coal) also identifies a flaw inherent to national stand-alone models: the representation of the international commodity market. In a national stand-alone model calibration, costs are optimised for the single country that the calibration represents, and hence, trade is also only optimised for this one country. In reality however, international commodity trade is balanced by supply and demand, and e.g. South Africa will not be able to decide just by itself how much coal to export, but it will be the international commodity markets that will balance supply and demand.

The values for $\boldsymbol{\mu}^*$, as shown in figure 4.6 for each group, gives an indication of the magnitude of variation caused by this group. Hence, table 4.3 supplements the insight by comparing the ranks (as given in figure 4.6) to the relative change that the variation of the input factor group causes.

The numbers show that the most influential trade-related costs, if varied by 30%, each have an impact in the magnitude of 7-26% of annual energy system costs. The wide margin between the import costs of oil and gas points out the different degrees of freedom the model has in the fuel application: the lock-in situation for oil, which is mostly used in the transport sector, is very stringent and thus, the effect of a price change is close to linear with a 30% price increase for fuel imports leading to 26% increase in energy system costs. Gas, however, is more diverse in its application, fuelling the industry but also the power sector, and can therefore more easily be replaced under cost pressure.

The impact on the GHG emissions in 2050 is, among the three top input factors, relatively equally spread, with each factor causing a variance of up to 20% each. This indicates the greater degree of freedom the model has to modulate the GHG emissions compared to the costs, which are, to a certain degree prescribed by the system lock-in. As expected, the measure for the direction of proportionality (indicated by $\boldsymbol{\mu}$) of the coal export costs is negative in relation to the energy system costs, and positive in relation to the GHG emissions (see figure 4.6).

Table 4.3: Comparison of input factor for their influence rank (R) and their impact size (S) for the GHG emission-unrestrained national stand-alone reference scenario (CURPOLnat).

	System Cost		**GHG Emission**		**RE Share**		**PPL Output**	
	R	S	R	S	R	S	R	S
Energy Resource Costs								
Oil Import Price	1	26%	6	18%	7	5%	10	3%
Gas Import Price	7	7%	3	21%	6	6%	4	10%
Coal Export Price	4	9%	4	20%	3	14%	8	5%
Biomass Cost	10	3%	7	11%	11	3%	18	1%
Useful Energy Demand								
Demand spec.	2	21%	2	22%	8	5%	2	21%
Demand therm.	5	8%	9	9%	x	0%	x	1%
Demand Transport	6	8%	8	10%	18	1%	x	1%
Electric Peak Load	16	1%	18	3%	9	4%	6	7%
Carbon Price								
Carbon Price	9	3%	1	25%	4	11%	5	10%

GHG: greenhouse gas, RE: renewable energy, PPL: power plant x: R > 20
R: Rank among all tested input factor groups. All values: 2050
S: Size of $\boldsymbol{\mu}^*$ in percent of absolute value of output metric in the reference scenario.

Energy Demand The second section in table 4.3 summarises the ranking of the input factor groups that relate to the energy demand. The table highlights the different effects that the more dynamic electric and thermal demands have in comparison to the more technology-constrained transport demand. In contrast to the electric and thermal demand, which are top ranking for all evaluated outputs, the transport demand has a strong impact on the system costs and the GHG emissions, but it has close to no effect on the other outputs. This indicates that a change in electric or thermal energy demand will lead to a change of the entire energy supply system, while an increase in transport demand will not. However, the results show that a 20% variation in demand will cause a variation in the magnitude of 8-22% in the energy system costs as well as the GHG emissions.

Furthermore, $\boldsymbol{\mu}$ indicates for both the transport energy demand and the electric peak load a positive correlation (see figure 4.6). In contrast, the renewable and nuclear power generation share reveals a negative correlation with the electric peak load factor. Hence, if the peak load factor increases, the demand is less uniformly distributed across the hours of a year, and hence a bigger share of more flexible power plants is required.

Carbon Price The ranking of the carbon price[21] among the other input factor groups is shown in the bottom section of table 4.3. The values emphasise the strong impact the carbon price has on the total energy system. Unsurprisingly, the carbon price is the dominant influence on the GHG emissions, reducing them by up to 24% if the carbon price is doubled from today's values.[22] However, caused by the formulation of the objective function, the carbon price is also among the top ranking factors concerning the energy system costs. But, as explained in section 3.2, the carbon costs are not to be considered system costs as such, and hence the cost impact is not representative here.

Discussion

In the national stand-alone model calibration (with no constraint on GHG emissions) of the South African energy system (*CURPOLnat*), the majority of variance in the main output metric, the energy system cost, is explained by changes in just two categories of input factors groups: (i) the global fossil fuel and domestic fuel prices, as well as the (ii) the useful energy demand. The dominance of these two categories is so significant that all other parameters summed together (this includes all technology costs for all energy supply technologies, the available renewable energy potentials, etc.), have a smaller influence than these. This effect, on the one hand, indicates the lock-in situation that the model experiences from a fuel perspective. For example, the limited and only slowly advancing set of options in the transportation sector forces the model to continue to consume oil despite high prices. Therefore, room for further research remains. For instance, a thorough analysis on the installation growth constraints for new technologies could identify, if the model is over-restrained or if this lock-in situation correctly represents the expected development.

[21]The carbon price, here, is the energy economy-wide price that is applied to all CO_2 emissions from combustion and all fugitive CH_4 emissions at a carbon equivalence level.

[22]In 2019 South Africa introduced a carbon tax. In line with the realised tax bill, in the model calibration the tax is introduced at an effective rate of 2.7 USD/tCO_2eq, and is increased by 3% per annum in the years thereafter (see section 2.5.2)

Furthermore, considering demand elasticity in the model could further shed light on the current *inflexibility* on several fuel demands. On the other hand, this effect indicates a shortcoming inherent to stand-alone models: the representation of international trade. As this model type does not establish commodity prices by supply and demand but rather as a flat-rate price per model period, fuel trade prices tend to introduce a flip-flop effect (either export/import as much as possible or as little as possible - depending on the price).

The dominance of the fuel prices and the useful energy demand is not as pronounced for the variability of the GHG emissions. However, here too, those two groups are among the top ranking. Additionally, the carbon price and the cost ratio between renewable and fossil fuel power plants are identified to have a major influence on the GHG emissions. These results can again be interpreted in two ways: (i) the modelled emission trajectory is susceptible to change and is strongly influenced by the input factor calibration (up to 25% in the case of the carbon price); (ii) there exist significant levers for altering the GHG emission trajectory of South Africa and some of these are in the hand of policy makers to change. However, by identifying the key input factors, these important results can work as a guide to choosing interesting and new scenarios for a scenario analysis that can explore a potentially new energy system development path.

4.5.2 Applying a GHG Emission Constraint

In this section the sensitivity analysis is re-applied to a version of same national stand-alone energy system model of South Africa as described above (*CURPOLnat*) but with an added constraint on GHG emissions. As a "middle-of-the-road" reference the partially conditional NDC emission constraint, as defined in the scenario analysis (see section 3.2) is applied (*PARCONnat*). This is done in order to establish which input factors are of the biggest influence under a GHG emission constraint using a wide screening of a large number of factors within a reasonable computational time demand.

Figure 4.7 summarises the results of the global sensitivity analysis. In line with the presentation of the results of the previous case (see figure 4.6), figure 4.7 shows the average absolute elementary effect $\boldsymbol{\mu}^*$ for the fifteen input factor groups with the biggest influence on the two main output metrics, each ranked in order of influence. However, in this case the evaluation addresses the effect on the marginal price of GHG emissions instead of the GHG emissions in the previous case. The marginal price is defined as the marginal value of the GHG emission constraint equation and can hence be interpreted as the economy-wide carbon price level, required in order to meet the applied emission constraint.

Here again, the dominant input factors are easily detectable. First and foremost is the GHG emission constraint that dominates both the total energy system costs as well as the carbon price. The input factors listed thereafter are similar to the ones already presented in the previous (non-restrained) scenario, i.e. the global fuel price and the energy demand (see table 4.4). However, the renewable energy potential of biomass as well as the cost of biomass are two factors gaining significance under the GHG emission-restrained conditions.

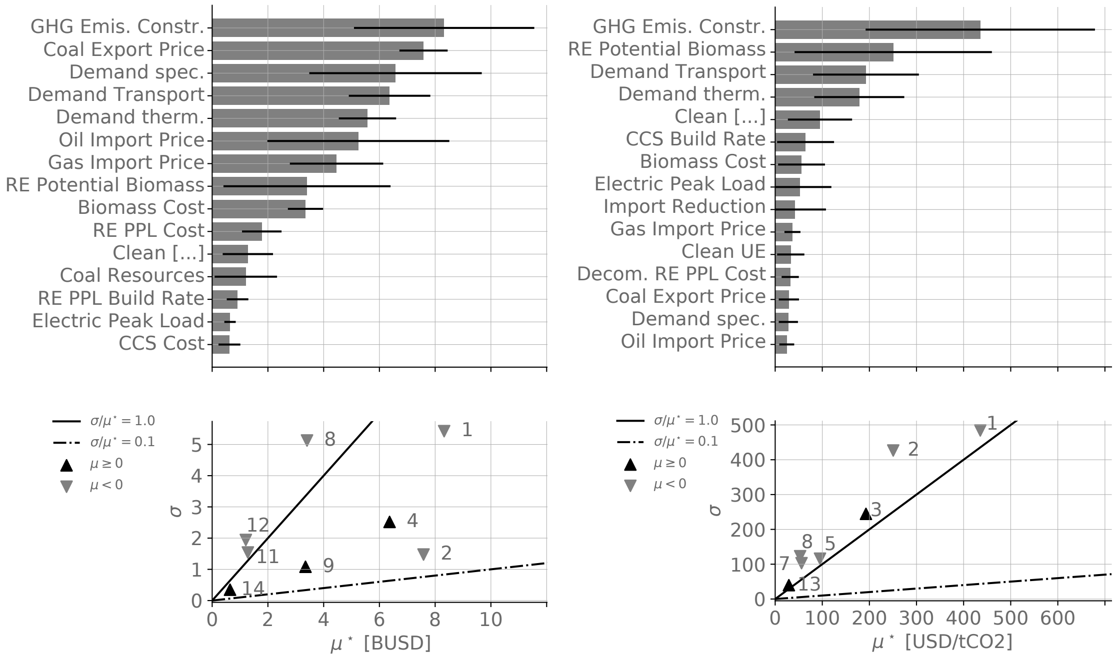

(a) Energy System Cost

(b) Marginal carbon price

Figure 4.7: Results of the initial screening of the GHG emission-restrained national stand-alone scenario (PARTCONnat) showing the 15 most influential input factor groups on the 2050 (a) energy system cost and (b) marginal carbon price. The numbers in the lower plots refer to the parameter rank in the top plot. Abbreviations: Demand spec. = electricity demand, RE = renewable energy, PPL = power plant, conv. = conventional.

Discussion

The sensitivity analysis of the GHG emission-restrained model calibration gives insights into the key cost drivers under a GHG emission reduction scenario. By limiting the GHG emissions, the sensitivity analysis provides information about how the mitigation costs emerge. Additionally, this analysis can be used to identify enablers but also inhibitors for a GHG emission reduction by the energy system.

The results show that in a GHG emission-restrained scenario the energy system costs are mainly driven by the GHG emission constraint itself. However, the GHG emission constraint does not generate costs as such. Thus, the cost impact induced by this input factor can be seen as a cumulative indicator of the system change that is made necessary by the GHG emission constraint. Furthermore, under the GHG emission constraint, the cost impact induced by the non-electric and the electric energy demand change rank. This effect can be attributed to the "ease of decarbonisation" of end-use energy supply. Hence, decarbonisation of the electricity comes at a lower cost than decarbonisation of the diverse thermal end-use supply or the liquid fuel-bound transport sector.

The impact of the input factors on the marginal carbon price allows for identifying so-called *decarbonisation inhibitors*. The results indicate that additional electric demand can be supplied at low-to-no additional GHG emissions. The electric energy demand, hence, has a low impact on the marginal carbon price. The transport and thermal energy demand, however, seem to be locked into an emission-intensive technology branch that limits the degree of electrification for the most supplies. This hypothesis is further supported as the single input factor group "*Clean Mobility Availability*" abbreviated in the bar chart of figure 4.7 as *Clean [...]* ranks among the top five influential input factors for the marginal carbon price - an indicator for the transport sectors lock-in situation in liquid fuel use.

Table 4.4: Comparison of input factors for their influence rank (R) and their impact size (S) for the GHG emission-restrained national stand-alone scenario (PARTCONnat).

	System Cost		**Carbon Price**		**RE Share**		**PPL Output**	
	R	S	R	S	R	S	R	S
Energy Resource Costs Related Groups:								
Oil Import Price	6	12%	15	12%	5	48%	8	0%
Gas Import Price	7	10%	10	18%	6	34%	3	1%
Coal Export Price	2	17%	13	14%	13	16%	5	0%
Biomass Cost	9	7%	7	27%	11	16%	19	0%
Useful Energy Demand Related Groups:								
Demand spec.	3	15%	14	14%	1	162%	11	0%
Demand therm.	5	12%	4	87%	7	31%	10	0%
Demand Transport	4	14%	3	94%	3	55%	15	0%
Electric Peak Load	14	1%	8	26%	18	5%	6	0%
GHG Emission Constraint:								
GHG Emission Constraint	1	18%	1	212%	2	116%	13	0%

GHG: greenhouse gas, RE: renewable energy, PPL: power plant x: R > 20
R: Rank among all tested input factor groups. All values: 2050
S: Size of μ^* in percent of absolute value of output metric in the reference scenario.

In summary, the results point at the importance of investing further research in both the model calibration and the real-world technology options.

Concerning the model, two further analyses are suggested by the model results: (i) an in-depth review of the model assumptions on technology change rates could eliminate possibly overrestictive transition rates; (ii) a comparative multi-scenario analysis that applies a model calibration of elasticity demand could identify the degree, to which the model calibration of inelastic demand overestimates the cost and emission impact of the useful energy demand.

However, the model results also indicate real-world implications: (i) investing in research of new, clean-technology options especially for currently "hard-to-decarbonise" technology branches (such as the transport sector, and means of fast implementation of the same) could reduce the susceptibility of the energy system costs to international market prices, demand hikes and GHG emission constraints; (ii) by appraising the cost burden of GHG emission reduction and its main cost drivers, effective means of realising such hypothetical GHG emission constraints in countries around the world can be established. This cost distribution can then further be applied to design efficient global mitigation strategies that are based on international compensation mechanisms.

4.5.3 Mixed-Granularity Reference Scenario

The following results are created by applying the *Sensitivity Analyser* to a mixed-granularity nested global model reference scenarios (*CURPOL*) that combines the data and granularity from both the national stand-alone (*CURPOLnat*) and a global model calibration (see section 2.5.2).

Due to the computational demands (10-15 minutes per model execution) of the mixed-granularity model calibrations that include both a representation of national detail of South Africa and a supra-national regional representation of the rest of the world, only a reduced set of input factor groups is evaluated in this sensitivity analysis. The selection of input factors is based on the results of the global sensitivity screening of the (GHG emission-unrestrained) national stand-alone reference scenario *CURPOLnat* as described above (see section 4.5.1). The 14 input factor groups of the national stand-alone model that were identified to be of the least influence (see table D.2 in the appendix) were fixed to their pre-calibrated levels. This approach is based on the hypothesis that the similar structure of both models' conditions that sensitivity of the input factors are of the same order of magnitude. Furthermore, international commodity trade prices are user-defined input factors only in the national stand-alone model. In the mixed-granularity model calibration, they are calculated endogenously by the model from the marginal values of the global commodity balance. As such, they are not user-defined and are not relevant for the input factor sample. In summary, the results of the sensitivity analysis of the mixed-granularity global model calibration, *CURPOL*, are formed from 280 separate model executions for the 166 remaining input factors aggregated into 27 groups.

Results

Out of the many mixed-granularity model calibrations established in this dissertation (see figure 3.2), the *CURPOL* calibration (described in section 3.1) was used for the sensitivity analysis. The *CURPOL* (current policies) calibration was designed under the assumption that the GHG emission-relevant energy policies in place today are maintained over the model horizon and that no other climate relevant policies are introduced. It serves as a reference for all other scenario calibrations.

Figure 4.8 summarises the results of the sensitivity analysis of the GHG emission-unrestrained *CURPOL* calibration. As presented before the figure depicts the value of the average absolute elementary effect ($\boldsymbol{\mu}^*$) for the fifteen input factor groups with the biggest influence on the two selected output metrics ranked by order of influence. The chosen metrics are the energy system cost, and the GHG emissions in the year 2050. In order to provide national-level insights and to establish comparability of the results with the results for the national stand-alone model, the outputs are evaluated for South Africa only.

Again, the input factors of biggest influence are clearly identifiable. The demand-related input factors as well as the carbon price are dominant among the top-ranking groups. Overall, the ranking of important input factors as well as the total influence ($\boldsymbol{\mu}^*$) remains similar to the national stand-alone model calibration.[23] Among the 15 top-ranking input factors for the energy system costs of the *CURPOL* calibration (see figure 4.8a) only four parameters are not ranked among the top 15 parameters of the national stand-alone counterpart *CURPOLnat*. However, all of those four parameters can be found among the top 20 ranking (not trade-related) input factor groups of the national-stand-alone model (see table D.2). The same can be observed for the impact on the GHG emissions. This indicates that the primary hypothesis of this analysis holds true, namely that the sensitivity analysis of the national stand-alone model calibrations provides good evidence for the sensitivity of the mixed granularity counterpart calibration, and that the global sensitivity screening of the national stand-alone model provides relevant insights into the sensitivities of the mixed-granularity model calibrations.

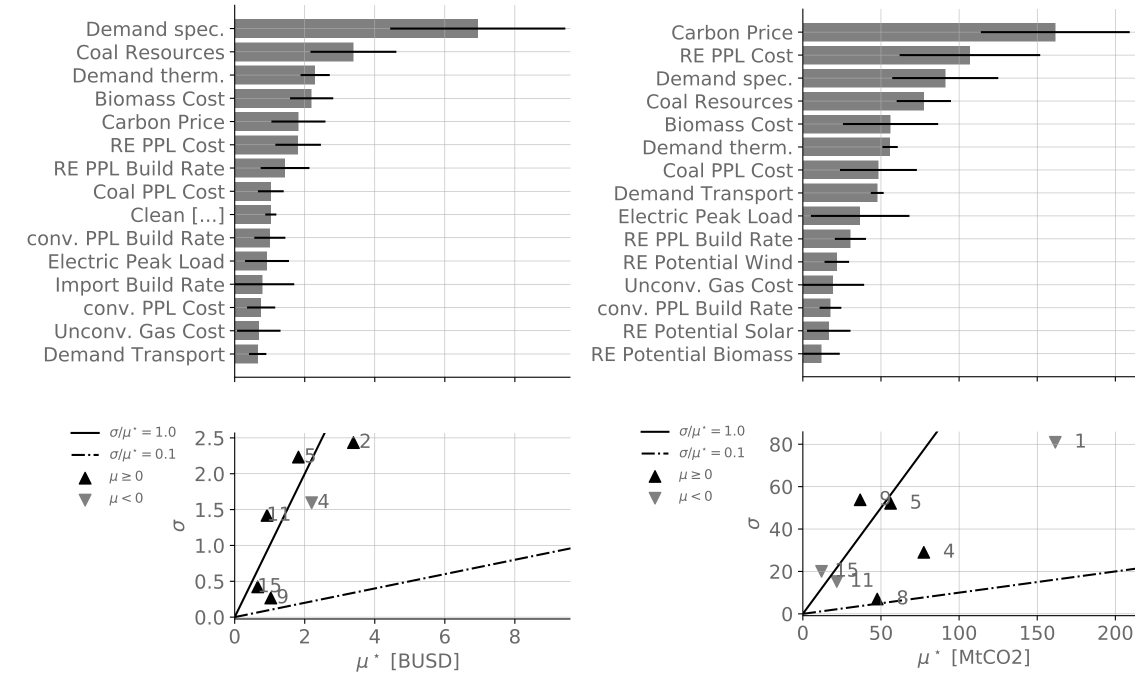

(a) *Energy System Cost* (b) *GHG Emissions*

Figure 4.8: Results of the GHG emission-unrestrained CURPOL reference scenario showing the 15 most influential input factor groups on the 2050 (a) energy system cost and (b) GHG emissions. The numbers in the lower plots refer to the parameter rank in the top plot. Abbreviations: Demand spec. = electricity demand, RE = renewable energy, PPL = power plant, conv. = conventional.

The most influential input factor groups for the *CURPOL* calibration are: (i) the energy costs, (ii) the useful energy demand, and (iii) the carbon price. These three factors are discussed in the following section. While the energy costs for the national stand-alone model are dominated by the commodity prices on the international commodity market, in

[23]The absolute value of the energy system cost variation, here in the *CURPOL* calibration, is smaller than in the national stand-alone counterpart *CURPOLnat*. However, the total energy system costs are too. Hence, the percentage of induced variation remains similar (see table 4.3 and 4.5).

this mix-granularity global case energy costs are defined as resource costs.

Energy Resource Costs Table 4.5 compares the ranks (as given in figure 4.8) to the relative change that the variation of the input factor group causes. The top section of table 4.5 summarises the ranking of the input factor groups that relate to the cost of energy commodities in the *CURPOL* calibration. In contrast to the results of the national stand-alone model calibrations the commodity trade costs are not listed, as these parameters are not applicable to the nested mixed-granularity model.[24] However, the table does list the resource volume of coal and the resource costs of biomass, as they remain among the most influential input factor groups. Both input factors each induce an up to 10% and 14% variation in costs and GHG emissions if shifted by 20% and 50%, respectively. However, due to the method of cost balancing in *MESSAGEix*, the sign of the $\boldsymbol{\mu}$ value changes for the coal resources between results of the sensitivity analysis of the national stand-alone *CURPOLnat* and the global *CURPOL* scenarios (see scatter plots in figure 4.6 and 4.8). While in both calibrations bigger coal resources lead to more coal being extracted and hence results in higher extraction costs for South Africa, in the stand-alone version these additional costs are superseded by the export revenue. In the global version, however, export revenues are not balanced, as the objective function will minimise the summed cost of all nodes, and hence trade costs are cancelled out.

Additionally, the table lists three high ranking input factors from the power sector: (i) the costs of renewable energy power plants, (ii) the costs of coal power plants, and (iii) the maximum build rate of renewable power plants. The numbers indicate that the cost of renewable power plants can have a strong influence on the share of renewable energy in power generation (up to 16%), which results in a major shift in GHG emissions (up to 19%). Of the two input factors, the strongest influence is also enacted on the renewable energy share and, hence, the GHG emissions. However, their influence is much smaller (6% influence on the renewable energy share and 5%-8% on the GHG emissions).

Energy Demand The second section of table 4.5 summarises the ranking of the demand-related input factor groups for the *CURPOL* calibration. The results closely resemble those observed in the analysis of the GHG emission-unrestrained national stand-alone model calibration *CURPOLnat* (see table 4.3). However, the demand in the transport sector that is strongly dependent on import costs reduces its impact on the energy system costs compared to the *CURPOLnat* calibration. This is due to the way costs are balanced in the mixed-granularity model calibrations where the fuel *producing* node has to *pay* for the fuel whether or not this node is also the *consumer*. Hence, in *CURPOL* calibration the increased liquid fuel requirements of South Africa are imposed on the country of fuel origin. In contrast, a 20% increase of the specific electric demand will cause a 20% cost increase, as electricity is not traded globally and hence, the generation costs will be balanced in South Africa.

Carbon Price The last line of table 4.5 lists the impact of the carbon price upon the four selected output metrics. It shows that in the *CURPOL* scenario, the carbon price

[24] The costs are not defined as input factors but endogenously calculated by the model (see section 2.5.2)

Table 4.5: Comparison of input factors for their influence rank (R) and their impact size (S) for the GHG emission-unrestrained mixed-granularity global reference scenario (CURPOL).

	System Cost		**GHG Emission**		**RE Share**		**PPL Output**	
	R	S	R	S	R	S	R	S
Energy Resource Costs Related Groups								
Coal Resources	2	10%	4	14%	7	4%	10	0%
Biomass Cost	4	6%	5	10%	12	1%	8	1%
RE PPL Cost	6	5%	2	19%	1	16%	6	1%
RE PPL Build Rate	7	4%	10	5%	4	6%	13	0%
Coal PPL Cost	8	3%	7	8%	5	6%	7	1%
Useful Energy Demand Related Groups								
Demand spec.	1	20%	3	16%	8	4%	1	23%
Demand therm.	3	7%	6	10%	18	0%	x	0%
Demand Transport	15	2%	8	8%	17	0%	3	2%
Electric Peak Load	11	3%	9	6%	6	5%	14	0%
Carbon Price								
Carbon Price	5	5%	1	28%	2	14%	5	1%

GHG: greenhouse gas, RE: renewable energy, PPL: power plant x: R > 20
R: Rank among all tested input factor groups. All values: 2050
S: Size of $\boldsymbol{\mu}^*$ in percent of absolute value of output metric in the reference scenario.

remains among the input factors with the most dominant influence on the outputs. Just as in the results of the national stand-alone model, also here the influence of the carbon price on the energy system costs remains low (5%) while the influence on the GHG emissions is high (28%). However, the impact of the carbon price on the total power generation changes between the national and the global scenarios. While in the national stand-alone model the carbon price was ranking fifth most important with respect to this output, the effect it has there is ten times higher compared to the global *CURPOL* scenario. This, together with the overall low sensitivity exhibited by the total power generation, indicates that electrification seems to be the overall more expensive GHG emission reduction strategy (e.g. as compared with the GHG emission reduction in the power supply through the application of renewable energy technologies or the GHG emission reduction of the total secondary energy transformation sector using carbon sequestration) as it was already observed in the scenario analysis presented in chapter 3.

Discussion

In the mixed-granularity global model calibration of the South African energy system (*CURPOL*) the majority of variance in the main output metric can be explained by variation in coal resources and the specific electric demand. In contrast, the variation in GHG emissions is far more diverse as a bigger number of input factors exhibits significant influence on this output. Nevertheless, the input factors of significant influence closely resemble the variation experienced by the national stand-alone model. The major influencing factors are the carbon price, the demands, and the domestic resource costs.

4.6 Conclusion

A general understanding exists that sensitivity analyses are important for establishing a deeper understanding of the results of scenario analyses (Saltelli 2008; Droste-Franke et al. 2015). However, they are, to date in the field energy systems analysis, often avoided as they are time-consuming, produce large amounts of data and are thus often regarded as a tedious and perhaps unwelcome exercise of modelling. Therefore, MIGRA-NEST is equipped with a *Sensitivity Analyser* add-on module that is dedicated to sensitivity analysis of MIGRA-NEST-generated model calibrations and makes the sensitivity analysis easier to perform. The implementation of the modules is based on the Sensitivity Analysis Library in Python (SALib) (see section 4.1). This workflow encompasses the generation of an input factor selection, the parallelised model execution and the evaluation, documentation and visualisation of the sensitivity analysis' results as important support for interpretation of the model sensitivities.

The *Sensitivity Analyser* provides the means to utilise both the national stand-alone calibrations from the *Rapid Prototyper* and the mixed-granularity global model calibrations from the *Model Nester*. This is useful as the evaluation of the national stand-alone models can support the reduced input factor selection for the sensitivity analysis of the mixed-granularity global model calibration.

A global sensitivity analysis was conducted for the national stand-alone model calibration of the South African energy system in both a GHG emission-restrained (*PARTCONnat*) and -unrestrained calibration (*CURPOLnat*) as well as on the GHG emission-unrestrained mixed-granularity global model calibration (*CURPOL*).

The sensitivity analyses show that the majority of variations of the model outputs can be assigned to three dominant input factor groups: (i) the energy resource cost, (ii) the useful energy demand, and (iii) the GHG emission constraint including the carbon price. Apart from demonstrating the *Sensitivity Analyser's* capacity, the sensitivity analysis provided several insights.

First, from the comparison of the conducted global sensitivity analyses on the national stand-alone and mixed-granularity calibration two methodological insights can be gained:

- The global sensitivity analyses of the national stand-alone model calibrations show that the commodity market costs are the dominant input factors. This indicates the significance of the representation of the commodity market for producing robust energy system transition strategies.
- The comparison of the results of the sensitivity analyses of the national and the mixed-granularity calibration shows that, apart from the trade parameters, the ranking and the absolute influence of the input factor groups remains of the same order of magnitude. This supports the chosen approach of using the computationally parsimonious national stand-alone model calibration rather than the complex mixed granularity global calibration for factor fixing and factor prioritisation model efforts.

Second, from the results of the conducted sensitivity analyses several real-world implications can be deducted.

- The slow change rate of the transport and thermal energy end-use sectors are, to date, South Africa's inhibitors to GHG emission reduction. By introducing clean technology options and increasing their speed of implementation, emissions mitigation cost can be significantly reduced.
- A push for clean technology could provide South Africa with the opportunity to reduce its import dependence and hence, to hedge against the country's energy system key cost driver, namely fluctuating international commodity prices.
- Technology costs for nuclear power stations do not rank among the twenty most influential input factors of any of the input factors. This indicates that for South Africa, with its vast renewable energy resources, nuclear energy does not pose an economical energy alternative - independent of its cost.[25]

4.7 Discussion

Important insights about a model and the model calibration can be gained through global sensitivity analyses. Nevertheless, in contrast to many other fields, they have not yet become state-of-the-art in energy system analysis (Usher 2016). However, several studies exist that use a comparative scenario analysis or sets of sensitivity scenarios in order to (i) test their model results reliability and (ii) identify the key driver and inhibitors to GHG emission reduction. In the following, the key findings presented above are bench-marked and compared to the recent literature on the topic.

In the presented sensitivity analysis it has been shown that in both the GHG-restrained and GHG-unrestrained model calibrations the useful energy demand is responsible for the majority of the variation in energy system costs as well as in GHG emission levels. This is in line with the findings of the study on the sensitivity of the SSP-scenario's long-term CO_2 emissions pathways by Marangoni et al. (2017). In their study, Marangoni et al. find that assumptions about energy intensity and economic growth (the two factors constituting the useful energy demand) are the most important determinants of future CO_2 emissions in their versions of both GHG emission-restrained and -unrestrained scenarios.

Furthermore, the presented results of all three sensitivity test cases indicate that the technological transition rate of the end-use sector is the biggest inhibitor to GHG emission reduction. Especially the transport sector is identified as being slow to introduce cleaner fuels and limited in total change potential. These findings confirm research focused on the end-use sector. For example, in their study on the role of the transport sector in climate stabilisation McCollum et al. (2014) identify the limited electrification potential of the transport sector to be an important driver for overall mitigation costs.

Biomass (used for power generation and for synthetic fuel production) can not only supply decarbonisation to change-resistant energy use sectors but it can loosen stringent GHG emission requirements by providing net negative emissions (by applying carbon capture and storage).

[25] In the sensitivity analysis the cost for nuclear energy power stations is varied by ± 50%

The main results of the sensitivity analysis of the GHG emission constraint model calibration confirms research results from many other studies (e.g. McCollum et al. (2014) and Riahi et al. (2015)): the model outputs are highly sensitive towards the calibration of the resource volume as well as the resource cost of biomass.

These results also point to an important topic of a current debate: in order to limit global emissions in line with the stringent GHG emission reduction goals (RCP1.9 and RCP2.6 pathways) the deployment of significant shares of using biomass as fuel in association with CCS technologies will be obligatory. While this finding is in line with literature on global energy analyses (e.g. Riahi et al. (2015)) scepticism has been voiced about whether these required high shares are realistic to implement (Fuss et al. 2014).

However, further work remains. First, the global model calibration should be extended to include a representation of elastic useful energy demand. This could create a more realistic picture of the overall cost impacts of limiting global GHG emissions to required levels. Second, the *Sensitivity Analyser* should be adjusted to address net costs for national energy system rather than the respective total global costs. With such an improvement the current analysis could provide more country-specific insights on the cost structure of the energy system. Third, by extending the sensitivity analysis to all regions of the global model calibration, the important cost components for commodity trade, could be more accurately represented for South Africa. However, here too, a significant increase in computing power will be required in order to remain within reasonable time frames, as the number of input factors increases by at least one order of magnitude.

Chapter 5

Summary & Outlook

> The game of science is, in principle, without end. He who decides one day that scientific statements do not call for any further test, and that they can be regarded as finally verified, retires from the game.
>
> Karl R. Popper (1902-1994)

5.1 Summary

This dissertation presents a novel modelling toolbox - MIGRA-NEST (Mixed Granularity Nested Energy System Toolbox) - to explore potential national energy system futures in a global context. A case study conducted on South Africa demonstrates how the toolbox can be employed to identify robust energy transition pathways under the consideration of a global GHG emission budget.

MIGRA-NEST

MIGRA-NEST was designed with the aim of being able to integrate national energy system model calibrations into global energy system model calibrations. Thus, the toolbox allows to create energy system model calibrations of mixed-spatial granularity, i.e. representing a country on national and the rest of the world on supra-national regional levels. This calibration type allows the evaluation of country-level policies in the context of international feedback effects especially from the global commodity markets.

MIGRA-NEST consists of four interconnected modules (see figure 2.2). The modules are each self-contained, each one with a specific purpose. The *Rapid Prototyper* module provides the tools that enable the fast prototyping of simple national stand-alone energy system model calibrations. It allows to adopt and refine the reference energy system (RES) of existing model calibrations of similar or lower spatial granularity and adapting them to national specifications. The module consists of three methods, which support (i) the adoption of RES from pre-existing model calibrations, (ii) the substitution of missing data points by approximations and (iii) an option for model testing feasibility and sanity of the resulting model (see figure 2.3).

The Model Nester produces mixed-granularity model calibrations by integrating national stand-alone model calibrations into global model calibrations. The module workflow consists of two process steps and two testing steps: (i) testing the alignment of the models; (ii) embedding the national stand-alone in the global model calibration; (iii) testing the embedded model; and (iv) finalising the nesting process by establishing trade links between the two sub-models and adjusting the global model parameterisation (see figure 2.4).

The *Scenario Analyser* provides all functionality required to set up, execute and evaluate a structured scenario analysis. Every scenario is defined by a specific reference calibration and a set of separately defined functions that are used to modify the reference. Thus, the *Scenario Analyser* ensures the reproducibility and transparency of the scenario creation process and analysis. In order to support the comparative evaluation, the module allows to aggregate scenarios of interest to scenario sets and evaluates them in a comparative analysis.

The *Sensitivity Analyser* provides tools for a documented and comprehensive global sensitivity analysis. The module supports the user in evaluating the sensitivity of the key model outputs toward the input factor calibration by supplying a standardised workflow for the problem definition, to the parallellised model execution to the calculation of the key measures for the evaluation of sensitivities, and the aggregation and visualisation of the results.

Case Study South Africa

MIGRA-NEST was applied to create a national energy system model of South Africa that is embedded into a representation of a multi-nodal global energy system (with respective global constraints on energy variables). Both energy system models are integrated with calculations of the resulting GHG emission balances.

The purpose of the case study was twofold. First, to investigate cost-effective options for the development of the South African energy system over the period 2020-2050 under different internal and external constraints, with a particular emphasis on mitigation of GHG emissions from the energy system, and on the feasibility for meeting GHG emission reduction targets. Second, to evaluate global GHG emission reduction strategies on their cost and mitigation impact and to identify the means, to which South Africa contributes in such scenario.

National Mitigation Scenarios - NDC Scenarios

The national mitigation scenarios are based on the GHG emission targets (Nationally Determined Contribution, NDC) pledged by South Africa at the 2015 Paris climate conference. South Africa's NDC emission goals are given as a GHG emission trajectory range that is conditional on international support: national GHG emissions would be lower with higher international support, but much higher with no support. Thus, scenarios have been constructed that consider (i) the pledged national GHG emissions with full support from the international community (*FULLCON*), (ii) the unconditional GHG emissions with no international support (*UNCON*), and (iii) a "middle" scenario that reflects partial support (*PARCON*). As reference scenario a *current policies* calibration was elaborated, in which only currently implemented measures were considered without any NDC reduction targets (*CURPOL*).

These four national scenarios were integrated in two global GHG emission reduction scenarios, namely (i) a global *current policies* framework (which forms the basis for the so-called *NDC* scenario set), and (ii) a global emission reduction trajectory that assumes that the three economically most advanced model regions - North America (NAM), Western Europe (WEU), Pacific OECD (PAO) - would reach their regional GHG emission mitigation trajectories as required in the RCP2.6 scenario (the *NDC-m* scenario set). The scenario that reflects the *current policies* base case in South Africa as well as in the global context (*CURPOL*), has been designated as the overall reference scenario.

The results of the scenario runs provided important insights. First, it is possible on a national as well as on a global scale to significantly reduce GHG emissions compared to *current policies* reference.

Second, even under the most lenient emission constraints the investment in carbon-intensive energy infrastructure is not economically competitive. In contrast, the model results show that the longevity and slow exchange rates of the energy supply sector require immediate action for even fulfilling the most lenient GHG emission constraints within the next decade.

Third, limiting South Africa's GHG emissions to the trajectories as suggested in the NDC targets increases total net energy system costs by up to 15%. However, if economically more advanced countries push for strong GHG emission reductions, they create market conditions that give South Africa options to follow their mitigation pathway: (i) a surplus of mid-range carbon-intensive fuels (e.g. natural gas) on the international commodity market makes them cost-competitive with GHG emission-intensive fuels; (ii) an increased global demand for new synthetic fuels, provides South Africa with the option to change their exports away from coal towards synthetic fuels (with a bigger margin). Both effects can lower the mitigation costs for South Africa up to 4%.

Finally, international mitigation efforts also increase the marginal carbon price; this would lead to more stringent reduction measures on a national level.

Global Mitigation Scenarios - RCP Scenarios

The global mitigation scenarios are based on the global GHG concentration trajectories (Representative Concentration Pathway (RCP)). The RCP concept sets the maximum allowable concentration of greenhouse gases according to respective maximum tolerable radiative warming assumptions. These RCP pathways, however, can be translated into maximum allowable global GHG emissions.

The scenarios are based on four RCP scenario developments, namely the relatively lenient RCP6.0, the medium RCP4.5 and RCP3.4, and the ambitious RCP2.6 pathways. In addition, the most ambitious, so-called *Paris Scenario* (RCP1.9) scenario was tested but proved infeasible for meaningful model results. This indicates that the ambitious Paris goals that require a -50% GHG reduction in the energy system within the next decade, and a further reduction to net-negative values by 2100 might pose a real-world challenge for the global community.

For all four RCP scenarios, two different implementations were defined, namely a reduction based on a globally cooperative optimised allocation (the *OPT* scenario set), and a reduction that is based on an equal-share contribution from all global model regions (the *EQU* scenario set). As before, the *current policies* (*CURPOL*) that contains no GHG emission constraint was used as reference.

The results of the scenario runs allow some robust conclusions. On a global level, the economic potential for GHG emission reduction in the energy system varies significantly among the model regions. While - the *current policies reference* - all model regions can reduce emissions up to -50% over the projection period (2021-2050), the cost efficiency of GHG emission reduction varies significantly among the regions. For example: reducing emissions by -25% (as required in the *EQU34* scenario) raises the average discounted net energy system costs by 11 USD/tCO_2eq in Sub-Saharan Africa (AFR), but 35 USD/tCO_2eq Pacific OECD (PAO) and Western Europe (WEU). Furthermore, the economically least advanced model regions are the ones with the overall biggest economical GHG emission reduction potential. This highlights the importance of international balancing mechanisms that would incentivise the utilisation of this potential but not burden to the ones contributing the most.

With a view on South Africa, the RCP scenario results indicate that in all *globally optimised* (*OPT*) scenarios South Africa reduces more GHG emissions than in the parallel *equal-share* (*EQU*) scenarios. This highlights the economic potential that a globally optimised mitigation approach holds for the country. As an economically export-dependent nation with vast renewable and abundant fossil resources, South Africa can monetise the growing international demand for clean synthetic fuels in the mitigation scenarios. However, high export revenues are needed to compensate for the necessary investments. Hence, in order to decouple the national mitigation from the export market, other incentives, such as an international GHG emission trading system, will be needed.

Sensitivity Analysis

The *Sensitivity Analyser* of MIGRA-NEST was used for a thorough check of three selected scenarios with respect to the sensitivity of results with variations of selected input factors. The sensitivity analysis was conducted for two versions of a national stand-alone model calibration of the South African energy system and one version of a mixed-granularity calibration of the South African energy system in a global context.

The two national stand-alone scenarios are a GHG emission-unrestrained (*CURPOLnat*) and a GHG emission-restrained (*PARTCONnat*) calibration. Both scenarios are stand-alone versions of the corresponding global scenarios - the *current policies* (*CURPOL*) reference and the partial NDC pledged emission reductions scenario (*PARCON*).

As the two stand-alone model implementations are much leaner with respect to computation time requirements these were selected for the initial sensitivity analyses, aimed at identifying the least important factors with respect to the key outputs in order to exclude them from the tedious and time-consuming model runs with the complex mixed-granularity model.

The results of the sensitivity analyses show that the majority of variations of the model outputs can be assigned to three dominant input factor groups: (i) the energy resource cost, (ii) the useful energy demand, and (iii) the GHG emission constraint including the carbon cost. Apart from demonstrating the Sensitivity Analyser's capacity, the sensitivity analysis provided several insights.

With respect to the energy system modelling methodology, is becomes clear that the commodity market costs are dominant input factors. This indicates the significance of including an adequate representation of the commodity market for producing robust energy system transition strategies. Furthermore, apart from the trade parameters, the ranking and the absolute influence of the input factor groups remains in the same order of magnitude between the two local stand-alone models and the complex global mixed-granularity model. This indicates that using the computationally parsimonious national stand-alone model calibration can be used for factor fixing and factor prioritisation.

With respect to policy implications, the results indicate that the slow change rate of the transport and thermal energy end-use sectors are, to date, inhibitors to reducing South Africa's energy related GHG emissions. By introducing clean technology options and increasing their speed of implementation, emission mitigation costs can be significantly reduced. A push for clean technology could provide South Africa with the opportunity to reduce its import dependence and hence, to hedge against the country's energy system key cost driver, namely fluctuating international commodity prices. Technology costs for nuclear power stations do not rank among the twenty most influential input factors of any of the input factors. This indicates that for South Africa, with its vast renewable energy resources, nuclear energy does not pose an economical energy alternative - independent of its cost.

5.2 Further Research

This dissertation identifies various fields of research that are presented in the fallowing.

Model Methodology

This dissertation creates parsimonious model calibrations of energy systems. While this enables the execution of a large number of scenarios, some relevant effects might be missed.

First, the results of the sensitivity analyses suggest that the end-use sector has a significant influence on both the GHG mitigation potential as well as the related mitigation costs. Thus, extending the representation of the end-use sector in the current calibration might allow for a more accurate assessment of the end-use related results. A first step towards this analysis of the end-use sector that has previously proved useful (Orthofer et al. 2019), could be to calibrate the macroeconomic *MESSAGEix* extension for the representation of demand elasticity's *MACRO* to the national stand-alone model calibrations.

Second, several region-specific characteristics were tested on their linear correlation to the economic GHG emission mitigation potential of the model regions. While this work identifies some of the relevant correlated factors, the created list is not exhaustive. Extending the analysis to more characteristics and to include non-linear correlations could provide further insights, into which typical features should describe a "cost-efficient to decarbonise" model region.

Third, in the current set-up the calibration of the historic energy supply structure has to be supplied to the *Rapid Prototyper* by the model user, a process that might discourage potential users. An extension to the module, which auto-generates a historic calibration prototype by providing the framework calibration data from an international energy use database (e.g. IEA (2018)) could further ease the prototyping process.

Data Needs

The case study presented in this dissertation provides useful insights into the dynamics of the South African energy system that are induced by national as well as international mitigation ambitions. While some general conclusions for structurally similar national energy systems can be drawn from this analysis, conducting additional case studies on these countries would be needed to confirm these presumptions.

Additionally, creating insights on the structural similarity of countries and regions could provide useful information for creating international mitigation strategies. MIGRA-NEST provides a useful framework for calibrating a fleet of comparable national energy system models, which could be applied to such an analysis.

Optimisation and Fairness

This dissertation offers insights into how global GHG emission mitigation could be distributed globally in a *technically feasible* and *cost-optimal* manner and how such a distribution would impact the participating countries and regions. However, the presented *cost-optimal* strategies are neither tested for *practicability* nor *fairness*. The provided allocation, thus, supplies a basis for further research on how to establish a fair distribution that would be acceptable to all involved parties. Here, further research that compares different approaches of a *fair* distribution could build a useful foundation for the negotiation of the mitigation distributions.

Furthermore, the identification of the policy instruments, (i.e. public regulations, and measures to implement the allocated GHG emission reduction) is essential in order to identify how, and to what degree, the technically *optimal* strategies can be realised. In line with current literature (e.g. Pollitt (2019)), this dissertation indicates that a global carbon market would be a suitable tool for incentivising cost-optimal GHG emission reduction, but the applied model calibration is currently not able to evaluate the practicability of the introduction of such a scheme. As such, the scenarios presented in this dissertation shall be considered a guideline for developing policy instruments that push in the direction of a globally coordinated *optimal* GHG emission reduction strategy.

Furthermore, this dissertation calculates the regional distribution of the mitigation cost in a variety of scenarios. However, recent literature suggests that the decarbonisation of the energy sector is not only a cost burden, as the results of the cost-optimised energy models might indicate, but can in many ways be viewed as a development option and economic stimulus (e.g Sen and Ganguly (2017) and McCollum et al. (2018a)). Hence, further research could employ a model that portrays economic feedback effects in order to more accurately portray the system costs.

5.3 Further Use of MIGRA-NEST

The presented model toolbox (MIGRA-NEST), including all documented workflows and scrips, will be published under an open-source licence. By utilising open-source software for model creation (*MESSAGEix/ixmp*) and for sensitivity analysis (SALib) this toolbox is designed as work-environment for the open modelling community. By connecting the underlying open software packages and connecting them into one standardised workflow, the toolbox provides for the creation and evaluation of models and scenarios within one transparent and reproducible modelling process. By easing model recreation and encouraging utilisation of existing model calibrations I hope to contribute to the growing open-source energy modelling community by strengthening cooperation and hence quality among the community.

Appendix A

Additional Material: Calibration Data

This appendix presents the data used for model calibration of the *MESSAGEix*-South Africa Model.

A.1 Installed Capacities

A.1.1 Installed Liquid Fuel Conversion Capacities

Table A.1: South Africa's installed liquid fuel production capacity. (Data from Nkomo (2009), Machete (2013), SA DoE (2016b), and SAPIA (2018))

Technology	**Name**	**Commissioning**	**Decommissioning**	**Capacity (bpd)**
Refinery	Enref	1954	>2050	120 000
Refinery	Sapref	1962	>2050	170 000
Refinery	Chevref	1966	>2050	100 000
Refinery	Natref	1971	>2050	108 000
CTL	Sasol 2&3	1980	2040	150 000
GTL	Mossel Bay	1992	2042	45 000
Total				**693 000**

A.1.2 Installed Power Generation Capacities

Table A.2: South Africa's installed power generation capacity. (Data from ESKOM (2018), IPPO (2018), and IPPO (2019))

		Station Owner	**Station Name**	**Station Location**	**Start-up Date**	**Capacity [MW]**
Base-load Stations	Coal	Eskom	Arnot	Middelburg	1971-1975	2 232
	Coal	Eskom	Camden	Ermelo	2005-2008	1 481
	Coal	Eskom	Duvha	Emalahleni	1980-1984	2 875
	Coal	Eskom	Grootvlei	Balfour	2008-2011	1 120
	Coal	Eskom	Hendrina	Middelburg	1970-1976	1 638
	Coal	Eskom	Kendal	Emalahleni	1988-1992	3 840
	Coal	Eskom	Komati	Middelburg	2009-2013	904
	Coal	Eskom	Kriel	Bethal	1976-1979	2 850
	Coal	Eskom	Kusile	Ogies	2017* (15%)	720
	Coal	Eskom	Lethabo	Vereeniging	1985-1990	3 558
	Coal	Eskom	Majuba	Volksrust	1996-2001	3 843
	Coal	Eskom	Matimba	Lephalale	1987-1991	3 690
	Coal	Eskom	Matla	Bethal	1979-1983	3 450
	Coal	Eskom	Medupi	Lephalale	2015* (50%)	2 157
	Coal	Eskom	Tutuka	Standerton	1985-1990	3 510
	Nuclear	Eskom	Koeberg	Cape Town	1984-1985	1 860
Peak-load Stations	Gas/Liquid fuel	Eskom	Acacia	Cape Town	1976-1976	171
	Gas/Liquid fuel	Eskom	Ankerlig	Atlantis	2007-2009	1 327
	Gas/Liquid fuel	Eskom	Gourikwa	Mossel Bay	2007-2008	740
	Gas/Liquid fuel	Eskom	Port Rex	East London	1976-1976	171
	Gas/Liquid fuel	IPP	multiple	-	**	1005
	Pump-Storage	Eskom	Drakensb.	Bergville	1981-1982	1 000
	Pump-Storage	Eskom	Ingula	Ladysmith	2016-2017	1 324
	Pump-Storage	Eskom	Palmiet	Grabouw	1988-1988	400
	Pump-Storage	Eskom	Gariep	Norvalspont	1971-1976	360
	Pump-Storage	Eskom	Vanderk.	Petrusville	1977-1977	240
Volatile RE	Wind energy	Eskom	Sere	Vredendal	2015	100
	Wind energy	IPP	multiple	-	**	1980
	Solar PV	IPP	multiple	-	**	1474
	Solar CSP	IPP	multiple	-	**	400
	Landfill	IPP	multiple	-	**	8
	Small hydro	Eskom	multiple	-	**	61
	Small hydro	IPP	multiple	-	**	14
	Total Capacity					**50 503**

* still under construction

** modelled commissioning date 2015

A.2 South Africa's Fossil Energy Resources

Table A.3: Model assumptions on South Africa's fossil resource potential. Data Sources: EPRI (2017), Hartnady (2010), SA DoE (2016b), Kock et al. (2017), and Thovhogi et al. (2015).

	Coal	Crude	Gas	Shale Gas	CBM
Volume [EJ]	661.78	0.08	0.38	15.21	7.59

Coal Despite the large amount of coal recovered in the last decades approximately three quarters of South Africa's proven coal reserves remain unrecovered to date (Pollet et al. 2015). Current estimates on viable coal reserves range between 290-2 000 EJ, depending on the views, on which resources are economic to mine (EPRI 2017; Hartnady 2010). In absence of more accurate data, in this dissertation a mid-range approximation also is applied.

Crude Oil and natural Gas South Africa's conventional fossil fuel resources are close to depletion and only minor resource volumes remain (SA DoE 2016a). In lack of assessment data on the actual resource size remaining, the volume was estimated based on current extraction rates and expected depletion dates. However, in February 2019 the French energy major *Total* announced that they may have identified a potential new deep-water oil and natural gas play located in area of the existing off-shore drilling platform Mossel Bay, holding up to 6.1 EJ of natural gas and liquid hydrocarbons (Sheppard et al. 2019). Those estimates, though potentially game-changing for South Africa's energy sector, have still to be scientifically verified, geologically tested and economically evaluated, especially since the play is located at an area that is difficult to access because of strong waves and currents (Sheppard et al. 2019) and were hence, not considered in this assessment.

Shale Gas In 2015 a report from the IEA attracted international attention when it announced that the Ecca Group's Whitehill Formation in the Southern Karoo Basin could possibly hold up to 392 EJ of shale gas, which equals 80 times South Africa's current annual primary energy consumption (BP 2018; US EIA 2015). Those estimates are speculative and based on geologic data such as carbonaceous shale thickness, area, depth, maturity and, the organic carbon content of the formation. However, those estimates were made without any measurements. A more recent report, which is based on several actual measurements estimates the technical recoverable potential to be in the range of 15 EJ might be more realistic (Kock et al. 2017).

Coal Bed Methane South Africa's coal bed methane (CBM) resources are estimated to lie in the range of 5.2 to 10.3 EJ (Thovhogi et al. 2015). In lack of more accurate estimates a mid-range value was applied in the analysis.

A.3 South Africa's Renewable Energy Potential

South Africa's renewable energy potential as included in the model is based on several national and international studies. All relevant sources are introduced below.

Solar PV and concentrated solar power (CSP) Solar energy is perhaps the most abundantly available and readily accessible renewable energy resource in South Africa. Most areas experience on average more than 6.8 hours of sunshine per day (2 500 hours per year), and solar-radiation levels between 4.5 and 6.5 kWh/m^2 (see figure A.1). This is more than double the average radiation experienced in the sunniest parts of the United States and Europe, which experience about 3.6 kWh/m^2 and 2.5 kWh/m^2 respectively (see figure A.1) (SA DoE 2015; SA DoE 2016a). According to Banks and Schäffler (2006), the solar energy of no more than 0.2% (3 000 km^2) of the country's land cover would be sufficient to supply South Africa's total energy demand. This vast potential is well suited for both i) solar thermal applications such as space and water heating in households and commerce or for industrial process heat provision, and ii) electricity generation from photovoltaic as well as concentrated solar power.

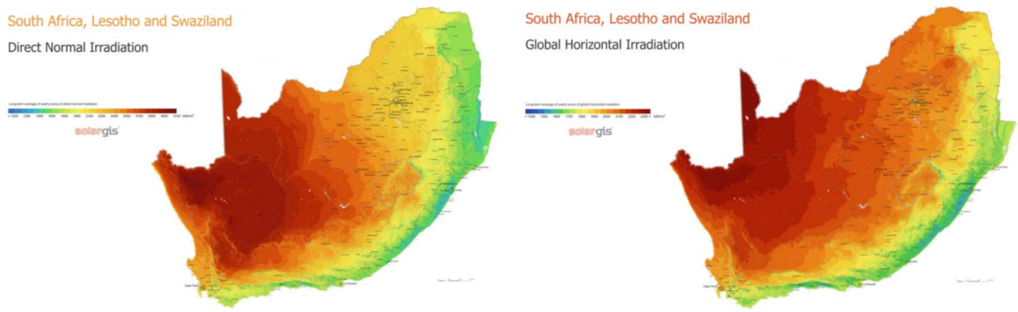

Figure A.1: Solar resource maps for South Africa, Lesotho and Swaziland (annual sum of direct normal irradiation and global horizontal irradiation, kWh/m^2), GeoModel Solar (SA DoE 2015)

The resource estimations for solar PV and CSP, applied to the model, are based on a global solar energy assessment by Pietzcker et al. (2014) and are adjusted to national recorded historical performance data on existing solar power generation in South Africa (Calitz and Wright 2019). This was necessary as for solar PV the data set by Pietzcker et al. (2014) specifies a maximum of 1 300 full load hours per year for the best solar PV categories, which lies 40% below the recorded average full load hours of solar PV installations in South Africa (Calitz and Wright 2019). Therefore, the capacity factor of the top solar PV potential category was increased to match the real recorded data. Furthermore, while the data set provided by Pietzcker et al. (2014) segments the available resource potential not only by regional capacity factor, but also by distance to the grid on country level this second differentiation is not applicable to the one-node model calibration. Hence, and in order to consider the economic aspects of electricity transmission, only the solar energy potentials in closest proximity ($\leq$ 50 km) to the closest settlement are considered in the model. The solar PV potential is displayed in top section, the CSP potential in the bottom half of table A.4 below.

Table A.4: Model assumptions on South Africa's solar PV & CSP energy potential aggregated by capacity factor. Data based on Pietzcker et al. (2014).

Cap. Factor		**≥ 0.26**	**0.26-0.14**	**0.14-0.13**	**0.13-0.11**	**0.11-0.1**	**≤ 0.1**
PV Potential	[GW]	22	407	1422	0	285	0

Cap. Factor		**≥ 0.6**	**0.59-0.57**	**0.57-0.55**	**0.55-0.53**	**0.53-0.5**	**≤ 0.5**
CSP Potential	[GW]	125	221	291	389	161	65

Furthermore, and in order to differentiate between utility-scale electricity production and the direct solar thermal use for residential, commercial but also industrial use, the latter two potentials are established as two separate energy resources. In lack of a more accurate assessment, the direct thermal solar energy potentials for both industrial and residential/commercial applications are estimated to be 0.3 EJ/a based on national calculations SA DoE (2018b) and SA DoE (2018c).

Wind Apart from its vast solar energy potential, South Africa has also been identified as one of the countries exhibiting a substantial wind energy potential. The recently released South African wind energy atlas (see figure A.2) indicates several areas where average annual wind speeds of up to 10 m/s occur (SA DoE 2015; SANEDI 2018).

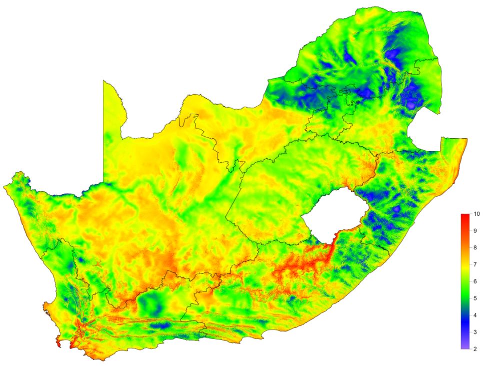

Figure A.2: High-resolution wind resource map showing mean wind speed (ms^{-1}) at 100 m. (SANEDI 2018)

The on- as well as off-shore wind energy potentials applied in the model are adopted from the a recent global assessment by Eurek et al. (2017). Similar to the solar power data set described above, the wind power data sets aggregate the wind power potential on the level of the whole country by capacity factor and distance to the grid. The offshore wind power potential data is further classified by water depth. However, considering South Africa's huge on-shore wind power potential and the economic favourably of on- over off-shore wind turbines, only the on-shore potential that is located in close proximity to a power sink or a grid access point is consideration in the model.

Table A.5: Model assumptions on South Africa's on-shore wind energy potential aggregated by capacity factor. Data based on Eurek et al. (2017).

Cap. Factor	**≥ 0.34**	**0.34-0.3**	**0.3-0.26**	**0.26-0.22**	**0.22-0.18**	**≤ 0.18**
Potential [GW]	2	64	146	168	317	937

Biomass Today, biomass is one of the predominant renewable energy sources in South Africa. Pelkmans (2018) records that more than half of South Africa's residential energy use is supplied by biomass in the form of primary solid bio-fuels and charcoal. This so called *unconventional* traditional biomass use is especially focused in poor households living in remote and rural communities, where modern boilers are not common. Those households use biomass for direct thermal applications, which comes at the cost of adverse impacts on human health and low energetic efficiency (IRENA 2015). However, biomass also finds commercial energetic use. Here, the main commercial biomass producers as well as consumers are the sugarcane industry (field residue and bagasse), the forest industry, the sawmills as well as the pulp and paper industry, which use the biomass for process heat generation as well as heat-and-power co-generation (Rago et al. 2018; SA DoE 2016a).

Despite the modern energetic use of biomass being underrepresented in South Africa to date, the huge country offers a vast potential of manure, agricultural and wood residues, energy crops as well as landfill gas (EPRI 2015). Recent assessments estimate the domestic biomass potential available today to be at around 0.355 EJ/a (Wim 2016). Additionally, estimates exist that the energy content of the currently unused domestic and industrial refuse alone amounts to about 0.04 EJ/a (SA DoE 2016a). While the majority of the waste's energy content is currently lost in landfills, it could instead be utilised by direct incineration for the production of electricity or conversion into biogas and methane.[26] Furthermore, the department of energy has announced plans to mandate a minimum of 5% bio-diesel blending with diesel and between 2% and 10% bio-ethanol blending with petrol starting mid-2019 in order to revitalise South Africa's bio-fuel industry. However, consultations are currently still taking place on the industry implications, the infrastructure requirements and costs associated with manufacturing and blending of bio-fuels as mandated by this regulation (SA DoE 2016a; Pelkmans 2018).

A large variety of fuels are considered under the term biomass. In the model they are aggregated to represent the potentials of non-commercial and commercial biomass, as well as landfill gas. The resulting volumes are summarised in table A.6.

Hydro Due to South Africa's geography and the persistent water scarcity, the inland commercial deployment of hydro-power is very limited and the remaining hydro-power potential is limited to a few domestic small-scale hydro energy power plants. The potential for new small-scale hydro development is believed to range between 0.2 to 0.5 GW(Miketa and Merven 2013; SA DoE 2015). In 2015 hydroelectricity accounted for only 0.3% of domestic power production (SA DoE 2016a). Today Eskom owns two hydroelectric power stations and four pumped storage schemes with a nominal capacity of 3.3 GW (ESKOM

[26] Several landfill sites already produce electricity from refuse, however, the total installed capacity collectively contributes less than 0.5% towards the total electricity generation (SA DoE 2016a).

Table A.6: Model assumptions on South Africa's biomass potential. Data based on Stecher et al. (2013), Batidzirai et al. (2016), Rago et al. (2018), Sustainable Energy Africa (2017), and Mokveld and Eije (2018).

	Non-Commercial Biomass	**Commercial Biomass**	**Landfill Gas**
Potential [EJ/a]	3.15	1.10	0.06

2017). However, due to climatic conditions, those plants cannot be relied upon during dry periods (SA DoE 2016a).

However, already today and thanks to the Southern African Power Pool (SAPP) that allows for the free trade of electricity between Southern African Development Community (SADC) member countries, South Africa imports a contractually fixed electricity supply (1.3 MW) of hydro-power from Mozambique's *Cahora Bassa Dam*. In 2017, despite cross-border purchases being well below target (due to low dam levels as a result of the continued drought in Mozambique's South) the hydroelectricity imported increased the share of hydro power generation to 5% of total electric demand (SA DoE 2016a; ESKOM 2018). Further, the governments of South Africa and the Democratic Republic of Congo have signed a treaty for the establishment of a 4.8 GW hydroelectric station on the Congo River, *Inga III*, of which 2.5 GW will be allocated to South Africa (ESKOM 2017; SA DoE 2016a). While the construction of the *Inga III* dam is about to start, the world's largest dam expansion project *Grand Inga* has been brought on the way, for which the South African government signalled willingness to double the amount it will purchase (Clowes 2018; Warner et al. 2019; Clowes and Burkhardt 2019).

In summary, the electric generation potential of hydro-power plants in South African amounts to about 6 GW, which in the model is split into equal shares of small- and large-scale project (SA DoE 2015).

A.4 Energy Demand

A.4.1 Calculation of the Useful Energy Demand

In the South African case study energy demand is represented as useful energy demand, i.e. as the energy service demand rather than a need for a certain energy commodity. However, at the time of the model creation, no forecasts on the future development of the useful energy demand for South Africa were publicly available. Hence, the useful energy demand forecasts are based on final energy demand records and forecasts as published by national sources SA DoE (2016a) and SA DoE (2018a). Based on these forecasts and the technical specifications (especially the efficiencies) of currently in use energy applications, the useful energy demand forecast is calculated based on the assumption that the technological share remains similar over the model horizon. The results are displayed in table A.7 alongside the calculated final energy demand.

Table A.7: Useful energy demand forecast for South Africa.

[EJ/a]	2030	2040	2050	2060	2070
Industry Sector					
Feedstock Demand	0.29	0.33	0.39	0.41	0.42
Specific Electric Demand	0.52	0.76	0.98	1.04	1.09
Thermal Demand	0.73	0.98	1.34	1.41	1.43
Residential & Commercial Sector					
Non-commercial Demand	0.04	0.03	0.03	0.02	0.01
Specific Electric Demand	0.25	0.38	0.47	0.50	0.53
Thermal Demand	0.29	0.29	0.32	0.33	0.34
Transport Sector					
Mobility Demand	0.97	1.30	1.72	1.84	1.95
Total Domestic Energy Demand	3.10	4.08	5.24	5.55	5.76

A.4.2 Peak Load Factor

South Africa's peak load factor, the proportion between average and peak electricity demand, currently lies at 1.3 (ESKOM 2019). However, the South African power system has not been keeping up with the rapid demand growth over the past decades and can thus, to date not provide the capacity margin required for safe operation. While in 2018 the actual capacity factor was below safe levels in the model, the goal of providing an adequate and safe capacity reserve is envisioned for the model year of 2050. Therefore, between the first model year 2030 and 2050, the peak load factor is gradually increased from today's peak load factor of 1.3 to the safe peak load factor of 1.7.

A.5 South Africa's Independent Power Procurement Program

In 2010, the Department of Energy launched the competitive Independent Power Producer Procurement Programme (IPPPP) in order to develop the power plant capacities as envisaged in the Integrated Resource Plan (IRP), through the private sector and to combat the ongoing power crisis (Calitz and Wright 2019). The main aims of the program were to introduce a competitive tendering system to diversify the power sector fuel mix and ownership structure and to further use the resulting competition to increase the system-efficiency. The IPPPP targets to procure 30 GW of power capacity from the private sector, as determined by the IRP to be connected to the grid by 2025 (IPPO 2019).

Renewable Energy Independent Power Producer Procurement Programme In 2011 the IPPPP was topped of by the introduction of the Renewable Energy IPPPP Programme. In line with the IPPPP the aim of the programme is to procure renewable power (power generation from onshore wind turbines, solar photovoltaics and concentrated solar power plants, thermal bio-, landfill-gas and biomass combustion as well as from small hydro power stations) from the private sector in multiple predefined biding rounds. For each of those tenderings, the programme establishes a technology-specific price cap and a maximum awardable capacity. Based on a 70 to 30 ratio for the offered price and their socioeconomic development concept, the preferred bidders are invited to sign a power procurement agreement with Eskom as well as an implementation agreement with the government. The signed contract established a two decades long guaranteed feed-in-tariff at the tendered price (Eberhard and Naude 2017).

Several independent assessments have described the renewable energy IPPPP a success story (Eberhard and Kåberger 2016; IRENA 2018). By 2019 6.4 GW of renewable power was commissioned from 112 so-called Independent Power Producer (IPP) in the course of seven highly competitive bid rounds (IPPO 2019). Of this allocated capacity, 4 GW were already connected to the grid by 2019 and had since the first project had become operational produced 36 TWh of electricity (IPPO 2019). To date, every new bid round had surprised by strong competition and a resulting drop in average tariffs. Since the first bid round, average tariffs decreased drastically: for example for solar PV prices dropped by 75% and for onshore wind by about 50% between the first and the last bid round, leading to renewable power generation prices that are, for the first time, below average generation costs of coal power plants (IRENA 2018; ESKOM 2018; Calitz and Wright 2019).

However, the project development speed has recently faced delays after Eskom refused to sign the financial contracts of the last bid windows in 2016 (IPPO 2019; Mathews 2017). Furthermore, the delayed publication of the 2018 IRP led to policy uncertainty for investors and finally put the programme on hold by 2017 (Khumalo 2018). However, by 2018 the energy minister Jeff Radebe finalised the 2016 bid rounds by signing the remaining 27 projects (IPPO 2019; ESKOM 2018). Furthermore, in an attempt to strengthen the shaken investors trust, the minister announced to open a new bid window of 1.8 GW by November 2018 (Creamer 2018). Yet, to date, no new bid window has been opened.

Non-Renewable Independent Power Producer Procurement Programme In order to guarantee the flexibility as well as reliability required by the power system, South Africa will, in the short to medium term, require conventional non-renewable power stations to complement the renewable power procured by the energy IPPPP. Therefore, the non-energy IPPPP aims at procuring non-renewable base-load, mid-merit and peaking power plants with a strong focus on gas turbines but also industrial co-generation and coal power plants.

Of the determined 3.1 GW of natural gas turbines, to date two gas peaking plants with a combined capacity of 1.3 GW have been commissioned and connected to the grid (IPPO 2019; ESKOM 2018). Beyond, supplying peak-load power, flexibility, and reliability to the South African power grid, the determined natural gas turbine capacity was also aimed at stimulating and catalysing South Africa's natural gas and liquefied natural gas (LNG) industry by the establishment of a local and reliable natural gas demand. However, major issues with the reliability of gas supply and the lacking gas infrastructure have so far prohibited the realisation of the determined required capacity and has led to the expensive situation, in which all natural gas turbines in South Africa are currently run on diesel rather than natural gas (ESKOM 2018). It is expected that the Gas Utilisation Master Plan (GUMP), as soon as published, will address those issues and thus to be able to reestablish policy trust and private sector investor interest. In the meantime the Department of Energy has announced that it is developing an LNG to Power IPPPP that focuses on installing LNG import terminals together with gas power plants at each of the Ports of Coega, Richards Bay and Saldanha Bay. While the procurement process that was initially expected to launch in 2016 was since put on hold, the strong gas focus of the 2018 IRP raises expectations to accelerate the reopening and bid documents are expected to be released soon after the adoption of the IRP (Creamer 2018; Radebe 2018).

The coal IPPPP, in line with the 2010 IRP aims at procuring 2.5 GW base-load coal power plants (IPPO 2019; SA DoE 2011). While 0.8 GW have already been awarded preferred bidder status in 2013 and the initial commercial operations date for the projects was set to be in 2015, continuing public critique and financial difficulties, have to date prevented the financial close (Mokgopo 2019). However, in the 2018 IRP the determined amount of new coal capacity is reduced to 1 GW and thus matches the capacity of the already awarded projects (SA DoE 2018a).

A.6 Model Benchmark Data

A.6.1 Results of the Integrated Energy Plan

Table A.8: Installed power generation capacity and electricity output as indicated in the Integrated Energy Plan by the SA DoE (2016a) and SA DoE (2016b).

Installed Power Generation Capacity GW								
[GW]		**Coal**	**NUC**	**Gas**	**Wind**	**Solar**	**Others**	**Total**
2020	BC	46	2	-	-	1	6	55
2050	BC	21	39	25	22	47	11	165
	EA	18	13	20	20	47	2	120
	GS	19	12	10	18	23	3	85
	RC	22	16	22	15	38	7	120
Electricity Output								
[TWh/a]		**Coal**	**NUC**	**Gas**	**Wind**	**Solar**	**Others**	**Total**
2020	BC	235	3	-	-	-	32	271
2050	BC	89	22	148	59	148	273	738
	EA	39	15	74	49	148	167	492
	GS	54	8	41	14	41	114	271
	RC	98	15	123	39	74	143	492

Scenarios: Base Case (BC), Environmental Awareness (AE), Green Shoots (GS), Resource Constrained (RC)

Fuel names: *Gas*: natural gas & liquefied natural gas (LNG), *NUC*: nuclear power stations

Table A.9: Final energy forecast as indicated by the Integrated Energy Plan (IEP) produced by South Africa's SA DoE (2016a) and SA DoE (2016b).

[EJ/a]		**Coal**	**Oil**	**Electr.**	**Gas**	**Other**	**Total**
2020	BC	0.95	0.85	1.10	0.05	0.02	**3.01**
2050	BC	2.50	1.95	3.00	0.50	0.03	**8.02**
	EA	1.20	2.05	2.00	0.20	0.03	**5.52**
	GS	0.90	1.65	1.10	0.30	0.02	**4.01**
	RC	1.30	1.95	2.00	0.20	0.03	**5.52**

Scenarios: Base Case (BC), Environmental Awareness (AE), Green Shoots (GS), Resource Constrained (RC)

Fuel names: *Oil*: all liquid fuels, *Gas*: natural gas & liquefied natural gas (LNG)

Table A.10: Liquid fuel supply as indicated by the Integrated Energy Plan (IEP) produced by South Africa's SA DoE (2016a) and SA DoE (2016b).

[EJ/a]		**Import**	**CtL**	**GtL**	**Refinery**	**Total**
2020	BC	0.35	0.10	0.01	0.77	**1.23**
2050	BC	1.30	0.05	0.35	0.75	**2.45**
	EA	1.02	0.00	0.35	0.63	**2.00**
	GS	1.19	0.05	0.35	0.62	**2.21**
	RC	0.98	0.05	0.35	0.65	**2.03**

Scenarios: Base Case (BC), Environmental Awareness (AE), Green Shoots (GS), Resource Constrained (RC)
Technologies: *CtL*: Coal Liquefaction, *GtL*: Gas Liquefaction

A.6.2 Results of other Sources

Table A.11: Installed power generation capacity and electricity output as indicated by Wright et al. (2019).

Installed Power Generation Capacity GW									
[GW]		**Coal**	**NUC**	**Gas**	**Wind**	**CSP**	**Solar**	**Others**	**Total**
2020	BAU	37	2	-	-	-	1	10	50
2050	BAU	25	20	36	30	-	16	9	136
	LC	10	-	56	85	-	74	9	234
	DC	-	-	43	83	13	84	25	248

Electricity Output									
[TWh/a]		**Coal**	**NUC**	**Gas**	**Wind**	**CSP**	**Solar**	**Others**	**Total**
2020	BAU	200	15	2	2	-	3	24	246
2050	BAU	172	148	50	93	-	28	37	528
	LC	59	-	67	257	-	110	38	531
	DC	-	-	30	251	70	113	68	532

Scenarios: Business-as-Usual (BAU), Least Cost (LC), Decarbonised (DC)
Fuel names: *Gas*: natural gas & liquefied natural gas (LNG), *NUC*: nuclear power stations

Appendix B

Additional Material: Global Model Calibration Specification

B.1 Model Regions

In the applied global calibration of the *MESSAGEix-GLOBIOM* model calibration the countries of the world are represented as eleven aggregated regions (Riahi et al. 2012). A full documentation on the model calibration is available online: `https://message.iiasa.ac.at/projects/global/en/latest/`. The specified model regions are:

Sub-Saharan Africa (AFR)
Angola, Benin, Botswana, British Indian Ocean Territory, Burkina Faso, Burundi, Cameroon, Cape Verde, Central African Republic, Chad, Comoros, Cote d'Ivoire, Congo, Djibouti, Equatorial Guinea, Eritrea, Ethiopia, Gabon, Gambia, Ghana, Guinea, Guinea-Bissau, Kenya, Lesotho, Liberia, Madagascar, Malawi, Mali, Mauritania, Mauritius, Mozambique, Namibia, Niger, Nigeria, Reunion, Rwanda, Sao Tome and Principe, Senegal, Seychelles, Sierra Leone, Somalia, South Africa, Saint Helena, Swaziland, Tanzania, Togo, Uganda, Zaire, Zambia, Zimbabwe

Centrally planned Asia and China (CPA)
Cambodia, China (incl. Hong Kong), Korea (DPR), Laos (PDR), Mongolia, Viet Nam

Central and Eastern Europe (EEU)
Albania, Bosnia and Herzegovina, Bulgaria, Croatia, Czech Republic, Estonia, The former Yugoslav Rep. of Macedonia, Latvia, Lithuania, Hungary, Poland, Romania, Slovak Republic, Slovenia, Yugoslavia

Former Soviet Union (FSU)
Armenia, Azerbaijan, Belarus, Georgia, Kazakhstan, Kyrgyzstan, Republic of Moldova, Russian Federation, Tajikistan, Turkmenistan, Ukraine, Uzbekistan (the Baltic republics are in the Central and Eastern Europe region)

Latin America and the Caribbean (LAC)
Antigua and Barbuda, Argentina, Bahamas, Barbados, Belize, Bermuda, Bolivia, Brazil, Chile, Colombia, Costa Rica, Cuba, Dominica, Dominican Republic, Ecuador, El Salvador, French Guyana, Grenada, Guadeloupe, Guatemala, Guyana, Haiti, Honduras, Jamaica, Martinique, Mexico, Netherlands Antilles, Nicaragua, Panama,

Paraguay, Peru, Saint Kitts and Nevis, Santa Lucia, Saint Vincent and the Grenadines, Suriname, Trinidad and Tobago, Uruguay, Venezuela)

Middle East and North Africa (MEA)
Algeria, Bahrain, Egypt (Arab Republic), Iraq, Iran (Islamic Republic), Israel, Jordan, Kuwait, Lebanon, Libya/SPLAJ, Morocco, Oman, Qatar, Saudi Arabia, Sudan, Syria (Arab Republic), Tunisia, United Arab Emirates, Yemen

North America (NAM)
Canada, Guam, Puerto Rico, United States of America, Virgin Islands

Pacific OECD (PAO)
Australia, Japan, New Zealand

Other Pacific Asia (PAS)
American Samoa, Brunei Darussalam, Fiji, French Polynesia, Gilbert-Kiribati, Indonesia, Malaysia, Myanmar, New Caledonia, Papua, New Guinea, Philippines, Republic of Korea, Singapore, Solomon Islands, Taiwan (China), Thailand, Tonga, Vanuatu, Western Samoa

South Asia (SAS)
Afghanistan, Bangladesh, Bhutan, India, Maldives, Nepal, Pakistan, Sri Lanka

Western Europe (WEU)
Andorra, Austria, Azores, Belgium, Canary Islands, Channel Islands, Cyprus, Denmark, Faeroe Islands, Finland, France, Germany, Gibraltar, Greece, Greenland, Iceland, Ireland, Isle of Man, Italy, Liechtenstein, Luxembourg, Madeira, Malta, Monaco, Netherlands, Norway, Portugal, Spain, Sweden, Switzerland, Turkey, United Kingdom

B.2 Representative Concentration Pathways

Following their mission for maximal transparency and hence, credibility of the climate change research, the climate change research community publishes the SSP/RCP scenario input data and the numeric results in an open access database `https://tntcat.iiasa.ac.at/SspDb/dsd?Action=htmlpage&page=welcome`.

The datasets on the emission trajectories in the RCP marker scenarios for the SSP2 scenario published in this database, act as the foundation for the RCP scenarios presented in this dissertation. However, in contrast to the integrated approach chosen for the assessments published in the database, in this dissertation, only CO_2 and CH_4 emissions from the energy sector are considered. In order to reflect this difference, the RCP marker scenario GHG emission trajectories were reduced to represent only the considered emissions share. Hence, the emission trajectories applied in the dissertation are lower because they (i) only consider CO_2 and CH_4 while the published scenario data contains all Kyoto-GHG emissions and (ii) because only emissions from the energy sector are considered in the dissertation in contrast to the integrated assessment of all emission sectors in the published scenarios. Thus, the original RCP GHG emission trajectories (Riahi et al. 2017; Rogelj et al. 2018; Gidden et al. 2019) are, in this dissertation, reduced to the modelled emission share based on the historical share as documented by Gütschow et al. (2019).

The reduced emission trajectories are calculated by scaling the future emission trajectories based on energy-share in 2017. The RCP trajectories as applied as GHG emission constraint are summarised in table B.1.

Table B.1: Emission trajectories as applied in the RCP scenarios.

[GtCO_2/a]	**2030**	**2040**	**2050**
RCP 1.9	24.0	12.7	5.7
RCP 2.6	34.2	26.5	17.9
RCP 3.4	41.3	37.6	33.4
RCP 4.5	43.5	43.6	43.3
RCP 6.0	45.2	48.5	53.0

Appendix C

Additional Material: Scenario Analysis

C.1 South Africa's GHG Emissions

Table C.1: South Africa's GHG emissions in 2017: (i) full emissions (with contributions from LULUCF), (ii) emissions excluding LULUCF, and (iii) emissions from only the energy sector. Total GHG emissions are resolved for contributions from CO_2 and CH_4 and other greenhouse gases. Data for LULUCF emissions are based CAT (2019a), data for other sectors are based on Gütschow et al. (2019).

[$MtCO_2eq$]	**CO_2**	**CH_4**	**Others**	**Total**
All sectors incl. LULUCF	515	77	25	617
All sectors excl. LULUCF*	540	77	25	642
Energy sector only	521	44	3	568

*Historically South Africa experienced net negative LULUCF GHG emission (Stevens 2018)

C.2 Further Results of the Explanation of the GHG Emission Reduction Potential

In order to find explaining variables for the economic GHG emission reduction potential of each node, in this dissertation the correlation coefficient was evaluated for several node specific characteristics. While three strong correlations could be identified (see section 3.3), several alternate tested correlation hypotheses had to be rejected. The results of the rejected correlation hypothesis of the total renewable energy potential and the total fossil energy potential are shown below. Additionally, the plot indicates the rejected additional hypothesis that the economic GHG mitigation potential might correlate with the total amount of high graded renewable energy potential, hence the renewable energy potential with the highest full load hours.

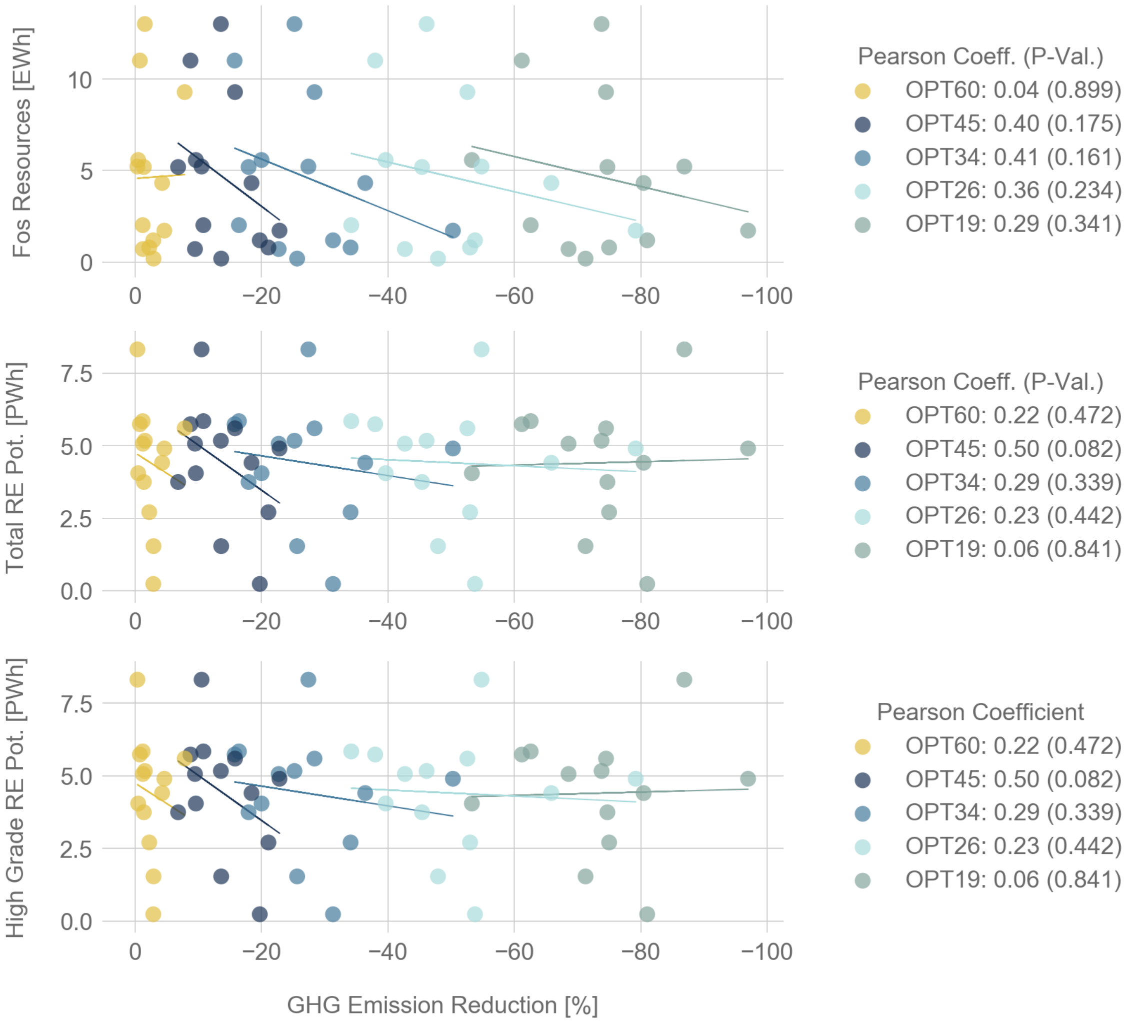

Figure C.1: Failing correlation between the GHG emission reduction (summed over the model horizon) and total fossil fuel resource (top), the total renewable energy potential (center) and the high graded renewable energy potential (bottom). The shown degree of GHG mitigation in a region in the globally optimised scenarios (OPT) is used as a measure for the economic GHG emission reduction potential. The markers indicate the scenario results in the model regions, the lines indicate the least-square-error linear trend per scenario. The GHG emission reduction is calculated relative to the reference scenario. The Pearson coefficient is a measure of linear correlation (here values <-0.5 are considered an indication for linear correlation), the P-Value is a measure of statistical significance (here values <0.05 are considered an indication for statistical significance). Projection Period: 2021-2050

C.3 Definition of the Scenario Calibrations and the Naming Convention

Table C.2: Specification of the national stand-alone model calibrations as applied in this dissertation. The gray shaded row highlights the calibration used as reference scenario.

			POLICY ASSUMPTION	
FULL NAME	**SHORT NAME**	**ACRONYM**	**NATIONAL**	**GLOBAL**
GHG emission-unrestrained national stand-alone model calibration	National current policies reference	CURPOLnat	Current policies	Current policies
GHG emission-restrained national stand-alone model calibration	National partially conditional NDC constrained calibration	PARTCONnat	Current policies + partially conditional NDC	Current policies

* m-regions: North America (NAM), Western Europe (WEU), Pacific OECD (PAO)

Table C.3: Specification of the mixed-granularity models' NDC- / national mitigation scenarios as applied in this dissertation. The gray shaded row highlights the calibration used as reference scenario.

FULL NAME	SHORT NAME	ACRONYM	ADDITION TO CURRENT POLICY NATIONAL	ADDITION TO CURRENT POLICY GLOBAL
GHG emission-unrestrained mixed-granularity global model calibration	Current policies reference	CURPOL	-	-
non-m Scenario Set				
Unconditional NDC constrained calibration		UNCON	Unconditional NDC	-
Partially conditional NDC constrained calibration		PARTCON	Partially conditional NDC	-
Fully conditional NDC constrained calibration		FULLCON	Fully conditional NDC	-
m-Scenario Set				Applied to m-regions:*
Unconditional NDC constrained m-calibration		UNCONm	Unconditional NDC	RCP2.6
Partially conditional NDC constrained m-calibration		PARTCONm	Partially conditional	RCP2.6
Fully conditional NDC constrained m-calibration		FULLCONm	Fully conditional NDC	RCP2.6

* m-regions: North America (NAM), Western Europe (WEU), Pacific OECD (PAO)

Table C.4: Specification of the mixed-granularity models' RCP- / global mitigation scenarios as applied in this dissertation. The gray shaded row highlights the calibration used as reference scenario.

			ADDITION TO CURRENT POLICY	
FULL NAME	**SHORT NAME**	**ACRONYM**	**NATIONAL**	**GLOBAL**
GHG emission-unrestrained mixed granularity global model calibration	Current policies reference	CURPOL	-	-
Globally optimised mitigation scenarios - OPT-Scenario Set				Applied to global sum:
		OPT19	-	RCP1.9
		OPT26	-	RCP2.6
		OPT34	-	RCP3.4
		OPT45	-	RCP4.5
		OPT60	-	RCP6.0
Equal share mitigation scenarios - EQU-Scenario Set				Applied to model regions:
		EQU19	RCP1.9	RCP1.9
		EQU26	RCP2.6	RCP2.6
		EQU34	RCP3.4	RCP3.4
		EQU45	RCP4.5	RCP4.5
		EQU60	RCP6.0	RCP6.0

Appendix D

Additional Material: Sensitivity Analysis

D.1 Input Factor Group Definition

Table D.1: Full list of the tested input factors, their grouping, description and applied domain from the initial screening of the emission-unrestrained national stand-alone model. abbreviations: carbon capture and storage (CCS), useful energy (UE), decommissioning (Decom.), conventional power plant (conv. PPL), extraction (Extr.), specific electric Demand (Demand spec.), renewable energy (RE), synthetic fuels (SynFuel), unconventional gas (Unconv. Gas)

Group	Technology	Parameter	Domain	
Clean Transport Growth	elec_share_trp	share_commodity_up	0.7	2
Biomass Build Rate	biomass_extr	growth_activity_up	0.5	1.5
Biomass Build Rate	biomass_extr	growth_activity_lo	0.8	1.2
Biomass Cost	biomass_extr	var_cost	0.5	1.5
CCS Build Rate	bio_istig_ccs	growth_activity_up	0.5	1.5
CCS Build Rate	coal_adv_ccs	growth_activity_up	0.5	1.5
CCS Build Rate	eth_bio_ccs	growth_activity_up	0.5	1.5
CCS Build Rate	gas_cc_ccs	growth_activity_up	0.5	1.5
CCS Build Rate	h2_bio_ccs	growth_activity_up	0.5	1.5
CCS Build Rate	h2_coal_ccs	growth_activity_up	0.5	1.5
CCS Build Rate	h2_smr_ccs	growth_activity_up	0.5	1.5
CCS Build Rate	coal_adv_ccs	bound_new_capacity_up	0.5	1.5
CCS Build Rate	igcc_ccs	growth_activity_up	0.5	1.5
CCS Build Rate	liq_bio_ccs	growth_activity_up	0.5	1.5
CCS Build Rate	meth_coal_ccs	growth_activity_up	0.5	1.5
CCS Build Rate	meth_ng_ccs	growth_activity_up	0.5	1.5
CCS Build Rate	syn_liq_ccs	growth_activity_up	0.5	1.5
CCS Build Rate	gas_cc_ccs	bound_new_capacity_up	0.5	1.5
CCS Build Rate	igcc_ccs	bound_new_capacity_up	0.5	1.5
CCS Capture Rate	bio_istig_ccs	emission_factor	0.5	1.05
CCS Capture Rate	coal_adv_ccs	emission_factor	0.5	1.05
			Continued on next page	

Table D.1 – continued from previous page

Group	Technology	Parameter	Domain	
CCS Capture Rate	eth_bio_ccs	emission_factor	0.5	1.05
CCS Capture Rate	gas_cc_ccs	emission_factor	0.5	1.05
CCS Capture Rate	h2_bio_ccs	emission_factor	0.5	1.05
CCS Capture Rate	h2_coal_ccs	emission_factor	0.5	1.05
CCS Capture Rate	h2_smr_ccs	emission_factor	0.5	1.05
CCS Capture Rate	igcc_ccs	emission_factor	0.5	1.05
CCS Capture Rate	liq_bio_ccs	emission_factor	0.5	1.05
CCS Capture Rate	meth_coal_ccs	emission_factor	0.5	1.05
CCS Capture Rate	meth_ng_ccs	emission_factor	0.5	1.05
CCS Capture Rate	syn_liq_ccs	emission_factor	0.5	1.05
CCS Cost	bio_istig_ccs	inv_cost	0.5	1.5
CCS Cost	coal_adv_ccs	inv_cost	0.5	1.5
CCS Cost	eth_bio_ccs	inv_cost	0.5	1.5
CCS Cost	gas_cc_ccs	inv_cost	0.5	1.5
CCS Cost	h2_bio_ccs	inv_cost	0.5	1.5
CCS Cost	h2_coal_ccs	inv_cost	0.5	1.5
CCS Cost	h2_smr_ccs	inv_cost	0.5	1.5
CCS Cost	igcc_ccs	inv_cost	0.5	1.5
CCS Cost	liq_bio_ccs	inv_cost	0.5	1.5
CCS Cost	meth_coal_ccs	inv_cost	0.5	1.5
CCS Cost	meth_ng_ccs	inv_cost	0.5	1.5
CCS Cost	syn_liq_ccs	inv_cost	0.5	1.5
CCS Decom.	bio_istig_ccs	growth_activity_lo	0.5	1.5
CCS Decom.	coal_adv_ccs	growth_activity_lo	0.5	1.5
CCS Decom.	eth_bio_ccs	growth_activity_lo	0.5	1.5
CCS Decom.	gas_cc_ccs	growth_activity_lo	0.5	1.5
CCS Decom.	h2_bio_ccs	growth_activity_lo	0.5	1.5
CCS Decom.	h2_coal_ccs	growth_activity_lo	0.5	1.5
CCS Decom.	h2_smr_ccs	growth_activity_lo	0.5	1.5
CCS Decom.	igcc_ccs	growth_activity_lo	0.5	1.5
CCS Decom.	liq_bio_ccs	growth_activity_lo	0.5	1.5
CCS Decom.	meth_coal_ccs	growth_activity_lo	0.5	1.5
CCS Decom.	meth_ng_ccs	growth_activity_lo	0.5	1.5
CCS Decom.	syn_liq_ccs	growth_activity_lo	0.5	1.5
Clean UE Build Rate	biomass_i	growth_activity_up	0.8	1.2
Clean UE Build Rate	biomass_rc	growth_activity_up	0.8	1.2
Clean UE Build Rate	elec_i	growth_activity_up	0.8	1.2
Clean UE Build Rate	elec_trp	growth_activity_up	0.8	1.2
Clean UE Build Rate	h2_fc_I	growth_activity_up	0.8	1.2
Clean UE Build Rate	h2_fc_RC	growth_activity_up	0.8	1.2
Clean UE Build Rate	h2_fc_trp	growth_activity_up	0.8	1.2
Clean UE Build Rate	h2_i	growth_activity_up	0.8	1.2
Clean UE Build Rate	h2_rc	growth_activity_up	0.8	1.2
Clean UE Build Rate	solar_i	growth_activity_up	0.8	1.2
Clean UE Build Rate	solar_rc	growth_activity_up	0.8	1.2
Clean UE Build Rate	sp_el_I	growth_activity_up	0.8	1.2
Clean UE Build Rate	sp_el_RC	growth_activity_up	0.8	1.2

Continued on next page

Table D.1 – continued from previous page

Group	Technology	Parameter	Domain	
Clean UE Cost	solar_i	inv_cost	0.5	1.5
Clean UE Cost	biomass_i	inv_cost	0.7	1.3
Clean UE Cost	elec_i	inv_cost	0.7	1.3
Clean UE Cost	h2_fc_I	inv_cost	0.7	1.3
Clean UE Cost	h2_fc_RC	inv_cost	0.7	1.3
Clean UE Cost	h2_fc_trp	inv_cost	0.7	1.3
Clean UE Cost	h2_i	inv_cost	0.7	1.3
Clean UE Decom.	biomass_i	growth_activity_lo	0.8	1.2
Clean UE Decom.	elec_i	growth_activity_lo	0.8	1.2
Clean UE Decom.	elec_trp	growth_activity_lo	0.8	1.2
Clean UE Decom.	h2_elec	growth_activity_lo	0.8	1.2
Clean UE Decom.	h2_fc_I	growth_activity_lo	0.8	1.2
Clean UE Decom.	h2_fc_RC	growth_activity_lo	0.8	1.2
Clean UE Decom.	h2_fc_trp	growth_activity_lo	0.8	1.2
Clean UE Decom.	h2_i	growth_activity_lo	0.8	1.2
Clean UE Decom.	h2_rc	growth_activity_lo	0.8	1.2
Clean UE Decom.	sp_el_I	growth_activity_lo	0.8	1.2
Clean UE Decom.	sp_el_RC	growth_activity_lo	0.8	1.2
Clean UE Decom.	sp_eth_I	growth_activity_lo	0.8	1.2
Clean UE Decom.	sp_liq_I	growth_activity_lo	0.8	1.2
Clean UE Decom.	sp_meth_I	growth_activity_lo	0.8	1.2
Coal Export Price	coal_exp	var_cost	0.8	1.2
Coal PPL Cost	coal_adv	inv_cost	0.7	1.3
Coal PPL Cost	coal_ppl	inv_cost	0.7	1.3
Coal PPL Cost	coal_ppl_u	inv_cost	0.7	1.3
Coal PPL Cost	igcc	inv_cost	0.7	1.3
Coal Resource Cost	coal	resource_cost	0.9	1.1
Coal Resources	coal	resource_volume	0.8	1.2
conv. PPL Build Rate	coal_adv	growth_activity_up	0.5	1.5
conv. PPL Build Rate	coal_ppl	growth_activity_up	0.5	1.5
conv. PPL Build Rate	coal_ppl_u	growth_activity_up	0.5	1.5
conv. PPL Build Rate	foil_ppl	growth_activity_up	0.5	1.5
conv. PPL Build Rate	gas_cc	growth_activity_up	0.5	1.5
conv. PPL Build Rate	gas_ppl	growth_activity_up	0.5	1.5
conv. PPL Build Rate	igcc	growth_activity_up	0.5	1.5
conv. PPL Build Rate	loil_cc	growth_activity_up	0.5	1.5
conv. PPL Build Rate	loil_ppl	growth_activity_up	0.5	1.5
conv. PPL Build Rate	nuc_hc	growth_activity_up	0.5	1.5
conv. PPL Build Rate	nuc_hc	bound_new_capacity_up	0.5	1.5
conv. PPL Build Rate	coal_adv	bound_new_capacity_up	0.7	1.3
conv. PPL Build Rate	coal_ppl	bound_new_capacity_up	0.7	1.3
conv. PPL Build Rate	coal_ppl_u	bound_new_capacity_up	0.7	1.3
conv. PPL Build Rate	foil_ppl	bound_new_capacity_up	0.7	1.3
conv. PPL Build Rate	gas_cc	bound_new_capacity_up	0.7	1.3
conv. PPL Build Rate	gas_ppl	bound_new_capacity_up	0.7	1.3
conv. PPL Build Rate	igcc	bound_new_capacity_up	0.7	1.3
conv. PPL Build Rate	loil_cc	bound_new_capacity_up	0.7	1.3

Continued on next page

Table D.1 – continued from previous page

Group	Technology	Parameter	Domain	
conv. PPL Build Rate	loil_ppl	bound_new_capacity_up	0.7	1.3
conv. PPL Cost	foil_ppl	inv_cost	0.7	1.3
conv. PPL Cost	gas_cc	inv_cost	0.7	1.3
conv. PPL Cost	gas_ppl	inv_cost	0.7	1.3
conv. PPL Cost	loil_cc	inv_cost	0.7	1.3
conv. PPL Cost	loil_ppl	inv_cost	0.7	1.3
conv. PPL Cost	nuc_hc	inv_cost	0.7	1.3
conv. PPL Decom.	nuc_hc	growth_activity_lo	0.5	1.5
conv. PPL Decom.	coal_adv	growth_activity_lo	0.8	1.2
conv. PPL Decom.	coal_ppl	growth_activity_lo	0.8	1.2
conv. PPL Decom.	coal_ppl_u	growth_activity_lo	0.8	1.2
conv. PPL Decom.	foil_ppl	growth_activity_lo	0.8	1.2
conv. PPL Decom.	gas_cc	growth_activity_lo	0.8	1.2
conv. PPL Decom.	gas_ppl	growth_activity_lo	0.8	1.2
conv. PPL Decom.	igcc	growth_activity_lo	0.8	1.2
conv. PPL Decom.	loil_cc	growth_activity_lo	0.8	1.2
conv. PPL Decom.	loil_ppl	growth_activity_lo	0.8	1.2
Conv. UE Build Rate	coal_i	growth_activity_up	0.8	1.2
Conv. UE Build Rate	coal_rc	growth_activity_up	0.8	1.2
Conv. UE Build Rate	eth_fc_trp	growth_activity_up	0.8	1.2
Conv. UE Build Rate	eth_i	growth_activity_up	0.8	1.2
Conv. UE Build Rate	eth_ic_trp	growth_activity_up	0.8	1.2
Conv. UE Build Rate	eth_rc	growth_activity_up	0.8	1.2
Conv. UE Build Rate	foil_i	growth_activity_up	0.8	1.2
Conv. UE Build Rate	foil_rc	growth_activity_up	0.8	1.2
Conv. UE Build Rate	foil_trp	growth_activity_up	0.8	1.2
Conv. UE Build Rate	gas_i	growth_activity_up	0.8	1.2
Conv. UE Build Rate	gas_rc	growth_activity_up	0.8	1.2
Conv. UE Build Rate	gas_trp	growth_activity_up	0.8	1.2
Conv. UE Build Rate	loil_i	growth_activity_up	0.8	1.2
Conv. UE Build Rate	loil_rc	growth_activity_up	0.8	1.2
Conv. UE Build Rate	loil_trp	growth_activity_up	0.8	1.2
Conv. UE Build Rate	meth_fc_trp	growth_activity_up	0.8	1.2
Conv. UE Build Rate	meth_i	growth_activity_up	0.8	1.2
Conv. UE Build Rate	meth_ic_trp	growth_activity_up	0.8	1.2
Conv. UE Build Rate	meth_rc	growth_activity_up	0.8	1.2
Conv. UE Build Rate	sp_eth_I	growth_activity_up	0.8	1.2
Conv. UE Build Rate	sp_liq_I	growth_activity_up	0.8	1.2
Conv. UE Build Rate	sp_meth_I	growth_activity_up	0.8	1.2
conv. UE Cost	coal_i	inv_cost	0.7	1.3
conv. UE Cost	eth_i	inv_cost	0.7	1.3
conv. UE Cost	foil_i	inv_cost	0.7	1.3
conv. UE Cost	gas_i	inv_cost	0.7	1.3
conv. UE Cost	loil_i	inv_cost	0.7	1.3
conv. UE Cost	meth_i	inv_cost	0.7	1.3
Conv. UE Decom.	coal_gas	growth_activity_lo	0.8	1.2
Conv. UE Decom.	coal_i	growth_activity_lo	0.8	1.2

Continued on next page

Table D.1 – continued from previous page

Group	Technology	Parameter	Domain	
Conv. UE Decom.	coal_rc	growth_activity_lo	0.8	1.2
Conv. UE Decom.	eth_fc_trp	growth_activity_lo	0.8	1.2
Conv. UE Decom.	eth_i	growth_activity_lo	0.8	1.2
Conv. UE Decom.	eth_ic_trp	growth_activity_lo	0.8	1.2
Conv. UE Decom.	eth_rc	growth_activity_lo	0.8	1.2
Conv. UE Decom.	foil_i	growth_activity_lo	0.8	1.2
Conv. UE Decom.	foil_rc	growth_activity_lo	0.8	1.2
Conv. UE Decom.	foil_trp	growth_activity_lo	0.8	1.2
Conv. UE Decom.	gas_i	growth_activity_lo	0.8	1.2
Conv. UE Decom.	gas_rc	growth_activity_lo	0.8	1.2
Conv. UE Decom.	gas_trp	growth_activity_lo	0.8	1.2
Conv. UE Decom.	loil_i	growth_activity_lo	0.8	1.2
Conv. UE Decom.	loil_rc	growth_activity_lo	0.8	1.2
Conv. UE Decom.	loil_trp	growth_activity_lo	0.8	1.2
Conv. UE Decom.	meth_fc_trp	growth_activity_lo	0.8	1.2
Conv. UE Decom.	meth_i	growth_activity_lo	0.8	1.2
Conv. UE Decom.	meth_ic_trp	growth_activity_lo	0.8	1.2
Conv. UE Decom.	meth_ng	growth_activity_lo	0.8	1.2
Conv. UE Decom.	meth_rc	growth_activity_lo	0.8	1.2
Demand spec.	i_spec	demand	0.8	1.2
Demand spec.	rc_spec	demand	0.8	1.2
Demand therm.	i_therm	demand	0.8	1.2
Demand therm.	rc_therm	demand	0.8	1.2
Demand Transport	transport	demand	0.8	1.2
Electric Peak Load	electr	peak_load_factor	0.8	1.2
Carbon Price		tax_emission	0.0	2
Export Build Rate	coal_exp	growth_activity_up	0.8	1.2
Fossil Extr. Reduction	cbm_extr	growth_activity_lo	0.8	1.2
Fossil Extr. Reduction	coal_extr	growth_activity_lo	0.8	1.2
Fossil Extr. Reduction	shalegas_extr	growth_activity_lo	0.8	1.2
Fossil Fuel Build Rate	cbm_extr	growth_activity_up	0.5	1.5
Fossil Fuel Build Rate	coal_extr	growth_activity_up	0.5	1.5
Fossil Fuel Build Rate	shalegas_extr	growth_activity_up	0.5	1.5
Gas Import Price	gas_imp	var_cost	0.6	1.4
Gas Import Price	LNG_imp	var_cost	0.6	1.4
Import Build Rate	elec_imp	growth_activity_up	0.8	1.2
Import Build Rate	eth_imp	growth_activity_up	0.8	1.2
Import Build Rate	foil_imp	growth_activity_up	0.8	1.2
Import Build Rate	gas_imp	growth_activity_up	0.8	1.2
Import Build Rate	lh2_imp	growth_activity_up	0.8	1.2
Import Build Rate	LNG_imp	growth_activity_up	0.8	1.2
Import Build Rate	loil_imp	growth_activity_up	0.8	1.2
Import Build Rate	meth_imp	growth_activity_up	0.8	1.2
Import Build Rate	oil_imp	growth_activity_up	0.8	1.2
Import Reduction	elec_imp	growth_activity_lo	0.8	1.2
Import Reduction	eth_imp	growth_activity_lo	0.8	1.2
Import Reduction	foil_imp	growth_activity_lo	0.8	1.2

Continued on next page

Table D.1 – continued from previous page

Group	Technology	Parameter	Domain	
Import Reduction	gas_imp	growth_activity_lo	0.8	1.2
Import Reduction	lh2_imp	growth_activity_lo	0.8	1.2
Import Reduction	LNG_imp	growth_activity_lo	0.8	1.2
Import Reduction	loil_imp	growth_activity_lo	0.8	1.2
Import Reduction	meth_imp	growth_activity_lo	0.8	1.2
Import Reduction	oil_imp	growth_activity_lo	0.8	1.2
Oil Import Price	eth_imp	var_cost	0.6	1.4
Oil Import Price	foil_imp	var_cost	0.6	1.4
Oil Import Price	loil_imp	var_cost	0.6	1.4
Oil Import Price	meth_imp	var_cost	0.6	1.4
Oil Import Price	oil_imp	var_cost	0.6	1.4
Other Fossil Resource	shalegas	resource_volume	0.5	1.5
Other Fossil Resource	cbm	resource_volume	0.5	1.5
Other Fossil Resource	crude_1	resource_volume	0.7	1.3
Other Fossil Resource	gas_1	resource_volume	0.7	1.3
Other Import Price	elec_imp	var_cost	0.6	1.4
Other Import Price	lh2_imp	var_cost	0.6	1.4
RE Decom.	geo_ppl_my	growth_activity_lo	0.8	1.2
RE Decom.	hydro_la_ppl_my	growth_activity_lo	0.8	1.2
RE Decom.	hydro_sm_ppl_my	growth_activity_lo	0.8	1.2
RE Decom.	solar_i	growth_activity_lo	0.8	1.2
RE Decom.	solar_pv_ppl_my	growth_activity_lo	0.8	1.2
RE Decom.	solar_rc	growth_activity_lo	0.8	1.2
RE Decom.	solar_th_ppl_my	growth_activity_lo	0.8	1.2
RE Decom.	wind_on_ppl_my	growth_activity_lo	0.8	1.2
RE Decom.	bio_istig	growth_activity_lo	0.8	1.2
RE Potential Biomass	biomass	renewable_potential	0.5	1.5
RE Potential Other	hydro_la	renewable_potential	0.5	1.5
RE Potential Other	geothermal	renewable_potential	0.5	1.5
RE Potential Other	hydro_sm	renewable_potential	0.5	1.5
RE Potential Other	lfgas	renewable_potential	0.5	1.5
RE Potential Solar	solar_th_i	renewable_potential	0.5	1.5
RE Potential Solar	solar_th_rc	renewable_potential	0.5	1.5
RE Potential Solar	solar_th	renewable_potential	0.5	1.5
RE Potential Solar	solar_pv	renewable_potential	0.5	1.5
RE Potential Wind	wind_on	renewable_potential	0.5	1.5
RE PPL Build Rate	solar_pv_ppl_my	bound_new_capacity_up	0.5	1.5
RE PPL Build Rate	solar_th_ppl_my	bound_new_capacity_up	0.5	1.5
RE PPL Build Rate	wind_on_ppl_my	bound_new_capacity_up	0.5	1.5
RE PPL Build Rate	bio_istig	growth_activity_up	0.5	1.5
RE PPL Build Rate	geo_ppl_my	growth_activity_up	0.5	1.5
RE PPL Build Rate	hydro_la_ppl_my	growth_activity_up	0.5	1.5
RE PPL Build Rate	hydro_sm_ppl_my	growth_activity_up	0.5	1.5
RE PPL Build Rate	solar_pv_ppl_my	growth_activity_up	0.5	1.5
RE PPL Build Rate	solar_th_ppl_my	growth_activity_up	0.5	1.5
RE PPL Build Rate	wind_on_ppl_my	growth_activity_up	0.5	1.5
RE PPL Cost	solar_pv_ppl_my	inv_cost	0.5	1.5

Continued on next page

Table D.1 – continued from previous page

Group	Technology	Parameter	Domain	
RE PPL Cost	solar_th_ppl_my	inv_cost	0.5	1.5
RE PPL Cost	wind_on_ppl_my	inv_cost	0.5	1.5
RE PPL Cost	geo_ppl_my	inv_cost	0.7	1.3
RE PPL Cost	hydro_la_ppl_my	inv_cost	0.7	1.3
RE PPL Cost	hydro_sm_ppl_my	inv_cost	0.7	1.3
RE PPL Cost	bio_istig	inv_cost	0.7	1.3
SynFuel Build Rate	bio_fuel	growth_activity_up	0.5	1.5
SynFuel Build Rate	coal_gas	growth_activity_up	0.5	1.5
SynFuel Build Rate	eth_bio	growth_activity_up	0.5	1.5
SynFuel Build Rate	gas_bio	growth_activity_up	0.5	1.5
SynFuel Build Rate	gtl	growth_activity_up	0.5	1.5
SynFuel Build Rate	h2_bio	growth_activity_up	0.5	1.5
SynFuel Build Rate	h2_coal	growth_activity_up	0.5	1.5
SynFuel Build Rate	h2_elec	growth_activity_up	0.5	1.5
SynFuel Build Rate	h2_smr	growth_activity_up	0.5	1.5
SynFuel Build Rate	liq_bio	growth_activity_up	0.5	1.5
SynFuel Build Rate	meth_coal	growth_activity_up	0.5	1.5
SynFuel Build Rate	meth_ng	growth_activity_up	0.5	1.5
SynFuel Build Rate	syn_liq	growth_activity_up	0.5	1.5
SynFuel Cost	syn_liq	inv_cost	0.5	1.5
SynFuel Cost	eth_bio	inv_cost	0.7	1.3
SynFuel Cost	gas_bio	inv_cost	0.7	1.3
SynFuel Cost	h2_bio	inv_cost	0.7	1.3
SynFuel Cost	liq_bio	inv_cost	0.7	1.3
SynFuel Cost	bio_fuel	inv_cost	0.7	1.3
SynFuel Cost	coal_gas	inv_cost	0.7	1.3
SynFuel Cost	gtl	inv_cost	0.7	1.3
SynFuel Cost	h2_coal	inv_cost	0.7	1.3
SynFuel Cost	h2_elec	inv_cost	0.7	1.3
SynFuel Cost	h2_liq	inv_cost	0.7	1.3
SynFuel Cost	h2_smr	inv_cost	0.7	1.3
SynFuel Cost	meth_coal	inv_cost	0.7	1.3
SynFuel Cost	meth_ng	inv_cost	0.7	1.3
SynFuel Decom.	bio_fuel	growth_activity_lo	0.8	1.2
SynFuel Decom.	eth_bio	growth_activity_lo	0.8	1.2
SynFuel Decom.	gtl	growth_activity_lo	0.8	1.2
SynFuel Decom.	h2_bio	growth_activity_lo	0.8	1.2
SynFuel Decom.	h2_coal	growth_activity_lo	0.8	1.2
SynFuel Decom.	h2_smr	growth_activity_lo	0.8	1.2
SynFuel Decom.	liq_bio	growth_activity_lo	0.8	1.2
SynFuel Decom.	meth_coal	growth_activity_lo	0.8	1.2
SynFuel Decom.	syn_liq	growth_activity_lo	0.8	1.2
Unconv. Gas Cost	cbm_extr	var_cost	0.5	1.5
Unconv. Gas Cost	shalegas_extr	var_cost	0.5	1.5

D.2 Additional Results

Table D.2: Results (μ^*) of the screening on the GHG emission-unrestrained national stand-alone reference scenario (CURPOLnat). All outputs are evaluated for 2050. GHG: greenhouse gas, PPL: power plant, CAP: Capacity, ACT: power output, RE: renewable energy, NUC: nuclear energy, CCS: carbon sequestration, BR: build rate

	System Cost [BUSD]	GHG Emission [MtCO2]	PPL CAP [GW]	PPL ACT [TWh]	Share of power gen. RE [%]	NUC [%]	CCS CAP [GW]
Oil Import Price	11.57	101.99	4.84	49.41	2.35	7.45	8.92
Demand spec.	9.41	122.81	33.42	157.37	1.99	6.61	1.66
Coal Resources	5.95	52.52	2.82	1.63	1.41	3.68	1.10
Coal Export Price	4.00	111.39	7.88	5.58	5.81	12.72	3.71
Demand therm.	3.74	52.55	1.34	1.07	0.20	0.16	0.11
Demand Transport	3.59	56.04	1.28	7.37	0.33	0.75	0.75
Gas Import Price	3.01	114.49	15.74	6.89	2.55	4.35	1.70
RE PPL Cost	1.45	111.17	48.13	5.09	7.53	0.89	0.15
Carbon Price	1.26	136.30	15.46	9.07	4.63	11.78	3.54
Biomass Cost	1.13	60.83	1.85	4.24	1.41	1.19	1.83
RE Potential Solar	0.60	35.80	10.83	0.53	2.90	4.09	0.25
Unconv. Gas Cost	0.60	15.43	1.94	0.32	0.42	0.61	0.38
SynFuel Cost	0.60	37.01	2.91	4.13	0.68	1.25	5.47
Coal PPL Cost	0.57	36.21	3.57	9.35	0.99	1.17	0.74
conv. PPL Cost	0.55	29.61	5.89	2.51	9.88	23.95	0.11
Electric Peak Load	0.49	16.40	11.40	2.63	1.86	3.37	0.07
Import BR	0.36	9.39	2.38	1.44	0.26	0.11	0.10
CCS Cost	0.34	19.54	1.61	4.51	0.28	0.30	11.39
Clean Transport G.	0.32	7.77	2.64	15.25	0.16	0.71	0.39
RE PPL BR	0.30	23.02	15.75	3.08	1.84	0.17	0.96
Clean UE Cost	0.26	1.07	0.27	1.13	0.01	0.04	0.23
conv. PPL BR	0.25	15.76	1.64	3.12	0.37	0.80	0.04
RE Potential Wind	0.23	19.57	4.10	0.56	1.41	0.24	0.31
Other Import Price	0.19	0.21	0.03	0.22	0.00	0.00	0.00
Import Reduction	0.17	6.77	0.59	1.15	0.07	0.12	0.30
CCS BR	0.15	9.28	0.61	1.60	0.05	0.14	1.80
Conv. UE BR	0.13	2.70	1.10	3.54	0.14	0.22	0.30
conv. UE Cost	0.11	0.97	0.07	0.05	0.00	0.01	0.07
Other fos. Resource	0.08	4.84	0.19	0.04	0.15	0.29	0.00
conv. PPL Decom.	0.07	4.87	0.48	0.58	0.14	0.24	0.00
SynFuel BR	0.07	1.50	0.76	2.55	0.06	0.06	0.28
SynFuel Decom.	0.06	2.03	0.39	0.03	0.05	0.03	0.01
Clean UE Decom.	0.05	1.75	0.39	0.83	0.04	0.06	0.10
CCS Capture Rate	0.04	3.89	0.17	0.64	0.01	0.01	0.28
Potential Biomass	0.04	9.42	0.34	2.53	0.13	0.08	0.37
RE Decom.	0.02	0.99	0.16	0.04	0.04	0.03	0.00
Conv. UE Decom.	0.01	0.81	0.18	0.06	0.03	0.01	0.01
Clean UE BR	0.00	0.32	0.01	0.08	0.00	0.01	0.01

…all other input factor groups are of less influence ($\mu^* < 0.01$).

Table D.3: Results (μ^*) of the initial screening on the GHG emission-restrained national stand-alone scenario (PARTCONnat). All outputs are evaluated for 2050. GHG: greenhouse gas, PPL: power plant, CAP: Capacity, ACT: power output, RE: renewable energy, NUC: nuclear energy, CCS: carbon sequestration, BR: build rate

	System Cost [BUSD]	GHG Emission [MtCO2]	PPL CAP [GW]	PPL ACT [TWh]	Share of power gen. RE [%]	NUC [%]	CCS CAP [GW]
GHG Emis. Constr.	8.32	133.53	20.34	66.31	0.63	0.92	14.02
Coal Export Price	7.58	4.50	5.40	9.04	1.88	3.39	7.97
Demand spec.	6.58	1.16	23.71	92.57	0.72	1.16	5.55
Demand Transport	6.36	1.52	13.31	31.56	0.61	1.14	6.88
Demand therm.	5.57	6.51	7.70	17.55	0.77	1.56	3.29
Oil Import Price	5.24	0.13	4.57	27.32	1.07	2.02	8.53
Gas Import Price	4.46	1.99	18.11	19.25	3.49	6.93	13.03
Potential Biomass	3.40	10.77	17.50	28.98	1.22	2.20	4.24
Biomass Cost	3.35	1.09	4.64	9.39	0.34	0.73	4.27
RE PPL Cost	1.78	2.59	35.06	8.94	4.23	6.29	6.15
Clean Transport G.	1.28	4.08	3.06	12.57	0.63	1.05	2.85
Coal Resources	1.21	0.00	2.25	2.69	0.84	1.66	2.27
RE PPL BR	0.91	2.42	28.95	9.30	1.96	2.89	3.44
Electric Peak Load	0.64	2.71	16.09	2.82	1.30	2.68	2.22
CCS Cost	0.62	3.54	5.02	11.99	0.67	0.80	8.81
RE Potential Solar	0.61	0.40	5.21	1.86	0.26	0.26	0.73
CCS BR	0.50	2.36	5.20	11.34	0.38	0.79	3.65
RE Potential Wind	0.42	0.00	3.43	1.80	0.45	0.80	1.29
conv. PPL Cost	0.41	2.66	2.87	1.14	4.99	9.37	2.92
Clean UE BR	0.35	1.13	1.01	1.41	0.23	0.41	0.64
conv. PPL BR	0.28	0.95	1.74	1.67	0.22	0.37	0.99
conv. PPL Decom.	0.26	0.17	2.69	2.34	0.14	0.20	1.58
Import Reduction	0.24	2.36	0.53	0.92	0.02	0.04	1.38
Other Import Price	0.20	0.10	0.34	2.13	0.46	0.76	0.51
Conv. UE BR	0.19	0.09	1.42	3.23	0.04	0.02	0.89
Clean UE Decom.	0.14	0.87	1.30	3.30	0.09	0.04	0.86
Clean UE Cost	0.14	0.34	1.47	4.57	0.18	0.19	1.07
Import BR	0.13	0.35	1.49	1.51	0.18	0.30	0.41
conv. UE Cost	0.13	0.00	0.29	1.23	0.06	0.12	0.15
Conv. UE Decom.	0.10	0.05	0.63	1.89	0.20	0.33	0.46
CCS Decom.	0.08	0.23	1.14	2.20	0.15	0.17	1.01
Unconv. Gas Cost	0.05	1.29	0.43	0.77	0.04	0.07	0.15
SynFuel Cost	0.05	0.26	0.18	1.76	0.01	0.04	0.52
SynFuel BR	0.03	0.00	0.18	0.56	0.01	0.02	0.23
SynFuel Decom.	0.03	0.00	0.09	0.22	0.03	0.05	0.17
RE Decom.	0.03	0.00	0.19	0.20	0.03	0.04	0.04
Coal PPL Cost	0.02	0.00	0.00	0.00	0.00	0.00	0.00
Fossil Fuel BR	0.02	0.01	0.18	0.12	0.16	0.31	0.16
...all other input factor groups are of less influence ($\mu^* < 0.01$).							

Table D.4: Results (μ^*) of the sensitivity screening on the global mixed-granularity CURPOL reference scenario. All outputs are evaluated for 2050. GHG: greenhouse gas, PPL: power plant, CAP: Capacity, ACT: power output, RE: renewable energy, NUC: nuclear energy, CCS: carbon sequestration, BR: build rate

	System Cost [BUSD]	GHG Emission [MtCO2]	PPL CAP [GW]	PPL ACT [TWh]	Share of power gen. RE [%]	NUC [%]	CCS CAP [GW]
Demand spec.	6.94	91.14	28.05	135.35	1.45	4.99	0.58
Coal Resources	3.39	77.42	7.19	1.50	1.63	0.09	0.95
Demand therm.	2.30	55.82	1.40	0.22	0.17	0.01	0.17
Biomass Cost	2.20	56.14	6.03	3.32	0.56	0.17	3.30
Carbon Price	1.82	161.57	24.09	5.70	5.90	7.15	5.18
RE PPL Cost	1.81	106.92	35.14	4.10	6.53	0.13	0.39
RE PPL BR	1.44	30.44	26.89	1.03	2.40	0.04	0.40
Coal PPL Cost	1.03	48.39	3.76	3.69	2.36	3.55	1.21
Clean Transport G.	1.03	10.60	4.87	26.05	0.30	0.99	0.26
conv. PPL BR	1.00	17.66	3.71	0.52	0.78	0.10	0.43
Electric Peak Load	0.92	36.68	16.99	1.00	2.14	0.04	0.31
Import BR	0.79	5.76	5.85	0.47	0.45	0.05	0.26
conv. PPL Cost	0.76	9.61	2.25	0.29	2.86	6.87	0.38
Unconv. Gas Cost	0.69	19.12	0.52	0.67	0.13	0.01	0.05
Demand Transport	0.66	47.61	2.15	11.35	0.21	0.38	0.30
RE Potential Solar	0.49	16.58	4.76	0.18	0.78	0.02	0.24
Import Reduction	0.40	7.32	0.98	0.44	0.11	0.04	0.08
RE Potential Wind	0.35	21.75	3.77	0.45	1.18	0.02	0.10
SynFuel Cost	0.34	5.18	0.59	1.33	0.05	0.09	0.22
Potential Biomass	0.33	11.96	0.64	0.98	0.29	0.04	0.84
CCS Cost	0.25	10.80	1.18	5.78	0.27	0.23	2.40
conv. UE Cost	0.16	0.27	0.08	0.00	0.01	0.00	0.00
CCS BR	0.15	2.68	0.29	2.13	0.04	0.09	0.85
SynFuel BR	0.09	1.91	0.31	1.41	0.01	0.06	0.15
Conv. UE Decom.	0.06	0.62	0.16	0.21	0.02	0.01	0.15

...all other input factor groups are of less influence ($\mu^* < 0.01$).

Appendix E

Related Author Publications

Contribution to the development of the new release version of *MESSAGEix*:

Huppmann, D., M. Gidden, O. Fricko, P. Kolp, C. Orthofer, M. Pimmer, N. Kushin, A. Vinca,A. Mastrucci, K. Riahi, and V. Krey (2019). The MESSAGE Integrated Assessment Model and the ix Modeling Platform (ixmp): An open framework for integrated and cross-cutting analysis of energy, climate, the environment, and sustainable development.Environmental Modelling & Software112, pp. 143–156.doi:doi.org/10/ggj67t.

Application of the new release version of *MESSAGEix* in a case study on South Africa's shale gas reserves:

Orthofer, C., D. Huppmann, and V. Krey (2019). South Africa after Paris: Fracking its way to the NDCs? Frontiers in Energy Research 7, p. 34. doi:doi.org/10.3389/fenrg.2019.00020.

Contribution to the development of a input-data handling framework for the *MESSAGEix-ixmp* environment:

Zipperle, T. and C. Orthofer (2019). d2ix: A model input-data management and analysis tool for MESSAGEix.Energies12.(8), p. 1483.doi:doi.org/10/ggf7zb.

Appendix F

Acronyms

MESSAGEix Model for Energy Supply Strategy Alternatives and their General Environmental Impact
ixmp ix modeling platform

AFR Sub-Saharan Africa
ANOVA Analysis of Variance
API Application Programming Interface

BESOM Brookhaven Energy Systems Optimisation Model

CBM Coal Bed Methane
CCS Carbon Capture and Storage
CPA centrally planned Asia and China
CSP Concentrated Solar Power

EEU Central and Eastern Europe
EMP-E Energy Modelling Platform for Europe
ETSAP Energy Technology Systems Analysis Program

FSU Former Soviet Union

GCAM Global Change Assessment Model
GDP Gross Domestic Product
GHG Greenhouse Gas
GIS Geographic Information System
GUMP Gas Utilisation Master Plan
GWP Global Warming Potential

HFCs Hydrofluorocarbons

IAM Integrated Assessment Model
IEA International Energy Agency
IEP Integrated Energy Plan
IIASA International Institute for Applied Systems Analysis

IPCC Intergovernmental Panel on Climate Change
IPP Independent Power Producer
IPPPP Independent Power Producer Procurement Programme
IRP Integrated Resource Plan

KTH-dESA Royal Institute of Technology - Department Energy System Analysis

LAC Latin America and the Caribbean
LNG Liquefied Natural Gas
LP Linear programming
LULUCF Land-use, Land-use Change and Forestry

MARKAL MARKet ALocation
MEA Middle East and North Africa

NAM North America
NDC Nationally Determined Contribution
NGO Non-Governmental Organisation

OAT One-at-a-time

PAO Pacific OECD
PAS non-OECD Pacific Asia
PFCs Perfluorocarbons
PPL power plant
PV Photovoltaics

RC Residential and Commercial
RCP Representative Concentration Pathway
RE Renewable Energy
RES Reference Energy System

SADC Southern African Development Community
SALib Sensitivity Analysis Library in Python
SAPP Southern African Power Pool
SAS South Asia
SDG Sustainable Development Goal
SSP Shared Socioeconomic Pathway
SSP2 "middle-of-the-road" SSP scenario

TIMES The Integrated MARKAL-EFOM System
TPES Total Primary Energy Supply

UE Useful Energy
UN United Nations
UNFCCC United Nations Framework Convention on Climate Change

VRE Volatile Renewable Energy

WEU Western Europe

ZAF South Africa

Bibliography

Agnew, M., L. Schrattenholzer, and A. Voss (1979). A model for energy supply systems alternatives and their general environmental impact. Laxenburg, Austria. URL: pure.iiasa.ac.at/id/eprint/1177/ (visited on 06/12/2019).

Andrews, R. (1989). The concise Columbia dictionary of quotations. Topic: The Future. New York, N.Y.: Columbia University Press.

Arndt, C., R. Davies, S. Gabriel, K. Makrelov, B. Merven, F. Hartley, and J. Thurlow (2016). A sequential approach to integrated energy modeling in South Africa. *Applied Energy* 161, pp. 591–599. DOI: 10.1016/j.apenergy.2015.06.053.

Banks, D. and J. Schäffler (2006). The potential contribution of renewable energy in South Africa: Draft update report. Johannesburg. URL: www.earthlife.org.za/wp-content/uploads/2009/04/potential-of-re-in-sa-feb06.pdf (visited on 05/30/2019).

Batidzirai, B., M. Valk, B. Wicke, M. Junginger, V. Daioglou, W. Euler, and A. Faaij (2016). Current and future technical, economic and environmental feasibility of maize and wheat residues supply for biomass energy application: Illustrated for South Africa. *Biomass and Bioenergy* 92, pp. 106–129. DOI: 10/f83cpg.

Bauer, N., I. Mouratiadou, G. Luderer, L. Baumstark, R. J. Brecha, O. Edenhofer, and E. Kriegler (2016). Global fossil energy markets and climate change mitigation: An analysis with REMIND. *Climatic Change* 136.(1), pp. 69–82. DOI: 10.1007/s10584-013-0901-6.

Bhattacharyya, S. C. and G. R. Timilsina (2010a). A review of energy system models. *International Journal of Energy Sector Management* 4.(4), pp. 494–518. DOI: 10.1108/17506221011092742.

Bhattacharyya, S. C. and G. R. Timilsina (2010b). Modelling energy demand of developing countries: Are the specific features adequately captured? *Energy Policy* 38.(4), pp. 1979–1990. DOI: 10.1016/j.enpol.2009.11.079.

Blaschke, T., M. Biberacher, S. Gadocha, and I. Schardinger (2013). Energy landscapes: Meeting energy demands and human aspirations. *Biomass & bioenergy* 55, pp. 3–16. DOI: 10.1016/j.biombioe.2012.11.022.

Bosetti, V., G. Marangoni, E. Borgonovo, L. Diaz Anadon, R. Barron, H. McJeon, S. Politis, and P. Friley (2016). Sensitivity to energy technology costs: A multi-model comparison analysis. DOI: 10.2139/ssrn.2718029.

Box, G. E. P. (1976). Science and Statistics. *Journal of the American Statistical Association* 71.(356), pp. 791–799. DOI: 10.1080/01621459.1976.10480949.

BP – British Petroleum (2018). Statistical Review of World Energy 2018. URL: www.bp.com/content/dam/bp/business-sites/en/global/corporate/pdfs/energy-economics/statistical-review/bp-stats-review-2018-full-report.pdf (visited on 05/21/2019).

Brown, T., J. Hörsch, and D. Schlachtberger (2018). PyPSA: Python for Power System Analysis. *Journal of Open Research Software* 6.(4). DOI: 10/gfb7m9. eprint: 1707.09913.

Bruckner, T., I. A. Bashmakov, Y. Mulugetta, H. Chum, A. De la Vega Navarro, J. Edmonds, A. Faaij, B. Fungtammasan, A. Garg, E. Hertwich, D. Honnery, D. Infield, M. Kainuma, S. Khennas, S. Kim, H. Nimir, K. Riahi, N. Strachan, R. Wiser, and X. Zhang (2014). Chapter 7 - Energy systems. *Climate change 2014: Mitigation of climate change. IPCC Working Group III contribution to Fifth Assessment Report of the Intergovernmental Panel on Climate Change*. Cambridge University Press. URL: pure.iiasa.ac.at/id/eprint/11118/.

Calitz, J. R. and J. G. Wright (2019). Statistics of utility-scale solar PV, wind and CSP in South Africa in 2018. Pretoria. URL: researchspace.csir.co.za/dspace/bitstream/handle/10204/10636/Calitz_21959_2019.pdf?sequence=1&isAllowed=y (visited on 06/09/2019).

Calvin, K., L. Clarke, V. Krey, G. Blanford, K. Jiang, M. Kainuma, E. Kriegler, G. Luderer, and P. R. Shukla (2012). The role of Asia in mitigating climate change: Results from the Asia modeling exercise. *Energy Economics* 34, S251–S260. DOI: 10.1016/j.eneco.2012.09.003.

Campolongo, F., J. Cariboni, and A. Saltelli (2007). An effective screening design for sensitivity analysis of large models. *Environmental Modelling & Software* 22.(10), pp. 1509–1518. DOI: 10.1016/j.envsoft.2006.10.004.

Campolongo, F., A. Saltelli, and J. Cariboni (2011). From screening to quantitative sensitivity analysis. A unified approach. *Computer Physics Communications* 182.(4), pp. 978–988. DOI: 10.1016/j.cpc.2010.12.039.

CAT – Climate Action Tracker (2019a). *Climate Action Tracker: South Africa*. URL: www.climateactiontracker.org/countries/south-africa/ (visited on 06/05/2020).

CAT – Climate Action Tracker (2019b). *Temperatures: Adressing Global Warming*. URL: www.climateactiontracker.org/global/temperatures/ (visited on 02/04/2020).

Clowes, W. (2018). Congo to start $13.9 billion hydropower project this year. *Bloomberg*. URL: www.bloomberg.com/news/articles/2018-06-13/congo-plans-to-start-13-9-billion-hydropower-project-this-year (visited on 05/28/2019).

Clowes, W. and P. Burkhardt (2019). South Africa may double power buy from Congo hydro plant. *fin24*. URL: www.fin24.com/Economy/South-Africa/south-africa-may-double-power-buy-from-congo-hydro-plant-20190121 (visited on 05/28/2019).

Connolly, D., H. Lund, B. V. Mathiesen, and M. Leahy (2010). A review of computer tools for analysing the integration of renewable energy into various energy systems. *Applied Energy* 87.(4), pp. 1059–1082. DOI: 10.1016/j.apenergy.2009.09.026.

Creamer, T. (2018). South Africa to release new-look renewables bid window in november. *Engineering News*. URL: www.engineeringnews.co.za/article/south-africa-to-release-new-look-renewables-bid-window-in-november-2018-06-01 (visited on 06/09/2019).

DeCarolis, J. F., K. Hunter, and S. Sreepathi (2012). The case for repeatable analysis with energy economy optimization models. *Energy Economics* 34.(6), pp. 1845–1853. DOI: 10.1016/j.eneco.2012.07.004.

Dioha, M. O. (2017). Energy system models for Sub-Saharan African countries: A systematic review. *Journal of Sustainable Energy* 8.(4), pp. 159–168. ISSN: 2067-5534. URL: www.energy-cie.ro/archives/2017/nr_4/v8-n4-5.pdf (visited on 06/13/2020).

Dodds, P. E., I. Keppo, and N. Strachan (2015). Characterising the evolution of energy system models using model archaeology. *Environmental Modeling & Assessment* 20.(2), pp. 83–102. DOI: 10.1007/s10666-014-9417-3.

Droste-Franke, B., M. Carrier, M. Kaiser, M. Schreurs, C. Weber, and T. Ziesemer, eds. (2015). Improving Energy Decisions. Ethics of Science and Technology Assessment. Cham: Springer International Publishing. ISBN: 978-3-319-11345-6. DOI: 10.1007/978-3-319-11346-3.

Eberhard, A. and T. Kåberger (2016). Renewable Energy Auctions in South Africa Outshine Feed-in Tariffs. *Energy Science & Engineering* 4.(3), pp. 190–193. DOI: 10/f3rzvj.

Eberhard, A. and R. Naude (2017). The South African renewable energy IPP Procurement Programme (IPPPP): Review, lessons learned & proposals to reduce transaction costs. URL: www.gsb.uct.ac.za/files/EberhardNaude_REIPPPPReview_2017_1_1.pdf (visited on 06/10/2019).

EPRI – Electric Power Research Institute (2015). Power generation technology data for integrated resource plan of South Africa: Technical update. Palo Alto. URL: www.energy.gov.za/IRP/2016/IRP-AnnexureA-EPRI-Report-Power-Generation-Technology-Data-for-IRP-of-SA.pdf (visited on 09/06/2019).

EPRI – Electric Power Research Institute (2017). Power generation technology data for the Integrated Resource Plan of South Africa: Technical update. Pretoria. URL: www.energy.gov.za/IRP/irp-update-draft-report2018/EPRI-Report-2017.pdf (visited on 05/29/2019).

Ellenbeck, S. and J. Lilliestam (2019). How modelers construct energy costs: Discursive elements in energy system and integrated asessment models. *Energy Research & Social Science* 47, pp. 69–77. DOI: 10/ggzhm2.

ERC – Energy Research Center - University of Cape Town (2013). Assumptions and methodologies in the South African TIMES (SATIM) energy model: version 2.1. Cape Town (SA). URL: erc.uct.ac.za/groups/esap/satim.

ESKOM (2017). Integrated Report 2017: Enabling economic growth. URL: www.eskom.co.za/IR2017/Documents/Eskom_integrated_report_2017.pdf (visited on 05/28/2019).

ESKOM (2018). Integrated Report 2018: Achieving sustained success. URL: www.eskom.co.za/IR2018/Documents/Eskom2018IntegratedReport.pdf (visited on 05/28/2019).

ESKOM (2019). Integrated Report 2019. URL: www.eskom.co.za/IR2019/Documents/Eskom_2019_integrated_report.pdf (visited on 05/28/2019).

Etminan, M., G. Myhre, E. J. Highwood, and K. P. Shine (2016). Radiative forcing of carbon dioxide, methane, and nitrous oxide: A significant revision of the methane radiative forcing. *Geophysical Research Letters* 43.(24), pp. 12, 614–12, 623. DOI: 10/gdkwbj.

Eurek, K., P. Sullivan, M. Gleason, D. Hettinger, D. Heimiller, and A. Lopez (2017). An improved global wind resource estimate for integrated assessment models. *Energy Economics* 64, pp. 552–567. DOI: 10/gbnz2c.

Fankhauser, S. and F. Jotzo (2018). Economic growth and development with low-carbon energy. *Wiley Interdisciplinary Reviews: Climate Change* 9.(1), e495. DOI: 10/gcz58q.

Ferretti, F., A. Saltelli, and S. Tarantola (2016). Trends in sensitivity analysis practice in the last decade. *The Science of the total environment* 568, pp. 666–670. DOI: 10.1016/j.scitotenv.2016.02.133.

Fricko, O., P. Havlik, J. Rogelj, Z. Klimont, M. Gusti, N. Johnson, P. Kolp, M. Strubegger, H. Valin, M. Amann, T. Ermolieva, N. Forsell, M. Herrero, C. Heyes, G. Kindermann, V. Krey, D. McCollum, M. Obersteiner, S. Pachauri, S. Rao, E. Schmid, W. Schoepp, and K. Riahi (2017). The marker quantification of the Shared Socioeconomic Pathway 2: A middle-of-the-road scenario for the 21st century. *Global Environmental Change* 42, pp. 251–267. DOI: 10/f9vdbp.

Fuss, S., J. G. Canadell, G. P. Peters, M. Tavoni, R. M. Andrew, P. Ciais, R. B. Jackson, C. D. Jones, F. Kraxner, N. Nakicenovic, C. Le Quéré, M. R. Raupach, A. Sharifi, P. Smith, and Y. Yamagata (2014). Betting on negative emissions. *Nature Climate Change* 4.(10), pp. 850–853. DOI: 10.1038/nclimate2392.

Gargiulo, M. and B. Ó. Gallachóir (2013). Long-term energy models: Principles, characteristics, focus, and limitations. *Wiley Interdisciplinary Reviews: Energy and Environment* 2.(2), pp. 158–177. DOI: 10.1002/wene.62.

Geoffrion, A. M. (1976). The purpose of mathematical programming is insight, not numbers. *Interfaces* 7.(1), pp. 81–92.

Ghanem, R., D. Higdon, and H. Owhadi, eds. (2017). Handbook of uncertainty quantification. Cham: Springer International Publishing. ISBN: 978-3-319-12384-4. DOI: 10/ggzhng.

Gidden, M. J., K. Riahi, S. J. Smith, S. Fujimori, G. Luderer, E. Kriegler, D. P. van Vuuren, M. van den Berg, L. Feng, D. Klein, K. Calvin, J. C. Doelman, S. Frank, O. Fricko, M. Harmsen, T. Hasegawa, P. Havlik, J. Hilaire, R. Hoesly, J. Horing, A. Popp, E. Stehfest, and K. Takahashi (2019). Global emissions pathways under different socioeconomic scenarios for use in CMIP6: a dataset of harmonized emissions trajectories through the end of the century. *Geoscientific Model Development* 12.(4), pp. 1443–1475. DOI: 10/gf8sgm. URL: www.geosci-model-dev.net/12/1443/2019/.

GEA – Global Energy Assessment (2012). Global Energy Assessment: Toward a sustainable future. Cambridge (UK), New York (USA), Laxenburg (AT): Global Energy Assessment. ISBN: 9781 10700 5198. URL: www.globalenergyassessment.org.

Grubler, A., C. Wilson, N. Bento, B. Boza-Kiss, V. Krey, D. McCollum, N. D. Rao, K. Riahi, J. Rogelj, S. de Stercke, J. Cullen, S. Frank, O. Fricko, F. Guo, M. Gidden, P. Havlík, D. Huppmann, G. Kiesewetter, P. Rafaj, W. Schoepp, and H. Valin (2018). A low energy demand scenario for meeting the 1.5 °C target and sustainable development goals without negative emission technologies. *Nature Energy* 3.(6), pp. 515–527. DOI: 10.1038/s41560-018-0172-6.

Gütschow, J., L. Jeffery, and R. Gieseke (2019). The PRIMAP-hist national historical emissions time sries (1850-2016): v2.0. DOI: 10/gftrpk. URL: www.pik-potsdam.de/paris-reality-check/primap-hist/ (visited on 06/13/2019).

Häfele, W. (1976). Second status report of the IIASA project on energy systems. Laxenburg (AT).

Hall, L. M. and A. R. Buckley (2016). A review of energy systems models in the UK: Prevalent usage and categorisation. *Applied Energy* 169, pp. 607–628. DOI: 10.1016/j.apenergy.2016.02.044.

Hamby, D. M. (1994). A review of techniques for parameter sensitivity analysis of environmental models. *Environmental monitoring and assessment* 32.(2), pp. 135–154. DOI: 10.1007/BF00547132.

Harmsen, M., O. Fricko, J. Hilaire, D. P. van Vuuren, L. Drouet, O. Durand-Lasserve, S. Fujimori, K. Keramidas, Z. Klimont, G. Luderer, L. Aleluia Reis, K. Riahi, F. Sano, and S. J. Smith (2019). Taking some heat off the NDCs? The limited potential of additional short-lived climate forcers' mitigation. *Climatic Change* 15, p. 8201. ISSN: 0165-0009. DOI: 10.1007/s10584-019-02436-3.

Hartnady, C. J. H. (2010). South Africa's diminishing coal reserves. *South African Journal of Science* 106.(9/10). DOI: 10.4102/sajs.v106i9/10.369.

Hedenus, F., D. Johansson, and K. Lindgren (2013). A critical assessment of energy-economy-climate models for policy analysis. *Journal of Applied Economics and Business Research*, pp. 118–132.

Herbst, A., F. Toro, F. Reitze, and E. Jochem (2012). Introduction to energy systems modelling. *Swiss Journal of Economics and Statistics* 148.(2), pp. 111–135. DOI: 10.1007/BF03399363.

Herman, J. and W. Usher (2017). SALib: An open-source Python library for sensitivity analysis. *The Journal of Open Source Software* 2.(9), p. 97. DOI: 10/ggxtbq.

Howard, D. C., P. J. Burgess, S. J. Butler, S. J. Carver, T. Cockerill, A. M. Coleby, G. Gan, C. J. Goodier, D. van der Horst, K. Hubacek, R. Lord, A. Mead, M. Rivas-Casado, R. A. Wadsworth, and P. Scholefield (2013). Energyscapes: Linking the energy system and ecosystem services in real landscapes. *Biomass and Bioenergy* 55, pp. 17–26. DOI: 10.1016/j.biombioe.2012.05.025.

Huppmann, D., M. Gidden, O. Fricko, P. Kolp, C. Orthofer, M. Pimmer, N. Kushin, A. Vinca, A. Mastrucci, K. Riahi, and V. Krey (2019). The MESSAGE Integrated Assessment Model and the ix Modeling Platform (ixmp): An open framework for integrated and cross-cutting analysis of energy, climate, the environment, and sustainable development. *Environmental Modelling & Software* 112, pp. 143–156. DOI: 10/ggj67t.

Huppmann, D., E. Kriegler, V. Krey, K. Riahi, J. Rogelj, S. Rose, J. Weyant, N. Bauer, C. Bertram, V. Bosetti, K. Calvin, J. Doelman, L. Drouet, J. Emmerling, S. Frank, S. Fujimori, D. Gernaat, A. Grubler, C. Guivarch, M. Haigh, C. Holz, G. Iyer, E. Kato, K. Keramidas, A. Kitous, F. Leblanc, J.-Y. Liu, K. Löffler, G. Luderer, A. Marcucci, D. McCollum, S. Mima, A. Popp, R. Sands, F. Sano, J. Strefler, J. Tsutsui, D. van Vuuren, Z. Vrontisi, M. Wise, and R. Zhang (2018). IAMC 1.5°C Scenario Explorer and data: Hosted by IIASA. Ed. by Integrated Assessment Modeling Consortium and International Institute for Applied Systems Analysis. DOI: 10/ggzhm8. URL: data.ene.iiasa.ac.at/iamc-1.5c-explorer (visited on 06/17/2019).

IPPO – Independent Power Producer Office (2018). Independent Power Producers Procurement Programme (IPPPP): An overview. Centurion. URL: www.ipp-projects.co.za/Publications.

IPPO – Independent Power Producer Office (2019). Independent Power Producers Procurement Programme (IPPPP): An overview. Centurion. URL: www.ipp-projects.co.za/Publications (visited on 05/29/2019).

IPCC – Intergovernmental Panel on Climate Change (2013). Climate Change 2013: Contribution of working group I to the Fifth Assessment Report of the Intergovernmental Panel on Climate Change. Ed. by T. Stocker, D. Qin, G.-K. Plattner, M. Tignor, and S. Allen. Cambridge (UK), New York (USA): Cambridge University Press.

IPCC – Intergovernmental Panel on Climate Change (2018). Summary for policymakers. *Global Warming of 1.5°C*. Ed. by V. Masson-Delmotte, P. Zhai, H.-O. Pörtner, D. Roberts, J. Skea, P. R. Shukla, W. Pirani, A. Moufouma-Okia, C. Péan, R. Pidcock, S. Connors, J. Matthews, Y. Chen, X. Zhou, M. Gomis, E. Lonnoy, T. Maycock, M. Tignor, and T. Waterfield. Intergovernmental Panel on Climate Change.

IEA – International Energy Agency (2018). World Energy Balances: 2018. URL: www.iea.org/statistics/?country=SOUTHAFRIC&year=2016&category=Energy%5C%20supply&indicator=TPESbySource&mode=table&dataTable=BALANCES (visited on 05/29/2019).

IEA – International Energy Agency (2019a). Technology Roadmap: Hydropower. Paris. URL: www.iea.org/reports/global-energy-co2-status-report-2019 (visited on 06/12/2019).

IEA – International Energy Agency (2019b). World Energy Model documentation: 2019 version. Paris (FR). URL: iea.blob.core.windows.net/assets/d496ff6a-d4ca-4f6a-9471-220adddf0efd/WEM_Documentation_WEO2019.pdf (visited on 02/10/2020).

IIASA – International Institute for Applied System Analysis (2018). Shared Socioeconomic Pathways (SSP) database: Version 2.0. URL: tntcat.iiasa.ac.at/SspDb/dsd?Action=htmlpage&page=about (visited on 06/18/2019).

IRENA – International Renewable Energy Agency (2015). Africa 2030: Roadmap for a renewable energy future. Abu Dhabi. URL: www.irena.org/publications/2015/Oct/Africa-2030-Roadmap-for-a-Renewable-Energy-Future (visited on 09/06/2019).

IRENA – International Renewable Energy Agency (2018). Renewable Energy Auctions: Cases from Sub-Saharan Africa. Abu Dhabi. URL: www.gsb.uct.ac.za/files/IrenaAuctionsSubSaharanAfrica2018.pdf (visited on 06/08/2019).

Iooss, B. and A. Saltelli (2017). Introduction to sensitivity analysis. *Handbook of uncertainty quantification*. Ed. by R. Ghanem, D. Higdon, and H. Owhadi. Vol. 3. Cham: Springer International Publishing, p. 1103–1122. ISBN: 978-3-319-12384-4. DOI: 10.1007/978-3-319-12385-1\textunderscore31.

Jebaraj, S. and S. Iniyan (2006). A review of energy models. *Renewable and Sustainable Energy Reviews* 10.(4), pp. 281–311. DOI: 10.1016/j.rser.2004.09.004.

Johnson, N., M. Strubegger, M. McPherson, S. C. Parkinson, V. Krey, and P. Sullivan (2017). A reduced-form approach for representing the impacts of wind and solar PV deployment on the structure and operation of the electricity system. *Energy Economics* 64, pp. 651–664. DOI: 10/ggzhnf.

Keynes, J. M. (1921). A Treatise on Probability. 128, p. 288. DOI: 10.7326/0003-4819-128-4-199802150-00007.

Khumalo, S. (2018). Jeff Radebe signs renewable energy Contracts after more than two years of delays. *Mail and Guardian*. URL: mg.co.za/article/2018-04-04-signing-of-renewable-energy-contracts-delayed-but-only-for-a-few-hours (visited on 06/09/2019).

Klaassen, G. and K. Riahi (2007). Internalizing externalities of electricity generation: An analysis with MESSAGE-MACRO. *Energy Policy* 35.(2), pp. 815–827. DOI: 10.1016/j.enpol.2006.03.007.

Kock, M. de, N. Beukes, E. Adeniyi, D. Cole, A. Götz, C. Geel, and F.-G. Ossa (2017). Deflating the shale gas potential of South Africa's main karoo basin. *South African Journal of Science* 113.(9/10). DOI: 10/gb254x.

Kristensen, M. H. and S. Petersen (2016). Choosing the appropriate sensitivity analysis method for building energy model-based investigations. *Energy and Buildings* 130, pp. 166–176. DOI: 10/f88c3t.

Kydes, A. S. (1980). The Brookhaven Energy System Optimization Model (BESOM): Its variants and uses. *United States and Canadian Experiences*. Ed. by W. T. Ziemba and S. L. Schwartz. Dordrecht: Springer Netherlands, p. 110–136. ISBN: 978-94-009-8751-7. DOI: 10.1007/978-94-009-8751-7\textunderscore7.

Lamontagne, J. R., P. M. Reed, G. Marangoni, K. Keller, and G. G. Garner (2019). Robust abatement pathways to tolerable climate futures require immediate global action. *Nature Climate Change* 9.(4), pp. 290–294. DOI: 10/gfws3c.

Loulou, R. and M. Labriet (2008). ETSAP-TIAM: the TIMES integrated assessment model Part I: Model structure. *Computational Management Science* 5.(1), pp. 7–40. DOI: 10.1007/s10287-007-0046-z.

Luenberger, D. G. and Y. Ye (2016). Linear and nonlinear programming. Vol. 228. Cham: Springer International Publishing. ISBN: 978-3-319-18841-6. DOI: 10.1007/978-3-319-18842-3.

Machete, M. J. (2013). Presentation to the IEP stakeholder consultation: Overview of the liquid fuel sector in South Africa. Nelspruit. URL: www.energy.gov.za/files/IEP/Mmabatho/Overview-of-the-Liquid-Fuels-Sector.pdf.

Mai, T., J. Logan, N. Blair, P. Sullivan, and M. Bzilian (2013). RE-ASSUME: A decision maker's guide to evaluating energy scenarios, modeling, and assumptions. URL: www.iea-retd.org/wp-content/uploads/2013/07/RE-ASSUME_IEA-RETD_2013.pdf (visited on 06/28/2019).

Marangoni, G., M. Tavoni, V. Bosetti, E. Borgonovo, P. Capros, O. Fricko, D. E. H. J. Gernaat, C. Guivarch, P. Havlik, D. Huppmann, N. Johnson, P. Karkatsoulis, I. Keppo, V. Krey, E. Ó Broin, J. Price, and D. P. van Vuuren (2017). Sensitivity of projected long-term CO2 emissions across the Shared Socioeconomic Pathways. *Nature Climate Change* 7.(2), pp. 113–117. DOI: 10/f9tqzn.

Mathews, C. (2017). What experts say about Eskom's excuses for renewable delays. *BussinessDay*. URL: www.businesslive.co.za/bd/companies/energy/2017-06-29-what-experts-say-about-eskoms-excuses-for-renewable-delays/ (visited on 06/10/2019).

McCollum, D., L. G. Echeverri, S. Busch, S. Pachauri, S. Parkinson, J. Rogelj, V. Krey, J. C. Minx, M. Nilsson, A.-S. Stevance, and K. Riahi (2018a). Connecting the sustainable development goals by their energy inter-linkages. *Environmental Research Letters* 13.(3), p. 033006. DOI: 10.1088/1748-9326/aaafe3.

McCollum, D., J. Jewell, V. Krey, M. Bazilian, M. Fay, and K. Riahi (2016). Quantifying uncertainties influencing the long-term impacts of oil prices on energy markets and carbon emissions. *Nature Energy* 1.(7). DOI: 10.1038/nenergy.2016.77.

McCollum, D., V. Krey, P. Kolp, Y. Nagai, and K. Riahi (2014). Transport electrification: A key element for energy system transformation and climate stabilization. *Climatic Change* 123.(3-4), pp. 651–664. DOI: 10.1007/s10584-013-0969-z.

McCollum, D., W. Zhou, C. Bertram, H.-S. de Boer, V. Bosetti, S. Busch, J. Després, L. Drouet, J. Emmerling, M. Fay, O. Fricko, S. Fujimori, M. Gidden, M. Harmsen, D. Huppmann, G. Iyer, V. Krey, E. Kriegler, C. Nicolas, S. Pachauri, S. Parkinson, M. Poblete-Cazenave, P. Rafaj, N. Rao, J. Rozenberg, A. Schmitz, W. Schoepp, D. van Vuuren, and K. Riahi (2018b). Energy investment needs for fulfilling the Paris Agreement and achieving the Sustainable Development Goals. *Nature Energy* 3.(7), pp. 589–599. DOI: 10.1038/s41560-018-0179-z.

Messner, S. (1984). User's guide for the matrix generator of Message II: Parts I and II: Model description and implementation guide, and appendices. Laxenburg, Austria. URL: pure.iiasa.ac.at/id/eprint/2447/ (visited on 06/13/2019).

Messner, S. (1997). Endogenized technological learning in an energy systems model. *Journal of Evolutionary Economics* 7.(3), pp. 291–313. DOI: 10.1007/s001910050045.

Messner, S. and M. Strubegger (1995). User's guide for MESSAGE III. Laxenburg, Austria. URL: pure.iiasa.ac.at/id/eprint/4527/ (visited on 06/14/2019).

Miketa, A. and B. Merven (2013). Southern African Power Pool: Planning and prospects for renewable energy. Abu Dhabi. URL: www.irena.org/DocumentDownloads/Publications/SAPP.pdf (visited on 05/29/2019).

Mokgopo, A. (2019). Financing new coal is the quick road to financial and environmental ruin. *Business Maverick*. URL: www.dailymaverick.co.za/article/2019-05-15-financing-new-coal-is-the-quick-road-to-financial-and-environmental-ruin/ (visited on 06/10/2019).

Mokveld, K. and S. von Eije (2018). Final energy: Report South Africa. The Hague. URL: www.rvo.nl/sites/default/files/2019/01/Final-Energy-report-South-Africa.pdf (visited on 06/09/2019).

Morris, M. D. (1991). Factorial sampling plans for preliminary computational experiments. *Technometrics* 33.(2), p. 161. DOI: 10.2307/1269043.

Musango, J. K., A. C. Brent, and A. Bassi (2009). South African energy model: A system dynamics approach. Pretoria (SA). URL: researchspace.csir.co.za/dspace/bitstream/handle/10204/3566/Musango_d2_2009.pdf?sequence=1&isAllowed=y.

Myhre, G., D. Shindell, F.-M. Bréon, W. Collins, J. Fuglestvedt, J. Huang, D. Koch, J.-F. Lamarque, D. Lee, B. Mendoza, T. Nakajima, A. Robock, G. Stephens, T. Takemura, and H. Zhang (2013). 2013: Anthropogenic and natural radiative forcing. *Climate Change 2013: Contribution of working group I to the Fifth Assessment Report of the Intergovernmental Panel on Climate Change*. Ed. by T. Stocker, D. Qin, G.-K. Plattner,

M. Tignor, and S. Allen. Cambridge (UK), New York (USA): Cambridge University Press.

NREL – National Renewable Energy Laboratory (2017). Preliminary findings of the South Africa power system capacity expansion and operational model study: Preprint. Cape Town (SA). URL: www.nrel.gov/docs/fy18osti/70319.pdf.

Nkomo, J. C. (2009). Energy security and liquid fuels in South Africa. *Journal of Energy in Southern Africa* 20.(1), pp. 20–24. URL: www.scielo.org.za/pdf/jesa/v20n1/03.pdf (visited on 05/30/2019).

Norton, J. P. (2009). Selection of Morris trajectories for initial sensitivity analysis. *IFAC Proceedings* 42.(10), pp. 670–674. DOI: 10.3182/20090706-3-FR-2004.00111.

O'Neill, B. C., E. Kriegler, K. Riahi, K. L. Ebi, S. Hallegatte, T. R. Carter, R. Mathur, and D. P. van Vuuren (2014). A new scenario framework for climate change research: The concept of shared socioeconomic pathways. *Climatic Change* 122.(3), pp. 387–400. DOI: 10.1007/s10584-013-0905-2.

Orthofer, C., D. Huppmann, and V. Krey (2019). South Africa after Paris: Fracking its way to the NDCs? *Frontiers in Energy Research* 7, p. 34. DOI: doi.org/10.3389/fenrg.2019.00020.

Pachauri, R. and L. Meyer, eds. (2014). Climate Change 2014: Synthesis Report. Contribution of Working Groups I, II and III to the Fifth Assessment Report of the Intergovernmental Panel on Climate Change. Geneva: Intergovernmental Panel on Climate Change. ISBN: 978-92-9169-143-2. URL: www.ipcc.ch/site/assets/uploads/2018/02/AR5_SYR_FINAL_Front_matters.pdf (visited on 06/02/2020).

Pauw, P., K. Mbeva, and H. van Asselt (2019). Subtle differentiation of countries' responsibilities under the Paris Agreement. *Palgrave Communications* 5.(1). DOI: 10/ggzhmx.

Pelkmans, L. (2018). South Africa: Bioenergy policies and status of implementation: 2018 update. DOI: 10/CountryReport2018. (Visited on 06/09/2019).

Pfenninger, S., J. DeCarolis, L. Hirth, S. Quoilin, and I. Staffell (2017). The importance of open data and software: Is energy research lagging behind? *Energy Policy* 101, pp. 211–215. DOI: 10/f9nvvx.

Pfenninger, S., A. Hawkes, and J. Keirstead (2014). Energy systems modeling for twenty-first century energy challenges. *Renewable and Sustainable Energy Reviews* 33, pp. 74–86. DOI: 10.1016/j.rser.2014.02.003.

Pietzcker, R. C., D. Stetter, S. Manger, and G. Luderer (2014). Using the sun to decarbonize the power sector: The economic potential of photovoltaics and concentrating solar power. *Applied Energy* 135, pp. 704–720. DOI: 10.1016/j.apenergy.2014.08.011.

Pittel, K., D. Rübbelke, and M. Altemeyer-Bartscher (2012). International efforts to combat global warming. *Handbook of Climate Change Mitigation.* Ed. by W.-Y. Chen, J. Seiner, T. Suzuki, and M. Lackner. Vol. 20. New York, NY: Springer US, p. 89–120. ISBN: 978-1-4419-7990-2. DOI: 10.1007/978-1-4419-7991-9.

PLEXOS Integrated Energy Model (2019). URL: www.energyexemplar.com/software/plexos-desktop-edition.

Pollet, B. G., I. Staffell, and K.-A. Adamson (2015). Current energy landscape in the Republic of South Africa. *International Journal of Hydrogen Energy* 40.(46), pp. 16685–16701. DOI: 10.1016/j.ijhydene.2015.09.141.

Pollitt, M. G. (2019). A global carbon market? *Frontiers of Engineering Management* 6.(1), pp. 5–18. ISSN: 2095-7513. DOI: 10.1007/s42524-019-0011-x.

Popper, K. R. (1959). The Logic of Scientific Discovery. First English edition by Hutchinson 1959. New English edition by Routledge Classics 2002. London and New York: Routledge Classics. ISBN: 0-203-99462-0. URL: gbv.eblib.com/patron/FullRecord.aspx?p=254228.

Radebe, J. (2018). Keynote address at the Africa Oil Week conference. Cape Town. URL: www.energy.gov.za/files/media/speeches/2018/KeynoteAddress-by-Minister-at-the-Africa-Oil-Week-Conference.pdf.

Rago, Y. P., R. Mohee, and D. Surroop (2018). A review of thermochemical technologies for the conversion of waste biomass to biofuel and energy in developing countries. *The Nexus: Energy, Environment and Climate Change*. Ed. by W. Leal Filho and D. Surroop. Vol. 32. Green Energy and Technology. Cham: Springer, p. 127–143. ISBN: 9783319636115. DOI: 10.1007/978-3-319-63612-2_8.

Riahi, K., F. Dentener, D. Gielen, A. Grubler, J. Jewell, Z. Klimont, V. Krey, D. McCollum, S. Pachauri, S. Rao, B. van Ruijven, D. P. van Vuuren, and C. Wilson (2012). Chapter 17: Energy pathways for sustainable development. *Global Energy Assessment*. Cambridge (UK), New York (USA), Laxenburg (AT): GEA, p. 1203–1306. ISBN: 9781 10700 5198. URL: www.globalenergyassessment.org (visited on 06/13/2019).

Riahi, K., E. Kriegler, N. Johnson, C. Bertram, M. den Elzen, J. Eom, M. Schaeffer, J. Edmonds, M. Isaac, V. Krey, T. Longden, G. Luderer, A. Méjean, D. McCollum, S. Mima, H. Turton, D. P. van Vuuren, K. Wada, V. Bosetti, P. Capros, P. Criqui, M. Hamdi-Cherif, M. Kainuma, and O. Edenhofer (2015). Locked into Copenhagen pledges — Implications of short-term emission targets for the cost and feasibility of long-term climate goals. *Technological Forecasting and Social Change* 90, pp. 8–23. DOI: 10.1016/j.techfore.2013.09.016.

Riahi, K., D. P. van Vuuren, E. Kriegler, J. Edmonds, B. C. O'Neill, S. Fujimori, N. Bauer, K. Calvin, R. Dellink, O. Fricko, W. Lutz, A. Popp, J. C. Cuaresma, S. KC, M. Leimbach, L. Jiang, T. Kram, S. Rao, J. Emmerling, K. Ebi, T. Hasegawa, P. Havlik, F. Humpenöder, L. A. D. Silva, S. Smith, E. Stehfest, V. Bosetti, J. Eom, D. Gernaat, T. Masui, J. Rogelj, J. Strefler, L. Drouet, V. Krey, G. Luderer, M. Harmsen, K. Takahashi, L. Baumstark, J. C. Doelman, M. Kainuma, Z. Klimont, G. Marangoni, H. Lotze-Campen, M. Obersteiner, A. Tabeau, and M. Tavoni (2017). The Shared Socioeconomic Pathways and their energy, land use, and greenhouse gas emissions implications: An overview. *Global Environmental Change* 42, pp. 153–168. DOI: 10/brg6.

Ringkjøb, H.-K., P. M. Haugan, and I. M. Solbrekke (2018). A review of modelling tools for energy and electricity systems with large shares of variable renewables. *Renewable and Sustainable Energy Reviews* 96, pp. 440–459. DOI: 10/gfgb5g.

Rogelj, J., M. den Elzen, N. Höhne, T. Fransen, H. Fekete, H. Winkler, R. Schaeffer, F. Sha, K. Riahi, and M. Meinshausen (2016). Paris Agreement climate proposals need a boost to keep warming well below 2°C. *Nature* 534.(7609), pp. 631–639. DOI: 10.1038/nature18307.

Rogelj, J., O. Fricko, M. Meinshausen, V. Krey, J. J. J. Zilliacus, and K. Riahi (2017). Understanding the origin of Paris Agreement emission uncertainties. *Nature communications* 8, p. 15748. DOI: 10/gc7jnb.

Rogelj, J., A. Popp, K. V. Calvin, G. Luderer, J. Emmerling, D. Gernaat, S. Fujimori, J. Strefler, T. Hasegawa, G. Marangoni, V. Krey, E. Kriegler, K. Riahi, D. P. van Vuuren, J. Doelman, L. Drouet, J. Edmonds, O. Fricko, M. Harmsen, P. Havlík, F. Humpenöder, E. Stehfest, and M. Tavoni (2018). Scenarios towards limiting global mean temperature increase below 1.5°C. *Nature Climate Change* 8.(4), pp. 325–332. DOI: 10/gdcsz6.

Saltelli, A. (2007). Sensitivity analysis in practice: A guide to assessing scientific models. Reprint. Hoboken, NJ: Wiley. ISBN: 978-0-470-87093-8.

Saltelli, A. (2008). Global sensitivity analysis: The primer. Chichester, England and Hoboken, NJ: John Wiley. ISBN: 9780470725184. DOI: 10.1002/9780470725184.

Saltelli, A., K. Aleksankina, W. Becker, P. Fennell, F. Ferretti, N. Holst, S. Li, and Q. Wu (2019). Why so many published sensitivity analyses are false: A systematic review of sensitivity analysis practices. *Environmental Modelling & Software* 114, pp. 29–39. DOI: 10/gf7mxr.

Seebregts, A. J., G. A. Goldstein, and K. Smekens (2002). Energy/Environmental modeling with the MARKAL family of models. *Operations Research Proceedings 2001*. Ed. by P. Chamoni, R. Leisten, A. Martin, J. Minnemann, and H. Stadtler. Operations Research Proceedings 2001, Selected Papers of the International Conference on Operations Research (OR 2001) Duisburg, September 3-5, 2001. Berlin and Heidelberg: Springer, p. 75–82. ISBN: 978-3-642-50282-8.

Sen, S. and S. Ganguly (2017). Opportunities, barriers and issues with renewable energy development – A discussion. *Renewable and Sustainable Energy Reviews* 69, pp. 1170–1181. ISSN: 13640321. DOI: 10.1016/j.rser.2016.09.137.

Sheppard, D., D. Keohane, and J. Cotterill (2019). Total strikes South African oil and gas find. *Financial Times*. URL: www.ft.com/content/07b7798c-2abc-11e9-a5ab-ff8ef2b976c7 (visited on 05/28/2019).

Sobol, I. (2001). Global sensitivity indices for nonlinear mathematical models and their Monte Carlo estimates. *Mathematics and Computers in Simulation* 55.(1-3), pp. 271–280. DOI: 10.1016/S0378-4754(00)00270-6.

SA DoE – South Africa Department of Energy (2011). Integrated Resource Plan 2010-2030: Final report (Revision 2) in promulgation). Pretoria. URL: www.energy.gov.za/IRP/irp%5C%20files/IRP2010_2030_Final_Report_20110325.pdf (visited on 06/09/2019).

SA DoE – South Africa Department of Energy (2015). State of renewable energy in South Africa: 2015. Pretoria. URL: www.energy.gov.za/files/media/Pub/2017-State-of-Renewable-Energy-in-South-Africa.pdf (visited on 05/28/2019).

SA DoE – South Africa Department of Energy (2016a). Integrated Energy Plan (IEP). Pretoria. URL: www.energy.gov.za/files/IEP/2016/Integrated-Energy-Plan-Report.pdf (visited on 05/28/2019).

SA DoE – South Africa Department of Energy (2016b). Integrated Energy Plan (IEP): Detailed scenarios for liquid fuels supply. Pretoria. URL: www.energy.gov.za/files/

IEP/2016/IEP-Detailed-Scenarios-for-Liquid-Fuels-Supply.pdf (visited on 06/09/2019).

SA DoE – South Africa Department of Energy (2018a). Integrated Resource Plan 2018: Final Draft For Public Input. Pretoria. URL: www.energy.gov.za/IRP/irp-update-draft-report2018/IRP-Update-2018-Draft-for-Comments.pdf (visited on 05/28/2019).

SA DoE – South Africa Department of Energy (2018b). The National Solar Water Heater Programme (NSWH). Pretoria. URL: www.solarwaterheating-programme.co.za/ (visited on 06/08/2019).

SA DoE – South Africa Department of Energy (2018c). The National Solar Water Heater Programme (NWHP). Pretoria. URL: www.solarwaterheating-programme.co.za/About (visited on 06/10/2019).

SA DoE – South Africa Department of Energy (2020). Energy statistics: Aggregated historical energy balances. Pretoria. URL: www.energy.gov.za/files/media/Energy_Balances.html (visited on 06/09/2019).

SA SCF – South Africa Standing Committee on Finance - National Assembly (2018). Carbon Tax Bill. URL: www.gov.za/sites/default/files/gcis_document/201902/bill-b46b-2018.pdf (visited on 06/09/2019).

SANEDI – South African National Energy Development Institute (2018). Wind atlas for South Africa. URL: www.wasaproject.info/ (visited on 06/09/2019).

SAPIA – South African Petroleum Industry Association (2018). Annual Report: 2017. Pretoria. URL: www.sapia.org.za/Portals/0/Annual-Reports/SAPIA_AR%5C%202017_FA_lowres.pdf (visited on 06/09/2019).

Stecher, K., A. Brosowski, and D. Thrän (2013). Biomass potential in Africa. Abu Dhabi. URL: www.irena.org/DocumentDownloads/Publications/IRENA-DBFZ_Biomass%5C%20Potential%5C%20in%5C%20Africa.pdf (visited on 09/06/2019).

Stevens, L. (2018). South Africa's greenhouse gas inventory report: 200-2015: Draft Report for Public Comments. Johannesburg. URL: environment.gov.za/sites/default/files/reports/southafricagreenhousegasinventory_draftreport2000_2015.pdf (visited on 05/22/2019).

Subramanian, A., T. Gundersen, and T. Adams (2018). Modeling and simulation of energy systems: A review. *Processes* 6.(12), p. 238. DOI: 10/gf8k32.

Sullivan, P., V. Krey, and K. Riahi (2013). Impacts of considering electric sector variability and reliability in the MESSAGE model. *Energy Strategy Reviews* 1.(3), pp. 157–163. DOI: 10.1016/j.esr.2013.01.001.

Sustainable Energy Africa (2017). Sustainable energy solutions for South African local government: A practical guide. Cape Town. URL: www.sustainable.org.za (visited on 03/09/2019).

Tennøe, S., G. Halnes, and G. T. Einevoll (2018). Uncertainpy: A Python toolbox for uncertainty quantification and sensitivity analysis in computational neuroscience. *Frontiers in Neuroinformatics* 12, p. 49. DOI: 10/gd5c4h.

Terrapon-Pfaff, J., M.-C. Gröne, C. Dienst, and W. Ortiz (2018). Impact pathways of small-scale energy projects in the global south – Findings from a systematic evaluation. *Renewable and Sustainable Energy Reviews* 95, pp. 84–94. DOI: 10/gfb3mt.

Thovhogi, T., S. Johnson, and X. Schalkwyk (2015). Assessment of the coal bed methane resource potential within coal-bearing strata of the Karoo supergroup, South Africa. *International Conference and Exhibition, Melbourne, Australia 13-16 September 2015*. Ed. by P. McCabe and S. Mackie. Society of Exploration Geophysicists and American Association of Petroleum Geologists, p. 341. DOI: 10.1190/ice2015-2211000.

Tian, W. (2013). A review of sensitivity analysis methods in building energy analysis. *Renewable and Sustainable Energy Reviews* 20, pp. 411–419. DOI: 10.1016/j.rser.2012.12.014.

Turton, H., V. Panos, M. Densing, and K. Volkart (2013). Global Multi-regional MARKAL (GMM) model update: Disaggregation to 15 regions and 2010 recalibration. Villigen (CH). URL: www.psi.ch/sites/default/files/import/eem/PublicationsTabelle/PSI-Bericht_13-03.pdf (visited on 02/10/2020).

UNEP – UN Environment Programme (2019). Emissions Gap Report 2018. New York, N.Y.: United Nations. ISBN: 9789210476690. DOI: 10/ggzhmz.

UNFCCC – United Nations Framework Convention on Climate Change (2015a). Adoption of the Paris Agreement: 21st Conference of the Parties. URL: sustainabledevelopment.un.org/content/documents/17853paris_agreement.pdf (visited on 04/06/2020).

UNFCCC – United Nations Framework Convention on Climate Change (2015b). Sustainable Development Goals: Affordable and Clean Energy. URL: www.un.org/sustainabledevelopment/energy/ (visited on 02/10/2020).

UNFCCC – United Nations Framework Convention on Climate Change (2016). South Africa's Intended Nationally Determined Contribution (INDC). Bonn. URL: www4.unfccc.int/sites/NDCStaging/Pages/Party.aspx?party=ZAF (visited on 05/30/2019).

US EIA – U.S. Energy Information Administration (2015). Technically recoverable shale oil and shale gas resources: South Africa. URL: www.eia.gov/analysis/studies/worldshalegas/pdf/South_Africa_2013.pdf (visited on 05/22/2019).

Usher, W. (2015). The value of global sensitivity analysis for energy system modelling. *International Energy Workshop*. Abu Dhabi: International Renewable Energy Agency. URL: irena.org/IEW (visited on 04/28/2020).

Usher, W. (2016). The value of learning about critical energy system uncertainties. Dissertation. London (UK): University College London.

Usher, W. and N. Strachan (2012). Critical mid-term uncertainties in long-term decarbonisation pathways. *Energy Policy* 41, pp. 433–444. DOI: 10.1016/j.enpol.2011.11.004.

van Vuuren, D. P., J. Edmonds, M. Kainuma, K. Riahi, A. Thomson, K. Hibbard, G. C. Hurtt, T. Kram, V. Krey, J.-F. Lamarque, T. Masui, M. Meinshausen, N. Nakicenovic, S. J. Smith, and S. K. Rose (2011). The representative concentration pathways: an overview. *Climatic Change* 109.(1-2), pp. 5–31. DOI: 10.1007/s10584-011-0148-z. (Visited on 04/10/2020).

van Vuuren, D. P., E. Kriegler, B. C. O'Neill, K. L. Ebi, K. Riahi, T. R. Carter, J. Edmonds, S. Hallegatte, T. Kram, R. Mathur, and H. Winkler (2014). A new scenario framework for climate change research: Scenario matrix architecture. *Climatic Change* 122.(3), pp. 373–386. DOI: 10.1007/s10584-013-0906-1.

Warner, J., S. Jomantas, E. Jones, M. Ansari, and L. de Vries (2019). The fantasy of the Grand Inga hydroelectric project on the river Congo. *Water* 11.(3), p. 407. DOI: 10/ggzhmw.

Wim, H. (2016). BioEnergy atlas for South Africa – Synopsis report. Pretoria. DOI: dx.doi.org/10.15493/SAEON.BEA.DOCS.10000001. (Visited on 06/06/2019).

Winkler, H. (2007). Energy policies for sustainable development in South Africa. *Energy for Sustainable Development* 11.(1), pp. 26–34. DOI: 10.1016/S0973-0826(08)60561.

WEC – World Energy Council (2019). World Energy Scenarios 2019: Exploring innovation pathways to 2040. London (UK). URL: www.worldenergy.org/assets/downloads/Scenarios_Report_FINAL_for_website.pdf (visited on 02/10/2020).

Wright, J. G., T. Bischof-Niemz, J. R. Calitz, C. Mushwana, and R. van Heerden (2019). Long-term electricity sector expansion planning: A unique opportunity for a least cost energy transition in South Africa. *Renewable Energy Focus* 30, pp. 21–45. DOI: 10/ggzhm3.

Zhang, S., F. Yang, C. Liu, X. Chen, X. Tan, Y. Zhou, F. Guo, and W. Jiang (2020). Study on Global Industrialization and Industry Emission to Achieve the 2 ?C Goal Based on MESSAGE Model and LMDI Approach. *Energies* 13.(4), e825. DOI: 10.3390/en13040825.

Zhou, Y., L. Clarke, J. Eom, P. Kyle, P. Patel, S. H. Kim, J. Dirks, E. Jensen, Y. Liu, J. Rice, L. Schmidt, and T. Seiple (2014). Modeling the effect of climate change on U.S. state-level buildings energy demands in an integrated assessment framework. *Applied Energy* 113, pp. 1077–1088. DOI: 10.1016/j.apenergy.2013.08.034.

Zipperle, T. (2020). Modellierung von Transformationspfaden für einen optimierten Energieeinsatz im Sektor Gewerbe, Handel, Dienstleistungen. Dissertation. München: Technische Universität München.

Zipperle, T. and C. Orthofer (2019). d2ix: A model input-data management and analysis tool for MESSAGEix. *Energies* 12.(8), p. 1483. DOI: 10/ggf7zb.